Identification of Specialized Pro-resolving Mediators: An Overview of Methods and Initial Efforts Towards New Methodology

Bojana Pavlovic

Dissertation for the degree of Master of Pharmacy
45 credits

Department of pharmaceutical chemistry
School of Pharmacy
Faculty of Mathematics and Natural Sciences

UNIVERSITY OF OSLO

April 2018

Identification of Specialized Pro-resolving Mediators: An Overview of Methods and Initial Efforts Towards New Methodology

Bojana Pavlovic

Dissertation for the degree of Master of Pharmacy
45 credits

Department of pharmaceutical chemistry
School of Pharmacy
Faculty of Mathematics and Natural Sciences

UNIVERSITY OF OSLO

April 2018

Supervisor
Trond Vidar Hansen

2018

Identification of Specialized Pro-resolving Mediators: An Overview of Methods and Initial Efforts towards New Methodology

Bojana Pavlovic

http://www.duo.uio.no/

Printed: Reprosentralen, University of Oslo

Acknowledgements

First of all, I would like to express my gratitude to my supervisor, Professor Trond Vidar Hansen, for all the help and guidance I received during my work on this thesis. Thank you for giving me the opportunity to work on this interesting project. Your intelligence, dedication to science and out-of-the-box thinking have been a true inspiration to me.

I would like to thank all the other members of the LIPCHEM group: Associate professor Anders Vik, Ph.D. student Renate Kristianslund, Dr Karoline G. Primdahl, postdoc. fellow Dr Jørn E. Tungen, Ph.D. student Jannicke I. Nesman, Ph.D. student Lars I.G. Johansen and master student Rawan Bero. Thank you for the valuable help and suggestions you provided me with during my work on this thesis.

I am greatly thankful to my chief, Celine Nguyen. You were ”the right person in the right place at the right time”, always flexible and ready to encourage. I am sincerely grateful. Many thanks, as well, to my colleagues Tormund, Isabelle and Anton for being good colleagues and good friends in these intense times for me.

Special thanks goes to my family and friends. As always, your support is what keeps me moving on.

Blindern, 2018

Bojana Pavlovic

Abstract

Resolution of inflammation has long been considered a passive process, until the discovery of specialized pro-resolving lipid mediators (SPMs). These molecules, derived from ω-3 fatty acids and arachidonic acid (ω-6 fatty acid) play a crucial role in shifting the process of inflammation towards resolution.

It has been almost 20 years since the first ω-3 fatty acid-derived SPM, resolvin E1, was discovered. Since then, research of biosynthetic pathways of the ω-3 fatty acids eicosapentaenoic acid, docosahexaenoic acid and n-3 docosapentaenoic acid has led to the discovery of several different families of SPMs: protectins, resolvins, maresins and their sulfido-conjugates.

The whole field of research of SPMs was accelerated by the advancement of analytical methods, especially liquid chromatography – tandem mass spectrometry (LC-MS/MS). Due to their sensitivity and specificity, LC-MS/MS methods overtook the central role that enzyme-linked immunosorbent assay (ELISA) and gas chromatography – mass spectrometry (GC-MS) had in SPM analysis.

However, the analysis of SPMs is still not without challenges. These molecules are produced *in vivo* in very low concentrations (picomolar to nanomolar), act locally and are readily further metabolized. The biggest challenge, however, remains that these molecules have several stereogenic centres, as well as isolated and conjugated double bonds, so a number of isomers are possible. Indeed, it was proven that the biosynthesis of SPMs is accompanied by the biosynthesis of their isomers, of which many have similar chromatographic and MS properties, but often lack pro-resolving activity. As a consequence, it is sometimes necessary to perform a chemical derivatisation of SPMs in order to unequivocally distinguish them from their isomers.

The first part of this master thesis provides an overview of the literature methods used for the discovery and analysis of SPMs. The second part of the thesis presents efforts towards application of new derivatisation agents that could enable the analysis of certain types of SPMs that are otherwise difficult to analyse.

Graphical abstract

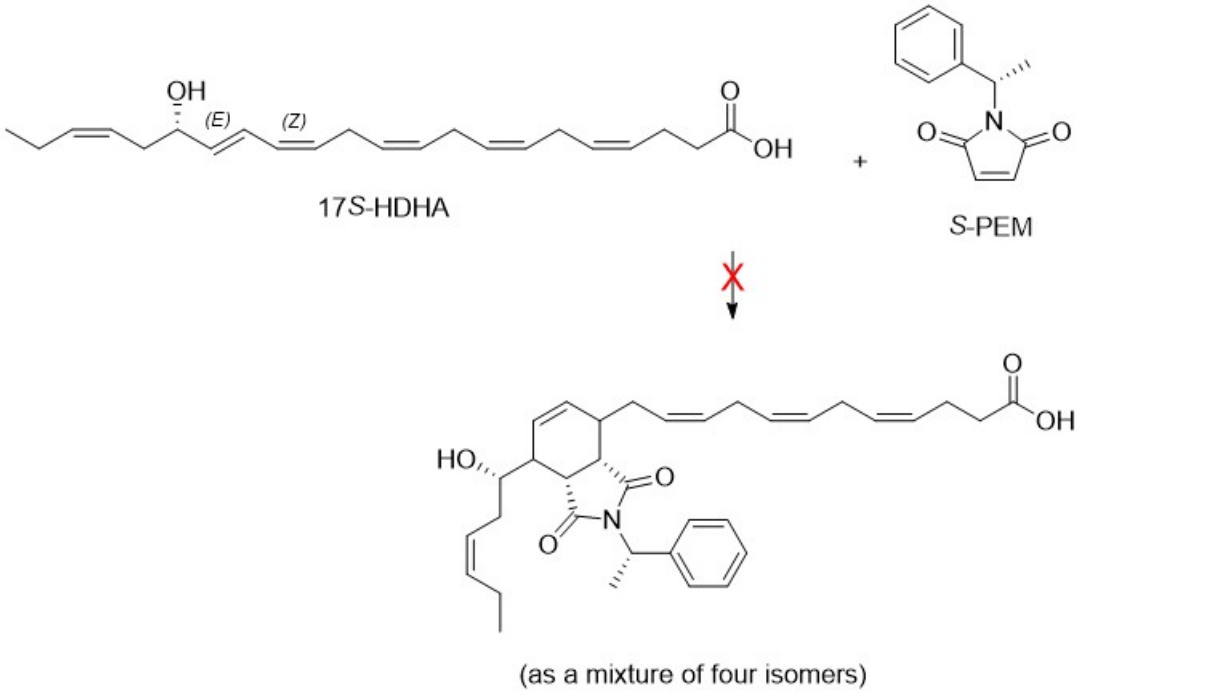

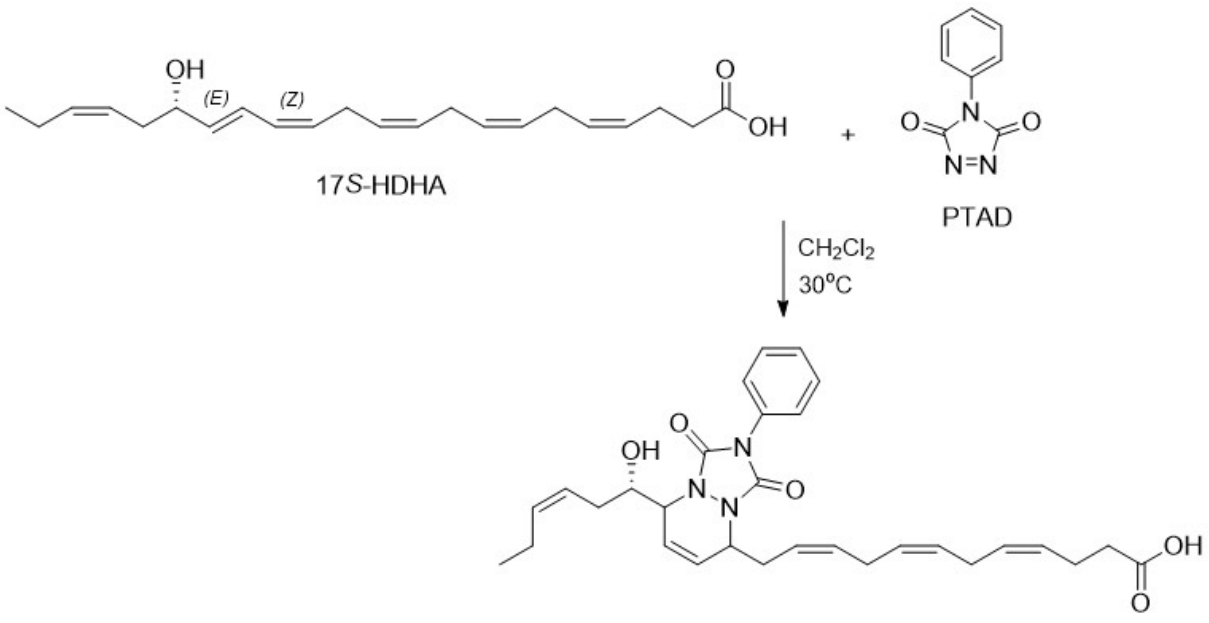

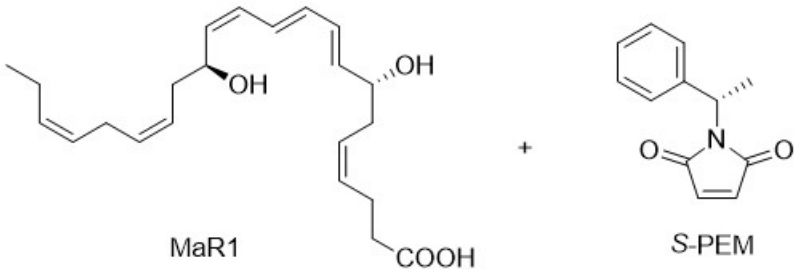

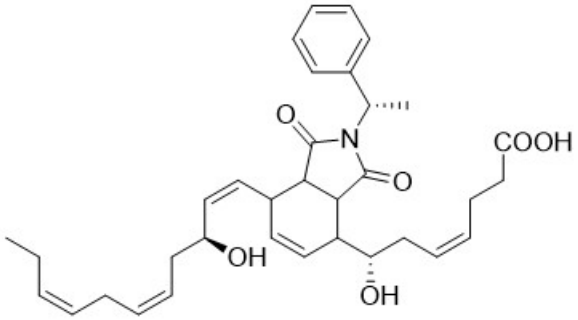

(as a mixture of four isomers)

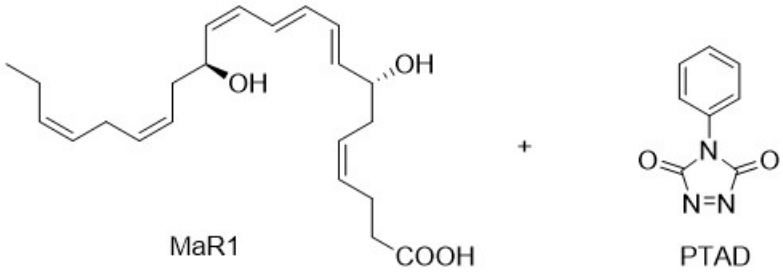

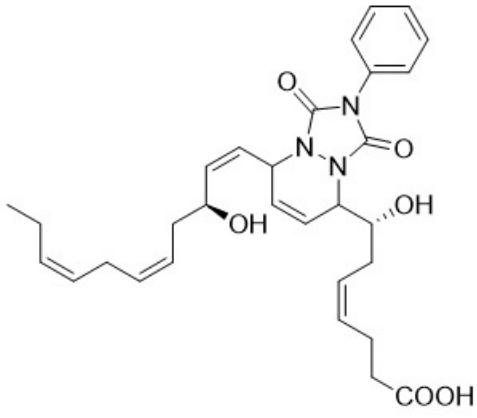

(as a mixture of two isomers)

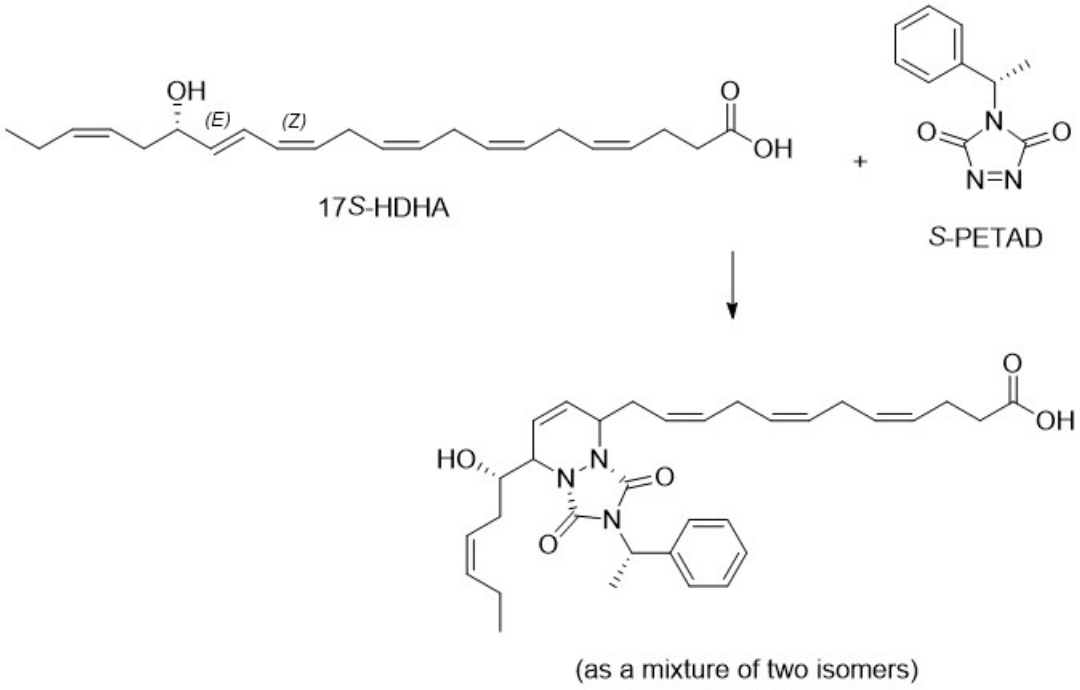
OH
(E)
(Z)
O
OH
17S-HDHA
+
O
O
N
N=N
S-PETAD
O
OH
HO
N
N
O
O
N
(as a mixture of two isomers)

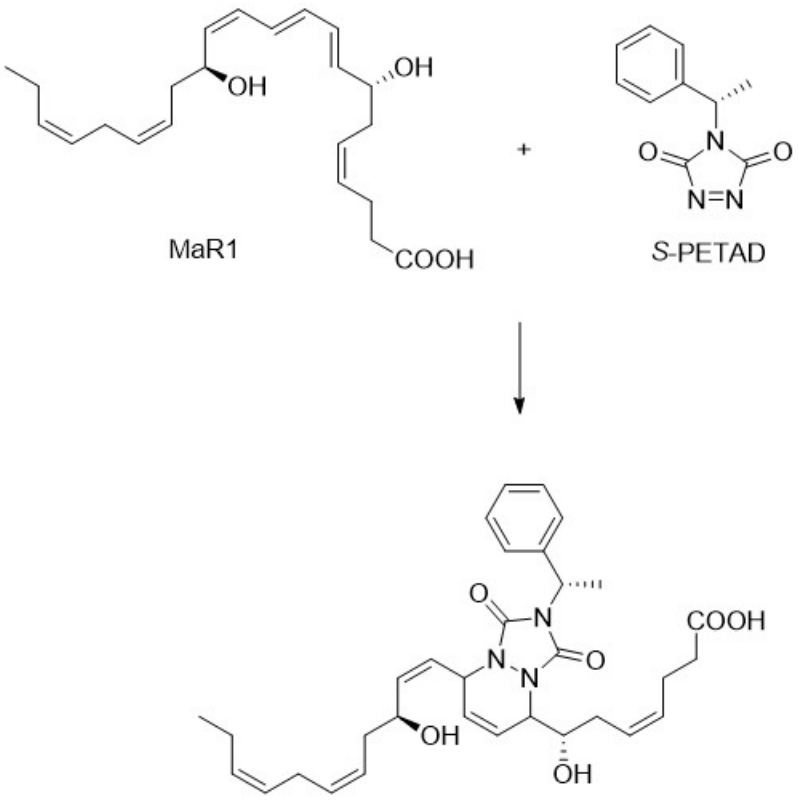
OH
OH
MaR1
COOH
+
O
O
N
N=N
S-PETAD
O
N
N
O
COOH
OH
OH
(as a mixture of two isomers)

List of abbreviations

AA	Arachidonic acid
APCI	Atmospheric pressure chemical ionization
CAM	Cerium ammonium molybdate
CID	Collision-induced dissociation
COX	Cyclooxygenase
CYP450	Cytochrome P450
DHA	Docosahexaenoic acid
DHAHDHA	Ester of docosahexaenoic acid and hydroxydocosahexaenoic acid
DHAHLA	Ester of docosahexaenoic acid and hydroxylinoleic acid
n-3 DPA	n-3 docosapentaenoic acid
ELISA	Enzyme-linked immunosorbent assay
EPA	Eicosapentaenoic acid
ESI	Electrospray-ionisation
FAHFA	Ester of fatty acid and hydroxy fatty acid
fMLP	Formyl-methionyl-leucyl-phenylalanine
GPCRs	G-protein coupled receptors
HDHA	Hydoxydocosahexaenoic acid
HEPE	Hydroxy-eicosapentaenoic acid
HETE	Hydroxyeicosatetraenoic acid
HODE	Hydroxylinoleic acid
H*p*ETE	Hydroperoxy-eicosatetraenoic acid

IS	Internal standard
LM	Lipid mediator
LOD	Limit of detection
LOX	Lipoxygenase
LT	Leukotriene
LXA_4	Lipoxin A_4
MaR1	Maresin 1
MRM	Multiple reaction monitoring
PAHSA	Ester of palmitic acid and hydroxystearic acid
PD1	Protectin D1
PETAD	4-(1-Phenylethyl)- 4,5-dihydro- 3*H*-1,2,4- triazole-3,5- dione
PG	Prostaglandin
PMN	Polymorphonuclear granulocyte
PTAD	4-Phenyl-1,2,4-triazoline-3,5-dione
PUFA	Polyunsaturated fatty acid
RT	Retention time
RvD1	Resolvin D1
RvE1	Resolvin E1
SPE	Solid-phase extraction
S-PEM	(*S*)-*N*-(1-phenylethyl)maleimide
SPM	Specialized pro-resolving mediator
SRM	Single reaction monitoring
TNF-α	Tumor necrosis factor-α

Table of contents

1 Introduction

1.1 Inflammation

Inflammation (lat. *inflammatio*) is a natural response of immune system to potentially harmful stimuli, such as pathogenic microorganisms, chemical and physical irritants or injury. Its primary function is protection of tissues and elimination of harmful factors.

Inflammation has been recognized from ancient times by its observable symptoms: redness, heat, swelling and pain (*rubor, calor, tumor, dolor*). It was not before 18th century it was concluded that inflammation was a consequence of injury or disease, and not a disease by itself. (1)

Today, it is well known that both cellular and chemical mediators of inflammation exist. In acute inflammation, vascular permeability rises, blood flow increases, pro-inflammatory cytokines and chemokines are produced and leukocytes are activated and recruited to the site of inflammation led by chemokines and other chemical inflammatory mediators. In the beginning, leukocytes recruited are predominantly polymorphonuclear granulocytes (PMN, neutrophils). In this early phase, pro-inflammatory mediators prostaglandins (such as PGE_2) and leukotrienes (such as LTB_4) are biosynthesized from arachidonic acid (AA). These mediators have an important role in stimulating vasodilatation and the formation of edema. As the inflammation process progresses, neutrophils are being replaced by monocytes and macrophages in the later stages of the inflammatory process. (1)

The ideal outcome is the complete resolution of the inflammation, where neutrophils cease to infiltrate, and apoptotic neutrophils and cellular debris are removed by macrophages via efferocytosis. Acute inflammation usually resolves within a couple of days, with surrounding tissue gradually returning to its previous state. However, sometimes instead of getting resolved, the inflammation becomes chronic, lasting for weeks, months or even years. Recruitment of leukocytes continues, tissues are infiltrated by monocytes, macrophages and lymphocytes (neutrophils decline, while monocytes, macrophages and lymphocytes arise). As a consequence of the persistent immune response and lasting inflammation, tissues are damaged and remodelled, and the loss of function is often irreversible. (2, 3)

Chronic inflammation is now recognized to be the root cause of many diseases, such as rheumatoid arthritis, chronic asthma, periodontal diseases, cardiovascular diseases, metabolic diseases, cancer and neurological disorders, like Alzheimer's disease. (4)

Resolution of inflammation has long been considered to be a passive process. Return to homeostasis was explained by catabolism of pro-inflammatory mediators. (5) Rising evidence from the last two decades proves otherwise - resolution of inflammation is an actively regulated process.

1.2 Polyunsaturated Fatty Acids

The polyunsaturated fatty acids (PUFAs) arachidonic acid (AA), eicosapentaenoic acid (EPA) and docosahexaenoic acid (DHA) play important roles in human physiology. There is a rising knowledge about metabolic pathways of PUFAs and effects of their metabolic products in the resolution of inflammation.

AA (C20:4 ω-6) is a ω-6 polyunsaturated fatty acid with four *Z*- double bonds. This fatty acid is a precursor to a range of both pro-inflammatory (prostaglandins, leukotrienes) and anti-inflammatory compounds (lipoxins).

DHA (docosahexaenoic acid, C22:6 ω-3) and EPA (eicosapentaenoic acid, C20:5 ω-3) are ω-3 PUFAs. These are the major dietary fatty acids, essential for normal body function and health. (6) DHA and EPA are not produced in mammalian tissues to any greater extent, and thus need to be part of the diet. One of the richest natural sources of ω-3 PUFAs is fish oil, but it is also found in canola oil and linseed. (7) (8)

Beneficial health effect of fish oil has long been known. As early as in 1929, experiments on rats showed that exclusion of ω-3 fatty acids from the diet could lead to a deficiency disease. (9) Those were the beginnings of realizing the essential role of ω-3 PUFAs. In 1999, a study conducted on myocardial infarct survivors taking 1g of ω-3 PUFAs daily, along with aspirin and other preventive medications, showed a significant decrease (of around 45%) in cardiovascular death. (7)

With these beneficial effects taken into account, it is no wonder there is a wide variety of dietary supplements with ω-3 fatty acids on the market. They are present either as solid dosage forms (mostly capsules, but also gelatine-free tablets) or as a highly concentrated fish oil. Different products on the Norwegian market contain 42-320 mg EPA per capsule (or ml) and 105-470 mg DHA per capsule (or ml). (10) Omacor® is the only registered medicine containing ω-3 PUFAs. It contains 1000 mg of PUFAs ethyl esters, of which 460 mg EPA and 380 mg DHA. Approved indications for Omacor® are secondary prophylaxis after myocardial infarction and hypertriglyceridemia. (11)

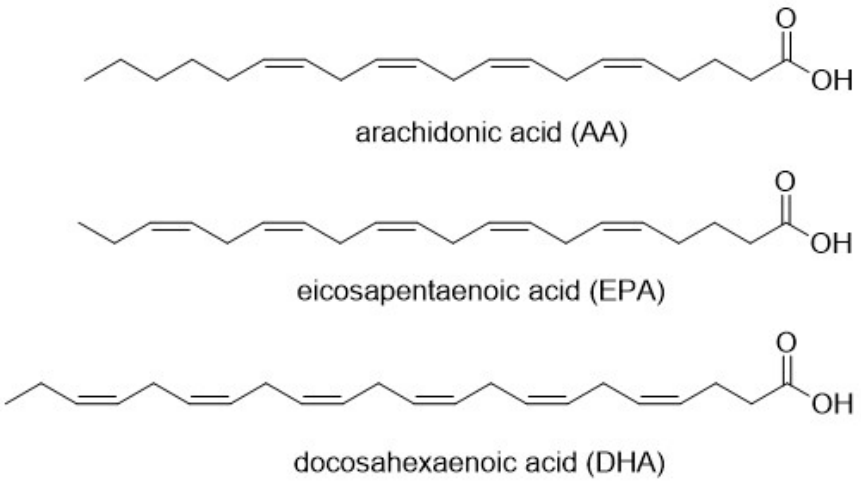

Figure 1. Structures of AA, EPA and DHA

AA and EPA are both C:20 PUFAs, and DHA is C:22. They are all-*cis* polyunsaturated fatty acids where the double bonds are methylene interrupted, in other words, their double bonds are non-conjugated.

EPA can be converted to DHA *in vivo*. EPA is biosynthesized from α-linoleic acid (ALA). To be converted to DHA, EPA is first enzymatically converted to n-3 docosapentaenoic acid (n-3 DPA). This acid was recently shown to be the origin of another class of SPMs with potent biological activity. (12)

1.3 Oxygenated Polyunsaturated Fatty Acids

PUFAs in organism are predominantly a part of phospholipid cell membranes, or present as triglycerides. When activated, they are released from the membrane, and then they undergo a series of oxidations mediated by either enzymes or free radicals. Oxygenated PUFAs are products of enzymatic oxygenation of PUFAs, and precursors of SPMs (specialized pro-resolving lipid mediators). There are three main enzymatic pathways: lipoxygenase (LOX), cyclooxygenase (COX) and cytochrome P450 (CYP450) pathway. (12)

Lipoxygenases are enzymes widely spread in plant, animal and human tissues. There are five isoforms of human LOX: 5-LOX, 12-LOX, 12R-LOX, 12/15-LOX and epithelial LOX, where number indicates the carbon atom in hydrocarbon chain which is most commonly oxygenised by the enzyme. Oxygenation is stereoselective, resulting in *S*-hydroperoxy-products that can be further conversed to *S*-hydroxy acids. (12)

In lipoxygenase (LOX) pathways, several SPMs are produced: lipoxins A_4 and B_4, protectins (PD), maresins and D-series resolvins.

Lipoxins A_4 and B_4 are products of AA, which is first oxygenised at position 15 by LOX-15 to form hydroperoxy-product 15*S*-H*p*ETE (15*S*-hydroperoxy-5*Z*,8*Z*,11*Z*,13*E*-eicosatetraenoic acid) and then 15*S*-HETE (15*S*-hydroxy-5*Z*,8*Z*,11*Z*,13*E*-eicosatetraenoic acid). Further oxidation at position 5 is mediated by 5-LOX. Along with lipoxins A_4 and B_4, some inactive isomers, like 6-epi-LXA_4, have been found as reaction products. (13)

AA is also a substrate for LOX-5, but final products in this pathway are pro-inflammatory leukotrienes. Intermediate hydroxy-PUFA is 5*S*-H*p*ETE.

In a similar way, D-resolvins are produced from DHA. At first stage, LOX-15 oxygenates DHA at position 17, giving 17*S*-H*p*DHA (17*S*-hydroperoxy-docosa-4*Z*,7*Z*,10*Z*,13*Z*,15*E*,19*Z*-hexaenoic acid) and in the next step 17*S*-HDHA. 17*S*-HDHA is further metabolized by 5-LOX to give D-series resolvins. (14)

Protectins are also products of DHA. DHA is first enzymatically oxygenised by 15-LOX to 17S-H*p*DHA and then to an epoxide. Further oxygenation of epoxide leads to formation of protectin D1 (PD1) or to PDx (dihydroxy acid protectin Dx). (15)

DHA can also be a substrate to 12-LOX, giving rise to maresin 1 (MaR1) via intermediate 14*S*-H*p*DHA (14*S*-hydroperoxy-docosa-4*Z*,7*Z*,10*Z*,12*E*,16*Z*,19*Z*-hexaenoic acid) and further enzymatic epoxidation and hydrolysis.

Of note, it has been shown that transgenic rabbits with overexpressed LOX-15 tend to develop a much milder form of inflammation and tissue damage when exposed to pro-inflammatory stimuli. (16)

In addition to lipoxygenase pathways, there are routes that include cyclooxygenase-2 (COX-2), where COX-2 is acetylated by aspirin (acetylsalicylic acid). Instead of inhibition of the enzyme, acetylation of COX-2 leads to the change of chirality of COX-2 enzymatic products. In case of LMs, this enzymatic pathway generates LOX-like products with hydroxyl group in *R*-configuration. (1) Oxygenated PUFAs that are produced in these reactions are 15*R*-HETE from AA, 17*R*-HDHA from DHA and 18*R*-HEPE from EPA. In further reaction series of aspirin-triggered pathways epimeric lipoxins (5-epi-LXA_4, 15-epi-LXB_4), E- and D-resolvins (17-epi-RvD1) and protectins (17-epi-PD1) arise. These compounds are also shown to be biologically active as anti-inflammatory and pro-resolving mediators. (13, 17) Early studies concluded that these aspirin-triggered lipid mediators could explain some of the beneficial effects of aspirin, and should therefore be further investigated as part of the efforts to discover new anti-inflammatory molecules with fewer side effects than those that are currently in use. (18)

The third enzymatic pathway is cytochrome P450 (CYP450) mediated. In this pathway, 15-epi-LXA_4 and 15-epi-LXB_4 are formed from AA via 15*R*-HETE and 15*R*-hydroxy-

5(6)-epoxy-ETE. CYP450 can also lead to production of RvE1 from EPA via 18*R*-H*p*EPE and 18*R*-HEPE. (13)

It was shown that some of oxygenated PUFAs also have pro-resolving properties. For example, 17-HDHA enhances humoral immune response against influenza virus. (19)

As outlined above, there exist numerous families of oxygenated PUFA products. These products contain both stereogenic centres and double bonds. Hence, several isomers of each product are possible.

1.4 Specialized Pro-resolving Lipid Mediators

Specialized pro-resolving lipid mediators (SPMs) are a class of biomolecules endogenously synthesized from AA and essential ω-3 PUFAs during the resolution phase of inflammation. They include lipoxins, protectins, resolvins and maresins, as well as their sulphido-conjugates. SPMs have the crucial role in the resolution of inflammation. Rising knowledge about their pro-resolving and anti-inflammatory properties depicts resolution of inflammation as actively regulated process. (1) A key step is class switching of lipid mediators from pro-inflammatory ones (prostaglandins, leukotrienes) to pro-resolving ones during the resolution phase. (5)

These potent bioactive molecules have a number of effects in common: they limit further neutrophil recruitment to the site inflammation, and stimulate macrophage uptake of apoptotic PMN and cellular remnants. They exert their actions at as low as picomolar to nanomolar concentrations. At the same time, members of different families act as ligands to specific G-protein–coupled receptors and have their individual specific actions. (4)

Lipoxins were the first SPMs to be discovered. They are derived from AA and formed by lipoxygenase pathways via cell-cell interactions (for example platelet-leukocyte interactions), or produced from single cells such as macrophages. Alternatively, aspirin can trigger epimeric lipoxin production via COX-2 acetylation. Lipoxins have trihydrohytetraene structures. It was shown that lipoxins limit PMN recruitment and adhesion to the site of insult. (1) They also stimulate macrophages to uptake the remains of the apoptotic cells. (20)

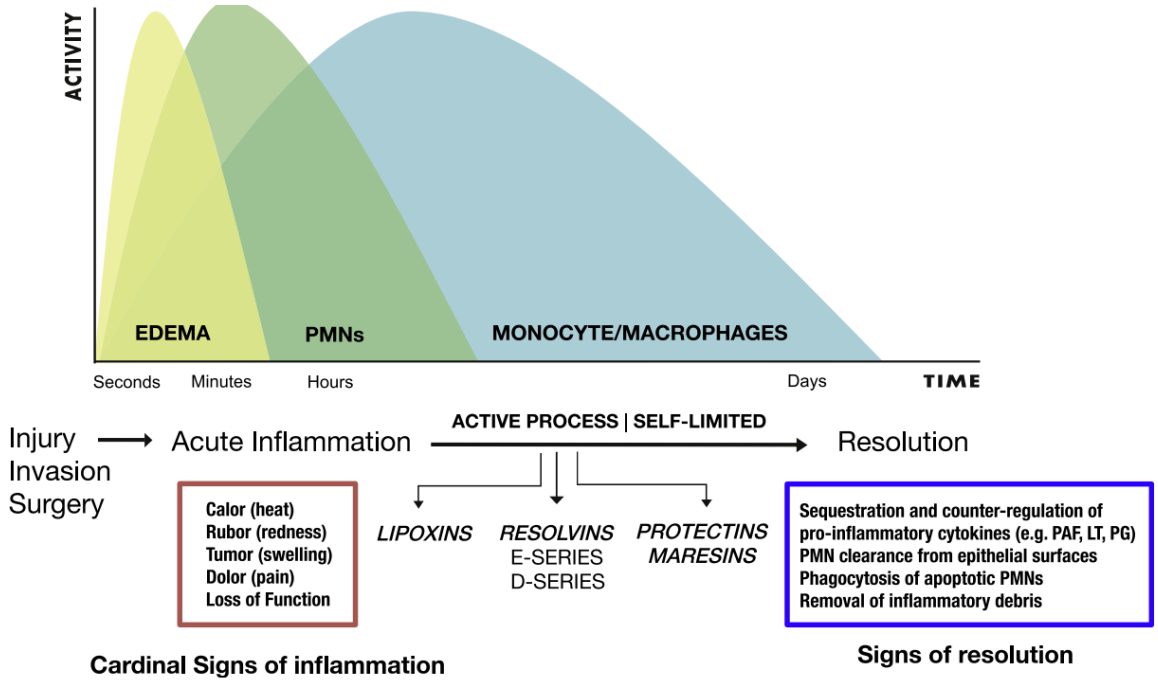

Figure 2. The ideal outcome of inflammation: edema is formed in acute inflammation, followed by PMN infiltration, and later monocyte and macrophage infiltration. SPMs (lipoxins, resolvins, protectins, maresins) biosynthesized in the resolution phase of self-limited inflammation. Adapted from reference (21)

Resolvins (or *resolution-phase interaction products*) include E-series resolvins (RvE1, RvE2 and RvE3) derived from EPA and D-series resolvins (RvD1 - RvD6) derived from DHA. The 17*R* series of resolvins are produced from DHA by COX-2 in the presence of aspirin – these are so-called aspirin-triggered resolvins (AT-Rv).

As mentioned, resolvin RvE1 was the first ω-3 PUFA derived SPM to be discovered, during the analysis of the inflammatory exudates in the mouse air pouch model. Its absolute configuration of stereogenic centres was confirmed by comparison with synthetic compounds. (12) Anti-inflammatory and pro-resolving actions of resolvins include stopping the production of pro-inflammatory mediators and regulating the recruitment of leukocytes, especially PMN. (1)

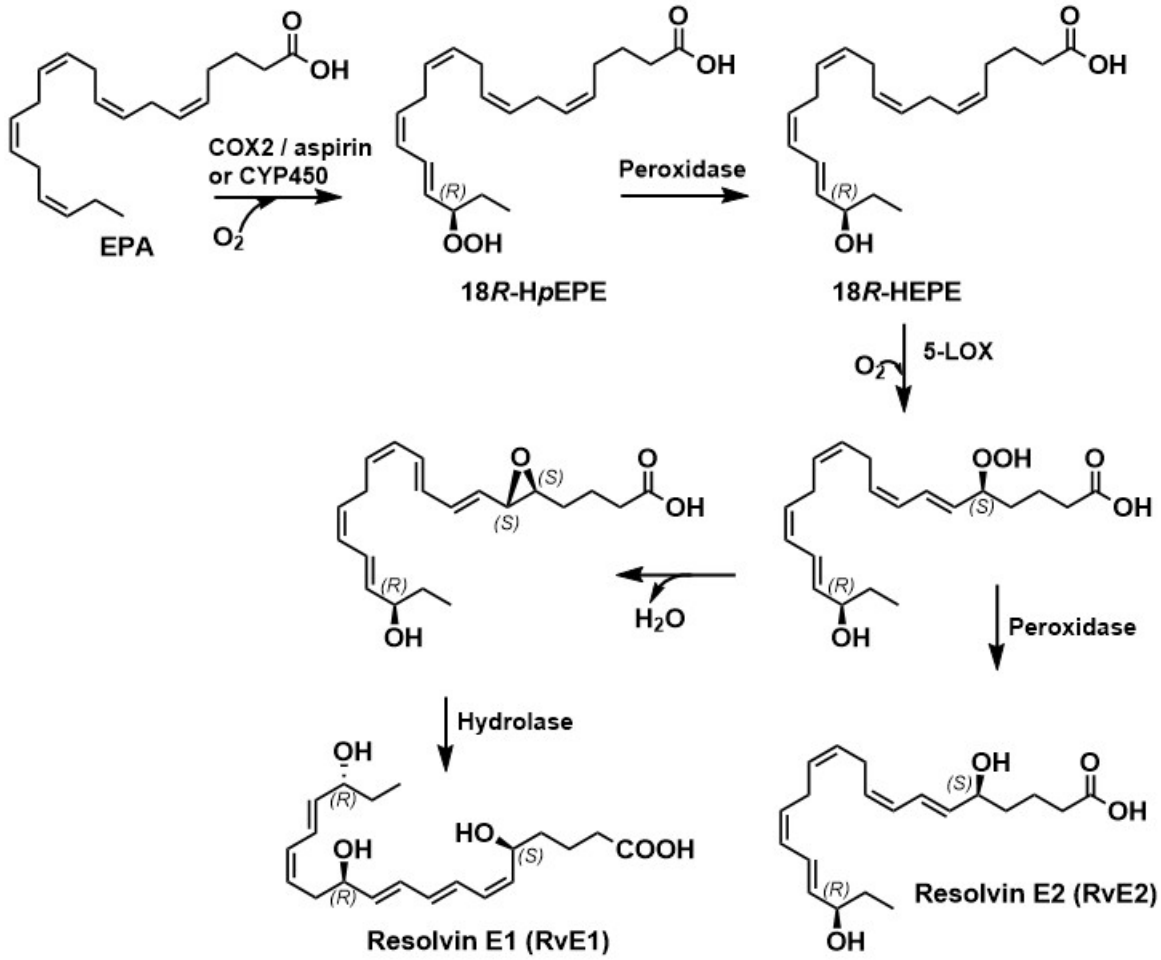

Figure 3. *In vivo* enzymatic synthesis of RvE1 and RvE2

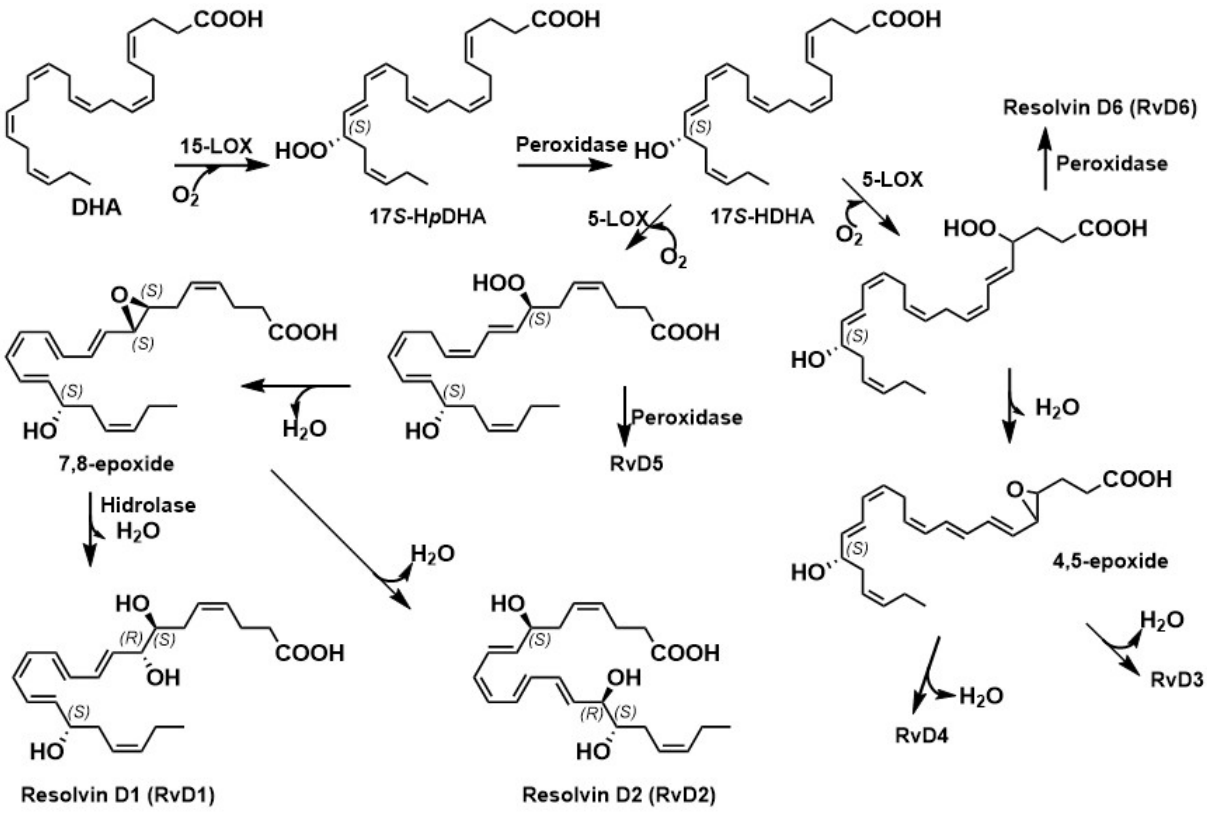

Figure 4. Biosynthetic pathways of DHA-derived LOX-mediated resolvins (RvD1-RvD6)

Protectins are derived from DHA. The first one to be discovered in 2002 in murine inflammatory exudate and human PMNs was protectin D1 (PD1). (12) These compounds are characterized by conjugated triene in their structure. In total they have six double bonds and 22 C atoms.

Maresins (*macrophage mediator in resolving inflammation*, or MaR1) are DHA products in 12/15-LOX pathway, with 14*S*-H*p*DHA and 14*S*-HDHA as intermediates. They are the first SPMs produced by macrophages. (1) Discovered in 2009, they resemble potent bioactions observed with earlier found SPMs. Potency of action can vary among different SPMs. It was, for instance, observed that MaR1 is a stronger stimulant of efferocytosis by macrophages than RvD1.

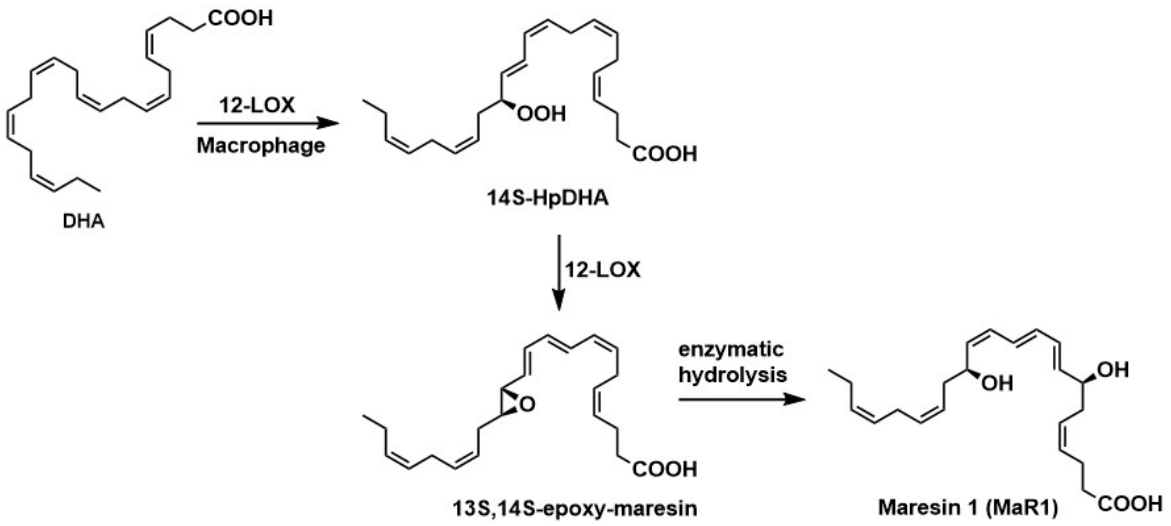

Figure 5. Biosynthesis of MaR1

Recently, it was proven that n-3 DPA (n-3 docosapentaenoic acid) is origin of several new members of SPMs family. (22) These SPMs are produced in LOX pathways and have the same structure as D-series resolvins, protectins and maresins, except for the *Z*-double bond in the C4-C5 position. Examples of this new group of SPMs are $PD1_{n\text{-}3\ DPA}$, $MaR1_{n\text{-}3\ DPA}$ and others. (12)

Sulfido-conjugates of resolvin, protectin and maresin, found in infectious murine exudates, *E. coli* infected mice and blood from sepsis patients, were recently also proven to possess pro-resolving and anti-inflammatory activity. (12)

Macrophages have the capability of producing different types and amounts of SPMs in their different states of activation and dependent of tissue of origin. (23)

1.5 Identification of Specialized Pro-resolving Mediators

The key for better understanding the role of SPMs *in vivo* is the development of sensitive and specific analytical methods for their identification, profiling and quantification in biological samples.

1.5.1 Challenges

In analysing SPMs, one needs to overcome several challenges: they appear in very low concentrations *in vivo*, act locally and are rapidly inactivated. In addition, SPMs show high stereoselectivity in their actions, and for that reason, it is very important to be able to distinguish them from related structures that are produced in the same metabolic pathways, but often lack biological activity. (24) Due to their structure, a multitude of isomeric structures is possible. (25) Some authors also warn about the *ex-vivo* formation of LMs during sample collection and sample clean-up, which could make further applied analytical methods less reliable. (26) It is also important to note that samples should not be stored for long periods of time prior to analysis, because LMs are prone to auto-oxidation and isomerization. (23)

1.5.2 Methods

There are different methods that have been used for the analysis of SPMs.

Enzyme-linked immunosorbent assay (ELISA) has long been a method of choice for quantitating LMs. ELISA can be used for highly sensitive detection and quantification of SPMs. The method requires specific antibody for each LM to be analysed. Its particular advantage is the possibility of quantitation of one specific SPM in a large number of samples in a relatively short time. Disadvantages of ELISA analysis are cross-reactivity and the fact that commercial ELISA-kits are not available for all of the compounds of interest. The method is quite expensive and only one LM can be determined in each assay, so it cannot be used for samples with a large number of different LMs. (27)

Another method that has been used is LC-UV. Here, samples are being analysed by their retention times and UV spectra. Limitation of this method is that it cannot be used for analysis of LMs that do not have chromophores. Another limitation is co-elution of peaks for some LMs with similar structures, and hence, inability to distinguish between them by using this method alone.

PUFAs are generally lacking characteristic UV spectra, due to non-conjugated double bonds. On the other hand, SPMs do have conjugated diene-, triene- and tetraene chromophores, giving them characteristic UV spectral properties.

GC-MS was the method that substituted ELISA as a method of choice for LM analysis in the past. Its particular advantage over ELISA is that it can detect multiple analytes in the same run. However, compounds need to be derivatized prior to analysis, and the sample preparation can be lengthy. A single derivatisation method is not always suitable for all the LMs in the sample. (27) Also, GC-MS methods are not applicable to all of the LMs – for example, there is a risk of thermal decomposition of oxygenated PUFAs. (28)

LC-MS/MS has proven to be the most reliable method. It usually does not require derivatisation prior to analysis, and its particular advantage is that it gives a possibility to multi-analyte testing. (25)

LC-MS/MS mediator lipidomics can be used for identification (matching), profiling, quantitation, structural elucidation, stereochemistry, and defining novel LMs. For compounds that have been identified, quantification or profiling is usually carried out by using multiple reaction monitoring (MRM) approach. It will be explained in more detail later in this thesis.

1.5.3 Sample preparation

The most common method for sample preparation and concentration is solid-phase extraction (SPE), though sometimes liquid-liquid extraction (LLE) and protein precipitation (PP) can also be used. In SPE, reverse-phase C18 cartridges are typically used. Samples are acidified prior to purification in order to protonate the carboxyl group. After elution, organic solvent used for the elution often needs to be removed (by nitrogen stream) in order to preserve the less stable eicosanoids. (25)

Samples are usually extracted together with the known amount of deuterium-labelled internal standard (IS). When available, IS has the same structure as the analyte. For example, RvD1 can be extracted with deuterated RvD1 as IS. When corresponding deuterium-labelled IS is not available, compounds with similar polarity are used as IS. The reason for using IS is to determine recovery and efficiency of extraction.

1.5.4 Introduction to LC-MS/MS

Liquid chromatography – tandem mass spectrometry (LC-MS/MS) is a technique that combines liquid chromatography as separation technique with highly diverse MS/MS detection that also separates different compounds based on their *m/z* (mass-to-charge) ratio. After chromatographic separation, samples are ionised and then identified or quantified based on their *m/z* ratios.

There are many different MS instruments with a wide variety of MS techniques. Development of LC-MS methods took place in early 1970s, about 20 years after GC-MS methods were introduced. In contrast to GC-MS, where gaseous samples can be directly introduced to MS detector, it took decades to develop an appropriate interface that would modify liquid eluate from LC (ionisation) so that the sample can then be introduced to MS detector. (29) Ionisation methods most frequently used in pharmaceutical analysis are electrospray-ionisation (ESI) and atmospheric pressure chemical ionisation (APCI). (30)

In LM metabololipidomics, approaches most commonly used are based on liquid chromatography - tandem mass spectrometry (LC-MS/MS). Here, LC separates LMs based on their physical and chemical properties. Then, the first mass analyser of the tandem mass spectrometer can isolate a selected ion. In the next step, this ion is being fragmented in vacuum, in the process of collision-induced dissociation (CID). The second mass analyser can then isolate a selected fragment ion. (30) Fragment ions and their abundances are determined by the structure of the precursor molecule. Therefore, fragmentation patterns are characteristic for the given analyte and thus can be used for identification and quantification. (31) This is the basis for single reaction monitoring (SRM), an approach widely used in lipidomics, where the analysis of lipids is based on the choice of characteristic precursor-product ion pairs. The advantage of LC-MS/MS is that more than one precursor-product ion pair can be observed in a single run; also, more than one product ion can be observed for the same precursor ion. This approach is called multiple reaction monitoring (MRM). (32) By using SRM and MRM, a much lower limit of detection (LOD) can be obtained in comparison to other standard techniques.

LC-MS/MS techniques have undergone a remarkable advancement in the last 20 years. There has been a high demand from the market, requiring shorter run times with maximised resolution for a growing number of samples. Thanks to that, methods have become more precise, sensitive and reliable. (33) Today, LC-MS techniques are the leading techniques in pharmaceutical analysis, especially because the majority of molecules analysed are thermally labile and hence cannot be analysed by GC-MS techniques. (34)

1.5.5 Application of LC-MS/MS and Metabololipidomic Techniques for the Identification of Specialized Pro-resolving Lipid Mediators

Metabololipidomics is a broad term that encompasses isolation and identification of new lipid molecules, but also their profiling, quantification and biological pathways: places of origin, precursors as biological markers, isomers with different biological activity, *in vivo* effects and metabolic inactivation. (28) It can include numerous biological samples taken at different time points. There are a plenty of lipid molecules found in these samples, and those of biological and medical interest are sometimes found in very low concentrations. That is why it was so important to develop methods that are sensitive, and that can be used to detect and analyse many lipid molecules at the same time. (28)

As already mentioned here, there are several analytical techniques that can be used for the identification of specialized pro-resolving lipid mediators. These techniques include LC-UV, ELISA, GC-MS and LC-MS, all of them with specific advantages and disadvantages. However, LC-MS/MS method proved to be the method of choice.

Chromatographic separation is usually done using C18 columns. When needed, chromatographic columns with chiral stationary phases can also be used. For detection, a combination of UV detector and MS/MS detector has shown its advantages. Using this combination of detectors, both UV spectra of the eluent and MS/MS spectra were obtained. These data, together with retention times (RT) were used to compare the analysed LM with known LMs or theoretical LMs, in order to identify it.

Therefore, one of the critical steps for successful identification of LMs was to create good databases with known and theoretical structures. These databases contained information about UV spectra, MS/MS spectra and retention times. The more information a database contained, the better were the chances that the right match would be found. (23)

When it comes to MS/MS analysis, it was important to find characteristic fragmentation ions for each SPM that could be used for targeted qualitative or quantitative analysis.

LC-UV-MS/MS combined the advantages of UV and MS/MS detection. However, after the advancement of MS/MS detectors and introduction of MRM in recent years, on-line UV detection is often omitted in most recent works.

1.5.6 Derivatization techniques

SPMs are PUFA-derived molecules with conjugated double bonds and hydroxy-groups (2^o alcohol) in their structure. This gives the possibility of a wide range of *E/Z* and *S/R* isomers. These isomers are often produced in the same biological pathways, but are either much less active, or are completely devoid of biological activity. Therefore, the analytical methods used need to be able to distinguish SPMs from their isomers. It is not always easy, as the example of maresin 1 (MaR1) and its double di-oxygenation isomer show (it will be explained in more detail later). Sometimes, even the most advanced methods, with long chiral chromatographic columns, are insufficient for a complete separation of isomers. In these cases, the use of derivatisation agents can lead to significant improvements. Sometimes, the derivatisation agent reacts with one of the isomers but not with the other; in other cases, both isomers react, but their properties are sufficiently modified to result in complete chromatographic separation. (35)

A derivatisation technique successfully applied by T.V.Hansen and his collaborators included the Diels-Alder reaction using 4-phenyl-1,2,4-triazoline-3,5-dione (PTAD) as a dienophile. It was well known that *E,E* conjugated dienes give the Diels-Alder reaction much more readily than *E,Z* conjugated dienes – it takes shorter time and milder reaction conditions. Most of the SPMs found so far have the *E,E*-moiety, while their double di-oxygenation isomers have the *E,Z*-moiety. Taking this into account, Hansen and collaborators foresaw that, under proper conditions, SPMs would react with PTAD and their double di-oxygenation isomers would not. (35)

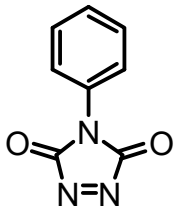

Figure 6. Structure of 4-phenyl-1.2.4-triazoline-3.5-dione (PTAD)

Indeed, their experiments and method development led to an easy and straightforward analysis of maresin 1 in the presence of its double di-oxygenation isomer, but other SPMs could be analysed with this method, as well. (35)

1.6 Structural Elucidation of Specialized Pro-resolving Mediators by matching with synthetic material

Whenever a novel putative SPM is found, it is important to unequivocally determine its structure in order to distinguish it from its isomers, as well as to be able to research its biosynthetic pathways and biological actions.

As shown on Fig. 7, analysis of novel active compounds includes both the analysis of their structure and of their functions in biological systems. That is why novel compounds need to be produced in higher amounts ("scale-up"), either by biogenic synthesis (like in the example of resolvin 1, using *B. megaterium*), or, most often, by total organic synthesis. In that way, structure of natural compounds can be compared to synthetic compounds with known structure, in order to unequivocally define the absolute configuration of the novel compounds. In addition to physical properties, it is important that bioactions of synthesized and novel molecules also match. (36) Higher amounts of synthesized compounds can then be used in further *in vitro* and *in vivo* experiments. (37)

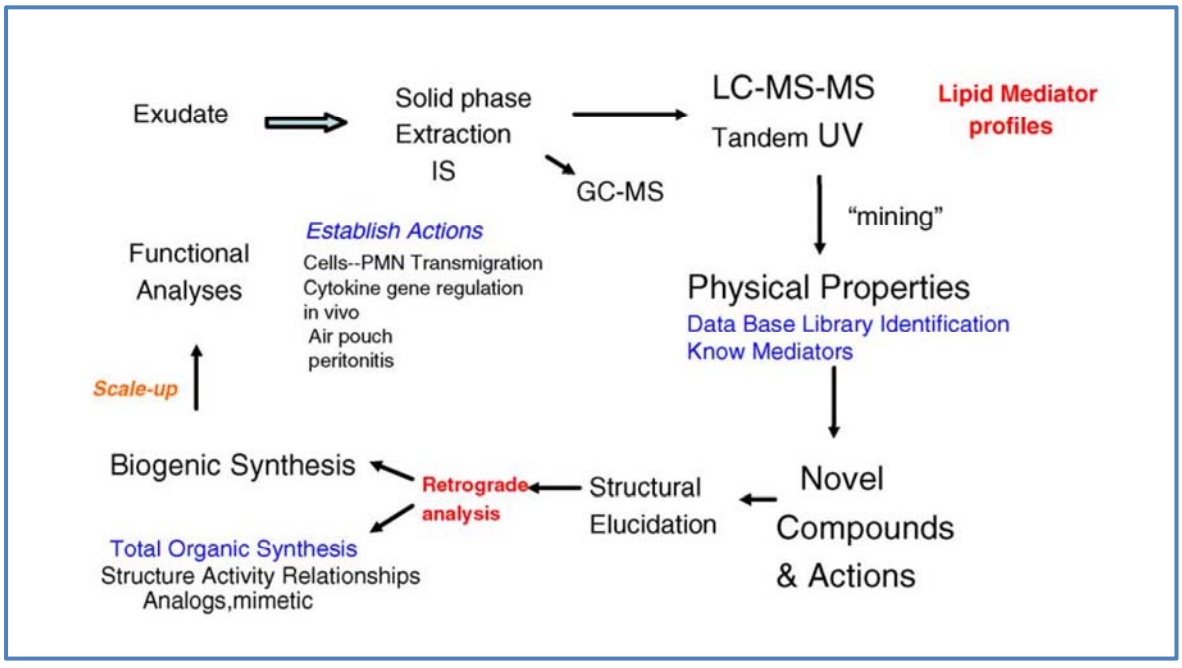

Figure 7. Mediator lipidomics: LC-MS/MS based analysis. Adapted from reference (37)

1.7 Novel Putative Specialized Pro-resolving Mediators

The advancement of several analytical methods in recent years has led to easier discovery of novel pro-resolving lipid mediators. A good example of this is the discovery of PUFA esters with hydroxy-PUFAs present in adipose tissue in 2016 (Prague). (38) These molecules were shown to have pro-resolving properties using *in vitro* experiments. Most prominent examples are esters of DHA with hydroxy-DHA and hydroxylinoleic acid (HODE): 13-DHAHLA, 9-DHAHLA and 14-DHAHDHA.

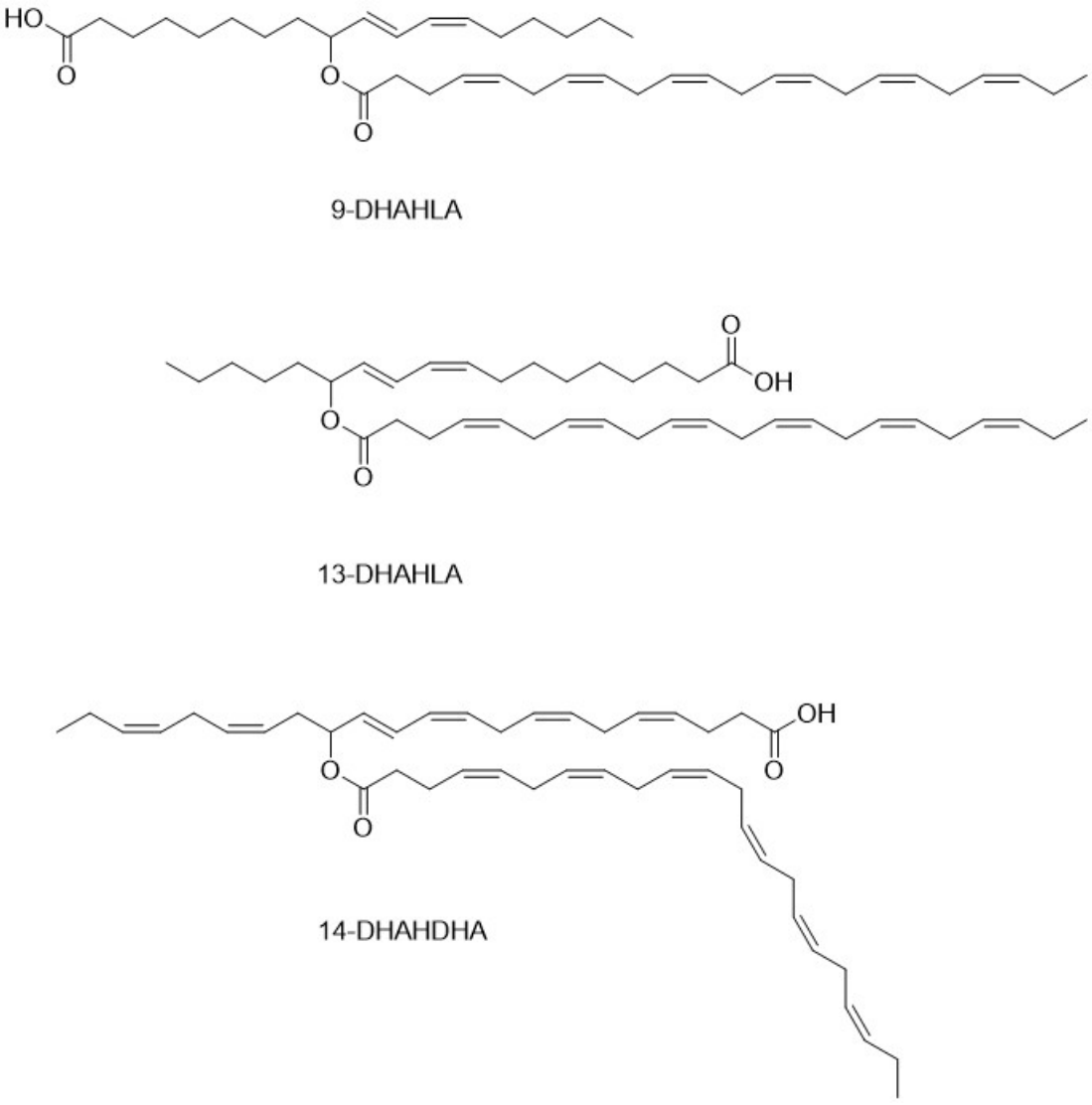

Figure 8. Structures of 9-DHAHLA, 13-DHAHLA and 14-DHAHLA

13-DHAHLA was particularly of interest for further investigation, because it was the only one found in significant amounts in human samples (in comparison to murine samples where all the above mentioned esters were found). (38)

In order to confirm pro-resolving properties on *in vivo* models, as well as to investigate the exact structure of the active molecules, higher amounts of 13-DHAHLA needed to be synthesized by total organic synthesis. The LIPCHEM group in Oslo has synthesized both the *R*- and the *S*- isomer of 13-DHAHLA. *In vivo* experiments gave promising results, however, exact structural elucidation of the isomer present in biological samples proved to be a challenge. The reason for this was the fact that *R*- and *S*- isomers of 13-DHAHLA gave a very similar signal when analysed by LC-MS/MS techniques. Namely, their retention times were so close that it was impossible to distinguish between the two isomers, and their mass spectra were essentially the same. [1]

1.8 Aim of Studies

- To provide an overview of the LC-MS/MS – metabololipidomic techniques used for SPMs (literature studies).

- To develop new methodology for the identification of SPMs.

Problems that scientists from Prague encountered when analysing 13-DHAHLA isomers gave the idea to the LIPCHEM group in Oslo to attempt derivatization of isomers, so that they could be more easily distinguished from one another. Since the isomers of 13-DHAHLA have the diene moiety in their structure, the idea of the LIPCHEM group was to attempt to induce the Diels-Alder reaction using a potent dienophile. This was the main goal of this master thesis – to try to develop a new method for the identification of novel special pro-resolving lipid mediators that are otherwise difficult to identify.

[1] Information obtained from professor Trond Vidar Hansen's personal correspondence

2 Results and Discussion

Part 1. An overview of the LC-MS/MS – metabololipidomic techniques used for the identification and analysis of SPMs

2.1 The initial efforts

SPMs are molecules that are produced in very small amounts *in vivo*, in picomolar to nanomolar concentrations. They act locally as ligands to specific G-protein coupled receptors (GPCRs), and disintegrate after a very short time. Thus, highly sensitive and selective methods need to be applied in their analysis. Finding a right isolation material and extraction techniques are equally important.

One of the first biological systems used to study the resolution of inflammation was the murine dorsal air pouch model. In this model, sterile air is injected in the back of the mouse or the rat. The air pouch that is developed mimics synovial cavity. Injection of pro-inflammatory agents into the air pouch gives a good environment for the research of cell trafficking and inflammatory response. After sufficient time has passed, air pouches are lavaged and fluids are collected and analysed. (39)

Murine air pouch model was particularly helpful because it allowed for direct analysis of where and when different LMs are produced during the resolution phase (temporal spatial differential analysis). It showed a class switch of lipid mediators. Namely, as the inflammatory exudate evolved in time, the lipid mediators produced switched from pro-inflammatory prostaglandins and leukotrienes to anti-inflammatory and pro-resolving SPMs. (20)

It has only been less than two decades since the first ω-3 derived SPM, resolvin E1, was discovered. The murine air pouch model was used. Mice were fed standard rodent diet containing 0,26% ω-3 PUFAs. TNF-α was injected into 6 days dorsal air pouches to induce inflammation, and after that aspirin was injected at 3,5h and EPA at 4h. Exudates were collected after 6h, purified using solid-phase extraction (SPE), and then analysed by LC-MS/MS. Selected ion chromatograms at *m/z* 317 showed the presence of 5-HEPE (product of 5-LOX pathway) and novel 18-HEPE. Cells found in aspirin and EPA-treated exudates were mostly PMN, and their number was 25-60% lower than in exudates with TNF-α alone. A novel trihydroxy-containing compound was also found. (7)

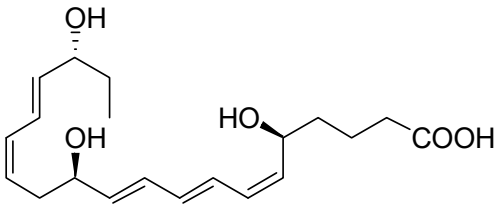

Figure 9. Structure of Resolvin E1 (RvE1)

MS/MS spectra with diagnostic ions for 18*R*-HEPE and 5,12,18*R*-triHEPE (later termed resolvin 1) are shown on Fig. 10. The absolute configuration of alcohol at C18 of 18-HEPE was shown to be *R*, using column with chiral stationary phase and comparing to the reference 18*R*-HEPE produced by biogenic synthesis using *B. megaterium*. (7)

Also, 18*R*-HEPE and 5,12,18*R*-HEPE (resolvin 1) were injected *i.v.* in the mouse tail to check whether they inhibit TNF-α stimulated PMN infiltration into murine dorsal air pouch. It was shown that as low levels as 100 ng of 5,12,18*R*-HEPE were a potent inhibitor of PMN infiltration, while 18*R*-HEPE was far less effective. (7)

These were the beginnings of mediator lipidomics for SPMs.

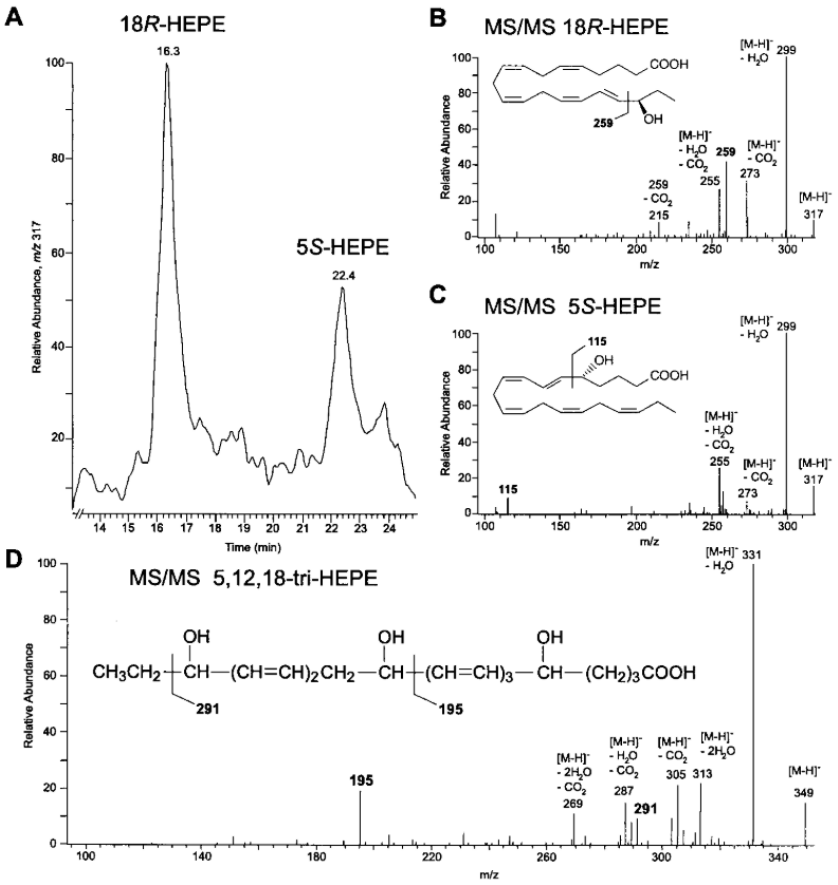

Figure 10. Inflammatory exudates from murine air pouches treated with aspirin and EPA give novel compounds. (A) Selected ion chromatogram of 5*S*-HEPE and 18*R*-HEPE; (B) MS/MS of 18*R*-HEPE; (C) MS/MS of 5*S*-HEPE; (D) MS/MS of 12,15,18*R*-triHEPE (resolvin 1). Adapted from reference (7)

Serhan and co-workers applied the same principle using the air pouch model in 2002, when they tested if DHA also was a substrate for aspirin-triggered COX-2. These experiments revealed new compounds that inhibited PMN migration and progress of inflammation. This time, rodent diet included DHA as well. (40) In addition to the air pouch model, another *in vivo* model was used: peritonitis in mice induced by intraperitoneal injection of zymosan A. In both *in vivo* models, selected ion chromatograms at *m/z* 343 proved the presence of 17-HDHA in exudates. Chiral stationary phase chromatography confirmed that over 95% of 17-HDHA was in the *R* configuration, which also indicated enzymatic origin. Also, novel 17*R*-trihydroxy products with the DHA backbone were identified at *m/z* 375: 4*S*,11,17*R*-triHDHA and trihydroxytetraene containing 7,8,17*R*-triHDHA. (40) These were later denoted AT-RvD3 and AT-RvD1.

Since 2002, the model of zymosan-induced sterile peritonitis in mice was the model of choice in the research and discovery of SPMs. (21) In this model, zymosan A, a polysaccharide component of *Saccharomyces cerevisiae* cell wall, is injected into the peritoneal cavity of mice. As a consequence, typical signs of inflammation occur, such

as leukocyte migration and infiltration and the production of inflammatory mediators. Sterile inflammation is self-resolved within 48 to 72 hours. (3)

This model has several advantages over the previously used murine air pouch model. One of the biggest advantages of the method is that it is time saving, since neutrophils reach their peak concentration within 4 hours after zymosan A injection, and the inflammation is completely resolved within 48-72 hours. Besides, peritoneal cavity is a natural serosal cavity, and compared to an artificial air pouch cavity it mimics the actual inflammation conditions more accurately. For example, the leukocytes can migrate from the inflammation site to regional lymph nodes by their natural ways. Peritoneal cavity is easily accessible, sufficient amounts of exudates are being produced for LMs analysis, and the overall technique is relatively simple and reproducible. (3)

2.2 The metabololipidomics era

Metabolomics is an integral part of systems biology and includes qualitative and quantitative analysis of the endogenous metabolome. Metabolome is a term used for small metabolites (under 1500 Da) and other small biochemical products that have a role in physiological processes. A metabolomics study usually involves the comparative analysis of a normal state and a perturbed state, where the perturbation can be of any kind, such as inflammation, use of a medicine or change in diet. (41)

Lipidomics is a term used to describe a process of identifying, profiling and quantifying lipids and lipid mediators in biosystems. It includes architecture/membrane lipidomics and mediator lipidomics. Lipidomics, together with proteomics and genomics, is a part of metabolomics, a rising field of research of metabolic pathways and pathway intermediates. (24)

In an article from 2006, Serhan and collaborators describe a LC-UV-MS/MS mediator lipidomics approach to analyse temporal production of SPMs, in other words, appearance and levels of lipid mediators in different time points of inflammation and resolution. *In vivo* models used are murine air pouch model and peritonitis model.

One of the most important steps in this research was to create databases with UV spectra, MS/MS spectra and retention times for well-known structures, as well as good search algorithms. Valuable approaches were taken from similar databases already developed for the GC-MS/MS analysis. The goal was to collect enough data to be able to define new structures based on their UV, MS/MS and chromatographic properties.

When using C-18 reverse-phase columns, elution takes place in the following order: trihydroxy-LMs elute first, then dihydroxy-, then monohydroxy-, and finally nonoxygenized molecules (like PUFAs).

Different structures give also their signature in UV spectrum: monohydroxy-compounds (like mono-HETEs, 17-HDHA etc.) have λ_{max} ~ 235 nm, conjugated trienes (like LTB_4 leukotriene) have triplet with λ_{max} ~ 270 nm, conjugated tetraenes (LXA_4 and LXB_4) have triplet with λ_{max} ~ 300 nm. Two conjugated dienes with methylene bridge (5*S*,15*S*-diHETE) have λ_{max} ~ 242 nm. Some of the lipid compounds of interest do not have chromophores, and consequently have absorption maximums in vacuum UV range, which makes them less applicable for UV analysis. They have namely λ_{max} < 210 nm, which falls in the cut-off wavelength range of chromatographic eluents. (23)

Table 1. Absorption maximums for different double bond systems found in LMs

Double bond system	λ_{max}
Conjugated diene (mono-HETEs, 17-HDHA, etc.)	λ_{max} ~ 235 nm
Two conjugated dienes (5*S*,15*S*-diHETE, RvD5)	λ_{max} ~ 242 nm
Conjugated diene + conjugated triene (RvE1, RvD3)	λ_{max} ~ 270 nm
Conjugated triene (LTB_4, MaR1, PD1)	triplet with λ_{max} ~ 270 nm
Conjugated tetraene (LXA_4, LXB_4, RvD1, RvD2)	triplet with λ_{max} ~ 300 nm

When it comes to MS/MS analysis, there are three different types of MS/MS fragment ions: 1) peripheral-cut ions are formed by neutral loss of H_2O, CO_2, amines, etc.; 2) chain-cut ions are formed by cleavage of a C-C bond in the carbon chain; 3) chain-plus-peripheral cut ions are a combination of the other two. Chain-cut ions are the most important because they are more specific – they give information about the position of functional groups and double bonds. Most common chain-cut ions are derived by α-cleavage – cleavage of a C-C bond next to the functional group like hydroxy group (23).

Therefore, in order to identify potential new LMs, Serhan and collaborators matched their UV and MS/MS spectra and retention times to those of authentic and synthetic standards, if they were available. If not, data were compared to the theoretical data – virtual UV and MS/MS spectra and retention times predicted for potential novel SPMs. For the development of the search algorithm, the logic diagram shown in Fig. 11 was used. Search includes several consecutive steps. For example, UV spectra can be

checked first, and further searches include only MS/MS spectra of compounds whose UV spectra match the one analysed. When MS/MS spectra are also matched (based on several diagnostic ions), further search includes comparison of retention times (RTs). In routine analysis, ≥ 6 diagnostic ions of tandem MS/MS spectrum are being analysed. COCAD (Cognoscitive-Contrast-Angle Algorithm and Databases) system was used to treat intensity of each peak based on the ion identity – it will not be explained in detail here. Search result gave a compound in the database (real or theoretical) with the highest matching score (23).

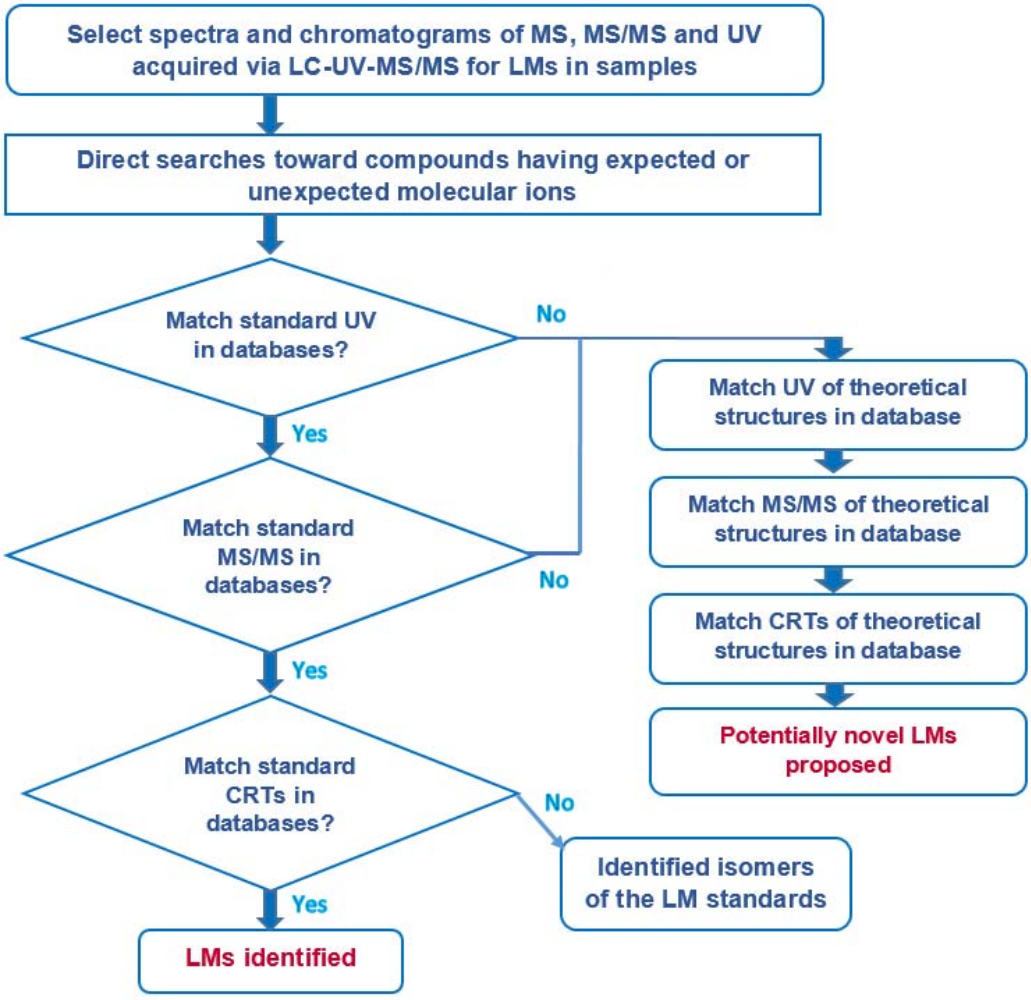

Figure 11. Logic diagram for developing LC-UV-MS/MS-based mediator lipidomic databases and search algorithms for PUFA-derived LMs (24)

2.3 Advancement of methods and the use of multiple reaction monitoring

As already said, it is of a particular advantage to use methods that can analyse a large number of lipid molecules from different biological samples in a relatively short time. This is where the use of MRM (multiple reaction monitoring) methods made a breakthrough.

In this highly sensitive approach, different chromatographic peaks are associated with MRM transitions of characteristic ion pairs, where the precursor ion is a molecular ion of SPM, and the product ion is a characteristic fragment ion. Instrument is usually run in the negative ionization mode, and the method of acquisition is Enhanced Production Ions (EPI). Many ion pairs can be followed in the same run – which is where the name "multiple" reaction monitoring comes from. MRM improves LC-MS/MS method sensitivity and detection limits as well. (28)

It was reported that "the number of published LC–MS/MS methods for eicosanoid analysis markedly increased as mass spectrometers with high sensitivity and the capability of fast data acquisition became commercially available". (25)

The first time MRM approach was used for the analysis of LMs was in 1996, when it was used to quantitate 14 arachidonic acid-derived eicosanoids from a biological sample. (27)

Masoodi, Serhan and co-workers reported the first analysis of novel SPMs using MRM in 2008. (28) They managed to simultaneously analyse twenty LMs, including protectins, resolvins and a number of oxygenated PUFAs by using LC/ESI-MS/MS assay. Tissue samples used were murine brain, liver and plasma. Sample purification and lipid extraction were performed using SPE cartridges, with 12-HETE-d_8 as internal standard. For each LM analysed, MS spectra were used to choose adequate precursor-product ion pairs. During method optimisation, for each precursor-product ion pair a proper collision energy was chosen to give the best abundance (Fig. 12). As shown here, isobaric molecules can be distinguished from one another by using characteristic fragmentation ions in MRM. Also, as a part of method optimisation, murine samples were spiked with standard solutions of LMs and then compared to unspiked samples, to obtain the recovery estimates.

Compound	MRM (*m/z*)	Collision energy (eV)
9-HODE	295 → 171	25
13-HODE	295 → 195	25
5-HEPE	317 → 115	20
18-HEPE	317 → 133	25
9-HEPE	317 → 149	20
8-HEPE	317 → 155	18
15-HEPE	317 → 175	18
12-HEPE	317 → 179	20
5-HETE	319 → 115	20
9-HETE	319 → 123	20
8-HETE	319 → 155	20
11-HETE	319 → 167	20
15-HETE	319 → 175	18
12-HETE	319 → 179	20
12-HETE-*d*8	328 → 185	17
LTB_4	335 → 195	17
17*S*-HDHA	343 → 281	15
RvE1	349 → 195	17
PD1	359 → 206	15
RvD1	375 → 141	15

Figure 12. MRM transitions and collision energies for precursor-product ion pairs of SPMs and oxygenated PUFAs (28)

For chromatographic separation, a C18 column was used. Different retention times and different precursor-product ion pairs allowed for several compounds to be distinguished (Fig. 13). In case of co-eluting compounds, like 8-HETE and 12-HETE, their specific product ions (*m/z* 319 > 155 for 8-HETE and *m/z* 319 > 179 for 12-HETE) allowed for simultaneous analysis. Conversely, 9-HEPE (*m/z* 317 > 179) shared a product ion with a number of other HEPEs (though at lower abundance), like 5-, 8-, 12-, 15- and 18-HEPE, which could lead to a cross-reactivity. However, these compounds were well separated chromatographically, so there was no problem of interference. (28) These two examples clearly show how the use of MRM improves sensitivity of the analysis compared to other conventional methods. The method proved to be sensitive, with detection limit of 10-20 pg and quantitation limit of 20-50 pg for different LMs. (28)

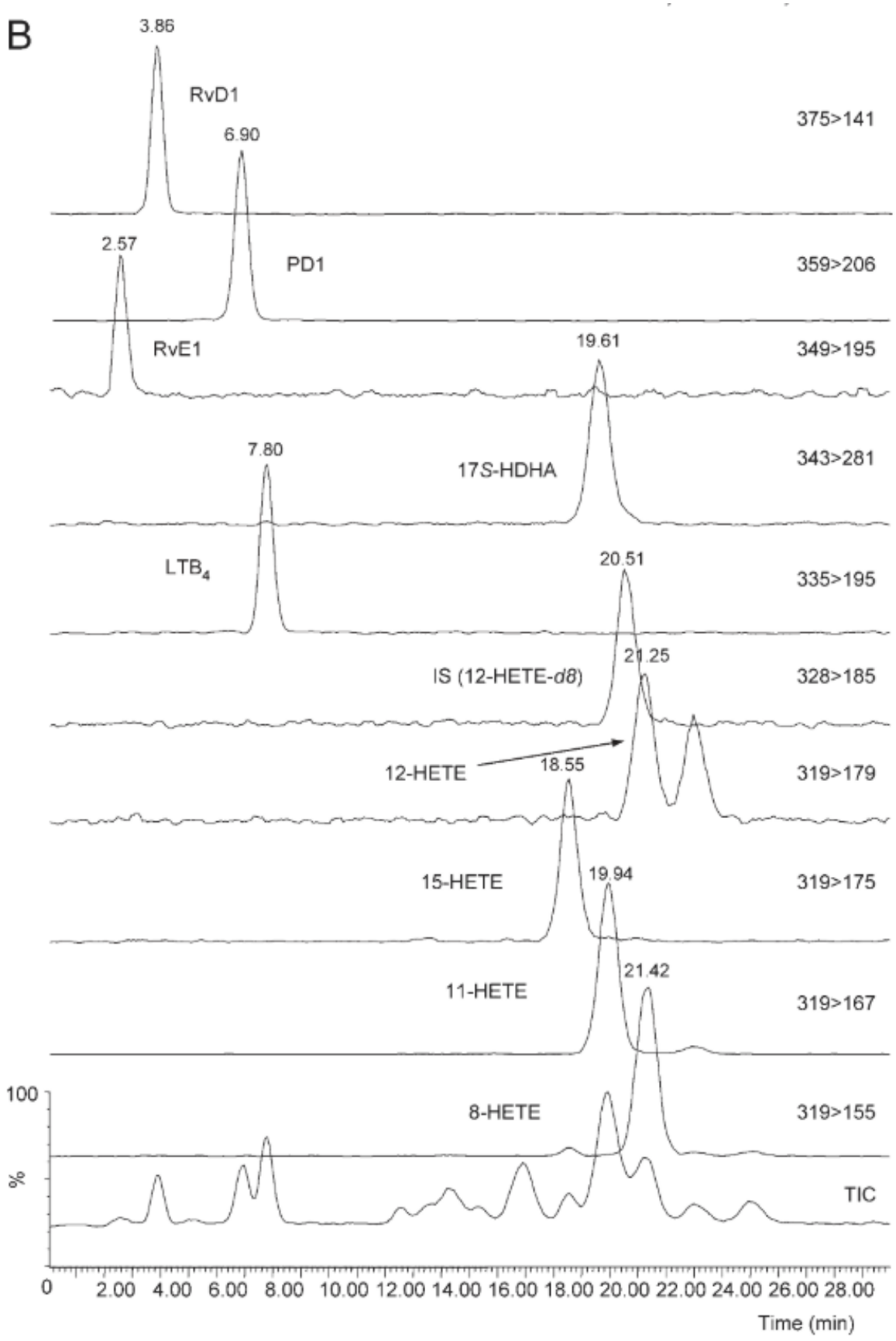

Figure 13. Chromatograms showing the LC/ESI-MS/MS analysis of some of the twenty hydroxy-fatty acids, leukotrienes, resolvins and protectins analysed in the same run. Adapted from reference (28)

In their more recent works, Serhan and co-workers reported that up to 52 LMs could be analysed in a single LC- MS/MS run using MRM method. (23) Typically, C18 chromatographic column is used, and instrument is run in negative ionisation mode. (23) If there are unmatched (unidentified) LMs with potent bioactivity, isotope trapping and chiral LC- MS/MS are used in order to determine pathways of biosynthesis. Fig. 9 depicts simultaneous LC-UV-MS/MS analysis of 12 authentic and synthetic SPMs and LMs in a single run. Online UV spectra and MS/MS spectra are shown for RvD1 and RvE1 as examples. Characteristic fragmentation of the molecule is shown for both SPMs – and there can also be seen fragments chosen for product ions in precursor-product ion pairs used for MRM analysis.

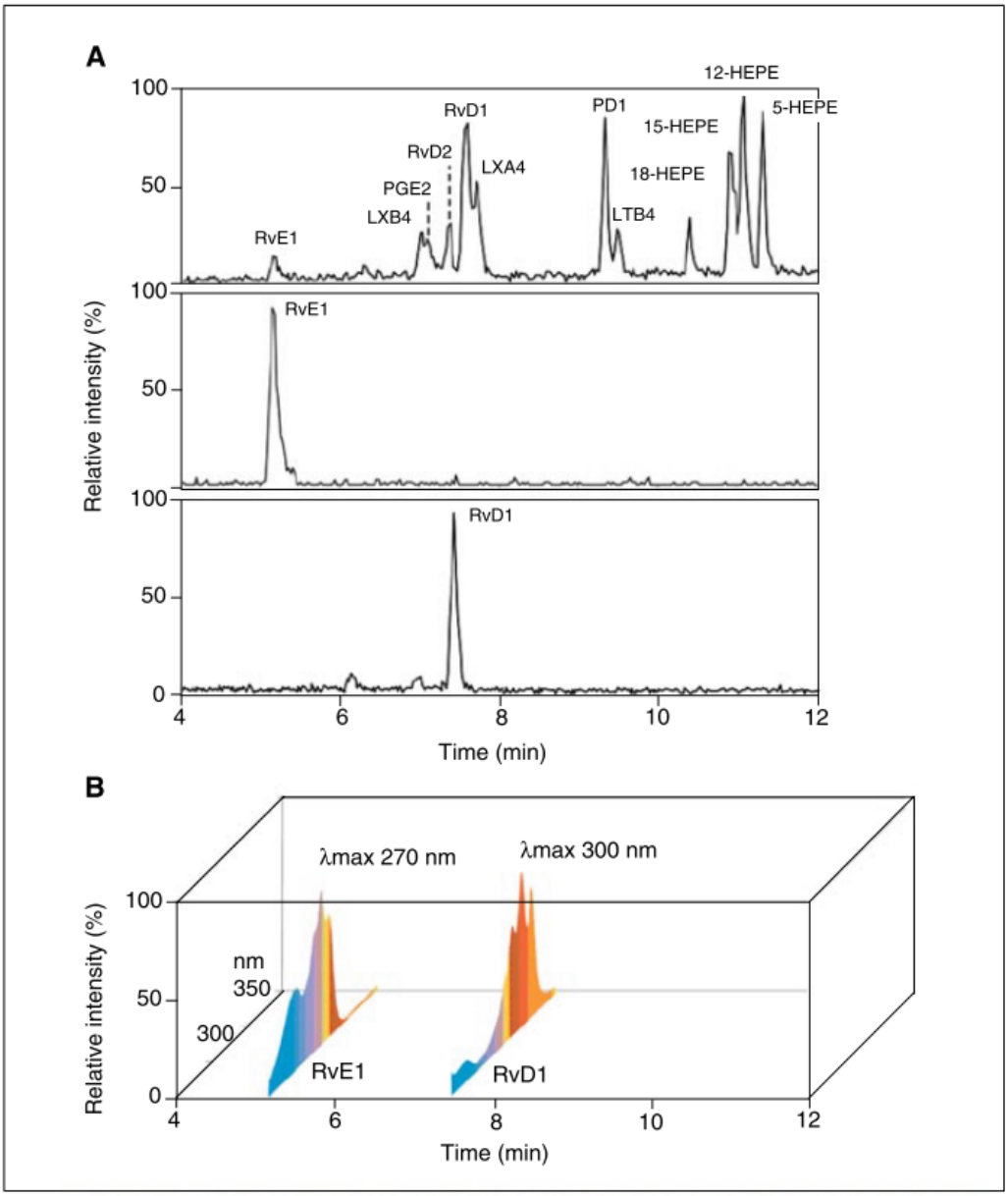

Figure 14. LC-UV-MS/MS lipidomics of 12 LMs. (A) Total ion chromatogram of 12 LMs; Chromatogram for precursor-product ion pairs *m/z* 349 > 195 (for RvE1) and *m/z* 375 > 141 for RvD1. (B) Online UV spectra of RvE1 and RvD1. Adapted from reference (23)

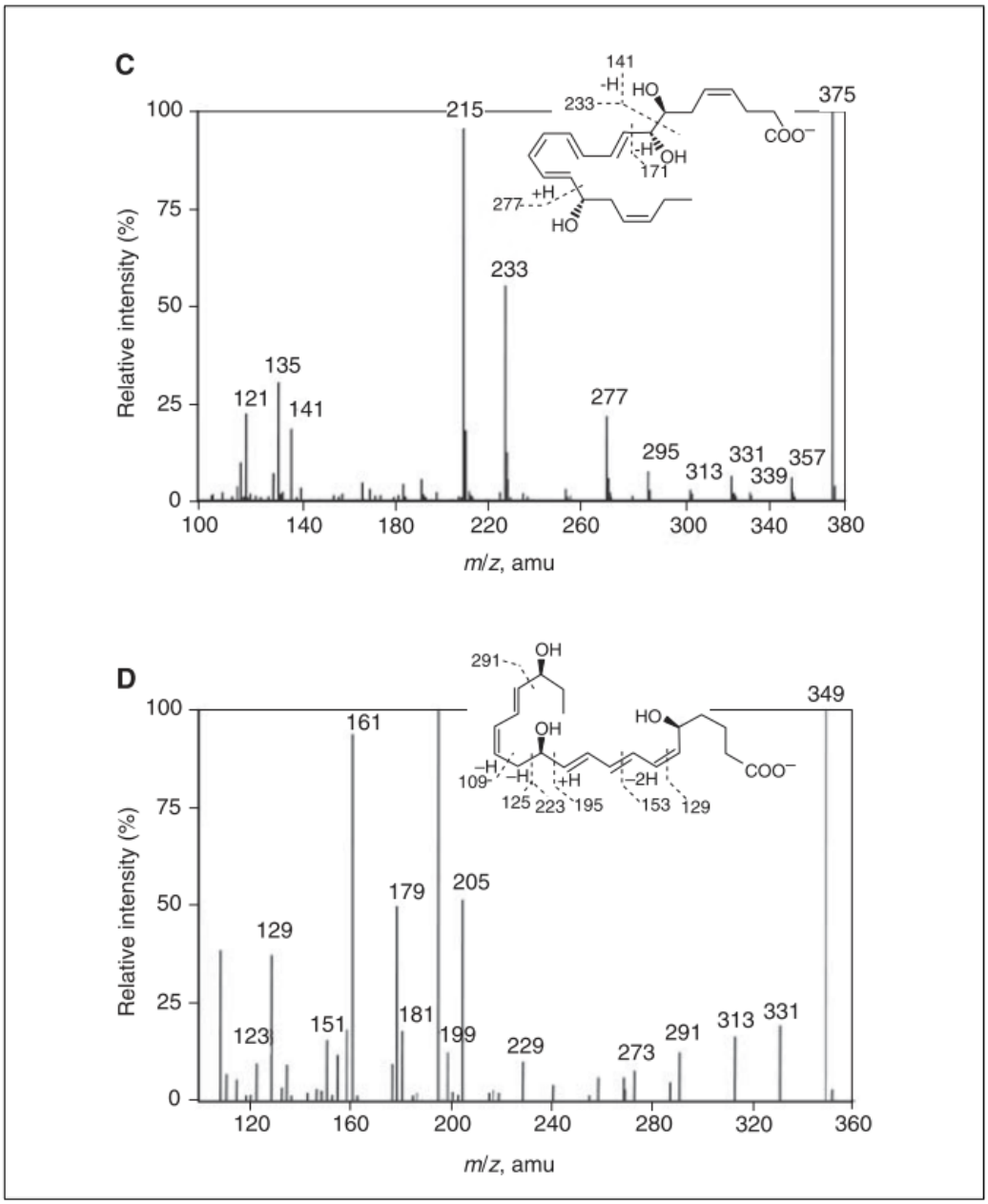

Figure 14. (continued): (C) MS/MS spectrum of RvD1. (D) MS/MS spectrum of RvE1. Adapted from reference (23)

Serhan and co-workers discovered maresin 1 (MaR1) in 2009. They used the zymosan A-induced peritonitis model as a self-resolving system to look for 17-HDHA as a marker of endogenous DHA conversion, but also to check for other possible pathways. Using the LC-MS/MS based targeted mediator lipidomics, they found 17*S*-HDHA as expected, and in addition 14*S*-HDHA, which accumulated with time during the resolution phase in 72 h course (Fig. 15). These two hydroxy-PUFAs were identified by characteristic diagnostic ions in their mass spectra. Here, MRM technique was used

again, to simultaneously measure the levels of 14*S*-HDHA and 17*S*-HDHA at different time points in the course of 72 h (Fig. 15).

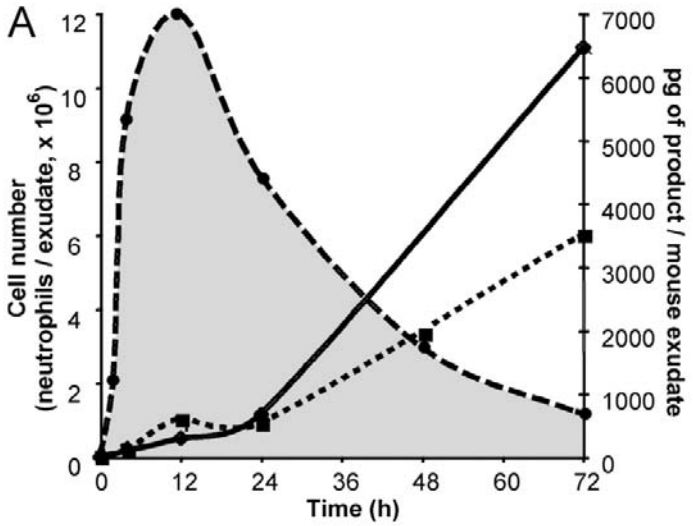

Figure 15. Zymosan-induced peritonitis: PMN accumulation and decline during 72 h (dashed line); 17*S*-HDHA (dotted line) and 14*S*-HDHA (continuous line) values obtained by using MRM. Adapted from reference (42)

As these authors had the experience with 17*S*-HDHA as a marker of biosynthetic pathways for D-series resolvins and protectins, they wanted to check whether 14*S*-HDHA was a precursor of novel bioactive molecules, too. In order to determine that, 14*S*-H*p*DHA (produced via biogenic synthesis) and DHA were individually incubated with resident peritoneal macrophages. LC-MS/MS mediator lipidomics of the incubate showed two 7,14-dihydroxy products. They had different retention times, but their mass spectra were basically the same (Fig. 17). This indicated that they could be isomers. To investigate whether this was the case, the material that gave two peaks on the chromatogram needed to be isolated. Further confirmation of a novel structure was carried out using GC-MS. Isotope incorporation experiments with $H_2{}^{18}O$ showed that the hydroxyl-group at C7 was derived from water, and not molecular O_2 as it tends to be when hydroxyl-group is enzymatically derived. To confirm that novel products are derived from DHA in presence of macrophages, deuterium (d_5)-labeled DHA (with 5 deuterium atoms at C21 and C22) was incubated with mouse macrophages. Dihydroxy products found in the incubate proved to carry d_5, too, and identification was confirmed by characteristic ions on mass spectra. (42)

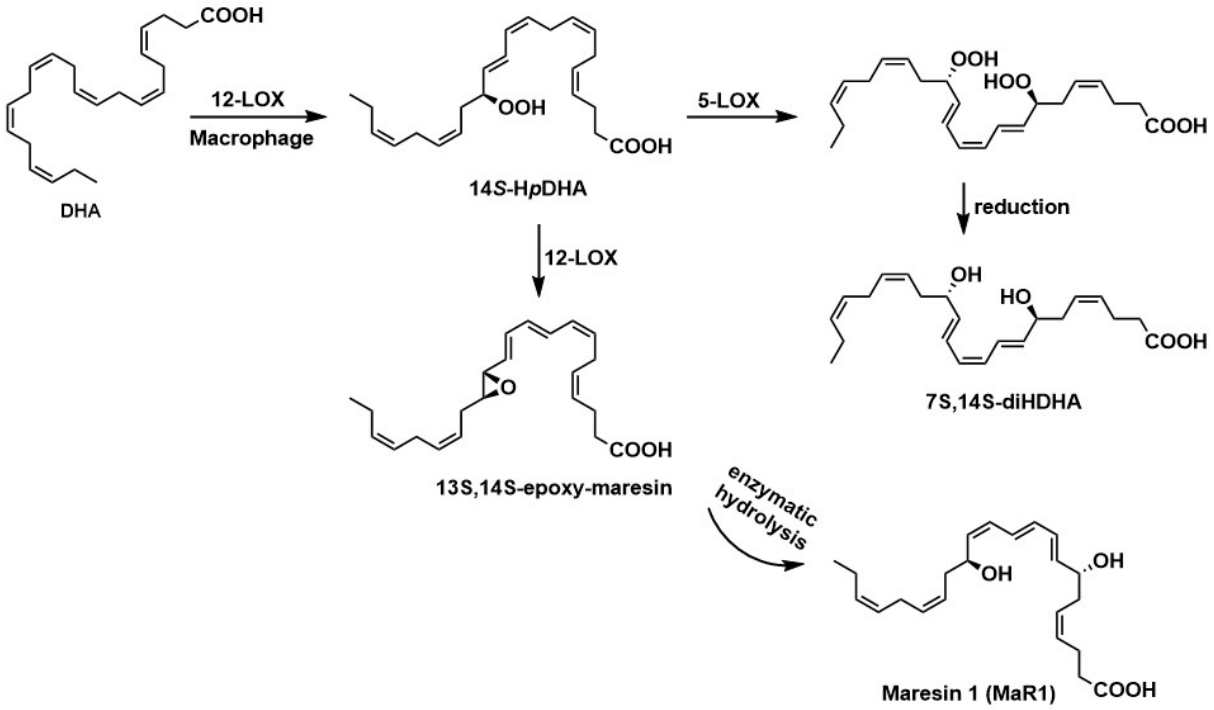

Figure 16. Biosynthesis of MaR1 and double dioxygenation product 7*S*,14*S*-diHDHA (42)

To monitor two 7,14-diHDHA isomers, LC-MS/MS was run in the negative ionization mode, and with EPI (enhanced product ion). For identification, precursor/product ion par 359.2/250.2 was used. Quantification was carried out using calibration curves. Deuterated internal standards 17-HDHA-d_5 and PGE_2-d_4 were used to monitor the recovery.

Of the two isomers, the one later termed MaR1 showed to have pro-resolving actions comparable to those of protectins and resolvins, while 7*S*,14*S*-dioxygenation isomer proved to be less potent. (42)

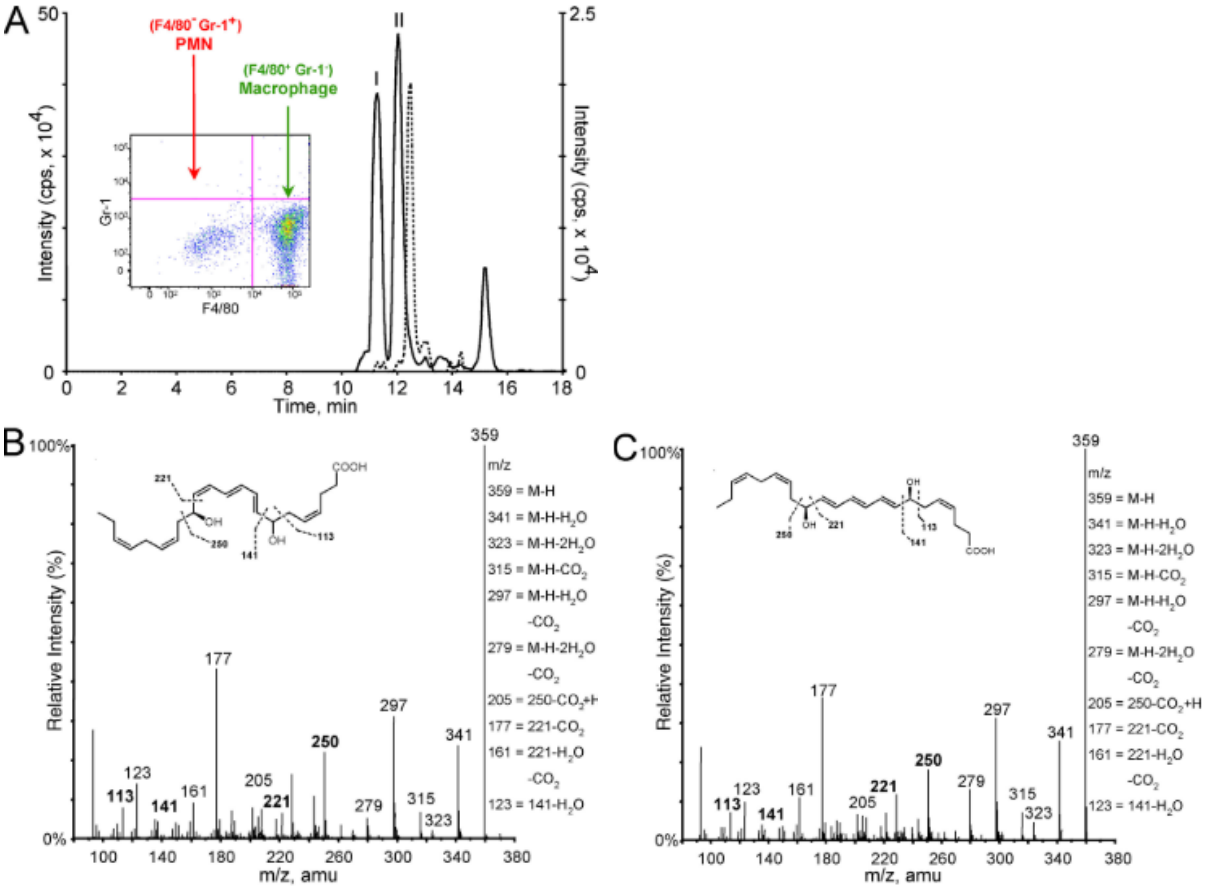

Figure 17. (A) targeted LC-MS/MS mediator lipidomics of incubate of mouse-resident macrophages with DHA or 14*S*-H*p*DHA. Selected ion chromatogram (*m/z* 359/250) of MaR1 and its 7*S*,14*S*-isomer. (B) and (C) mass spectra of MaR1 and its 7*S*,14*S*-isomer. Adapted from reference (42)

The examples given above illustrate the use of LC-MS/MS metabololipidomics in the discovery and identification of SPMs.

LC-MS/MS metabololipidomic methods are also used to measure the capacity of different cells to produce SPMs. SPMs are often produced as a result of cell-cell interaction. These interactions can be simulated *in vitro*, in order to determine transcellular pathways for SPMs. (23) Cells can be stimulated by a range of agonists, like phagocytic (zymosan, urate crystals, apoptotic PMNs) and soluble (thrombin, calcium ionophores) agonists. The most important are agonists who react over cellular receptors.

Two different cell types can be co-incubated, in order to determine whether their interaction during incubation (and stimulation by agonist specific for each cell type) gives rise to new pathways for new products. In order to do this, it is important to first analyse SPMs production of individual cell types before and after specific stimuli, as well as SPMs production of co-incubated cells exposed to the agonist to just one of the

cells. Indeed, it was shown that, when co-incubating neutrophils with platelets, in presence of both thrombin (platelet agonist) and fMLP (formyl-methionyl-leucyl-phenylalanine, neutrophil agonist), novel products occurred in addition to cell-specific products. (23)

Even though LC-MS/MS is the most powerful method for the LM identification, it should be underlined that the absolute configuration of novel LMs cannot be distinguished by this method alone. In order to determine the absolute configuration of novel putative SPMs, candidate structures need to be synthesized. Endogenous compound is then compared to candidate synthetic structures. It is important to match both their physical properties and their bioactivities, in order to unambiguously identify a new structure. (23)

LC-MS/MS chiral analysis alone (without synthetic compounds for comparison) does have important applications in SPMs analysis. It can help distinguish whether an oxygenated metabolome is a product of auto-oxidation or enzymatic oxidation. PUFAs are particularly prone of auto-oxidation, and as a result, a racemic mixture of oxygenated products is formed. In contrast, when enzymatically oxidised, PUFAs tend to give products that have predominant isomeric ratios – for example, 14-HDHA, an intermediate in production of maresin 1 from DHA, was shown to be in 98% *S*-configuration. *R*- and *S*- isomer gave 2 peaks on chromatogram, where peak area of the *S*-isomer was much bigger than peak area of R-isomer. Retention time (RT) of the *S*-isomer was confirmed by using synthetic compound (Fig. 18). For this purpose, chiral reverse-phase columns are used for chromatographic separation. (23)

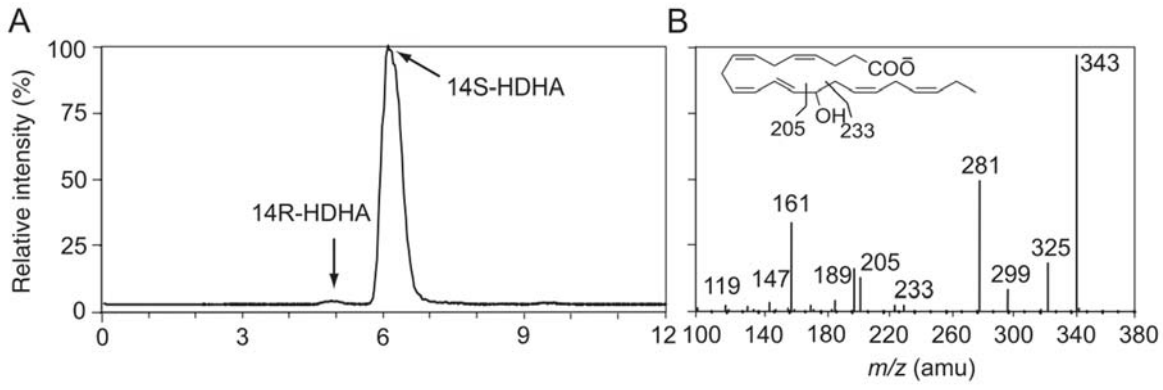

Figure 18. (A) LC-UV-MS/MS-based analysis of 14-HDHA using chiral stationary phase columns after incubation of DHA with porcine 12-LOX. (B) MS/MS spectrum of 14-HDHA. Adapted from reference (23)

2.4 The metabololipidomics era – challenges

As the example of maresin MaR1 shows, biosynthetic pathways during which SPMs are produced often lead to the by-production of molecules with similar chromatographic behaviour and similar MS spectra and, thus, can be difficult to distinguish from SPMs with potent activity by using LC-MS/MS mediator lipidomics approach only. This is not surprising, since SPMs discovered so far contain conjugated triene or tetraene moiety in their structure, as well as two or three secondary alcohols. This gives the possibility of a range of *S/R* and *cis/trans* isomers.

In their work from 2016, Hansen, Dalli and Serhan (35) elaborated a new approach for easier identification of SPMs in the presence of double di-oxygenation isomers of SPMs – by chemical derivatization. Namely, most of the SPMs found have *E,E,Z* or *E,E,Z,E* moiety in their structure. In parallel, their double di-oxygenation isomers have *E,Z,E* moiety (Fig. 19). This difference gave the idea to the authors of using a reactive Diels-Alder reagent (dienophile) as a derivatization agent, since *E,E* conjugated double bonds give the Diels-Alder reaction much more promptly and under milder reaction conditions than *E,Z* conjugated double bonds. Only dienes that adopt the s-*cis* conformation can participate in the Diels-Alder reaction. (35)

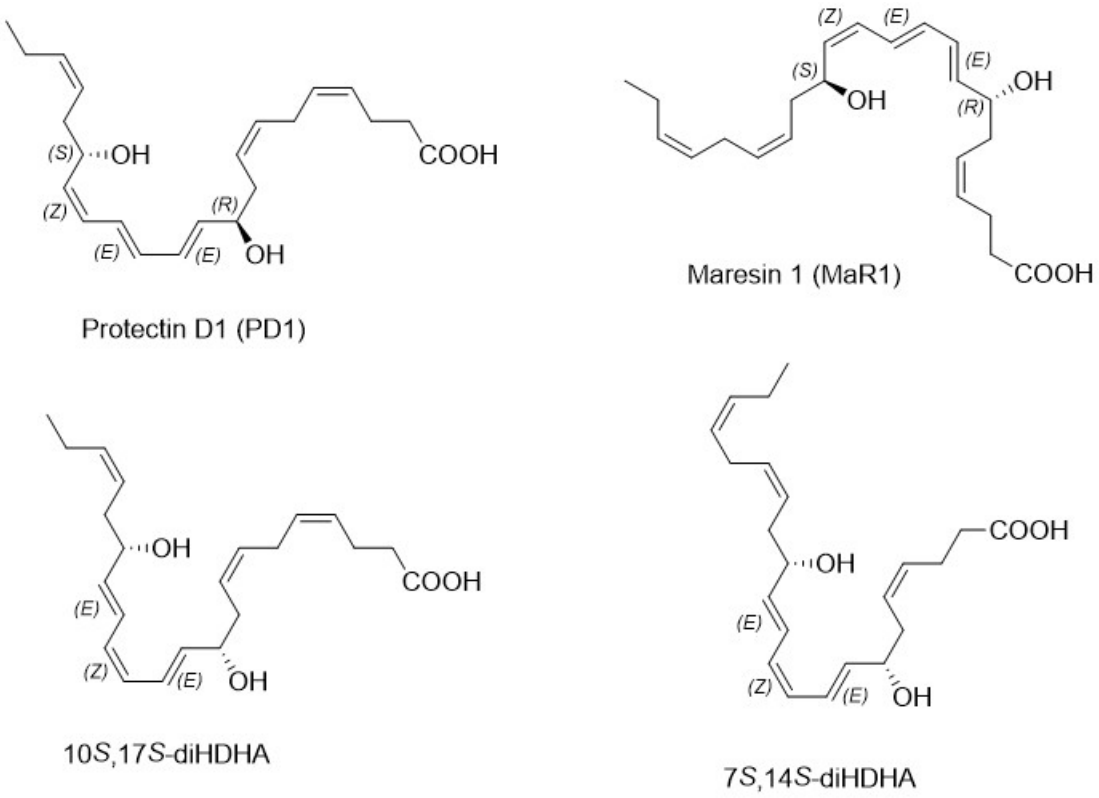

Figure 19. PD1, MaR1 and their double di-oxygenation isomers

It was important to find a reactive dienophile, and at the same time not use too harsh conditions, since SPMs are sensitive compounds. The dienophile 4-phenyl-1,2,4-triazole-3,5-dione (PTAD), which was commercially available, proved to be a good choice.

Fig. 20 depicts the reaction between PTAD and SPMs with the *E,E*- conjugated diene moiety.

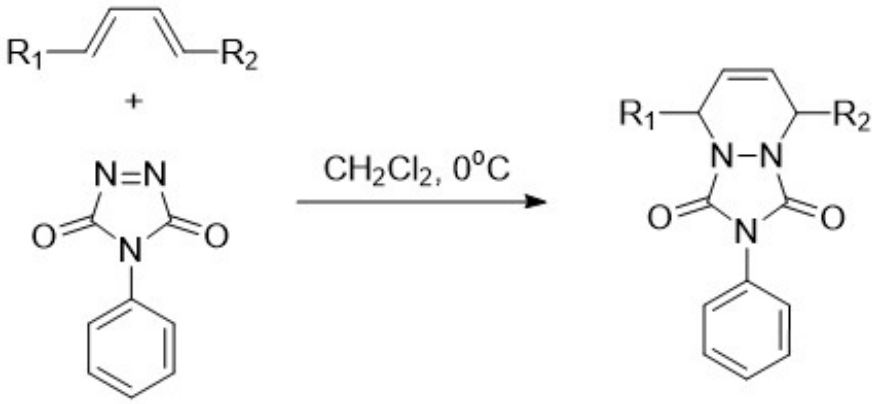

Figure 20. The Diels-Alder reaction between PTAD and a 1,4-disubstituted diene

It was already known that PTAD adducts give MS spectra that are relatively simple and easy to interpret. They are characterised by abundant molecular ions, as well as fragment ions where fragmentation happens in the alpha position to nitrogen. Hence, these fragment ions give information about the position of the conjugated diene. (43) PTAD has been successfully used for the derivatisation of unsaturated fatty acids prior to analysis of positional isomers. It is hard to obtain reliable mass spectra of underivatised fatty acids because their double bonds can migrate during MS analysis, but with PTAD this problem was overcome. (44) PTAD has also been used as derivatisation agent to improve the sensitivity of the assay for vitamin D metabolites, 1,25-dihydroxyvitamin D_2 and 1,25-dihydroxyvitamin D_3. (45)

To develop the method for *in vivo* samples, Hansen et al inoculated *E. coli* in the mouse peritoneum. Exudates were collected after 12 h and analysed using LC-MS/MS metabololipidomics. Chromatograms obtained showed that signals from MaR1 and its double di-oxygenation isomer, as well as PD1 and its double di-oxygenation isomer, are so close that it was difficult to distinguish between two peaks (Fig. 21). That is why a method improvement was needed in the first place.

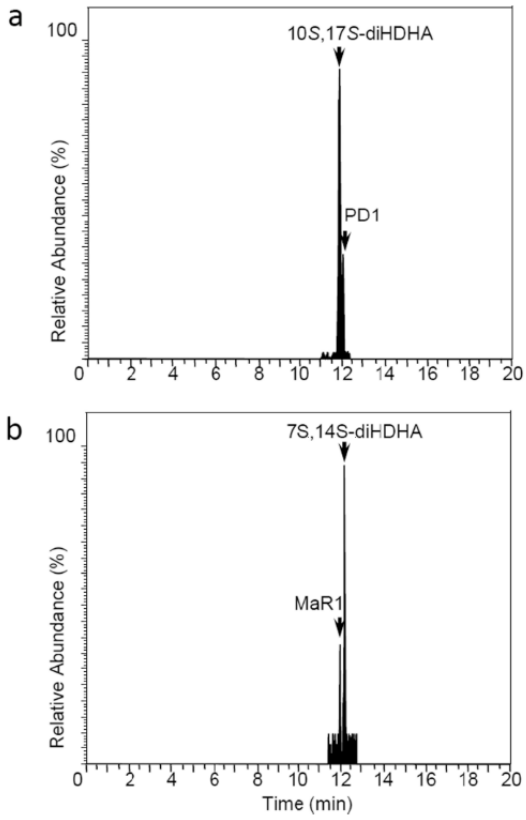

Figure 21. MRM chromatograms of mouse peritoneal exudates after inoculation of *E. coli*. (a) PD1 and its double di-oxygenation isomer, *m/z* 359->153; (b) MaR1 and 7S,14S-diHDHA, *m/z* 359->250. Adapted from reference (35)

In order to develop a method with PTAD derivatisation, synthetic material of PD1 and $PD1_{n\text{-}3\ DPA}$ was used in separate experiments. Compounds were reacted with PTAD in CH_2Cl_2 at 0°C and analysed using LC-MS/MS metabololipidomics. MS spectra showed characteristic ions for the PD1-PTAD reaction product: *m/z* = 516 $[M\text{-}H^+\text{-}H_2O]-$, *m/z* = 498 $[M\text{-}H^+\text{-}2H_2O]-$ and *m/z* = 490 $[M\text{-}H^+\text{-}CO_2]-$, with signature ions *m/z* = 397, *m/z* = 371 $[M\text{-}H^+\text{-}CO_2PhCNO]-$ and *m/z* = 352 (Fig. 22). Corresponding fragmentation ions were found for the $PD1_{n\text{-}3\ DPA}$-PTAD reaction product, but no PTAD products were found for 7*S*,14*S*-diHDHA and 10*S*,17*S*-diHDHA, in line with the authors' expectations. (35)

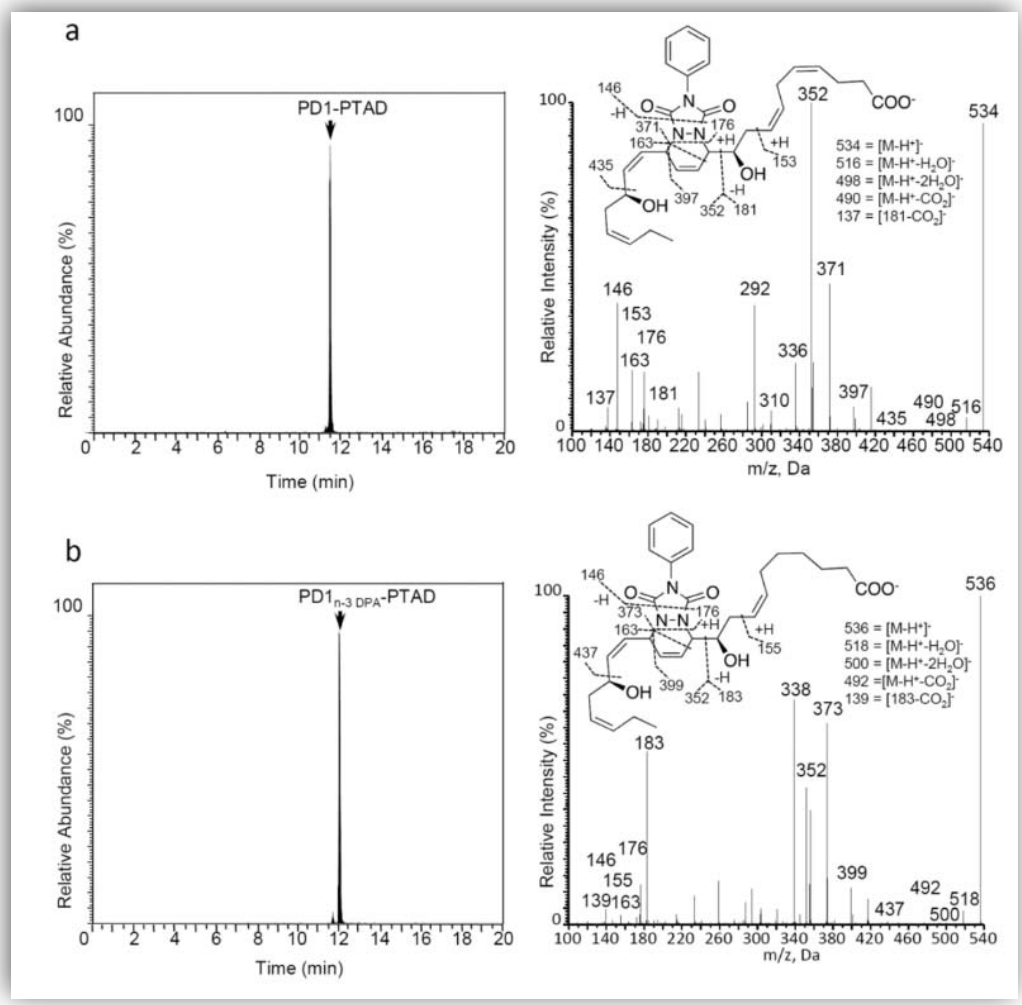

Figure 22. LC-MS/MS chromatogram (left) and MS spectra (right) of the Diels-Alder reaction products between PTAD and PD1 (a) and PTAD and PD1 $_{n\text{-}3\ DPA}$. Adapted from reference (35)

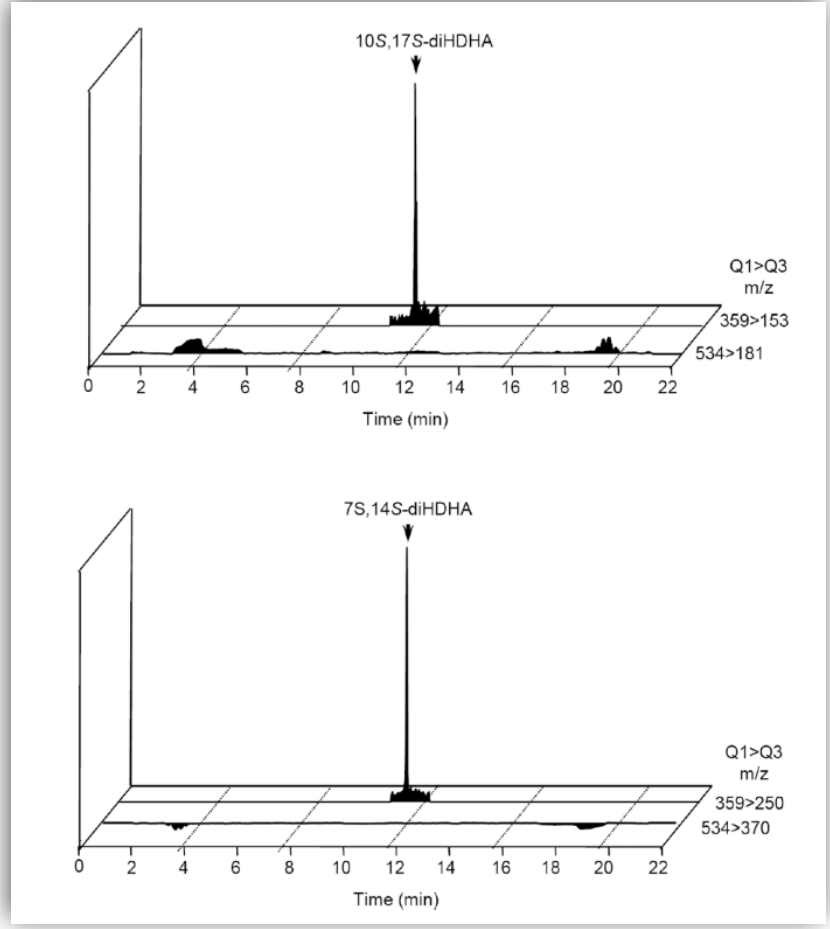

Figure 23. LC-MS/MS metabololipidomics of the reaction mixture of PTAD with 10*S*,17*S*-diHDHA (top) and PTAD with 7*S*,14*S*-diHDHA (bottom), showing that there was no reaction product. Adapted from reference (35)

This method was confirmed using *in vivo* samples, as well as with a range of different SPMs. In conclusion, this is a fast and convenient approach to distinguish SPMs from their double di-oxygenation isomers, given that these SPMs have conjugated double bonds with the *E,E* conformation and that the isomers of these SPMs lack the *E,E* moiety.

2.5 Potential novel SPMs and challenges in their analysis

Driven by the success of Serhan and his team, scientific teams from around the world continue to explore pro-resolving lipid mediators. In their work from 2016, Kuda and his collaborators in Prague described novel molecules with pro-resolving properties produced in white adipose tissue. (38) These molecules are esters of fatty acids and hydroxy fatty acids. According to FAHFA nomenclature, where FA stands for fatty acid, HFA for hydroxy fatty acid and a number for the position of hydroxyl-group, these new molecules were termed 13-DHAHLA, 9-DHAHLA and 14-DHAHDHA.

To discover whether adipose tissue has the ability to produce SPMs, Kuda et al used serum and white adipose tissue samples of murine and human origin. In both cases, half of the group was supplemented with ω-3 PUFAs, and the other half was not. (38)

Samples were purified using SPE with 5-PAHSA-$^{2}H_{31}$ and 9-PAHSA-$^{13}C_{4}$ (PAHSA = palmitic acid ester of hydroxystearic acid) as internal standards. After that, a highly advanced metabololipidomics approach was used, where both quantitative and qualitative analysis could be performed in a single run, thanks to the possibility of switching from the triple-quadrupole scan mode to full-scan ion trap mode. The principle of analysis is shown on (Fig. 24) on the example of 9-PAHSA. For quantification, MRM analyses were performed using one quantifier and two qualifier ions per FAHFA. Quantifier ions were fatty acid fragments, while qualifier ions were hydroxy fatty acid derived, with or without water loss. Further fragmentation of hydroxy fatty acid fragment gave characteristic fragments that could be used for identification, since they gave information about the position of the alcohol group. (38)

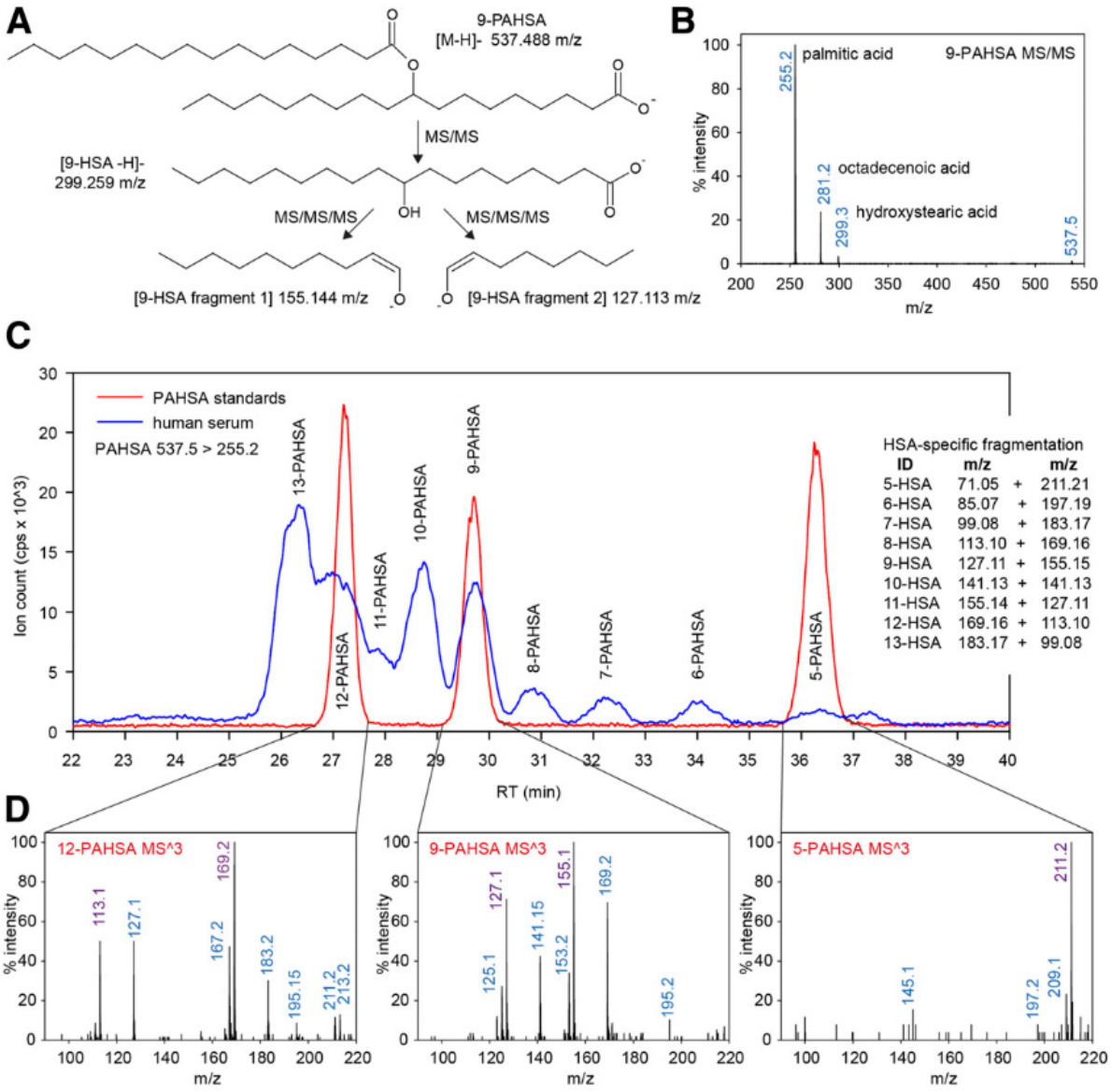

Figure 24. Analysis of PAHSA isomers. A: 9-PAHSA gives specific 9-HSA fragments. B: MS/MS spectrum of 9-PAHSA and three major fragments. C: Chromatographic profile of PAHSA isomers (MRM 537.5 > 255.2) in human serum (blue) and synthetic standards (red). The inserted table shows MS/MS/MS fragments (three stages of fragmentation) characteristic for different positional isomers of hydroxy group on HAS. C and D: Combination of triple-quadrupole scan mode and highly sensitive full-scan ion trap mode within one analysis – specific fragments of HSA highlighted in magenta. Adapted from reference (38)

Nine positional isomers of PAHSA were found in human samples. Supplementation with ω-3 PUFAs did not change the serum levels of PAHSA, but it proved to increase the levels of DHA-derived esters. The same approach explained for PAHSA was used to identify and quantify DHA-derived esters. As shown on (Fig. 25), 13-DHAHLA gives characteristic fragments of 13-HLA through two steps of fragmentation. These fragments can be used for qualitative analysis, whereas 13-DHAHLA and DHA ions (605,4 > 327.2) are used as precursor-product ion pair for quantitative analysis with

MRM approach. The levels of DHAHLA and DHAHDHA found were in the same range as the levels of SPMs (picomolar to nanomolar concentrations). (38)

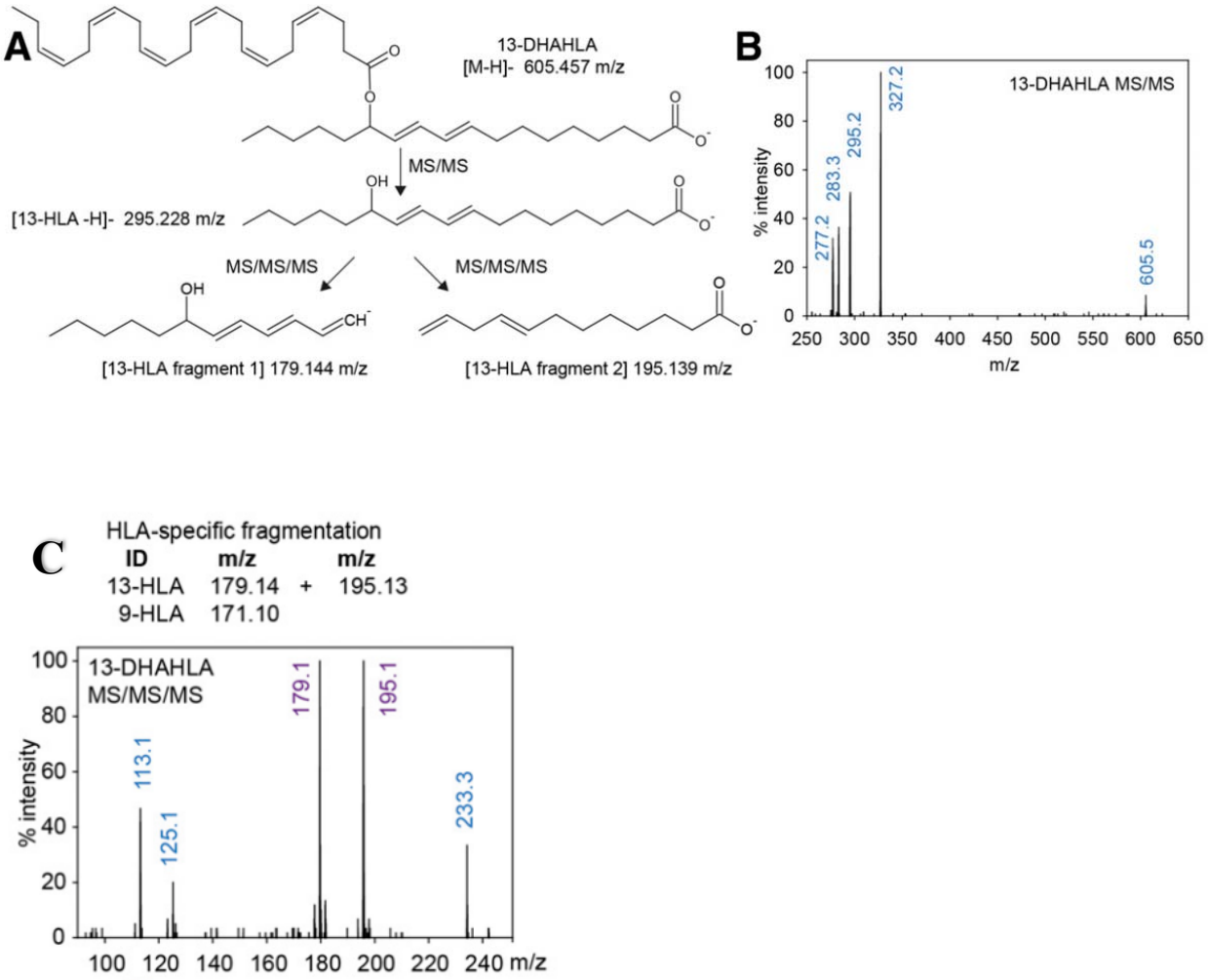

Figure 25. Analysis of DHAHLA isomers. A: Fragmentation of 13-DHAHLA and 13-HLA specific fragments. B: MS/MS spectrum of 13-DHAHLA. C: MS/MS/MS spectrum of 13-DHAHLA with specific fragments in magenta. Adapted from reference (38)

Kuda and co-workers showed using *in vitro* experiments that 13-DHAHLA has anti-inflammatory and pro-resolving properties, at least *in vitro* – it reduced activation of macrophages by LPS and stimulated phagocytosis of zymosan A particles. (38) However, they pointed out that in order to perform further analysis of *in vivo* actions of 13-DHAHLA and related molecules, as well as further structural elucidation, higher amounts of 13-DHAHLA needed to be synthesized by total organic synthesis. (38) To meet all these needs, collaboration between the Prague group and the LIPCHEM group in Oslo was started. Associate professor Anders Vik has prepared both the *R*- and *S*- stereoisomer of 13-DHAHLA:

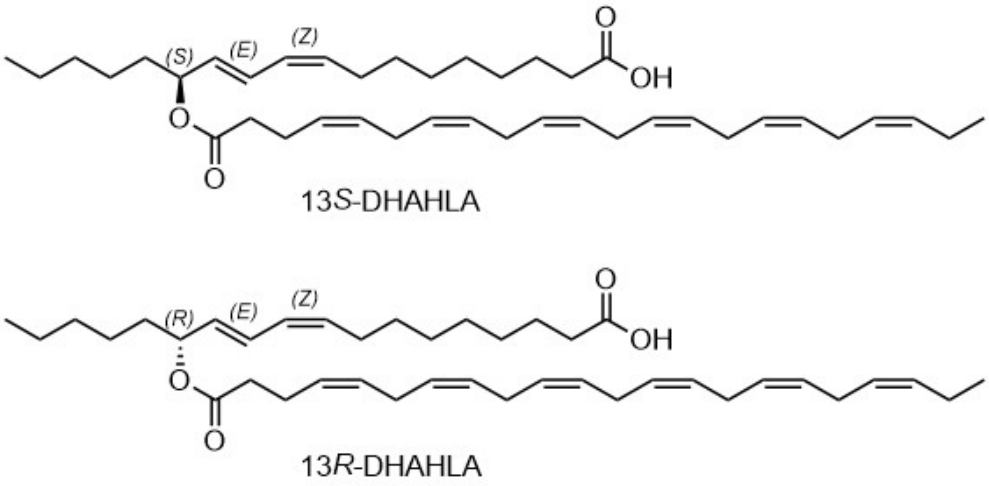

Figure 26. Structures of 13*S*-DHAHLA and 13*R*-DHAHLA

The exact structural elucidation of *in vivo* produced 13-DHAHLA proved to be a challenge, since chromatographic separations of the two isomers failed, even with long HPLC columns with chiral stationary phases using different eluent combinations. Consequently, it was hard to distinguish between these two isomers and develop a good identification method. That is why a derivatisation with PTAD was tried in this case, as well.[2] As mentioned before, SPMs with *E,E* moiety give the Diels-Alder reaction much more readily than their *E,Z*-isomers. However, *E,Z* isomers do react with dienophiles when they are given enough time and energy (higher reaction temperature). Kuda and co-workers attempted to induce reaction of *R*- and *S*- isomers of 13-DHAHLA with PTAD. After a prolonged reaction at room temperature using an excess amount of PTAD, two signals for each isomer of the Diels-Alder adduct were

[2] Information obtained from personal communication between dr Ondrej Kuda and professor Trond Vidar Hansen

observed on HPLC chromatogram. When co-injected, separation of signals was not complete (Fig. 27).

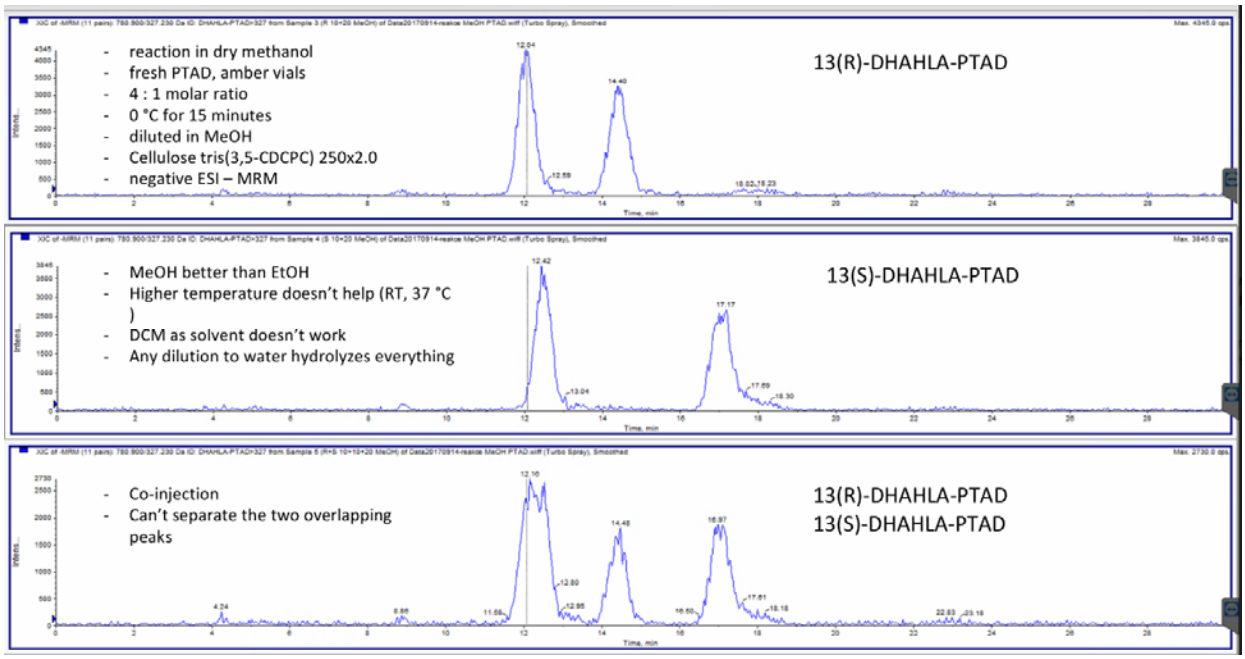

Figure 27. Chromatographic separation of 13R-DHAHLA and 13S-DHAHLA reaction products with PTAD[3]

Of note, in accordance with the reaction mechanism of the Diels-Alder reaction, two isomers of both the *R*- and *S*-stereoisomers of 13-DHAHLA are expected. (46) The two peaks observed on chromatograms for each isomer of 13-HDHA after reaction with PTAD are the peaks of the racemic mixture of the two Diels-Alder adducts formed. This is depicted in Fig. 28.

[3] Figure obtained from professor T. V. Hansen's personal correspondence

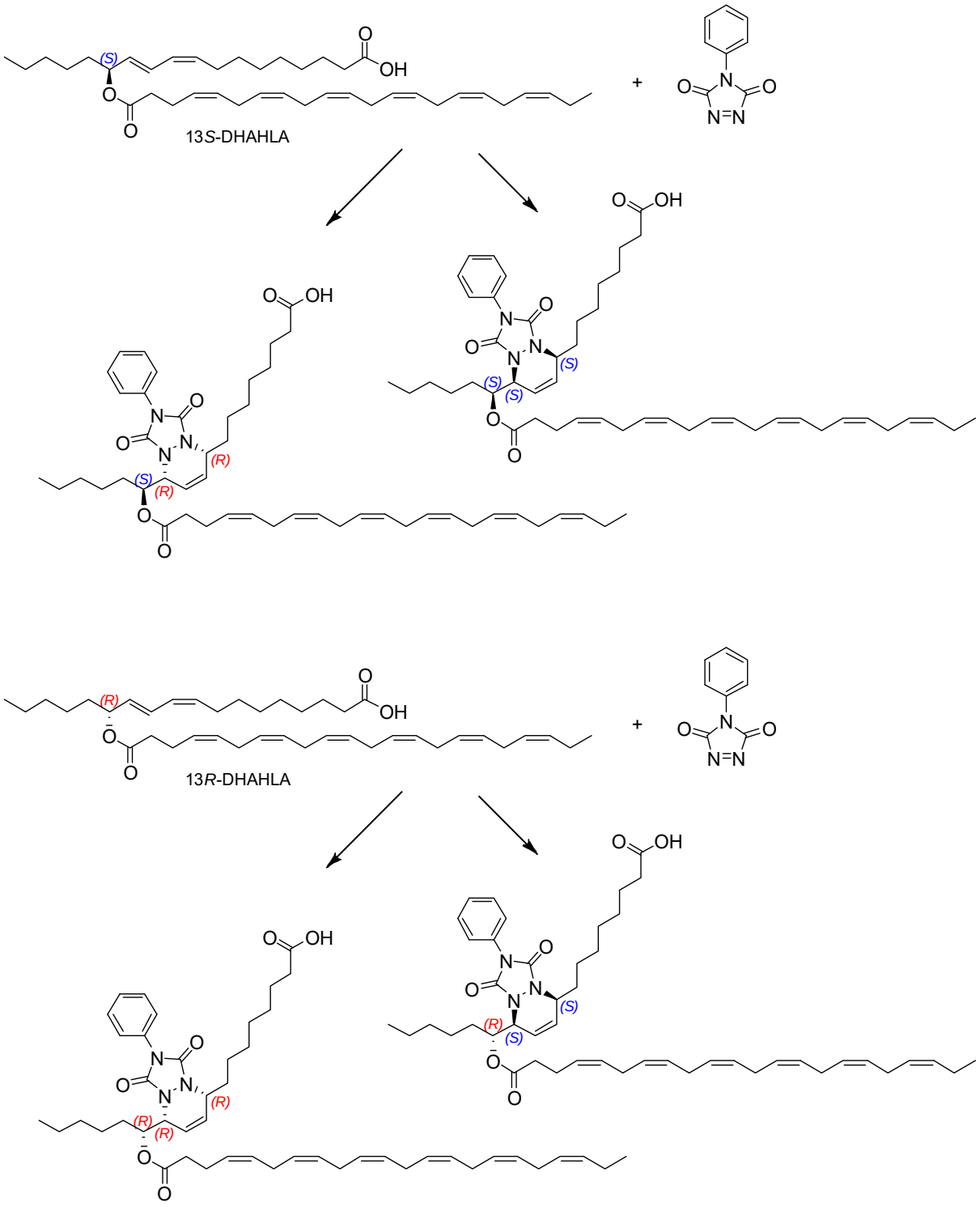

Figure 28. Diels-Alder reaction between *R*- and *S*- isomers of 13-DHAHLA and PTAD - two possible outcomes for each isomer

Part 2. Initial Efforts Towards New Methodology

As previously described, PTAD derivatisation of 13-DHAHLA isomers did not lead to the satisfactory chromatographic separation. Both *R*- and *S*- stereoisomers gave two reaction products when reacted with PTAD. As a result, chromatograms of both isomers using a chiral chromatographic column gave two peaks, but they could not be completely separated when co-injected, since two of the four peaks had a very close retention times, and could not be separated well even with long chromatographic column with chiral stationary phase.

This gave the idea to T. V. Hansen and the LIPCHEM group in Oslo to try the derivatisation of 13-DHAHLA isomers with a dienophile that has a stereogenic centre. This was the main objective of this master thesis – to attempt to find the optimal conditions for the chosen dienophiles to react with LMs with the *E,Z*- moiety, and hence, with isomers of 13-DHAHLA, and after that, develop a protocol for LC-MS/MS analysis.

Dienophiles chosen as putative derivatization agents for our experiments were commercially available (*R*)- and (*S*)-*N*-(1-phenylethyl)maleimide. These molecules have one stereogenic center. The idea was to introduce a new stereogenic centre in the reaction product, in order to possibly make the separation and analysis easier. We started our experiments with (*S*)-*N*-(1-phenylethyl)maleimide (*S*-PEM).

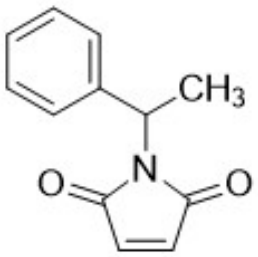

Figure 29. Structure of *N*-(1-phenylethyl)maleimide (PEM)

Outline of the putative Diels-Alder reaction between *S*-PEM and an *E,Z*-conjugated diene is shown on (Fig. 30). As depicted here, reaction products have five stereogenic centers. The absolute configuration on C1 and C4 of the diene in the reaction product is defined by the general rules of the Diels-Alder reaction, where the “inside groups” of the s-*cis* conformation of the diene are on the same side of the new formed six-membered ring in the reaction product (and on the other side are the “outside groups” of the s-*cis* conformation). (46) That is why in the case of an *E,Z*-conjugated diene the

remainders of hydrocarbon chain are on the opposite sides of the six-membered ring. In theory, four possible reaction products occur.

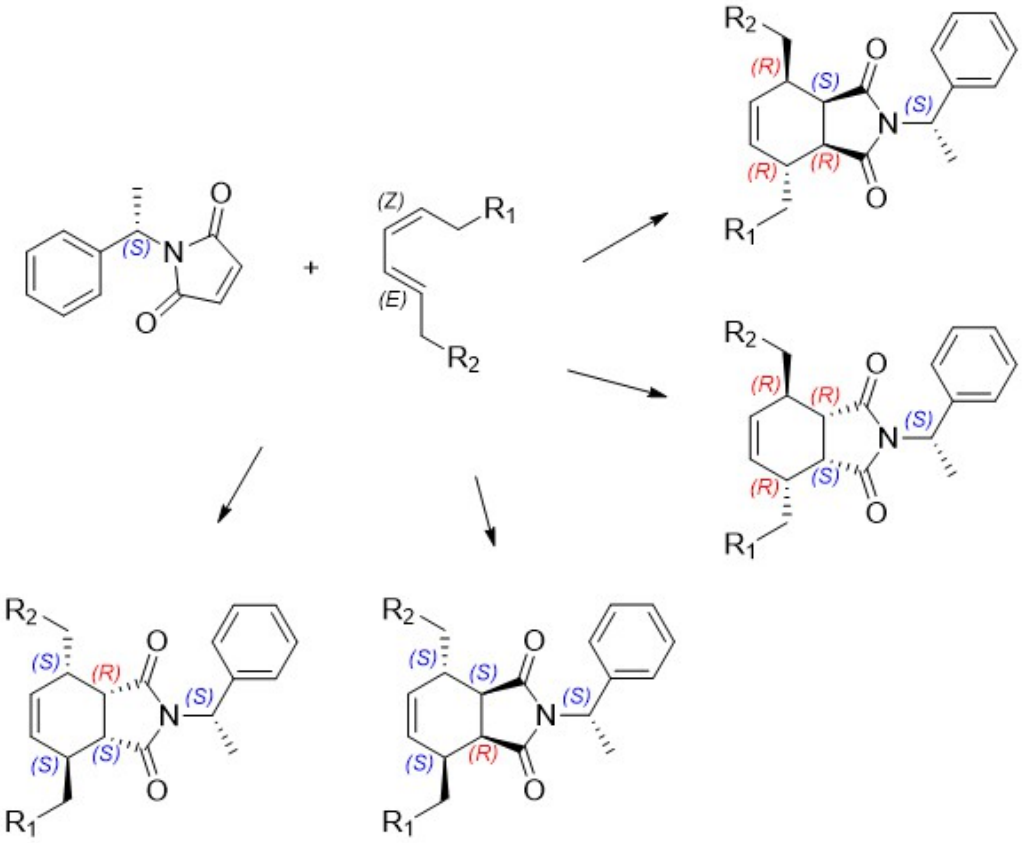

Figure 30. Diels-Alder reaction between an *E,Z*-conjugated diene and *(S)-N*-(1-phenylethyl)maleimide with four possible reaction products

Our goal was to develop a method that could be used for the derivatization and further identification of *E,Z*-conjugated dienes in general, with special focus on 13-DHAHLA isomers. However, since 13-DHAHLA isomers are not commercially available, and only limited amounts of them were obtained by total organic synthesis, we started our experiments by using 17*S*-HDHA. This hydroxy PUFA is commercially available as a 0,1 mg/ml ethanol solution and has an *E,Z*-moiety, which made it an ideal candidate for the development of our method.

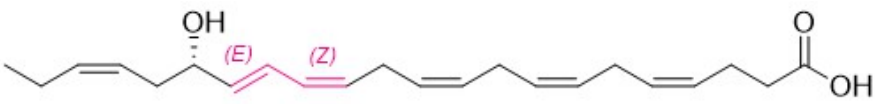

Figure 31. Structure of 17*S*-HDHA

We tried to make the Diels-Alder reaction happen with different solvents, different reaction temperatures and after different periods of time. In order to check whether the reaction took place, UV spectrometry and TLC were used.

17*S*-HDHA is partially UV active due to the presence of conjugated double bonds. Its absorption maximum is at λ = 237 nm. Therefore, the idea was to monitor the reaction between 17*S*-HDHA and *S*-PEM by recording spectra in UV range at different time points and checking whether the change of the absorption maximum or the overall signal occurs.

In order to do so, a solution of 17*S*-HDHA was mixed with a solution of the desired dienophile in the same solvent. Different reaction conditions were attempted. Summary of the reaction conditions used and the results obtained is provided in Table 2.

Table 2. An overview of the Diels-Alder reaction conditions attempted for this master thesis, as well as the reaction outcomes obtained

	LM	c_{LM} [mg/ml]	Dienophile	Dienophile molar access [%]	Solvent	Temperature	Duration	Reaction took place		
								UV	TLC	MS
1	17*S*-HDHA	0,002	*S*-PEM	5	ethanol	room temp.	4 h	no	/	no
2	17*S*-HDHA	0,01	*S*-PEM	10	ethanol	40°C	24 h	no	/	no
3	17*S*-HDHA	0,01	*S*-PEM	10	ethanol	60°C	24 h	no	/	no
4	17*S*-HDHA	0,01	PTAD	5	ethanol	room temp.	4 h	no	/	no
5	17*S*-HDHA	0,01	PTAD (3 days old)	5	dichloromethane	room temp.	2 h	no	no	no
6	17*S*-HDHA	0,01	*S*-PEM	10	ethanol	80°C	24 h	no	no	no
7	17*S*-HDHA	0,01	PTAD	5	dichloromethane	35°C	4 h	**yes**	**yes**	**yes**
8	MaR1	0,01	PTAD	100	methanol	room temp.	4 h	**yes**	**yes**	**yes**
9	MaR1	0,01	*S*-PEM	5	methanol	room temp.	4 h	no	no	no
10	MaR1	0,01	*S*-PEM	1000	methanol	room temp.	4 h	no	no	no
11	17-oxo-DHA	0,01	PTAD	10	dichloromethane	room temp.	2 h	no	no	no
12	17-oxo-DHA	0,01	PTAD	10	dichloromethane	35°C	2 h	no	no	no
13	17-oxo-DHA	0,01	*S*-PEM	10	dichloromethane	room temp.	2 h	no	no	no
14	17-oxo-DHA	0,01	*S*-PEM	10	dichloromethane	35°C	2 h	no	no	no
15	(±)17-HDHA	0,02	*S*-PETAD	5	dichloromethane	room temp.	24 h	unsure	**yes**	**yes**
16	(±)17-HDHA	0,02	*S*-PETAD	300	dichloromethane	35°C	24 h	**yes**	**yes**	**yes**
17	17S-HDHA	0,02	*S*-PETAD	5	dichloromethane	35°C	24 h	unsure	unsure	**yes**
18	17S-HDHA	0,02	*S*-PETAD	300	dichloromethane	35°C	24 h	**yes**	unsure	**yes**
19	MaR1	0,02	*S*-PETAD	5	dichloromethane	35°C	24 h	unsure	unsure	**yes**
20	MaR1	0,02	*S*-PETAD	300	dichloromethane	35°C	24 h	**yes**	unsure	**yes**

Herein, the obtained results are presented in more detail:

1) *S*-PEM, ethanol solution, room temperature, c = 0,002 mg/ml

The mixture of 0,002 mg/ml ethanol solution of 17*S*-HDHA and *S*-PEM (5% molar excess) was kept in a dark place at room temperature. UV spectrum was taken at 0 min, 15 min, 30 min, 60 min, 120 min, 180 min and 240 min. λ_{max} of the mixture was at 224-231 nm. No major change of spectrum took place, indicating that the reaction most probably did not take place.

2) *S*-PEM, ethanol solution, 40°C, c = 0,01 mg/ml

This time, a higher concentration of 17*S*-HDHA was used: 0,01 mg/ml, and the excess of *S*-PEM was 10%. UV spectrum was taken at 0 min, 120 min and 240 min. After initial UV measurement, the mixture was warmed up in oil bath at 40°C. Since there was no significant change of spectrum after 2h, the solution was kept at 40°C overnight. The next day UV measurement was taken, and no significant change of spectrum took place.

3) *S*-PEM, ethanol solution, 60°C, c = 0,01 mg/ml

The concentration of 17*S*-HDHA was 0,01 mg/ml, and the excess of *S*-PEM was 10%. UV spectrum was taken at 0 min, 120 min, 240 min and after keeping the mixture at 60°C overnight. After the initial UV measurement, the mixture was warmed up in oil bath at 60°C. Once again, no significant change of spectrum took place.

In parallel, we decided to check if we can induce 17*S*-HDHA to react with PTAD. PTAD was previously successfully used as dienophile in the Diels-Alder reaction to distinguish between LMs with *E,E*-conjugated diene moiety and *E,Z*-moiety (MaR1, PD1 and their double di-oxygenation isomers). This time, it was presumed that it will take longer time and higher temperature in order for *E,Z*-conjugated diene to react.

4) PTAD, ethanol solution, room temperature, c = 0,01 mg/ml

The mixture of 0,01 mg/ml 17*S*-HDHA in ethanol solution and PTAD (5% molar excess) was kept in a dark place at room temperature. UV spectrum was taken at 0 min, 15 min, 30 min, 60 min, 120 min, 180 min and 240 min. λ_{max} of 17*S*-HDHA alone was at 237 nm, PTAD alone at 227 nm and mixture at 233 nm. No major change of spectrum took place, indicating that no reaction occurred.

Of note, PTAD is commercially available as a powder with intense ruby colour. When dissolved in ethanol, the solution readily changed colour to orange, and at the same time bubbles of gas occurred. This gave the reason to suspect that PTAD may be reacting with ethanol. Therefore, we decided to try another solvent – dichloromethane (CH_2Cl_2).

5) PTAD, dichloromethane solution, room temperature, c = 0,01 mg/ml

The ethanol from the sample of commercial 17*S*-HDHA was first removed with the stream of nitrogen. After that, 17*S*-HDHA was dissolved in dichloromethane to a concentration of 0,01 mg/ml. λ_{max} of 17*S*-HDHA alone was at 232 nm, PTAD alone at 228 nm and mixture at 229 nm. UV spectra were taken at 0 min, 15 min, 30 min, 60 min and 120 min. No significant change of spectrum took place.

All of the samples derived from experiments mentioned above were kept at -18^{o}C. MS spectra of all the samples were taken. Sample with dichloromethane solution was first treated with nitrogen stream to remove dichloromethane, and residuals were dissolved in ethanol prior to the MS analysis. Fragments on MS spectra did not indicate the formation of the Diels-Alder adduct.

At this point, we decided to introduce TLC method as a double check for the results obtained from UV analysis. To do so, we needed to find a right eluent composition for the mobile phase, as well as derivatisation reagent for 17*S*-HDHA. The mixture of 17*S*-HDHA and PTAD was also analysed, to see whether the signal is different from the one of 17*S*-HDHA.

- Mixture of CH_2Cl_2 and methanol in ratio 95:5 did not lead to satisfactory chromatographic development.
- Mobile phase of ethyl-acetate : hexane = 50:50 proved to be a good choice with CAM (Cerium ammonium molybdate) as a staining agent. The Rf value of 17*S*-HDHA was 0,17, and the mixture of 17*S*-HDHA and PTAD gave the spot with the same Rf value.

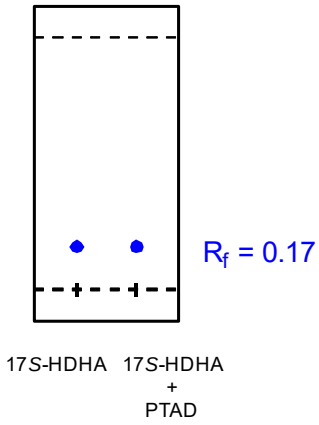

- Mobile phase of ethyl-acetate : hexane = 70:30 gave even better result, with Rf = 0,53. This mobile phase was chosen for further experiments.

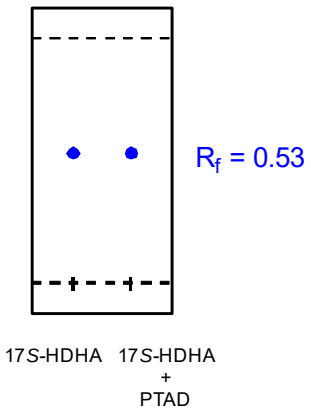

6) *S*-PEM, ethanol solution, 80ºC, c = 0,01 mg/ml

We decided to attempt to induce the reaction with a temperature slightly higher than the ethanol boiling point. A completely closed system was used, in order to prevent ethanol from evaporating. Spectra were taken after 2h and after keeping the mixture at 80ºC overnight. No significant change of UV spectrum took place. TLC analysis showed a clear presence of 17*S*-HDHA in the 17*S*-HDHA-PTAD mixture.

7) PTAD, dichloromethane solution, 35ºC, c = 0,01 mg/ml

Dichloromethane evaporates easily, so solution was warmed at 35ºC for 2 h. This time, a **freshly prepared** solution of PTAD in dichloromethane was used, after noticing that colour of the stock solution fades away, even when kept at refrigerator.

UV spectra showed the change of signal. TLC analysis showed no sign of 17*S*-HDHA in the 17*S*-HDHA-PTAD mixture. In addition, the sample was analysed on MS, and MS spectrum showed fragments that were expected for the Diels-Alder reaction product of 17*S*-HDHA and PTAD. In other words, we succeeded to get 17*S*-HDHA to react with PTAD.

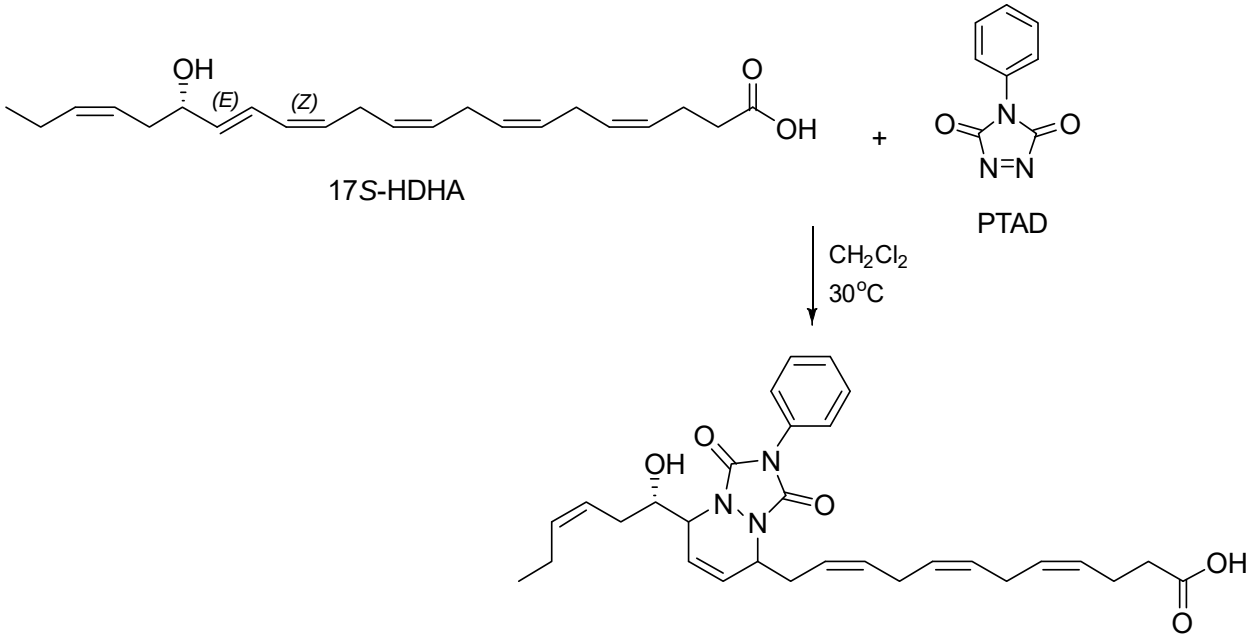

Figure 32. The Diels-Alder reaction between 17*S*-HDHA and PTAD

However, our goal to successfully induce the reaction between 17*S*-HDHA and *S*-PEM was yet to be reached.

We decided to check if *S*-PEM reacts with LMs with *E,E*-conjugated diene moiety. As mentioned before, *E,E*-conjugated dienes react in Diels-Alder reaction much more readily than *E,Z*-conjugated dienes. For that purpose, maresin 1 (MaR1) obtained by the LIPCHEM group by total organic synthesis (47) was used.

8), 9) and 10) MaR1, methanol solution, room temperature, c = 0,01 mg/ml

All solutions were made in methanol, because MaR1 obtained by total organic synthesis was kept in methanol. Both PTAD and *S*-PEM were used as dienophiles. UV

spectrum of MaR1 showed absorption maximum at 270 nm, with shoulders on both sides of the main signal (triplet).

- With 5% excess of PTAD the peak of MaR1 on UV spectrum got lower, and with 100% excess of PTAD the peak disappeared completely. TLC analysis with 100% excess of PTAD confirmed that the reaction took place, since there was no spot of MaR1 in the mixture. MS spectrum of the sample confirmed that the reaction took place.

- With 5% excess of *S*-PEM the peak on UV spectrum remained the same.

- Even with as much as 1000% excess of *S*-PEM there was no change of signal.

As experiments with MaR1 showed, *S*-PEM is hard to react even with LMs that have *E,E*-conjugated diene moiety.

We decided to try another approach: oxidation of 2º alcohol in 17-HDHA to ketone – 17-oxo-DHA. We believed that the carbonyl group would cause the conjugated diene to become more reactive, and hence easier to react with a dienophile.

A racemic mixture of 17-HDHA isomers was used. 17-HDHA was oxidised to the corresponding oxo-compound (17-oxo-DHA) using the Dess-Martin periodinane reagent (DMP). (48) TLC method was used to check whether the oxidation of 17-HDHA was complete. The oxidation was continued overnight, and when finished, solvents were evaporated using nitrogen stream, and residues were dissolved in dichloromethane to the concentration of 0,05 mg/ml. This concentration was proposed assuming that the 17-HDHA was completely oxidised to 17-oxo-DHA.

Figure 33. Oxidation of 17-HDHA to corresponding ketone

11) 17-oxo-DHA c = 0,01 mg/ml, PTAD, dichloromethane solution, room temperature

UV spectrum of dichloromethane solution of 17-oxo-DHA alone showed a peak at 232 nm, and another one, much lower at 275 nm. PTAD alone had λ_{max} at 229 nm. A solution of 17-oxo-DHA with 10% excess of PTAD was kept at room temperature for 2

hours. UV spectrum showed absorption maximum at 229 nm, and there was no peak at 275 nm, which could be a sign that the reaction took place. However, TLC signals were too pale and therefore could not be used as an indicator whether the reaction took place. MS spectrum of the sample did not contain ions that would be indicative of the reaction product.

12) 17-oxo-DHA c = 0,01 mg/ml, PTAD, dichloromethane solution, 35°C

A solution of 17-oxo-DHA with 10% excess of PTAD was kept at 35°C for 2 hours. No significant change of signal on UV spectrum occurred. TLC signals were too pale and therefore could not be used as an indicator whether the reaction took place. Once again, MS spectrum of the sample did not contain ions that would be indicative of the reaction product.

13) 17-oxo-DHA c = 0,01 mg/ml, *S*-PEM, dichloromethane solution, room temperature

As previously observed, UV spectrum of dichloromethane solution of 17-oxo-DHA showed a peak at 232 nm, and another one, much lower at 275 nm. *S*-PEM in dichloromethane gives a high peak at 230 nm. Hence, the mixture of the two compounds gave a high peak on UV spectrum at 230 nm. After 2 hours, no significant change of spectrum occurred. TLC signals were too pale and therefore inappropriate as an indicator whether the reaction took place. MS spectrum of the sample did not contain ions that would be indicative of the reaction product.

14) 17-oxo-DHA c = 0,01 mg/ml, *S*-PEM, dichloromethane solution, 35°C

A solution of 17-oxo-DHA with 10% excess of *S*-PEM was kept at 35°C for 2 hours. After 2 hours no significant change of spectrum occurred. TLC signals were too pale and therefore inappropriate as an indicator whether the reaction took place. MS spectrum of the sample did not contain ions that would be indicative of the reaction product.

After these experiments, we concluded that our attempts to make the dienes of interest react with *S*-PEM did not succeed. Even at higher reaction temperatures and with prolonged reaction time, *S*-PEM as derivatisation agent did not serve the purpose, as we could not prove the presence of cycloaddition product by any of the methods used. Therefore, Professor Trond V. Hansen came to a new idea: to try the Diels-Alder

reaction with a new dienophile, that would have a combined structure of PTAD and PEM:

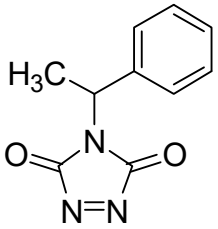

Figure 34. Structure of 4-(1-phenylethyl)-*3H*-1,2,4-triazole-3,5(*4H*)-dione (PETAD)

This compound was expected to have all the advantages and reactivity of PTAD. At the same time, the fact that it has a stereogenic center would possibly contribute to better separation of reaction products with conjugated dienes. Another advantage over PEM is the fact that the double bond that forms a ring with the diene in the Diels-Alder reaction in between two nitrogen atoms, and not carbon atoms, which gives fewer possible isomeric reaction products in the Diels-Alder reaction (Fig. 35) compared to PEM.

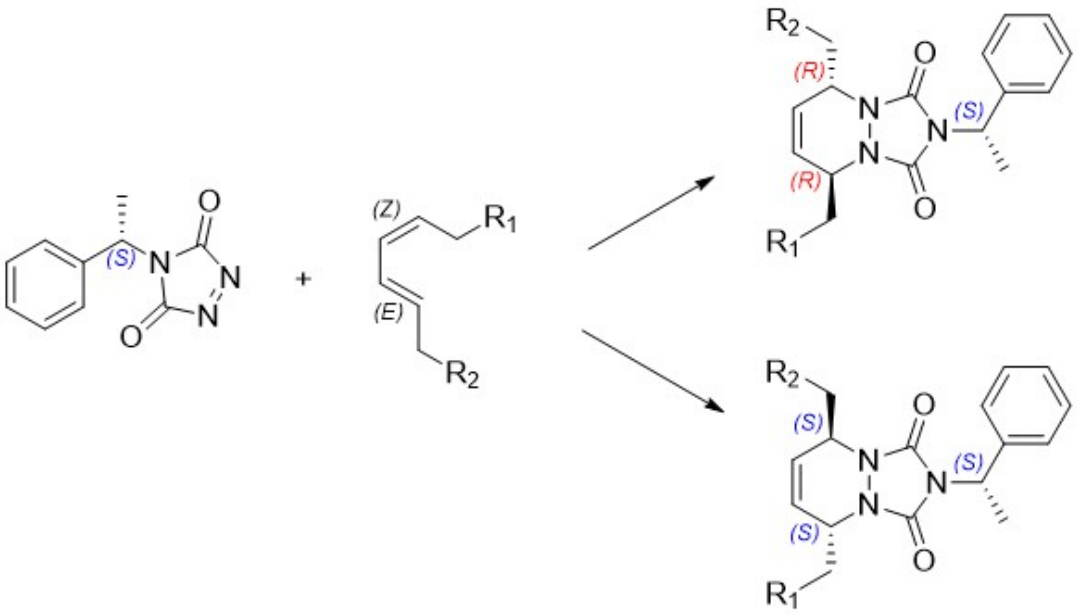

Figure 35. Diels-Alder reaction between *S*-PETAD and *E,Z*-conjugated diene, with two possible reaction products

However, this new dienophile was not commercially available. Therefore it had to be made by total organic synthesis. The dienophile was ordered from a synthesis laboratory in Krakow, Poland.

The synthesis of the new dienophile proved to be a lengthy process. Ordered in the end of October 2017, with estimated delivery in January 2018, was followed by several delays. However, it was finally delivered to the LIPCHEM group in the first half of March 2018. The late delivery of the new reagent did not leave a lot of time for additional and more extensive laboratory trials, having in mind that the deadline for the submission of the master thesis was 3rd April 2018. However, we managed to repeat the initial experiments with the new dienophile, using following dienes: (±)17-HDHA, 17*S*-HDHA and MaR1. The solvent used was dichloromethane, since the producer provided the information that PETAD is unstable in the alcohol solutions.

15) (±)17-HDHA c = 0,02 mg/ml, *S*-PETAD, dichloromethane solution, room temperature

Ethanol was removed from 20 µl of the commercially available stock solution of (±)17-HDHA. The dichloromethane solution of *S*-PETAD (5% molar excess) was used to dissolve the residues, and dichloromethane was added to the final volume of 100 µl. The mixture was kept at room temperature. UV spectra were taken initially, after 2h and after 24 h. Absorbance maximum of the mixture was at 232 nm. No significant change of UV spectrum was observed over time. TLC analysis, however, showed no sign of (±)17-HDHA in the mixture. MS spectrum showed fragment that was expected for the Diels-Alder reaction product of (±)17-HDHA and *S*-PETAD, which confirmed that the reaction took place.

16) (±)17-HDHA c = 0,02 mg/ml, *S*-PETAD 300% excess, dichloromethane solution, 35°C

The mixture was prepared as explained in 15), and kept at 35°C in oil bath. UV spectra were taken initially and after 2h. Absorbance maximum of the mixture was at 232 nm. Since no significant change of UV spectrum was observed after 2h, additional amount of *S*-PETAD was added, so that there was 300% excess of it in the final solution. This led to an immediate change of spectrum – the absorbance at 237 nm (where the absorbance maximum of (±)17-HDHA is) became much lower. The mixture was kept at 35°C overnight, and the UV spectrum was taken again after 24 h. TLC analysis showed no sign of (±)17-HDHA in the mixture. MS spectrum showed characteristic molecular ion that was expected for the Diels-Alder reaction product of (±)17-HDHA and *S*-PETAD, which confirmed that the reaction took place. Compared to the sample with 5% excess of *S*-PETAD, this sample had a much higher abundance of the

molecular ion, indicating that the reaction was incomplete with only 5% excess of *S*-PETAD.

17) 17*S*-HDHA c = 0,02 mg/ml, *S*-PETAD, dichloromethane solution, 35ºC

20 µl of the commercially available stock solution of 17*S*-HDHA was transferred to a HPLC vial, and ethanol was removed under the stream of nitrogen. The dichloromethane solution of *S*-PETAD (5% molar excess) was used to dissolve the residues, and dichloromethane was added to the final volume of 100 µl. The mixture was kept at 35ºC in oil bath. UV spectra were taken initially, after 2h and after 24h. Absorbance maximum of the mixture was initially at 238 nm, but changed after 2h to 232 nm. Signals on TLC plate were too pale to be indicative of whether the reaction took place. MS spectrum showed characteristic molecular ion that was expected for the Diels-Alder reaction product of 17*S*-HDHA and *S*-PETAD, which confirmed that the reaction took place.

18) 17*S*-HDHA c = 0,02 mg/ml, *S*-PETAD 300% excess, dichloromethane solution, 35ºC

20 µl of the commercially available stock solution of 17*S*-HDHA was transferred to a HPLC vial, and ethanol was removed under the stream of nitrogen. The dichloromethane solution of *S*-PETAD (300% molar excess) was used to dissolve the residues, and dichloromethane was added to the final volume of 100 µl. The mixture was kept at 35ºC in oil bath. UV spectra were taken initially, after 2h and after 24h. Absorbance maximum of the mixture was initially at 238 nm, but changed after 2h to 230 nm. Signals on TLC plate were too pale to be indicative of whether the reaction took place. MS spectrum showed characteristic molecular ion that was expected for the Diels-Alder reaction product of 17*S*-HDHA and *S*-PETAD, which confirmed that the reaction took place.

19) MaR1 c = 0,02 mg/ml, *S*-PETAD, dichloromethane solution, 35ºC

20 µl of the stock solution of MaR1 synthesized by the LIPCHEM group was transferred to a HPLC vial, and methanol was removed under the stream of nitrogen. The dichloromethane solution of *S*-PETAD (5% molar excess) was used to dissolve the residues, and dichloromethane was added to the final volume of 100 µl. The mixture was kept at 35ºC in oil bath. UV spectra were taken initially, after 2h and after 24h. Absorbance maximum of the mixture was initially at 274 nm, with characteristic shoulders on both sides of the signal. This characteristic triplet signal was still present on UV spectrum after 2h and after 24h, though with lower absorbance. Signals on TLC plate were too pale to be indicative of whether the reaction took place. MS spectrum

showed characteristic molecular ion that was expected for the Diels-Alder reaction product of MaR1 and *S*-PETAD, which confirmed that the reaction took place. Molecular ion of MaR1 was also present on MS spectrum, showing that the reaction was incomplete with 5% excess of *S*-PETAD.

20) MaR1 c = 0,02 mg/ml, *S*-PETAD 300% excess, dichloromethane solution, 35^{o}C

20 µl of the stock solution of MaR1 synthesized by the LIPCHEM group was transferred to a HPLC vial, and methanol was removed under the stream of nitrogen. The dichloromethane solution of *S*-PETAD (300% molar excess) was used to dissolve the residues, and dichloromethane was added to the final volume of 100 µl. The mixture was kept at 35^{o}C in oil bath. UV spectra were taken initially, after 2h and after 24h. Absorbance maximum of the mixture was initially at 229 nm, with the characteristic triplet of MaR1 at 274 nm completely absent.

This indicated that the reaction took place completely. Signals on TLC plate were too pale to be indicative of whether the reaction took place. MS spectrum showed dominant characteristic molecular ion that was expected for the Diels-Alder reaction product of MaR1 and *S*-PETAD.

3 Conclusions and future studies

Our efforts towards the development of a new derivatization protocol for SPMs included experiments with three different dienophiles: the two known reagents PTAD and *S*-PEM, and the novel reagent *S*-PETAD. We already knew that PTAD reacted with *E,Z*-conjugated dienes under suitable conditions. Indeed, we managed to induce the reaction of 17*S*-HDHA and MaR1 with PTAD. However, chromatographic analysis of PTAD adducts of novel putative SPMs discovered by the Praha group did not lead to the satisfactory separation of signals. That is why we focused on developing a new derivatization protocol, where an extra stereogenic center would be introduced by using *S*-PEM as a dienophile. Different solvents, reaction temperatures and reaction duration were attempted, and the reaction outcome was investigated by using three different analytical methods: UV spectrometry, TLC and MS. Oxidation of 17-HDHA to the corresponding ketone was also studied. Given that the reaction took place, our goal was to establish a HPLC method for the separation of the Diels-Alder adducts obtained.

Unfortunately, we did not succeed in inducing the *S*-PEM react with either 17*S*-HDHA, as *E,Z*-diene, or MaR1, as *E,E*-diene. Therefore, the novel reagent *S*-PETAD, with the combined structure of PTAD and *S*-PEM was ordered. Experiments were repeated in the same manner as for *S*-PEM, using dichloromethane as a solvent. This time, our attempts led to success. *S*-PETAD reacted with racemic 17-HDHA, 17*S*-HDHA and MaR1, as unambiguously confirmed by MS spectra. Our conclusion is that dienophiles with double bond between two carbon atoms are far less reactive in the Diels-Alder reaction than dienophiles with the -N=N- moiety.

To the great disappointment of the student, the novel reagent *S*-PETAD was delivered to the LIPCHEM group too late to be able to continue with HPLC experiments as initially proposed in this master thesis. Still, there is a reason for satisfaction - a new reagent has been introduced, with the potential of becoming a powerful tool in the future analysis of SPMs. This gives plenty of opportunity for further studies, perhaps for some new master thesis.

The first part of this thesis gives a thorough overview of methods that have been used for the analysis of SPMs in the last two decades.

4 Experimental

4.1 Materials and apparatus

All commercially available reagents and solvents were used without further purification, unless otherwise stated. *S*-PETAD (4-[(1*S*)-1-phenylethyl]-4,5-dihydro- 3*H*-1,2,4-triazole-3,5-dione) was not commercially available and was therefore ordered from the chemical synthesis laboratory Selvita services in Krakow, Poland. MaR1 was synthesized by the LIPCHEM group.

UV spectrometry was performed on Agilent Technologies Cary 8454 UV-Vis spectrophotometer. Thin layer chromatography (TLC) was performed on TLC Silica gel 60 F_{254} aluminium-backed plates from Merck. Mass spectra were recorded at 70 eV on a Waters Prospec Q, with ESI as a method of ionization.

4.2 Experimental procedures

4.2.1 Attempted reaction between 17*S*-HDHA and *S*-PEM in ethanol at room temperature

2 µl of the commercially available stock solution of 17*S*-HDHA c = 0,1 mg/ml was mixed with 10 µl of 0,0123 mg/ml *S*-PEM ethanol solution in a HPLC vial, and 88 µl of ethanol was added to the final volume of 100 µl. UV spectrum of the mixture was taken at 0 min, 15 min, 30 min, 60 min, 120 min, 180 min and 240 min, using ethanol as a blank. Maximum absorbance was at 237 nm. No change of UV spectrum was observed. Theoretical exact mass of the reaction product was 545.31. MS spectrum of the sample did not indicate that the reaction took place.

4.2.2 Attempted reaction between 17*S*-HDHA and *S*-PEM in ethanol at 40°C

10 µl of the commercially available stock solution of 17*S*-HDHA c = 0,1 mg/ml was mixed with 10 µl of 0,0615 mg/ml *S*-PEM ethanol solution in a HPLC vial, and 80 µl of ethanol was added to the final volume of 100 µl. After the initial measurement, the mixture was kept at 40°C in the oil bath. UV spectrum of the mixture was taken at 0

min, 120 min, 240 min and 24 h, using ethanol as a blank. Maximum absorbance was at 237 nm. No change of UV spectrum was observed. Theoretical exact mass of the reaction product was 545.31. MS spectrum of the sample did not indicate that the reaction took place.

4.2.3 Attempted reaction between 17*S*-HDHA and *S*-PEM in ethanol at 60°C

10 µl of the commercially available stock solution of 17*S*-HDHA c = 0,1 mg/ml was mixed with 10 µl of 0,0615 mg/ml *S*-PEM ethanol solution in a HPLC vial, and 80 µl of ethanol was added to the final volume of 100 µl. After the initial measurement, the mixture was kept at 60°C in the oil bath. UV spectrum of the mixture was taken at 0 min, 120 min, 240 min and 24 h, using ethanol as a blank. Maximum absorbance was at 237 nm. No change of UV spectrum was observed. Theoretical exact mass of the reaction product was 545.31. MS spectrum of the sample did not indicate that the reaction took place.

4.2.4 Attempted reaction between 17*S*-HDHA and PTAD in ethanol at room temperature

10 µl of the commercially available stock solution of 17*S*-HDHA c = 0,1 mg/ml was mixed with 10 µl of 0,05338 mg/ml PTAD ethanol solution in a HPLC vial, and 80 µl of ethanol was added to the final volume of 100 µl. UV spectrum of the mixture was taken at 0 min, 15 min, 30 min, 60 min, 120 min, 180 min and 240 min, using ethanol as a blank. Maximum absorbance was at 233 nm. No change of UV spectrum was observed. PTAD changed color from ruby red to orange when dissolved in ethanol, and the gas bubbles appeared. That indicated that PTAD is not stable in ethanol. Theoretical exact mass of the reaction product was 519.27. MS spectrum of the sample did not indicate that the reaction took place.

4.2.5 Attempted reaction between 17*S*-HDHA and PTAD in dichloromethane at room temperature

10 µl of the commercially available stock solution of 17*S*-HDHA c = 0,1 mg/ml was transferred to a HPLC vial, and the solvent (ethanol) was evaporated under a nitrogen stream. 10 µl of 0,05338 mg/ml PTAD dichloromethane solution was then added, and 80 µl of dichloromethane was added to the final volume of 100 µl. UV spectrum of the mixture was taken at 0 min, 15 min, 30 min, 60 min and 120 min, using dichloromethane as a blank. Maximum absorbance of the mixture was at 229 nm. No

change of UV spectrum was observed. Dichloromethane was evaporated from the sample prior to MS analysis, and the residuals were dissolved in ethanol. Theoretical exact mass of the reaction product was 519.27. MS spectrum of the sample did not indicate that the reaction took place.

4.2.6 Attempted reaction between 17*S*-HDHA and *S*-PEM in ethanol at 80°C

10 µl of the commercially available stock solution of 17*S*-HDHA c = 0,1 mg/ml was mixed with 10 µl of 0,0615 mg/ml *S*-PEM ethanol solution in a HPLC vial, and 80 µl of ethanol was added to the final volume of 100 µl. After the initial measurement, the mixture was kept at 80°C in the oil bath. UV spectrum of the mixture was taken at 0 min, 2 h and 24 h, using ethanol as a blank. Maximum absorbance was at 224 nm. No change of UV spectrum was observed. TLC was performed using ethyl-acetate : hexane = 70:30 as a mobile phase. TLC plate was developed by using CAM stain and heating until spots appeared. The spot obtained from the 17*S*-HDHA-*S*-PEM mixture had the same Rf value as the spot obtained from 17*S*-HDHA, indicating that there was still 17*S*-HDHA present in the mixture. Theoretical exact mass of the reaction product was 545.31. MS spectrum of the sample did not indicate that the reaction took place.

4.2.7 Attempted reaction between 17*S*-HDHA and PTAD in dichloromethane at 35°C

0,05338 mg/ml PTAD dichloromethane solution was prepared *ex tempore*, since it was observed during previous experiments that the color of PTAD stock solution faded away after few days. 10 µl of the commercially available stock solution of 17*S*-HDHA c = 0,1 mg/ml was transferred to a HPLC vial, and the solvent (ethanol) was evaporated under a nitrogen stream. 10 µl of 0,05338 mg/ml PTAD dichloromethane solution was then added, and 80 µl of dichloromethane was added to the final volume of 100 µl. After the initial measurement, the mixture was kept at 35°C in the oil bath.UV spectrum of the mixture was taken initially, after 2 h and after 24 h, using dichloromethane as a blank. Maximum absorbance of the mixture was at 229 nm. UV spectrum has changed with time, indicating that the reaction took place. TLC was performed using ethyl-acetate : hexane = 70:30 as a mobile phase. TLC plate was developed by using CAM stain and heating until spots appeared. No spot of 17*S*-HDHA was observed in the 17*S*-HDHA-PTAD mixture on the developed TLC plate. Dichloromethane was evaporated from the sample prior to MS analysis, and the residuals were dissolved in ethanol. Theoretical exact mass of the reaction product was 519.27. Molecular ion of the reaction product was observed on the MS spectrum ($[M+Na]^+$, m/z = 542.26), confirming that the reaction took place.

4.2.8 Attempted reaction between MaR1 and PTAD in methanol at room temperature

MaR1 was prepared by the LIPCHEM group by total organic synthesis, and kept as 0.1 mg/ml methanol solution at -80ºC. 10 µl of the stock solution of MaR1 c = 0,1 mg/ml was mixed with 10 µl of the freshly prepared 0,051 mg/ml PTAD methanol solution in a HPLC vial, and 80 µl of methanol was added to the final volume of 100 µl. Maximum absorbance of MaR1 methanol solution alone was a triplet with maximum at 271 nm, and shoulders at 262 nm and 282 nm. UV spectrum of the mixture after 2 h showed a much lower absorbance at 271 nm, indicating that the reaction took place, however, the characteristic triplet signal of MaR1 was still observed. Therefore, the solvent was removed under a nitrogen stream. Then, additional 30 µl of the 0,051 mg/ml PTAD methanol solution and 70 µl of methanol were added, so that there was 300% molar excess of PTAD in the final solution. UV spectrum of this solution lacked the characteristic triplet signal of MaR1. TLC was performed as previously described. No spot of MaR1 was observed in the MaR1-PTAD mixture on the developed TLC plate. Theoretical exact mass of the reaction product was 535.27. Molecular ion of the reaction product was observed on the MS spectrum ($[M+Na]^+$, *m/z* = 558.26; $[M-H]^-$, *m/z* = 534.26), though with lower abundance, confirming that the reaction took place.

4.2.9 Attempted reaction between MaR1 and *S*-PEM in methanol at room temperature

10 µl of the stock solution of MaR1 c = 0,1 mg/ml was mixed with 4 µl of the freshly prepared 0,1544 mg/ml *S*-PEM methanol solution in a HPLC vial, and 86 µl of methanol was added to the final volume of 100 µl. Maximum absorbance of MaR1 methanol solution alone was a triplet with maximum at 271 nm, and shoulders at 262 nm and 282 nm. UV spectrum of the mixture after 2 h showed no change of signal.

4.2.10 Attempted reaction between MaR1 and *S*-PEM (1000% excess) in methanol at room temperature

The solvent from the mixture of MaR1 and *S*-PEM described in 4.2.9 was removed under a nitrogen stream. Then, additional 40 µl of the 0,1544 mg/ml *S*-PEM methanol solution and 60 µl of methanol were added, so that there was approximately 1000% molar excess of *S*-PEM in the final solution. UV spectrum of the mixture after 2 h showed no change of signal. TLC was performed as previously described. The spot obtained from the MaR1-*S*-PEM mixture had the same Rf value as the spot obtained from MaR1, indicating that there was still MaR1 present in the mixture. Theoretical exact mass of the reaction product was 561.31. MS spectrum of the sample did not indicate that the reaction took place.

4.2.11 Attempted reaction between 17-oxo-HDHA and PTAD in dichloromethane at room temperature

Racemic 17-HDHA was oxygenized to 17-oxo-HDHA following the procedure described in the supplementary data of the reference (48). 1000 µl of the stock solution of 0.1 mg/ml 17-HDHA in ethanol was transferred to a HPLC vial. Ethanol was evaporated under the nitrogen stream. Residuals were dissolved in 40 µl dichloromethane. Suspension of 0,00016 g DMP in dichloromethane was added to the 17-HDHA solution. Mixture was stirred for four hours at room temperature. TLC analysis showed that there was still 17-HDHA in the mixture, so the stirring was continued over night. Next day, aqueous solution of $Na_2S_2O_3$ and saturated aqueous solution of $NaHCO_3$ (1:1) were added to the mixture. Aqueous layer was removed using automatic pipette, and then it was extracted three times with diethyl ether. Organic layers were combined and washed with brine, and then dried using Na_2SO_4. Solution over Na_2SO_4 was taken with syringe and filtered through HPLC filter. Obtained solution was clear and colorless. Organic solvents were removed under the nitrogen stream, and the residuals were dissolved in 1 ml of dichloromethane. Calculated concentration of 17-oxo-DHA solution was 0,05 mg/ml. Absorption maximum of the solution was at 229 nm.

20 µl of the stock solution of 17-oxo-HDHA in dichloromethane c = 0,05 mg/ml was mixed with 10 µl of the freshly prepared 0,05338 mg/ml PTAD. 70 µl of dichloromethane was added to the final volume of 100 µl. The mixture was kept at room temperature for 2 hours. UV spectrum showed no change of signal. TLC was performed as previously described. Spots on the developed TLC plate were too pale, and thus could not be used as an indicator of whether the reaction took place. Theoretical exact mass of the reaction product was 517.25. MS spectrum of the sample did not indicate that the reaction took place.

4.2.12 Attempted reaction between 17-oxo-HDHA and PTAD in dichloromethane at 35°C

20 µl of the stock solution of 17-oxo-HDHA in dichloromethane c = 0,05 mg/ml was mixed with 10 µl of the freshly prepared 0,05338 mg/ml PTAD. 70 µl of dichloromethane was added to the final volume of 100 µl. The mixture was kept at 35°C for 2 hours. UV spectrum showed no change of signal. TLC was performed as previously described. Spots on the developed TLC plate were too pale, and thus could not be used as an indicator of whether the reaction took place. Theoretical exact mass of the reaction product was 517.25. MS spectrum of the sample did not indicate that the reaction took place.

4.2.13 Attempted reaction between 17-oxo-HDHA and *S*-PEM in dichloromethane at room temperature

20 µl of the stock solution of 17-oxo-HDHA in dichloromethane c = 0,05 mg/ml was mixed with 10 µl of the freshly prepared 0,0615 mg/ml *S*-PEM. 70 µl of dichloromethane was added to the final volume of 100 µl. The mixture was kept at room temperature for 2 hours. UV spectrum showed no change of signal. TLC was performed as previously described. Spots on the developed TLC plate were too pale, and thus could not be used as an indicator whether the reaction took place. Theoretical exact mass of the reaction product was 543.29. MS spectrum of the sample did not indicate that the reaction took place.

4.2.14 Attempted reaction between 17-oxo-HDHA and *S*-PEM in dichloromethane at 35°C

20 µl of the stock solution of 17-oxo-HDHA in dichloromethane c = 0,05 mg/ml was mixed with 10 µl of the freshly prepared 0,0615 mg/ml *S*-PEM. 70 µl of dichloromethane was added to the final volume of 100 µl. The mixture was kept at 35°C for 2 hours. UV spectrum showed no change of signal. TLC was performed as previously described. Spots on the developed TLC plate were too pale, and thus could not be used as an indicator whether the reaction took place. Theoretical exact mass of the reaction product was 543.29. MS spectrum of the sample did not indicate that the reaction took place.

4.2.15 Attempted reaction between (±)17-HDHA and *S*-PETAD in dichloromethane at room temperature

20 µl of the 0,1 mg/ml stock solution of (±)17-HDHA in ethanol was transferred to a HPLC vial and ethanol was evaporated under the nitrogen stream. 20 µl of the freshly prepared 0.062 mg/ml *S*-PETAD solution in dichloromethane was added, and 80 µl of dichloromethane was added to the final volume of 100 µl. After the initial UV measurement, the mixture was kept at room temperature. UV spectra were taken initially, after 2h and after 24h. Absorption maximum changed from 239 nm to 232 nm. TLC was performed as previously described. Spots on the developed TLC plate were too pale, and thus could not be used as an indicator whether the reaction took place. Theoretical exact mass of the reaction product was 547.30. Molecular ion of the reaction product was observed on the MS spectrum ($[M+Na]^+$, m/z = 570.29), though with lower abundance, confirming that the reaction took place.

4.2.16 Attempted reaction between (±)17-HDHA and *S*-PETAD (300% excess) in dichloromethane at 35ºC

20 µl of the 0,1 mg/ml stock solution of (±)17-HDHA in ethanol was transferred to a HPLC vial and ethanol was evaporated under the nitrogen stream. 80 µl of the freshly prepared 0.062 mg/ml *S*-PETAD solution in dichloromethane was added, and 20 µl of dichloromethane was added to the final volume of 100 µl. After the initial UV measurement, the mixture was kept at 35ºC in oil bath. UV spectra were taken initially, after 2h and after 24h. Absorption maximum changed from 239 nm to 232 nm. TLC was performed as previously described. Spots on the developed TLC plate were too pale, and thus could not be used as an indicator whether the reaction took place. Theoretical exact mass of the reaction product was 547.30. Molecular ion of the reaction product was observed on the MS spectrum, confirming that the reaction took place.

4.2.17 Attempted reaction between 17*S*-HDHA and *S*-PETAD in dichloromethane at 35ºC

20 µl of the 0,1 mg/ml stock solution of 17*S*-HDHA in ethanol was transferred to a HPLC vial and ethanol was evaporated under the nitrogen stream. 20 µl of the freshly prepared 0.062 mg/ml *S*-PETAD solution in dichloromethane was added, and 80 µl of dichloromethane was added to the final volume of 100 µl. After the initial UV measurement, the mixture was kept at 35ºC in oil bath. UV spectra were taken initially, after 2h and after 24h. Absorption maximum changed from 239 nm to 230 nm. TLC was performed as previously described. Spots on the developed TLC plate were too pale, and thus could not be used as an indicator whether the reaction took place. Theoretical exact mass of the reaction product was 547.30. Molecular ion of the reaction product was observed on the MS spectrum ($[M+Na]^+$, m/z = 570.29), though with lower abundance, confirming that the reaction took place.

4.2.18 Attempted reaction between 17*S*-HDHA and *S*-PETAD (300% excess) in dichloromethane at 35ºC

20 µl of the 0,1 mg/ml stock solution of 17*S*-HDHA in ethanol was transferred to a HPLC vial and ethanol was evaporated under the nitrogen stream. 80 µl of the freshly prepared 0.062 mg/ml *S*-PETAD solution in dichloromethane was added, and 20 µl of dichloromethane was added to the final volume of 100 µl. After the initial UV measurement, the mixture was kept at 35ºC in oil bath. UV spectra were taken initially, after 2h and after 24h. Absorption maximum was at 229 nm from the initial measurement. TLC was performed as previously described. Spots on the developed TLC plate were too pale, and thus could not be used as an indicator whether the

reaction took place. Theoretical exact mass of the reaction product was 547.30. Molecular ion of the reaction product was observed on the MS spectrum ([M+Na]$^+$, *m/z* = 570.29), confirming that the reaction took place.

4.2.19 Attempted reaction between MaR1 and *S*-PETAD (5% excess) in dichloromethane at 35^{o}C

20 µl of the 0,1 mg/ml stock solution of MaR1 in methanol was transferred to a HPLC vial, and methanol was evaporated under the nitrogen stream. 19 µl of the freshly prepared 0.062 mg/ml *S*-PETAD solution in dichloromethane was added, and 81 µl of dichloromethane was added to the final volume of 100 µl. After the initial UV measurement, the mixture was kept at 35^{o}C in oil bath. UV spectra were taken initially, after 2h and after 24h. Absorption maximum was at 274 nm, with characteristic shoulders on both sides of the peak, and did not change at consecutive measurements. TLC was performed as previously described. Spots on the developed TLC plate were too pale, and thus could not be used as an indicator whether the reaction took place. Theoretical exact mass of the reaction product was 563.30. Molecular ion of the reaction product was observed on the MS spectrum ([M+Na]$^+$, *m/z* = 586.29), confirming that the reaction took place.

4.2.20 Attempted reaction between MaR1 and *S*-PETAD (300% excess) in dichloromethane at 35^{o}C

20 µl of the 0,1 mg/ml stock solution of MaR1 in methanol was transferred to a HPLC vial, and methanol was evaporated under the nitrogen stream. 76 µl of the freshly prepared 0.062 mg/ml *S*-PETAD solution in dichloromethane was added, and 24 µl of dichloromethane was added to the final volume of 100 µl. After the initial UV measurement, the mixture was kept at 35^{o}C in oil bath. UV spectra were taken initially, after 2h and after 24h. Absorption maximum was at 229 nm from the initial measurement, and no characteristic triplet at 274 nm was observed, indicating that the reaction took place at once and completely. TLC was performed as previously described. Spots on the developed TLC plate were too pale, and thus could not be used as an indicator whether the reaction took place. Theoretical exact mass of the reaction product was 563.30. Molecular ion of the reaction product was clearly present on the MS spectrum ([M+Na]$^+$, *m/z* = 586.29), confirming that the reaction took place.

5 References

1. Fredman G, Serhan CN. Specialized pro-resolving mediators: wiring the circuitry of effector immune and tissue homeostasis. Endodontic Topics. 2011;24(1):39-58.
2. Ferrero-Miliani L, Nielsen OH, Andersen PS, Girardin SE. Chronic inflammation: importance of NOD2 and NALP3 in interleukin-1β generation. Clinical and Experimental Immunology. 2007;147(2):227-35.
3. Cash JL, White GE, Greaves DR. Chapter 17 Zymosan-Induced Peritonitis as a Simple Experimental System for the Study of Inflammation. Methods in Enzymology. 461: Academic Press; 2009. p. 379-96.
4. Dalli J, Serhan CN. Specific lipid mediator signatures of human phagocytes: microparticles stimulate macrophage efferocytosis and pro-resolving mediators. Blood. 2012;120(15):e60-e72.
5. Buckley CD, Gilroy DW, Serhan CN, Stockinger B, Tak PP. The resolution of inflammation. Nature Reviews Immunology. 2012;13:59.
6. Sandrone SS, Repossi G, Candolfi M, Eynard AR. Polyunsaturated fatty acids and gliomas: A critical review of experimental, clinical, and epidemiologic data. Nutrition. 2014;30(10):1104-9.
7. Serhan CN, Clish CB, Brannon J, Colgan SP, Chiang N, Gronert K. Novel Functional Sets of Lipid-Derived Mediators with Antiinflammatory Actions Generated from Omega-3 Fatty Acids via Cyclooxygenase 2–Nonsteroidal Antiinflammatory Drugs and Transcellular Processing. The Journal of Experimental Medicine. 2000;192(8):1197-204.
8. Yang R, Chiang N, Oh SF, Serhan CN. Metabolomics-Lipidomics of Eicosanoids and Docosanoids Generated by Phagocytes. Current Protocols in Immunology: John Wiley & Sons, Inc.; 2001.
9. Burr GO, Burr MM. A New Deficiency Disease Produced by the Rigid Exclusion of Fat from the Diet. Nutrition Reviews. 1973;31(8):148-9.
10. Komplettapotek.no. Tran og omegaprodukter - Kosttilskudd og mat: Komplettapotek.no; https://www.komplettapotek.no/category/1806/kosttilskudd-og-mat/tran-og-omegaprodukter?nlevel=18%C2%A71806&CrmOnly=true&hits=48 (accessed 25.12.2017).
11. Felleskatalogen AS. Omacor: Felleskatalogen; 2017; https://www.felleskatalogen.no/medisin/omacor-pronova-562393 (accessed 25.12.2017)
12. Primdahl KG. PhD Dissertation: Stereoselective Syntheses of Oxygenated Polyunsaturated Fatty Acid Mediators and Investigations of Biosynthetic Pathways

Department of Pharmacy, Faculty of Mathematics and Natural Sciences, University of Oslo; 2017.
13. Homann J, Lehmann C, Kahnt AS, Steinhilber D, Parnham MJ, Geisslinger G, et al. Chiral chromatography–tandem mass spectrometry applied to the determination of pro-resolving lipid mediators. Journal of Chromatography A. 2014;1360(Supplement C):150-63.
14. Hong S, Gronert K, Devchand PR, Moussignac R-L, Serhan CN. Novel Docosatrienes and 17S-Resolvins Generated from Docosahexaenoic Acid in Murine Brain, Human Blood, and Glial Cells: AUTACOIDS IN ANTI-INFLAMMATION. Journal of Biological Chemistry. 2003;278(17):14677-87.

15. Serhan CN, Gotlinger K, Hong S, Lu Y, Siegelman J, Baer T, et al. Anti-Inflammatory Actions of Neuroprotectin D1/Protectin D1 and Its Natural Stereoisomers: Assignments of Dihydroxy-Containing Docosatrienes. The Journal of Immunology. 2006;176(3):1848-59.
16. Serhan CN, Jain A, Marleau S, Clish C, Kantarci A, Behbehani B, et al. Reduced Inflammation and Tissue Damage in Transgenic Rabbits Overexpressing 15-Lipoxygenase and Endogenous Anti-inflammatory Lipid Mediators. The Journal of Immunology. 2003;171(12):6856-65.
17. Bannenberg G, Serhan CN. Specialized pro-resolving lipid mediators in the inflammatory response: An update. Biochimica et Biophysica Acta (BBA) - Molecular and Cell Biology of Lipids. 2010;1801(12):1260-73.
18. Clish CB, O'Brien JA, Gronert K, Stahl GL, Petasis NA, Serhan CN. Local and systemic delivery of a stable aspirin-triggered lipoxin prevents neutrophil recruitment in vivo. Proceedings of the National Academy of Sciences. 1999;96(14):8247-52.
19. Ramon S, Baker SF, Sahler JM, Kim N, Feldsott EA, Serhan CN, et al. The Specialized Proresolving Mediator 17-HDHA Enhances the Antibody-Mediated Immune Response against Influenza Virus: A New Class of Adjuvant? The Journal of Immunology. 2014;193(12):6031-40.
20. Serhan CN. Systems approach with inflammatory exudates uncovers novel anti-inflammatory and pro-resolving mediators. Prostaglandins, Leukotrienes and Essential Fatty Acids. 2008;79(3):157-63.
21. Chiang N, Serhan CN. Structural elucidation and physiologic functions of specialized pro-resolving mediators and their receptors. Molecular Aspects of Medicine. 2017;58(Supplement C):114-29.
22. Dalli J, Colas RA, Serhan CN. Novel n-3 Immunoresolvents: Structures and Actions. Scientific Reports. 2013;3:1940.
23. Yang R, Chiang N, Oh SF, Serhan CN. Metabolomics-Lipidomics of Eicosanoids and Docosanoids Generated By Phagocytes. Current Protocols in Immunology. 2011;CHAPTER:Unit-14.26.
24. Serhan CN, Hong S, Lu Y. Lipid mediator informatics-lipidomics: Novel pathways in mapping resolution. The AAPS Journal. 2006;8(2):E284-E97.
25. Kortz L, Dorow J, Ceglarek U. Liquid chromatography–tandem mass spectrometry for the analysis of eicosanoids and related lipids in human biological matrices: A review. Journal of Chromatography B. 2014;964(Supplement C):1-11.
26. Tsikas D, Zoerner AA. Analysis of eicosanoids by LC-MS/MS and GC-MS/MS: A historical retrospect and a discussion. Journal of Chromatography B. 2014;964(Supplement C):79-88.
27. Deems R, Buczynski MW, Bowers-Gentry R, Harkewicz R, Dennis EA. Detection and Quantitation of Eicosanoids via High Performance Liquid Chromatography-Electrospray Ionization-Mass Spectrometry. Methods in Enzymology. 432: Academic Press; 2007. p. 59-82.
28. Masoodi M, Mir AA, Petasis NA, Serhan CN, Nicolaou A. Simultaneous lipidomic analysis of three families of bioactive lipid mediators leukotrienes, resolvins, protectins and related hydroxy-fatty acids by liquid chromatography/electrospray ionisation tandem mass spectrometry. Rapid Communications in Mass Spectrometry. 2008;22(2):75-83.
29. Niessen WMA. Liquid chromatography--mass spectrometry. Boca Raton: Taylor & Francis; 2007.
30. Stig Pedersen-Bjergaard KER. Legemiddelanalyse: Fagbokforlaget; 2004 (p. 239-268).
31. Cohen Freue GV, Borchers CH. Multiple Reaction Monitoring (MRM). Principles and Application to Coronary Artery Disease. 2012;5(3):378-.

32. Murray KK, Boyd RK, Eberlin MN, Langley GJ, Li L, Naito Y. Definitions of terms relating to mass spectrometry (IUPAC Recommendations 2013). Pure and Applied Chemistry. 2013.
33. Petrovic M, Barceló D. Liquid chromatography–tandem mass spectrometry. Analytical and Bioanalytical Chemistry. 2013;405(18):5857-8.
34. Dass C. Hyphenated Separation Techniques. Fundamentals of Contemporary Mass Spectrometry: John Wiley & Sons, Inc.; 2006. p. 151-94.
35. Hansen TV, Dalli J, Serhan CN. Selective identification of specialized pro-resolving lipid mediators from their biosynthetic double di-oxygenation isomers. RSC Adv. 2016;6(34):28820-9.
36. Vik A, Dalli J, Hansen TV. Recent advances in the chemistry and biology of anti-inflammatory and specialized pro-resolving mediators biosynthesized from n-3 docosapentaenoic acid. Bioorganic & Medicinal Chemistry Letters. 2017;27(11):2259-66.
37. Serhan CN. Mediator lipidomics. Prostaglandins & Other Lipid Mediators. 2005;77(1):4-14.
38. Kuda O, Brezinova M, Rombaldova M, Slavikova B, Posta M, Beier P, et al. Docosahexaenoic Acid–Derived Fatty Acid Esters of Hydroxy Fatty Acids (FAHFAs) With Anti-inflammatory Properties. Diabetes. 2016;65(9):2580-90.
39. MuriGenics. Air Pouch Model (APM); http://www.murigenics.com/in-vivo/disease-models/air-pouch-model-apm/ (accessed 30.11.2017).
40. Serhan CN, Hong S, Gronert K, Colgan SP, Devchand PR, Mirick G, et al. Resolvins: a family of bioactive products of omega-3 fatty acid transformation circuits initiated by aspirin treatment that counter proinflammation signals. J Exp Med. 2002;196(8):1025-37.
41. Drexler DM, Reily MD, Shipkova PA. Advances in mass spectrometry applied to pharmaceutical metabolomics. Analytical and Bioanalytical Chemistry. 2011;399(8):2645-53.
42. Serhan CN, Yang R, Martinod K, Kasuga K, Pillai PS, Porter TF, et al. Maresins: novel macrophage mediators with potent antiinflammatory and proresolving actions. The Journal of Experimental Medicine. 2009;206(1):15-23.
43. Young DC, Vouros P, Holick MF. Gas chromatography—mass spectrometry of conjugated dienes by derivatization with 4-methyl-1,2,4-triazoline-3,5-dione. Journal of Chromatography A. 1990;522:295-302.
44. Shah U, Lay JO, Proctor A. Significance of 4-Phenyl-1,2,4-triazoline-3,5-dione (PTAD) in the GC–MS Identification of Conjugated Fatty Acid Positional Isomers. Journal of the American Oil Chemists' Society. 2013;90(1):155-8.
45. Hedman CJ, Wiebe DA, Dey S, Plath J, Kemnitz JW, Ziegler TE. Development of a sensitive LC/MS/MS method for vitamin D metabolites: 1,25 Dihydroxyvitamin D2&3 measurement using a novel derivatization agent. Journal of Chromatography B. 2014;953-954:62-7.
46. MasterOrganicChemistry.com. Stereochemistry of the Diels-Alder Reaction: MasterOrganicChemistry.com; https://www.masterorganicchemistry.com/2017/11/13/stereochemistry-of-the-diels-alder-reaction/ (accessed 17.12.2017).
47. Tungen JE, Aursnes M, Hansen TV. Stereoselective synthesis of maresin 1. Tetrahedron Letters. 2015;56(14):1843-6.
48. Primdahl KG, Stenstrøm Y, Hansen TV, Vik A. Synthesis of 5-(S)-HETE, 5-(S)-HEPE and (+)-zooxanthellactone: Three hydroxylated polyunsaturated fatty acid metabolites. Chemistry and Physics of Lipids. 2016;196:1-4.

6 Appendix

6.1 UV spectra

Method file : <method not saved>
Information : Default Method
Data File : <data not saved>

Overlaid Spectra:

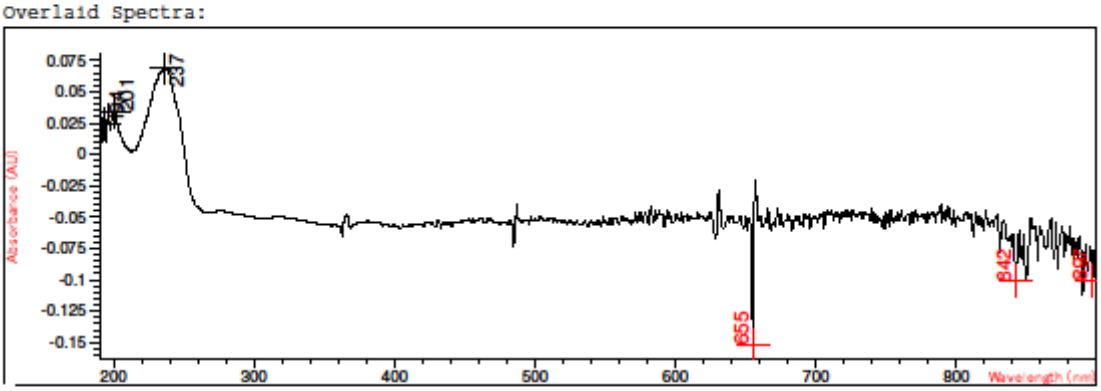

#	Name	Peaks(nm)	Abs(AU)	Valleys(nm)	Abs(AU)
1		237.0	6.8937E-2	655.0	-0.15193
1		201.0	3.4524E-2	897.0	-0.10103
1		194.0	2.4917E-2	842.0	-0.10098

Figure A 1. UV-VIS spectrum of 0.002 mg/ml 17*S*-HDHA in ethanol

Method file : <method not saved>
Information : Default Method
Data File : <data not saved>

Overlaid Spectra:

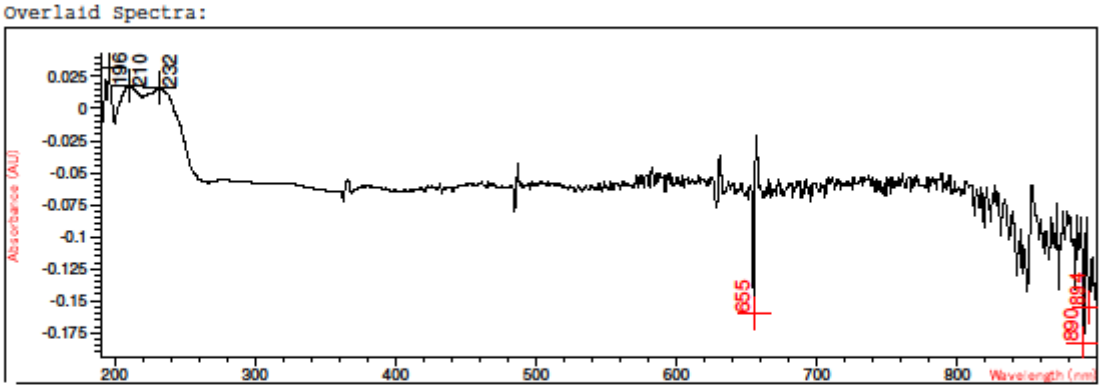

#	Name	Peaks(nm)	Abs(AU)	Valleys(nm)	Abs(AU)
1		196.0	3.1595E-2	890.0	-0.18312
1		210.0	1.7569E-2	655.0	-0.15950
1		232.0	1.5913E-2	894.0	-0.15490

Figure A 2. UV-VIS spectrum of the mixture of 0.002 mg/ml 17*S*-HDHA and *S*-PEM (5% excess) in ethanol right after mixing

Method file : <method not saved>
Information : Default Method
Data File : <data not saved>

Overlaid Spectra:

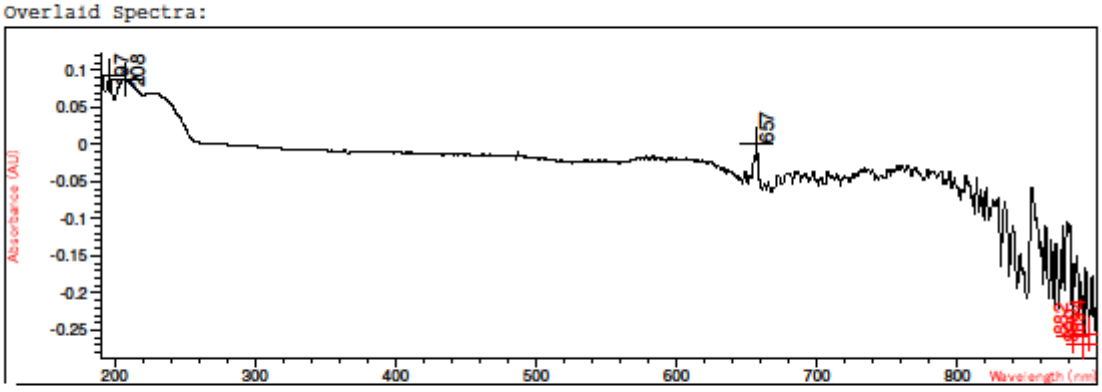

#	Name	Peaks(nm)	Abs(AU)	Valleys(nm)	Abs(AU)
1		197.0	9.2340E-2	890.0	-0.26904
1		208.0	8.8058E-2	882.0	-0.25814
1		657.0	5.2834E-4	894.0	-0.25527

Figure A 3. UV-VIS spectrum of the mixture of 0.002 mg/ml 17*S*-HDHA and *S*-PEM (5% excess) in ethanol after 15 min

Method file : <method not saved>
Information : Default Method
Data File : <data not saved>

Overlaid Spectra:

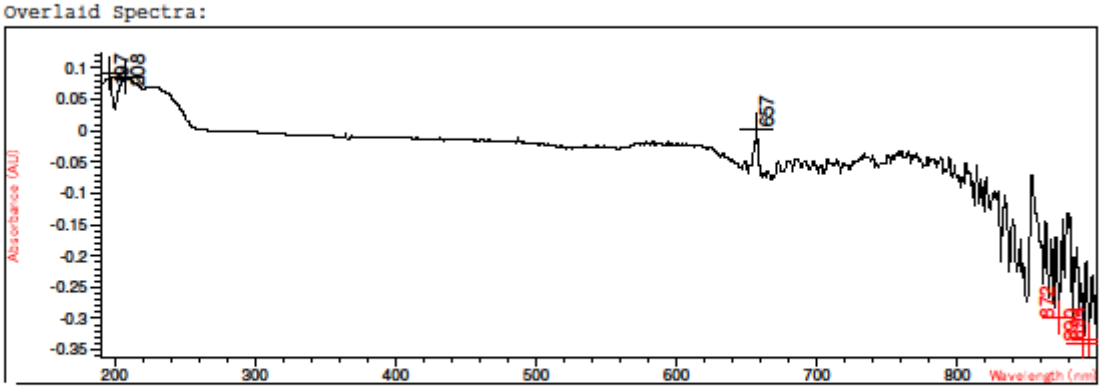

#	Name	Peaks(nm)	Abs(AU)	Valleys(nm)	Abs(AU)
1		197.0	9.2422E-2	890.0	-0.33977
1		208.0	8.5396E-2	894.0	-0.33445
1		657.0	3.8071E-3	872.0	-0.29945

Figure A 4. UV-VIS spectrum of the mixture of 0.002 mg/ml 17*S*-HDHA and *S*-PEM (5% excess) in ethanol after 30 min

Method file : <method not saved>
Information : Default Method
Data File : <data not saved>

Overlaid Spectra:

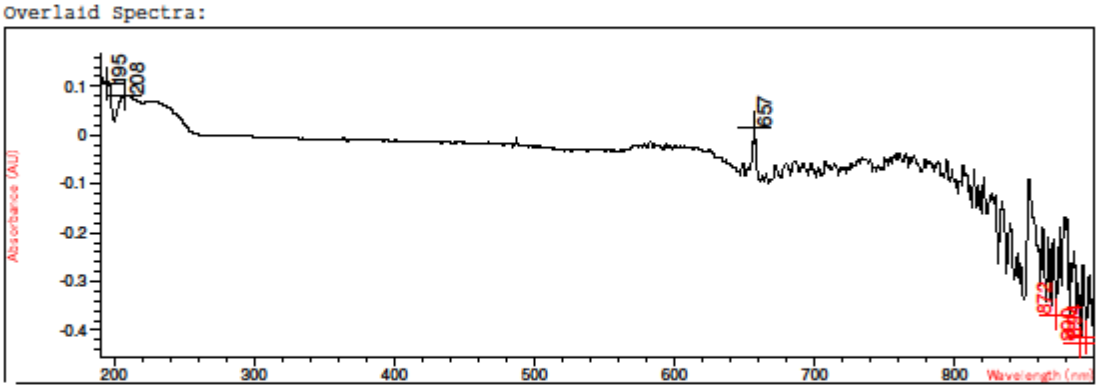

#	Name	Peaks(nm)	Abs(AU)	Valleys(nm)	Abs(AU)
1		195.0	0.10621	890.0	-0.42642
1		208.0	8.3001E-2	894.0	-0.41497
1		657.0	1.5068E-2	872.0	-0.36744

Figure A 5. UV-VIS spectrum of the mixture of 0.002 mg/ml 17*S*-HDHA and *S*-PEM (5% excess) in ethanol after 45 min

Method file : <method not saved>
Information : Default Method
Data File : <data not saved>

Overlaid Spectra:

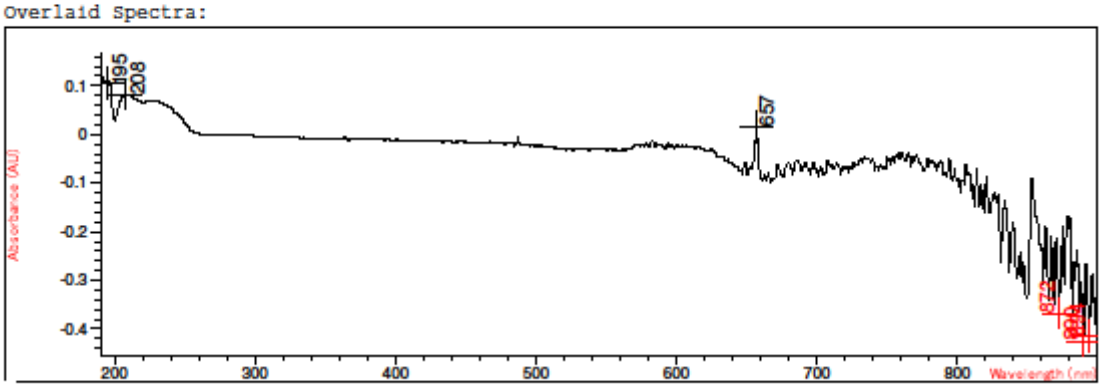

#	Name	Peaks(nm)	Abs(AU)	Valleys(nm)	Abs(AU)
1		195.0	0.10621	890.0	-0.42642
1		208.0	8.3001E-2	894.0	-0.41497
1		657.0	1.5068E-2	872.0	-0.36744

Figure A 6. UV-VIS spectrum of the mixture of 0.002 mg/ml 17*S*-HDHA and *S*-PEM (5% excess) in ethanol after 60 min

Method file : <method not saved>
Information : Default Method
Data File : <data not saved>

Overlaid Spectra:

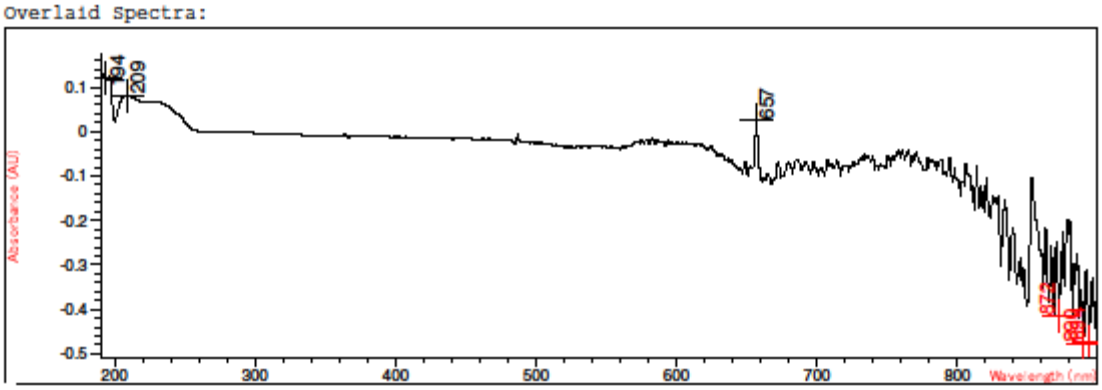

#	Name	Peaks(nm)	Abs(AU)	Valleys(nm)	Abs(AU)
1		194.0	0.12169	890.0	-0.47792
1		209.0	8.1801E-2	894.0	-0.47129
1		657.0	2.4322E-2	872.0	-0.41410

Figure A 7. UV-VIS spectrum of the mixture of 0.002 mg/ml 17*S*-HDHA and *S*-PEM (5% excess) in ethanol after 120 min

Method file : <method not saved>
Information : Default Method
Data File : <data not saved>

Overlaid Spectra:

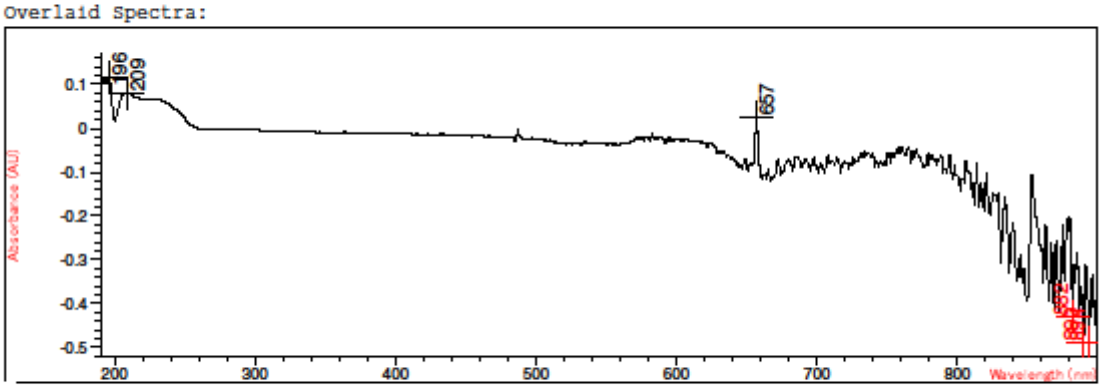

#	Name	Peaks(nm)	Abs(AU)	Valleys(nm)	Abs(AU)
1		196.0	0.11564	890.0	-0.48889
1		209.0	8.1132E-2	894.0	-0.48855
1		657.0	2.6467E-2	882.0	-0.42829

Figure A 8. UV-VIS spectrum of the mixture of 0.002 mg/ml 17*S*-HDHA and *S*-PEM (5% excess) in ethanol after 180 min

Method file : <method not saved>
Information : Default Method
Data File : <data not saved>

Overlaid Spectra:

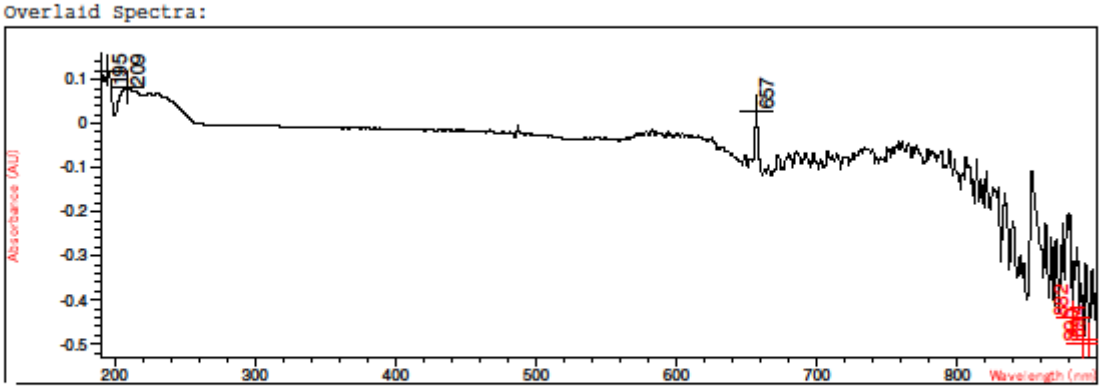

#	Name	Peaks(nm)	Abs(AU)	Valleys(nm)	Abs(AU)
1		195.0	0.12046	890.0	-0.49854
1		209.0	8.0478E-2	894.0	-0.48855
1		657.0	2.7747E-2	882.0	-0.43790

Figure A 9. UV-VIS spectrum of the mixture of 0.002 mg/ml 17*S*-HDHA and *S*-PEM (5% excess) in ethanol after 240 min

Method file : <method not saved>
Information : Default Method
Data File : <data not saved>

Overlaid Spectra:

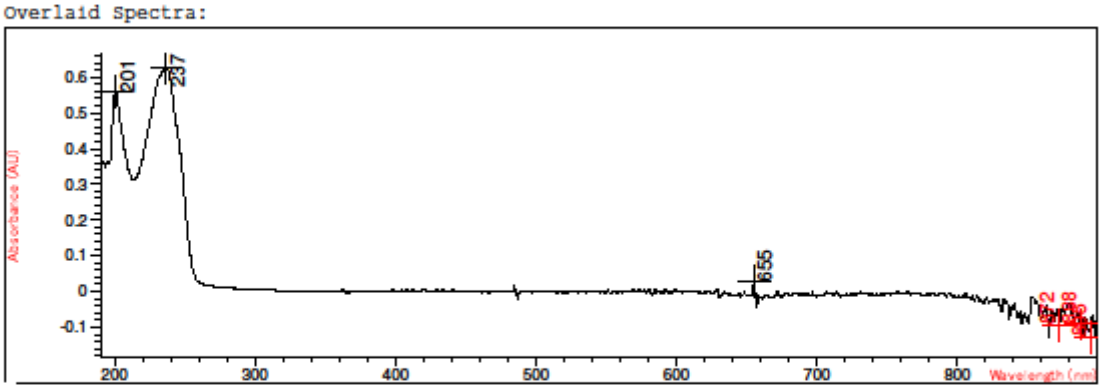

#	Name	Peaks(nm)	Abs(AU)	Valleys(nm)	Abs(AU)
1		237.0	0.62515	895.0	-0.12589
1		201.0	0.55783	872.0	-9.2443E-2
1		655.0	2.7801E-2	888.0	-9.1539E-2

Figure A 10. UV-VIS spectrum of 0.01 mg/ml 17*S*-HDHA in ethanol

Method file : <method not saved>
Information : Default Method
Data File : <data not saved>

Overlaid Spectra:

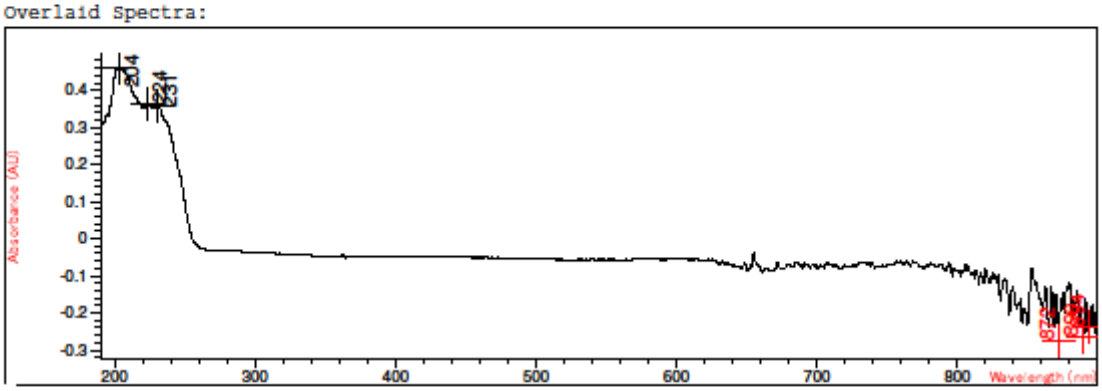

#	Name	Peaks(nm)	Abs(AU)	Valleys(nm)	Abs(AU)
1		204.0	0.45939	872.0	-0.27512
1		224.0	0.36305	890.0	-0.26570
1		231.0	0.35654	894.0	-0.23824

Figure A 11. UV-VIS spectrum of the mixture of 0.01 mg/ml 17*S*-HDHA and *S*-PEM (5% excess) in ethanol right after mixing

Method file : <method not saved>
Information : Default Method
Data File : <data not saved>

Overlaid Spectra:

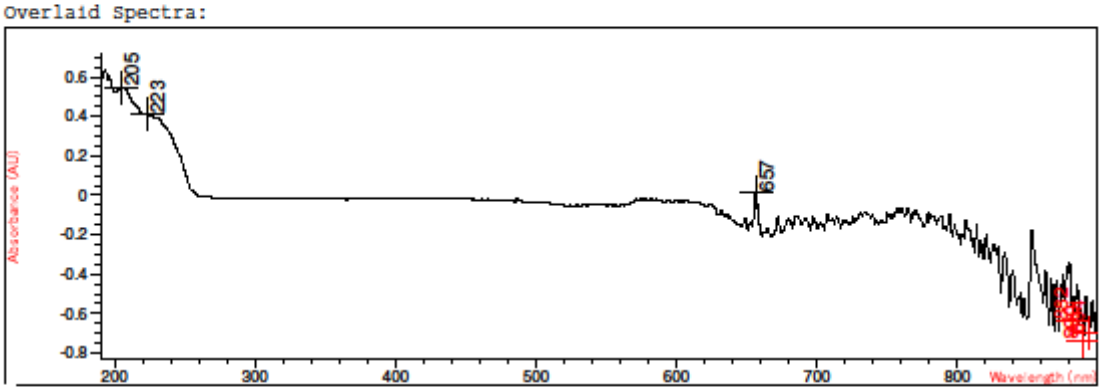

#	Name	Peaks(nm)	Abs(AU)	Valleys(nm)	Abs(AU)
1		205.0	0.54757	890.0	-0.73563
1		223.0	0.41560	894.0	-0.70230
1		657.0	1.2212E-2	882.0	-0.63745

Figure A 12. UV-VIS spectrum of the mixture of 0.01 mg/ml 17*S*-HDHA and *S*-PEM (5% excess) in ethanol after 2h at 40°C

Method file : <method not saved>
Information : Default Method
Data File : C:\USERS\TVH\DESKTOP\BOJANA\161017 SYRE OG PEM 4H 40OC.SD
Created : 10/16/17 15:22:17

Overlaid Spectra:

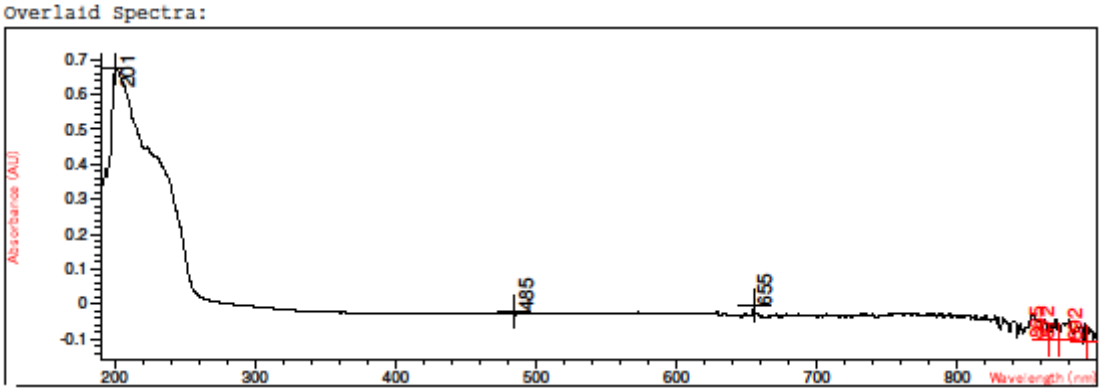

#	Name	Peaks(nm)	Abs(AU)	Valleys(nm)	Abs(AU)
1		201.0	0.67455	892.0	-0.10720
1		655.0	-4.3144E-3	872.0	-0.10203
1		485.0	-2.0291E-2	865.0	-9.9611E-2

Figure A 13. UV-VIS spectrum of the mixture of 0.01 mg/ml 17*S*-HDHA and *S*-PEM (5% excess) in ethanol after 4h at 40°C

Method file : <method not saved>
Information : Default Method
Data File : C:\USERS\TVH\DESKTOP\BOJANA\171017 SYRE OG PEM OVER NATTA.SD
Created : 10/17/17 9:16:20

Overlaid Spectra:

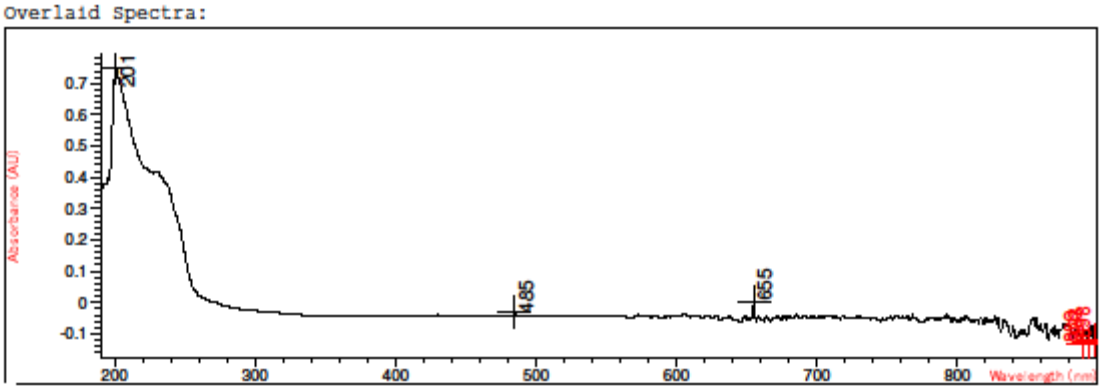

#	Name	Peaks(nm)	Abs(AU)	Valleys(nm)	Abs(AU)
1		201.0	0.74952	889.0	-0.13148
1		655.0	3.3617E-3	893.0	-0.12943
1		485.0	-3.1416E-2	898.0	-0.11841

Figure A 14. UV-VIS spectrum of the mixture of 0.01 mg/ml 17*S*-HDHA and *S*-PEM (5% excess) in ethanol after staying at 40ºC over night

Method file : <method not saved>
Information : Default Method
Data File : C:\USERS\TVH\DESKTOP\BOJANA\171017 SYRE OG PEM 60 OC 2H.SD
Created : 10/17/17 12:01:15

Overlaid Spectra:

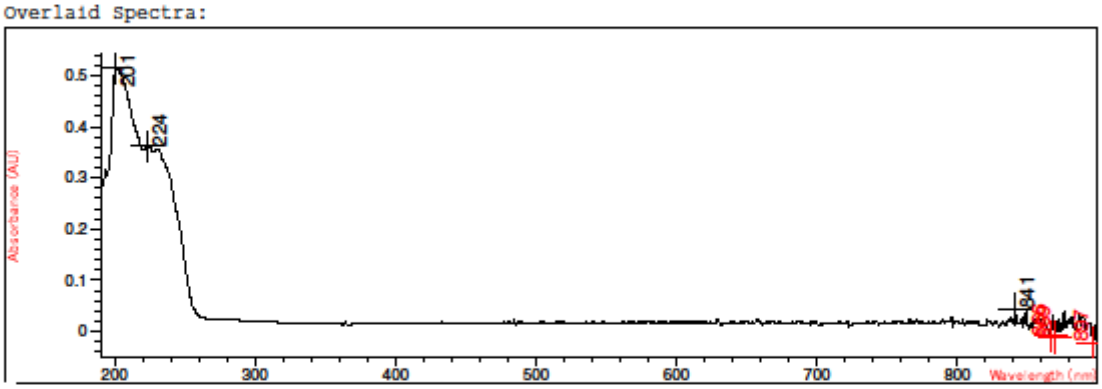

#	Name	Peaks(nm)	Abs(AU)	Valleys(nm)	Abs(AU)
1		201.0	0.51521	897.0	-2.2579E-2
1		224.0	0.36177	869.0	-1.1796E-2
1		841.0	4.3877E-2	866.0	-9.6493E-3

Figure A 15. UV-VIS spectrum of the mixture of 0.01 mg/ml 17*S*-HDHA and *S*-PEM (5% excess) in ethanol after 2h at 60ºC

Method file : <method not saved>
Information : Default Method
Data File : C:\USERS\TVH\DESKTOP\BOJANA\171017 SYRE OG PEM 60 OC 4H.SD
Created : 10/17/17 14:10:25

Overlaid Spectra:

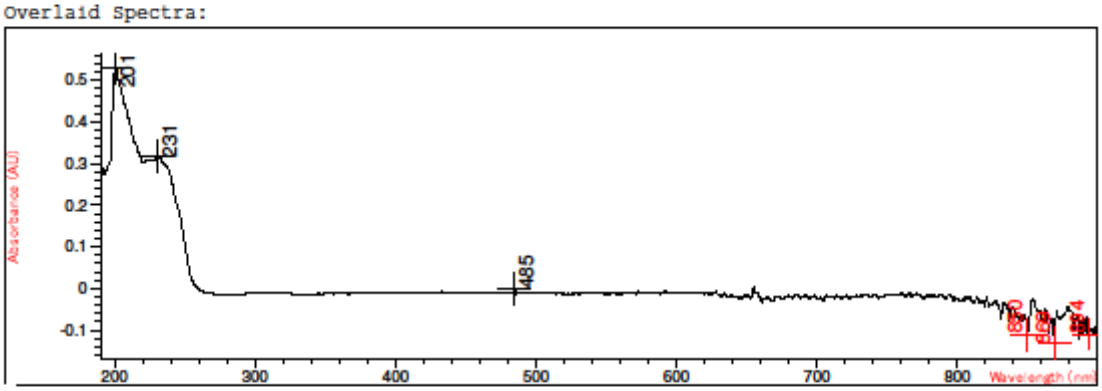

#	Name	Peaks(nm)	Abs(AU)	Valleys(nm)	Abs(AU)
1		201.0	0.52951	869.0	-0.13184
1		231.0	0.31666	850.0	-0.11000
1		485.0	2.8896E-4	894.0	-0.10914

Figure A 16. UV-VIS spectrum of the mixture of 0.01 mg/ml 17*S*-HDHA and *S*-PEM (5% excess) in ethanol after 4h at 60ºC

Method file : <method not saved>
Information : Default Method
Data File : C:\USERS\TVH\DESKTOP\BOJANA\181017 SYRE OG PEM 60 OC OVER NATTA.SD
Created : 10/18/17 9:30:00

Overlaid Spectra:

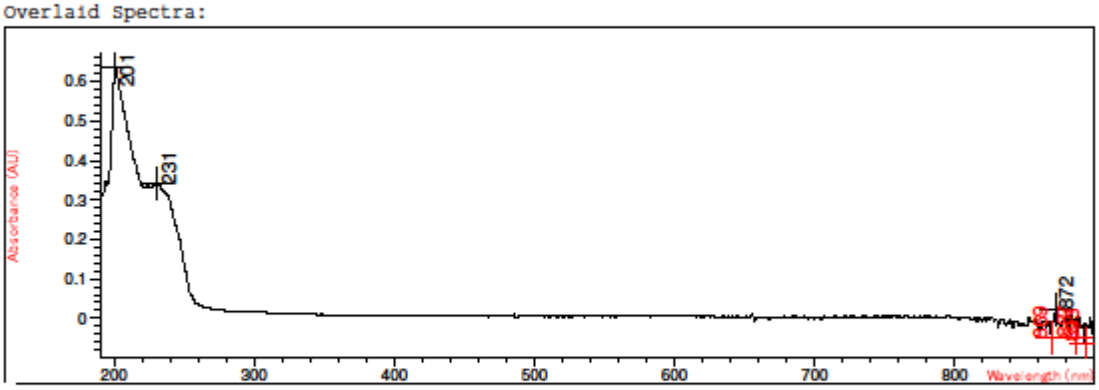

#	Name	Peaks(nm)	Abs(AU)	Valleys(nm)	Abs(AU)
1		201.0	0.63603	893.0	-6.3298E-2
1		231.0	0.34128	869.0	-4.9608E-2
1		872.0	2.1553E-2	887.0	-4.9427E-2

Figure A 17. UV-VIS spectrum of the mixture of 0.01 mg/ml 17*S*-HDHA and *S*-PEM (5% excess) in ethanol after staying at 60oC over night

Method file : <method not saved>
Information : Default Method
Data File : C:\USERS\TVH\DESKTOP\BOJANA\171017 PTAD 0 005338 UG UL .SD
Created : 10/17/17 10:35:26

Overlaid Spectra:

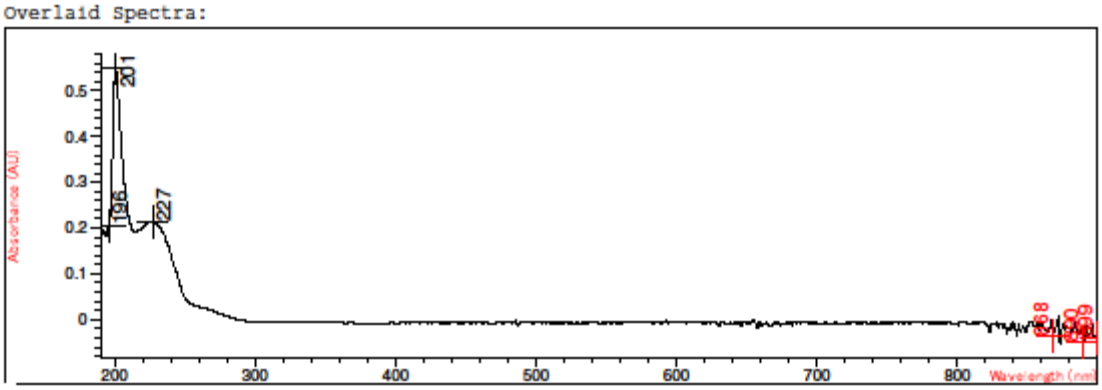

#	Name	Peaks(nm)	Abs(AU)	Valleys(nm)	Abs(AU)
1		201.0	0.55015	890.0	-5.0960E-2
1		227.0	0.21405	899.0	-3.9183E-2
1		196.0	0.20599	868.0	-3.6023E-2

Figure A 18. UV-VIS spectrum of 0,005338 mg/ml PTAD in ethanol

Method file : <method not saved>
Information : Default Method
Data File : C:\USERS\TVH\DESKTOP\BOJANA\171017 SYRE OG PTAD 0 MIN.SD Created : 10/17/17 10:45:57

Overlaid Spectra:

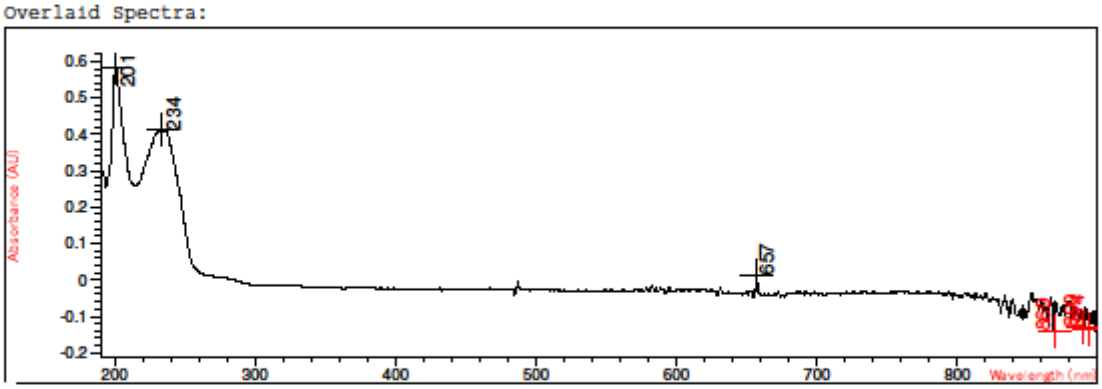

#	Name	Peaks(nm)	Abs(AU)	Valleys(nm)	Abs(AU)
1		201.0	0.58251	869.0	-0.14036
1		234.0	0.41167	894.0	-0.13354
1		657.0	1.1873E-2	890.0	-0.13045

Figure A 19. UV-VIS spectrum of the mixture of 0.01 mg/ml 17*S*-HDHA and PTAD (5% excess) in ethanol right after mixing

Method file : <method not saved>
Information : Default Method
Data File : C:\USERS\TVH\DESKTOP\BOJANA\171017 SYRE OG PTAD 15 MIN.SD
Created : 10/17/17 10:45:57

Overlaid Spectra:

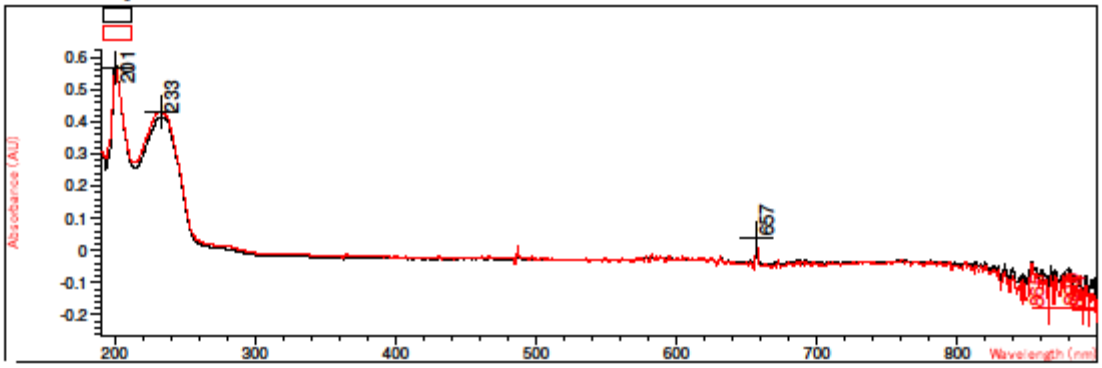

#	Name	Peaks(nm)	Abs(AU)	Valleys(nm)	Abs(AU)
1		201.0	0.58251	869.0	-0.14036
1		234.0	0.41167	894.0	-0.13354
1		657.0	1.1873E-2	890.0	-0.13045
2		201.0	0.56523	894.0	-0.18184
2		233.0	0.43024	890.0	-0.17681
2		657.0	4.1071E-2	865.0	-0.17645

Figure A 20. UV-VIS spectrum of the mixture of 0.01 mg/ml 17*S*-HDHA and PTAD (5% excess) in ethanol after 15 min at room temperature – overlay with the initial UV spectrum

Method file : <method not saved>
Information : Default Method
Data File : C:\USERS\TVH\DESKTOP\BOJANA\171017 SYRE OG PTAD 30 MIN.SD
Created : 10/17/17 11:16:28

Overlaid Spectra:

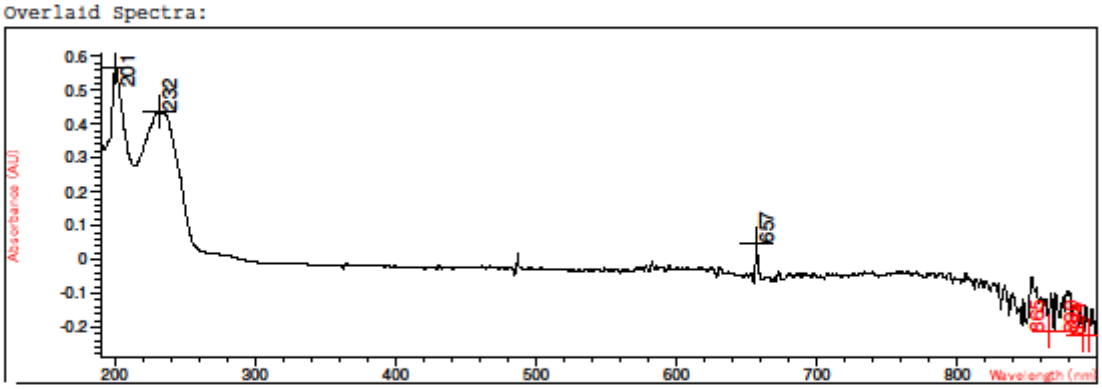

#	Name	Peaks(nm)	Abs(AU)	Valleys(nm)	Abs(AU)
1		201.0	0.56668	894.0	-0.22531
1		232.0	0.43562	890.0	-0.22315
1		657.0	4.5038E-2	865.0	-0.21303

Figure A 21. UV-VIS spectrum of the mixture of 0.01 mg/ml 17*S*-HDHA and PTAD (5% excess) in ethanol after 30 min at room temperature

```
Method file :         <method not saved>
Information :         Default Method
Data File   :         C:\USERS\TVH\DESKTOP\BOJANA\171017 SYRE OG PTAD 60 MIN.SD
                      Created : 10/17/17 11:45:47
```

Overlaid Spectra:

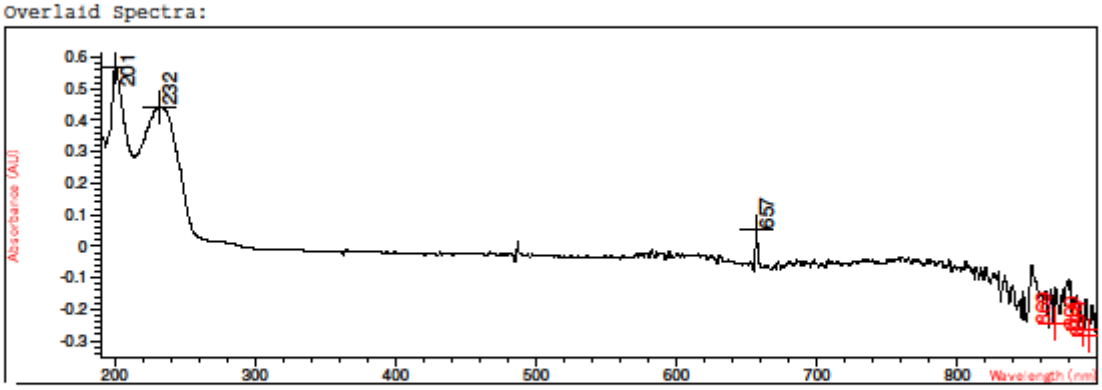

#	Name	Peaks(nm)	Abs(AU)	Valleys(nm)	Abs(AU)
1		201.0	0.56793	894.0	-0.28330
1		232.0	0.44214	890.0	-0.26740
1		657.0	5.0401E-2	869.0	-0.24779

Figure A 22. UV-VIS spectrum of the mixture of 0.01 mg/ml 17*S*-HDHA and PTAD (5% excess) in ethanol after 60 min at room temperature

```
Method file :         <method not saved>
Information :         Default Method
Data File   :         <data not saved>
```

Overlaid Spectra:

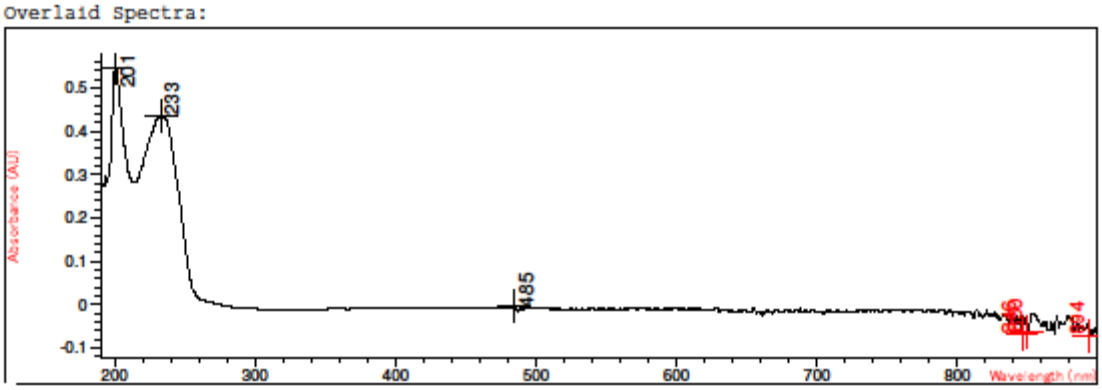

#	Name	Peaks(nm)	Abs(AU)	Valleys(nm)	Abs(AU)
1		201.0	0.54534	894.0	-7.1356E-2
1		233.0	0.43549	846.0	-6.8566E-2
1		485.0	-3.6116E-3	850.0	-6.5110E-2

Figure A 23. UV-VIS spectrum of the mixture of 0.01 mg/ml 17*S*-HDHA and PTAD (5% excess) in ethanol after 120 min at room temperature

Method file : <method not saved>
Information : Default Method
Data File : C:\USERS\TVH\DESKTOP\BOJANA\171017 SYRE OG PTAD 180 MIN.SD
Created : 10/17/17 13:48:03

Overlaid Spectra:

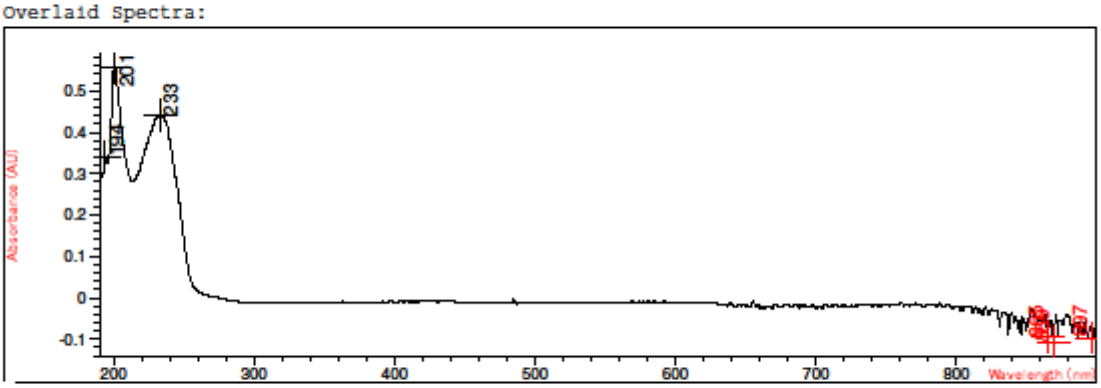

#	Name	Peaks(nm)	Abs(AU)	Valleys(nm)	Abs(AU)
1		201.0	0.55635	869.0	-0.10707
1		233.0	0.43944	897.0	-9.5826E-2
1		194.0	0.34193	865.0	-9.4263E-2

Figure A 24. UV-VIS spectrum of the mixture of 0.01 mg/ml 17*S*-HDHA and PTAD (5% excess) in ethanol after 180 min at room temperature

Method file : <method not saved>
Information : Default Method
Data File : C:\USERS\TVH\DESKTOP\BOJANA\181017 PTAD I CH2CL2 0 005358 UG UL.SD
Created : 10/18/17 13:47:31

Overlaid Spectra:

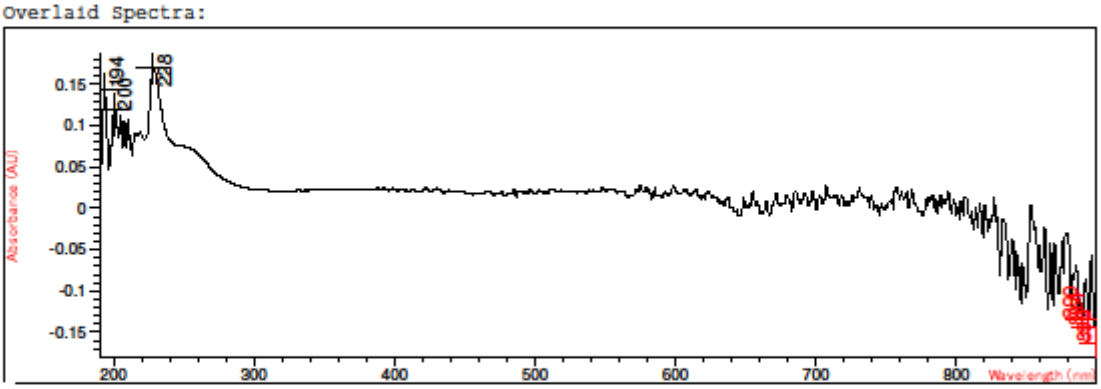

#	Name	Peaks(nm)	Abs(AU)	Valleys(nm)	Abs(AU)
1		228.0	0.17025	899.0	-0.16308
1		194.0	0.14451	894.0	-0.14391
1		200.0	0.11947	890.0	-0.13454

Figure A 25. UV-VIS spectrum of PTAD 0.005358 mg/ml in dichloromethane

Method file : <method not saved>
Information : Default Method
Data File : C:\USERS\TVH\DESKTOP\BOJANA\181017 SYRE I CH2CL2 0 01 UG UL.SD
Created : 10/18/17 13:54:15

Overlaid Spectra:

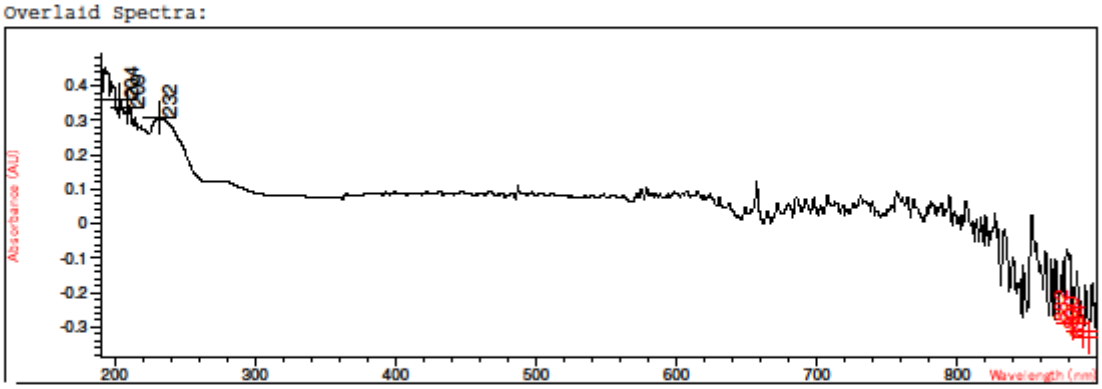

#	Name	Peaks(nm)	Abs(AU)	Valleys(nm)	Abs(AU)
1		204.0	0.36208	894.0	-0.33099
1		209.0	0.33577	890.0	-0.31053
1		232.0	0.30705	882.0	-0.28771

Figure A 26. UV-VIS spectrum of 0.01 mg/ml 17*S*-HDHA in dichloromethane

Method file : <method not saved>
Information : Default Method
Data File : C:\USERS\TVH\DESKTOP\BOJANA\181017 SYRE OG PTAD I CH2CL2 15 MIN.SD
Created : 10/18/17 14:14:16

Overlaid Spectra:

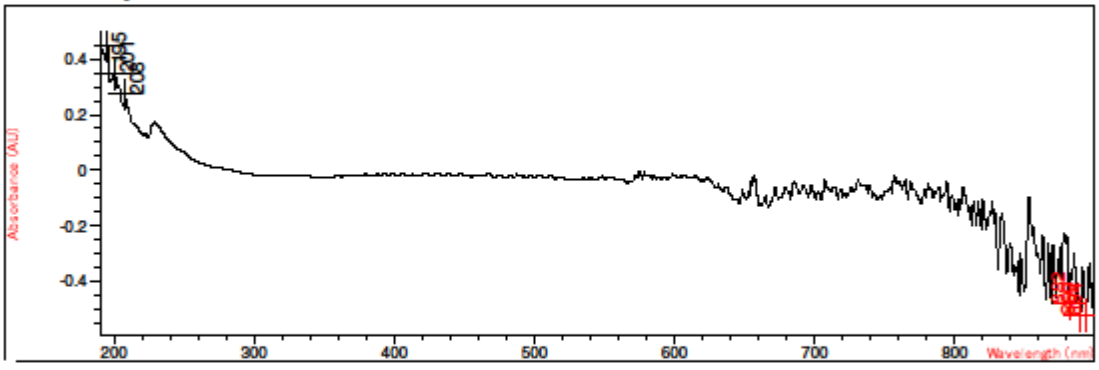

#	Name	Peaks(nm)	Abs(AU)	Valleys(nm)	Abs(AU)
1		195.0	0.44675	890.0	-0.52284
1		201.0	0.34792	894.0	-0.52132
1		208.0	0.27244	882.0	-0.47860

Figure A 27. UV-VIS spectrum of the mixture of 0.01 mg/ml 17*S*-HDHA and PTAD (5% excess) in dichloromethane after 15 min at room temperature

Method file : <method not saved>
Information : Default Method
Data File : C:\USERS\TVH\DESKTOP\BOJANA\181017 SYRE OG PTAD I CH2CL2 30 MIN.SD
Created : 10/18/17 14:26:24

Overlaid Spectra:

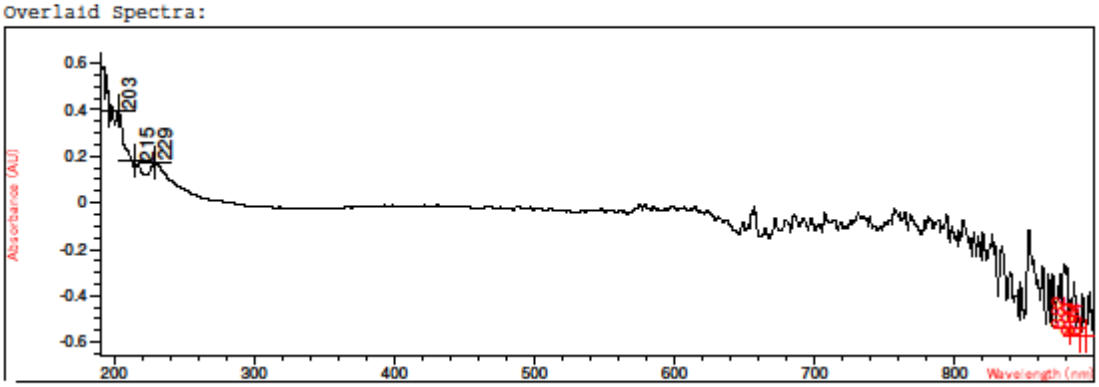

#	Name	Peaks(nm)	Abs(AU)	Valleys(nm)	Abs(AU)
1		203.0	0.39772	890.0	-0.57611
1		215.0	0.18139	894.0	-0.57403
1		229.0	0.17328	882.0	-0.54124

Figure A 28. UV-VIS spectrum of the mixture of 0.01 mg/ml 17*S*-HDHA and PTAD (5% excess) in dichloromethane after 30 min at room temperature

Method file : <method not saved>
Information : Default Method
Data File : C:\USERS\TVH\DESKTOP\BOJANA\181017 SYRE OG PTAD I CH2CL2 60 MIN.SD
Created : 10/18/17 15:00:20

Overlaid Spectra:

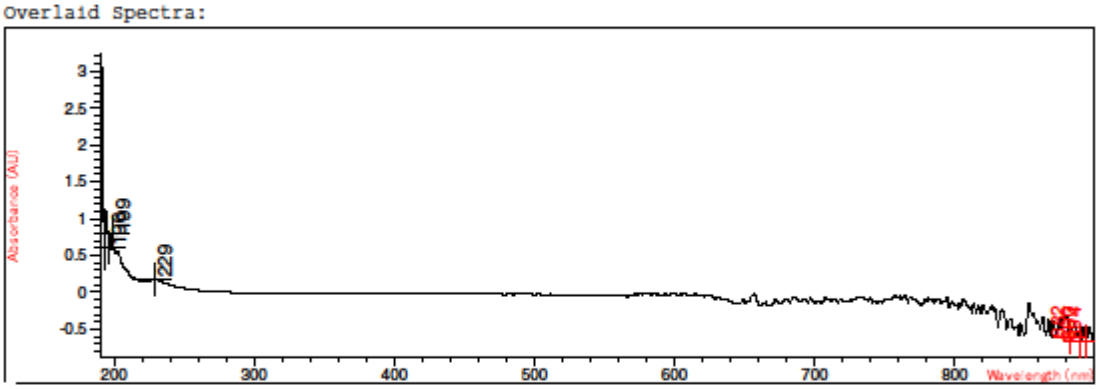

#	Name	Peaks(nm)	Abs(AU)	Valleys(nm)	Abs(AU)
1		199.0	0.80075	890.0	-0.66613
1		196.0	0.61137	894.0	-0.66005
1		229.0	0.18130	882.0	-0.61878

Figure A 29. UV-VIS spectrum of the mixture of 0.01 mg/ml 17*S*-HDHA and PTAD (5% excess) in dichloromethane after 60 min at room temperature

Method file : <method not saved>
Information : Default Method
Data File : C:\USERS\TVH\DESKTOP\BOJANA\181017 SYRE OG PTAD I CH2CL2 120 MIN.SD
Created : 10/18/17 16:02:35

Overlaid Spectra:

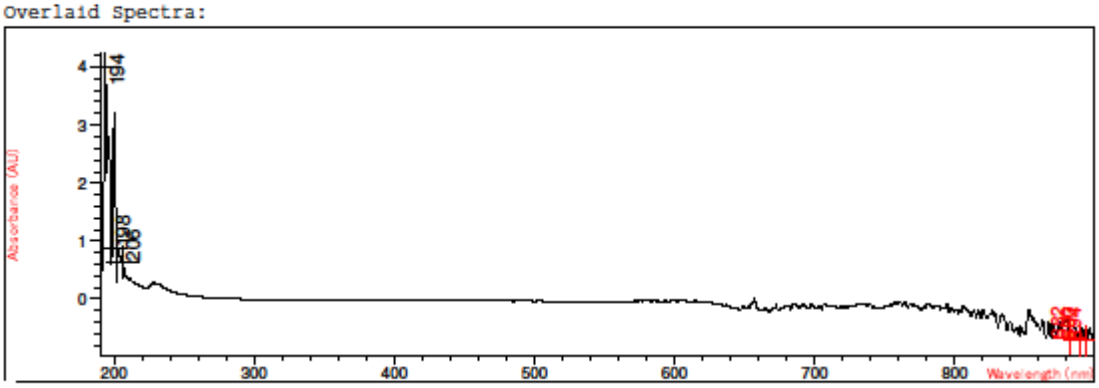

#	Name	Peaks(nm)	Abs(AU)	Valleys(nm)	Abs(AU)
1		194.0	4.00000	890.0	-0.72111
1		198.0	0.87963	894.0	-0.72016
1		206.0	0.62635	882.0	-0.66857

Figure A 30. UV-VIS spectrum of the mixture of 0.01 mg/ml 17*S*-HDHA and PTAD (5% excess) in dichloromethane after 120 min at room temperature

Method file : <method not saved>
Information : Default Method
Data File : C:\USERS\TVH\DESKTOP\BOJANA\241017 SYRE OG S-PEM På 80 GRADER 2 TIMER.SD Created : 10/24/17 15:36:15

Overlaid Spectra:

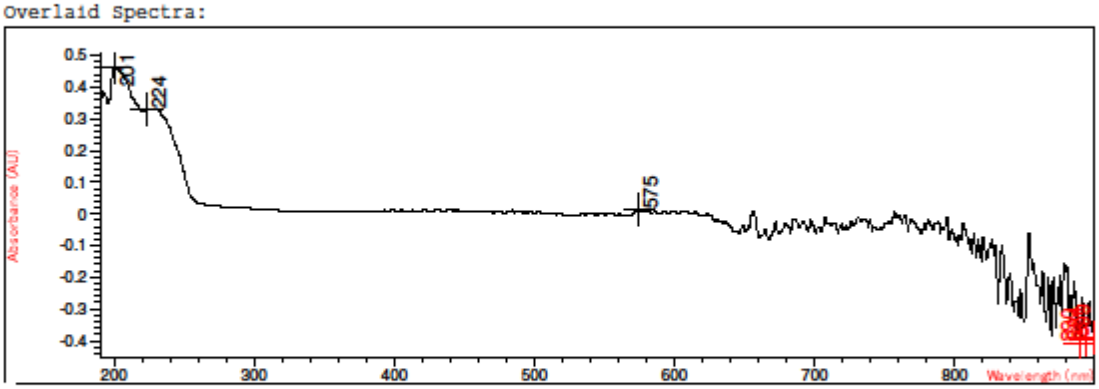

#	Name	Peaks(nm)	Abs(AU)	Valleys(nm)	Abs(AU)
1		201.0	0.46269	890.0	-0.40876
1		224.0	0.33281	894.0	-0.39794
1		575.0	1.5368E-2	899.0	-0.39009

Figure A 31. UV-VIS spectrum of the mixture of 0.01 mg/ml 17*S*-HDHA and *S*-PEM (10% excess) in ethanol after 2h at 80°C

Method file : <method not saved>
Information : Default Method
Data File : C:\USERS\TVH\DESKTOP\BOJANA\251017 SYRE OG PTAD (NY) PÅ 30 GRADER 2 TIMER.SD Created : 10/25/17 13:43:14

Overlaid Spectra:

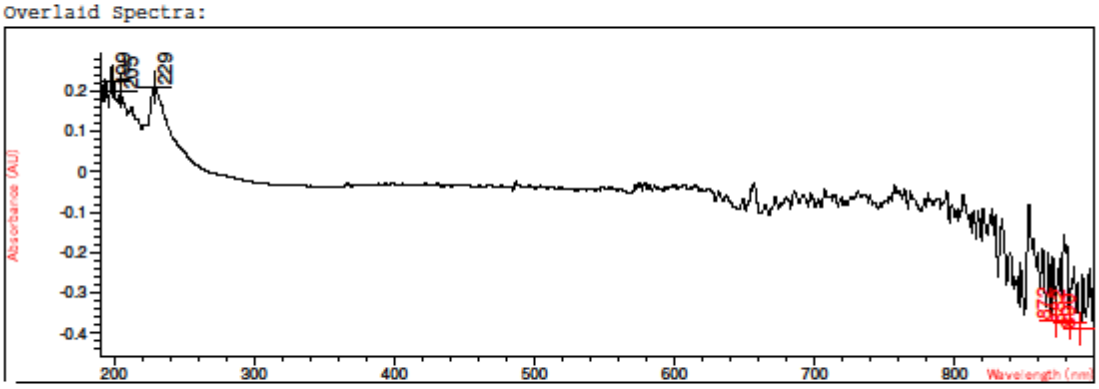

#	Name	Peaks(nm)	Abs(AU)	Valleys(nm)	Abs(AU)
1		199.0	0.22596	890.0	-0.38887
1		229.0	0.21080	882.0	-0.37407
1		205.0	0.20037	872.0	-0.36732

Figure A 32. UV-VIS spectrum of the mixture of 0.01 mg/ml 17*S*-HDHA and freshly made PTAD (5% excess) in dichloromethane after 2h at 35ºC

Method file : <method not saved>
Information : Default Method
Data File : C:\USERS\TVH\DESKTOP\BOJANA\261017 MAR1 I MEOH 0-1 MG ML.SD
Created : 10/26/17 10:50:58

Overlaid Spectra:

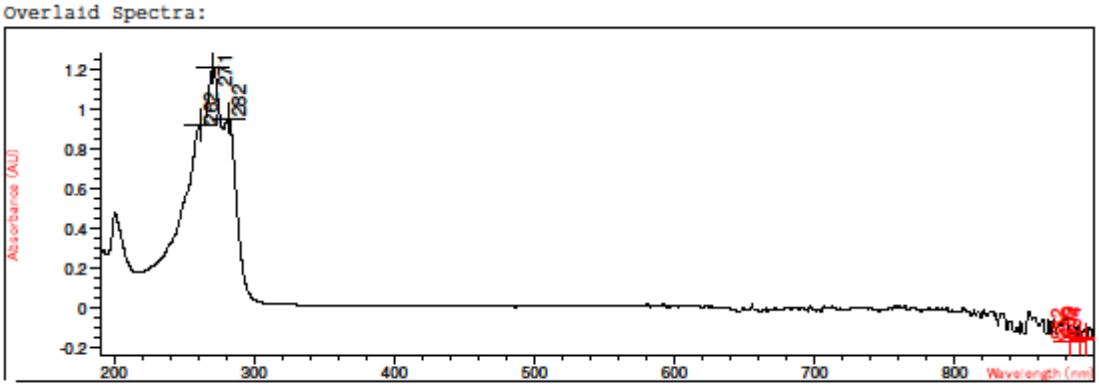

#	Name	Peaks(nm)	Abs(AU)	Valleys(nm)	Abs(AU)
1		271.0	1.21230	882.0	-0.16571
1		282.0	0.95815	894.0	-0.15836
1		262.0	0.92097	889.0	-0.15077

Figure A 33. UV-VIS spectrum of 0.1 mg/ml MaR1 in methanol

Method file : <method not saved>
Information : Default Method
Data File : C:\USERS\TVH\DESKTOP\BOJANA\261017 MAR1 OG PTAD I MEOH.SD
Created : 10/26/17 13:49:50

Overlaid Spectra:

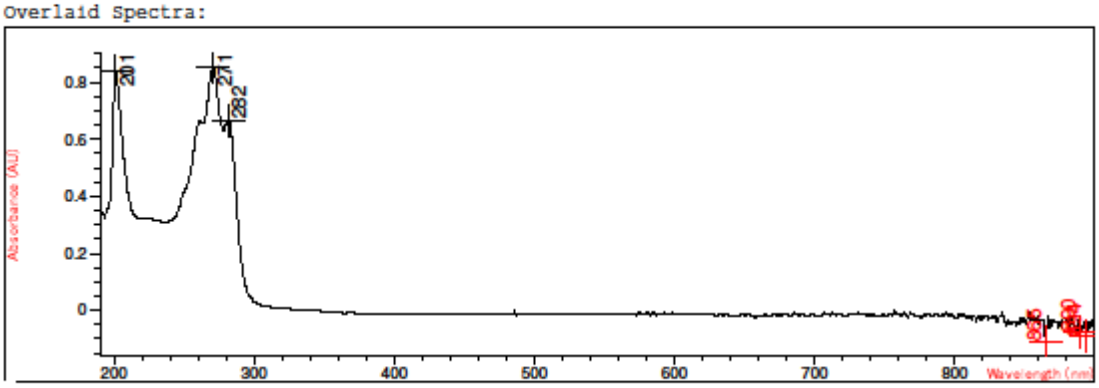

#	Name	Peaks(nm)	Abs(AU)	Valleys(nm)	Abs(AU)
1		271.0	0.85298	865.0	-0.10985
1		201.0	0.84067	894.0	-9.0177E-2
1		282.0	0.66550	890.0	-7.6416E-2

Figure A 34. UV-VIS spectrum of the mixture of 0.1 mg/ml MaR1 and PTAD (10% excess) in methanol

Method file : <method not saved>
Information : Default Method
Data File : C:\USERS\TVH\DESKTOP\BOJANA\261017 MAR1 OG PTAD HØY C I MEOH.SD
Created : 10/26/17 15:07:01

Overlaid Spectra:

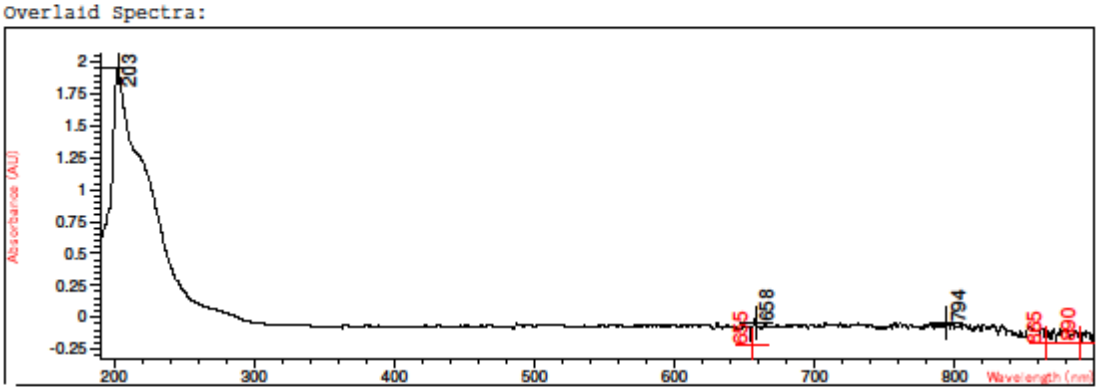

#	Name	Peaks(nm)	Abs(AU)	Valleys(nm)	Abs(AU)
1		203.0	1.95560	655.0	-0.21543
1		658.0	-3.9243E-2	865.0	-0.20671
1		794.0	-4.2460E-2	890.0	-0.20138

Figure A 35. UV-VIS spectrum of the mixture of 0.1 mg/ml MaR1 and PTAD (300% excess) in methanol

Method file : <method not saved>
Information : Default Method
Data File : C:\USERS\TVH\DESKTOP\BOJANA\261017 MAR1 OG S-PEM I MEOH.SD
Created : 10/26/17 13:55:39

Overlaid Spectra:

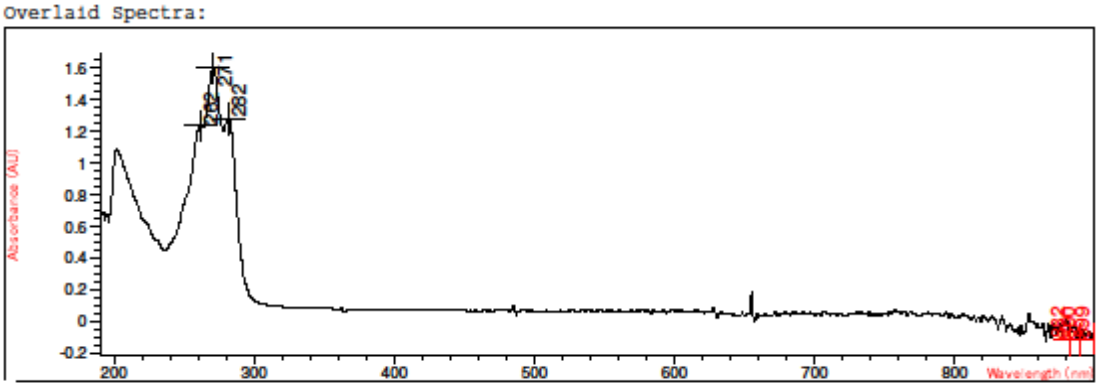

#	Name	Peaks(nm)	Abs(AU)	Valleys(nm)	Abs(AU)
1		271.0	1.60470	890.0	-0.11427
1		282.0	1.28410	882.0	-0.10550
1		262.0	1.23620	899.0	-0.10435

Figure A 36. UV-VIS spectrum of the mixture of 0.1 mg/ml MaR1 and *S*-PEM (10% excess) in methanol

Method file : <method not saved>
Information : Default Method
Data File : C:\USERS\TVH\DESKTOP\BOJANA\261017 MAR1 OG S-PEM HøY C I MEOH.SD
Created : 10/26/17 15:11:09

Overlaid Spectra:

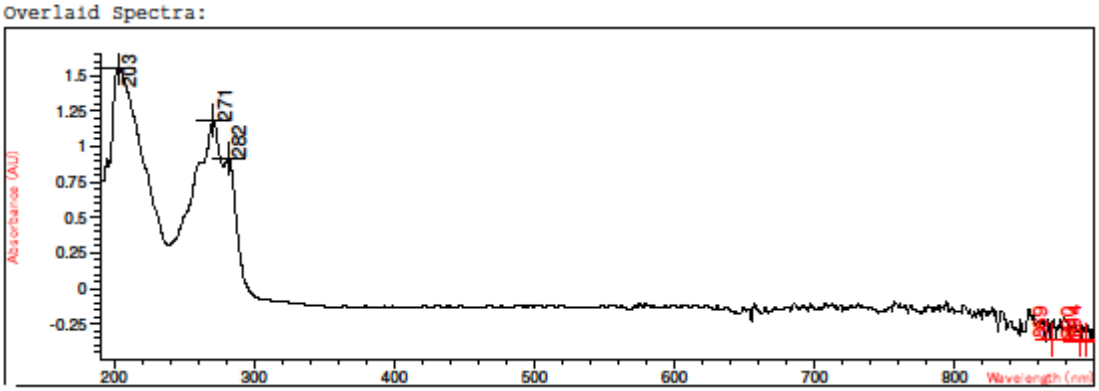

#	Name	Peaks(nm)	Abs(AU)	Valleys(nm)	Abs(AU)
1		203.0	1.55270	890.0	-0.36718
1		271.0	1.18100	894.0	-0.35902
1		282.0	0.91505	869.0	-0.35375

Figure A 37. UV-VIS spectrum of the mixture of 0.1 mg/ml MaR1 and *S*-PEM (300% excess) in methanol

Method file : <method not saved>
Information : Default Method
Data File : C:\USERS\TVH\DESKTOP\BOJANA\261017 MAR1 OG S-PEM I MEOH 1000%
OVERSKUDD.SD Created : 10/26/17 15:38:39

Overlaid Spectra:

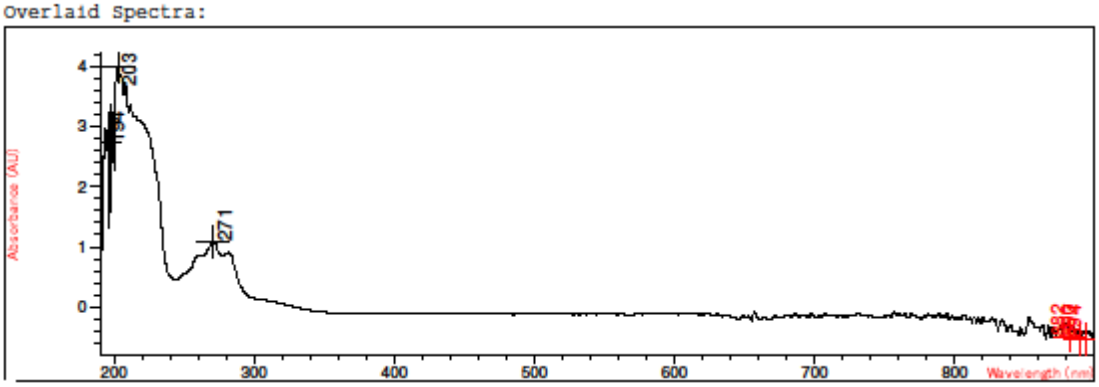

#	Name	Peaks(nm)	Abs(AU)	Valleys(nm)	Abs(AU)
1		203.0	4.00000	890.0	-0.53739
1		194.0	2.72580	894.0	-0.52904
1		271.0	1.08760	882.0	-0.49342

Figure A 38. UV-VIS spectrum of the mixture of 0.1 mg/ml MaR1 and *S*-PEM (1000% excess) in methanol

Method file : <method not saved>
Information : Default Method
Data File : C:\USERS\TVH\DESKTOP\BOJANA\311017 OXO 0 1 UG UL I CH2CL2.SD
Created : 10/31/17 12:32:00

Overlaid Spectra:

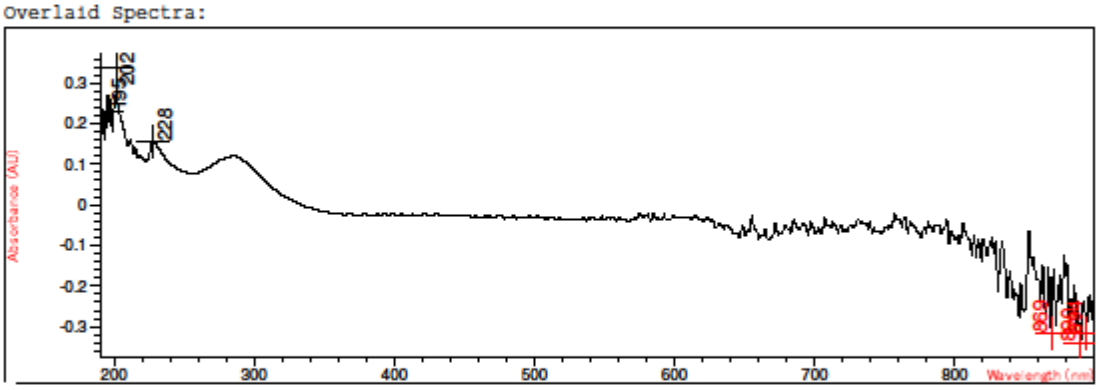

#	Name	Peaks(nm)	Abs(AU)	Valleys(nm)	Abs(AU)
1		202.0	0.33755	890.0	-0.34045
1		195.0	0.23063	894.0	-0.31742
1		228.0	0.15737	869.0	-0.31587

Figure A 39. UV-VIS spectrum of 0.1 mg/ml 17-oxo-DHA in dichloromethane

Method file : <method not saved>
Information : Default Method
Data File : C:\USERS\TVH\DESKTOP\BOJANA\011117 OXO 40UL (2 UG) OG PTAD 10%
OVERSKUDD I CH2CL2.SD Created : 11/1/17 13:22:11

Overlaid Spectra:

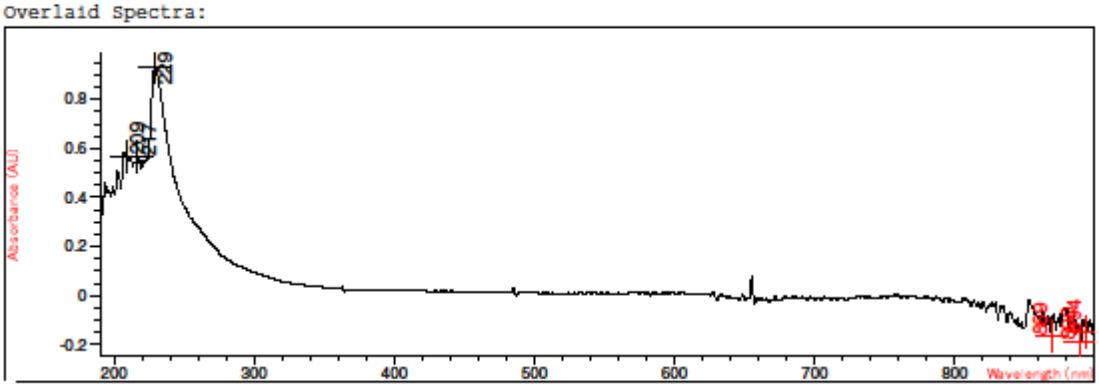

#	Name	Peaks(nm)	Abs(AU)	Valleys(nm)	Abs(AU)
1		229.0	0.93034	890.0	-0.18728
1		217.0	0.56864	869.0	-0.16166
1		209.0	0.56827	894.0	-0.15039

Figure A 40. UV-VIS spectrum of the mixture of 17-oxo-DHA and PTAD (10% excess) in dichloromethane

Method file : <method not saved>
Information : Default Method
Data File : C:\USERS\TVH\DESKTOP\BOJANA\011117 OXO 40UL (2 UG) OG PTAD 110%
OVERSKUDD I CH2CL2.SD Created : 11/1/17 14:44:51

Overlaid Spectra:

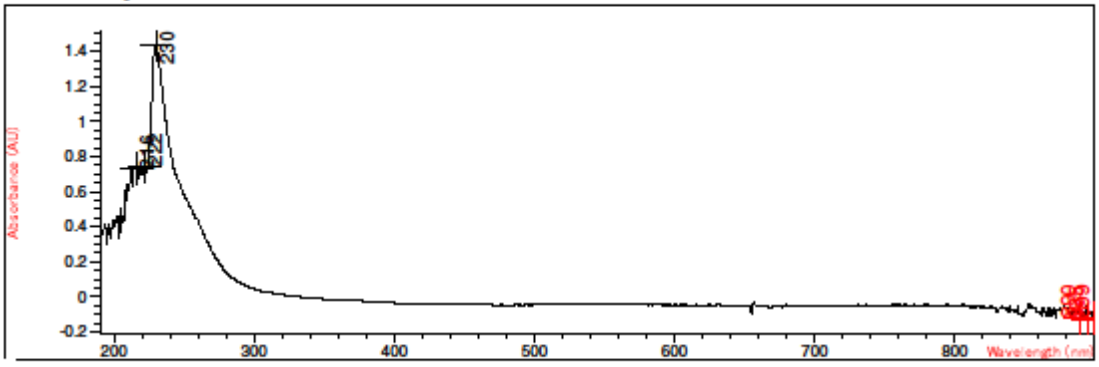

#	Name	Peaks(nm)	Abs(AU)	Valleys(nm)	Abs(AU)
1		230.0	1.43500	895.0	-0.12996
1		222.0	0.74211	890.0	-0.12187
1		216.0	0.73162	899.0	-0.11863

Figure A 41. UV-VIS spectrum of the mixture of 17-oxo-DHA and PTAD (110% excess) in dichloromethane

Method file : <method not saved>
Information : Default Method
Data File : C:\USERS\TVH\DESKTOP\BOJANA\011117 PTAD 20 UL (0 1 UG-UL) I CH2CL2.SD Created : 11/1/17 14:53:47

Overlaid Spectra:

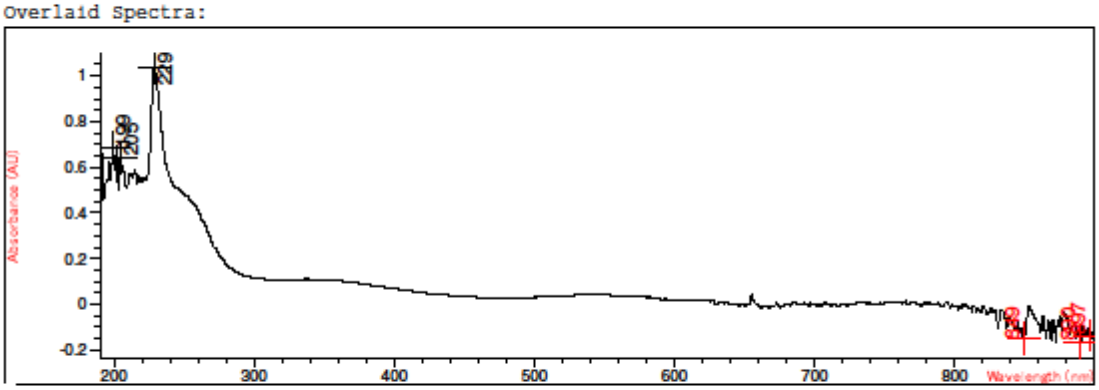

#	Name	Peaks(nm)	Abs(AU)	Valleys(nm)	Abs(AU)
1		229.0	1.03580	890.0	-0.16594
1		199.0	0.68140	849.0	-0.15053
1		205.0	0.64425	897.0	-0.13573

Figure A 42. UV-VIS spectrum of 0.1 mg/ml PTAD in dichloromethane

Method file : <method not saved>
Information : Default Method
Data File : C:\USERS\TVH\DESKTOP\BOJANA\011117 OXO 40UL (2 UG) OG S-PEM 10% OVERSKUDD I CH2CL2.SD Created : 11/1/17 13:13:19

Overlaid Spectra:

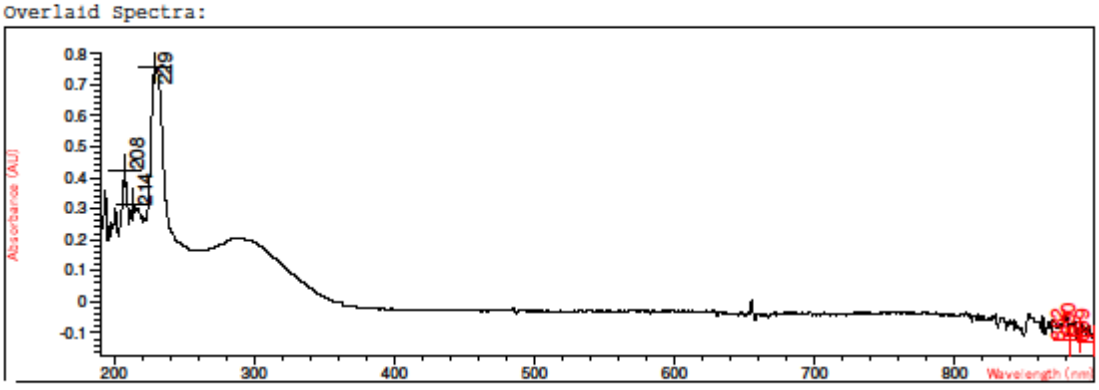

#	Name	Peaks(nm)	Abs(AU)	Valleys(nm)	Abs(AU)
1		229.0	0.75598	899.0	-0.12854
1		208.0	0.42347	882.0	-0.12644
1		214.0	0.31279	890.0	-0.11244

Figure A 43. UV-VIS spectrum of the mixture of 17-oxo-DHA and *S*-PEM (10% excess) in dichloromethane

Method file : <method not saved>
Information : Default Method
Data File : C:\USERS\TVH\DESKTOP\BOJANA\011117 OXO 40UL (2 UG) OG S-PEM 110%
OVERSKUDD I CH2CL2.SD Created : 11/1/17 14:40:19

Overlaid Spectra:

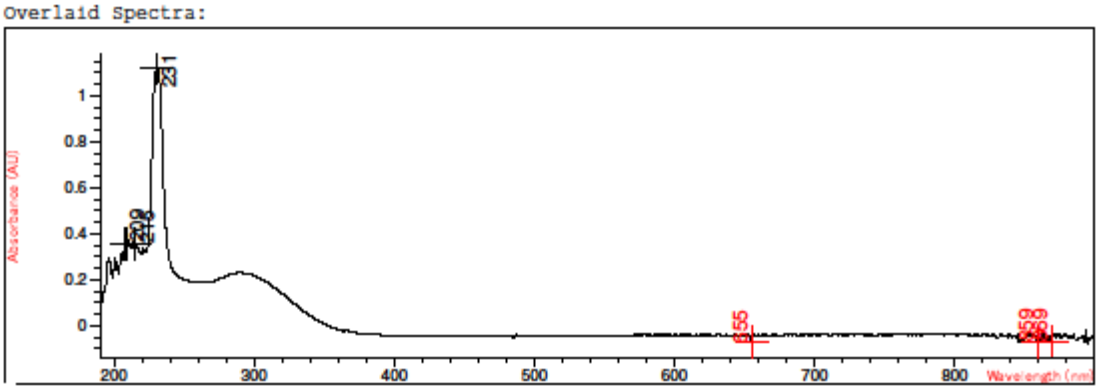

#	Name	Peaks(nm)	Abs(AU)	Valleys(nm)	Abs(AU)
1		231.0	1.11950	655.0	-7.0727E-2
1		209.0	0.35645	859.0	-6.6779E-2
1		215.0	0.35583	869.0	-6.6014E-2

Figure A 44. UV-VIS spectrum of the mixture of 17-oxo-DHA and *S*-PEM (110% excess) in dichloromethane

Method file : <method not saved>
Information : Default Method
Data File : C:\USERS\TVH\DESKTOP\BOJANA\011117 S-PEM 20 UL (0 1 UG-UL) I
CH2CL2.SD Created : 11/1/17 14:49:29

Overlaid Spectra:

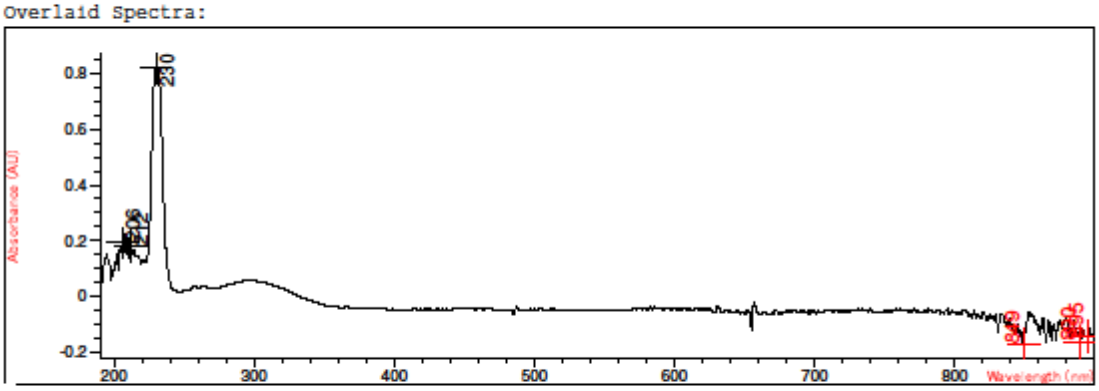

#	Name	Peaks(nm)	Abs(AU)	Valleys(nm)	Abs(AU)
1		230.0	0.82095	849.0	-0.17016
1		206.0	0.19265	890.0	-0.16172
1		212.0	0.17905	895.0	-0.14233

Figure A 45. UV-VIS spectrum of 0.1 mg/ml *S*-PEM in dichloromethane

```
Method file :         <method not saved>
Information :         Default Method
Data File   :         C:\USERS\TVH\DESKTOP\BOJANA\080318 PETAD 20 MCL OG 80 MCL CH2CL2.SD
                         Created : 3/8/18 12:40:08
```

Overlaid Spectra:

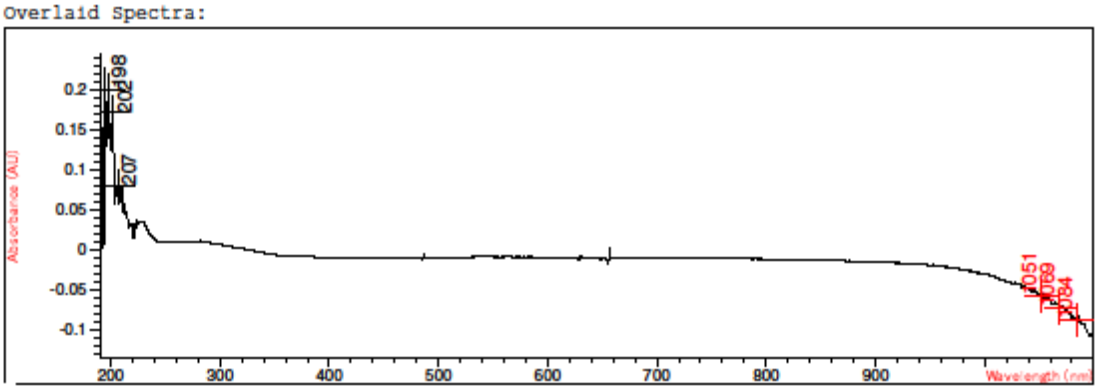

#	Name	Peaks(nm)	Abs(AU)	Valleys(nm)	Abs(AU)
1		198.0	0.19954	1084.0	-8.6522E-2
1		202.0	0.17142	1069.0	-7.2158E-2
1		207.0	7.9444E-2	1051.0	-5.6872E-2

Figure A 46. UV-VIS spectrum of *S*-PETAD in dichloromethane

```
Method file :         <method not saved>
Information :         Default Method
Data File   :         C:\USERS\TVH\DESKTOP\BOJANA\080318 17-RAC 0 02 MG-ML OG PETAD ETTER
                      3 TIMER ROM T.SD     Created : 3/8/18 15:17:14
```

Overlaid Spectra:

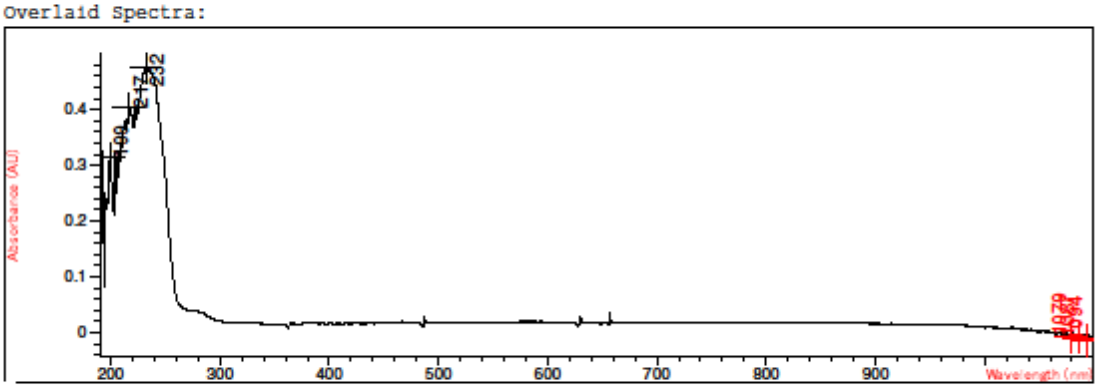

#	Name	Peaks(nm)	Abs(AU)	Valleys(nm)	Abs(AU)
1		232.0	0.47528	1094.0	-1.4350E-2
1		217.0	0.40226	1087.0	-9.3579E-3
1		199.0	0.31303	1079.0	-6.1722E-3

Figure A 47. UV-VIS spectrum of the mixture of (±)17-HDHA and *S*-PETAD (5% excess) in dichloromethane after 3 h at room temperature

Method file : <method not saved>
Information : Default Method
Data File : C:\USERS\TVH\DESKTOP\BOJANA\090318 17S-HDHA 0 02 MG-ML OG PETAD OVER NATT ROM T.SD Created : 3/9/18 10:24:03

Overlaid Spectra:

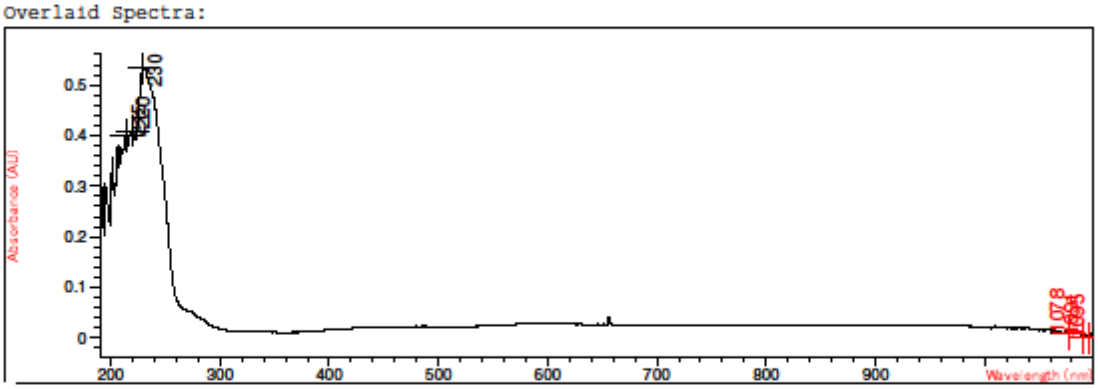

#	Name	Peaks(nm)	Abs(AU)	Valleys(nm)	Abs(AU)
1		230.0	0.53389	1095.0	-2.0456E-4
1		220.0	0.40989	1091.0	2.8505E-3
1		215.0	0.39889	1078.0	8.8086E-3

Figure A 48. UV-VIS spectrum of the mixture of (±)17-HDHA and *S*-PETAD (5% excess) in dichloromethane after 24 h at room temperature

Method file : <method not saved>
Information : Default Method
Data File : C:\USERS\TVH\DESKTOP\BOJANA\080318 17 RAC 0 02 MG-ML OG PETAD ETTER 3 TIMER 30 OC T.SD Created : 3/8/18 15:36:33

Overlaid Spectra:

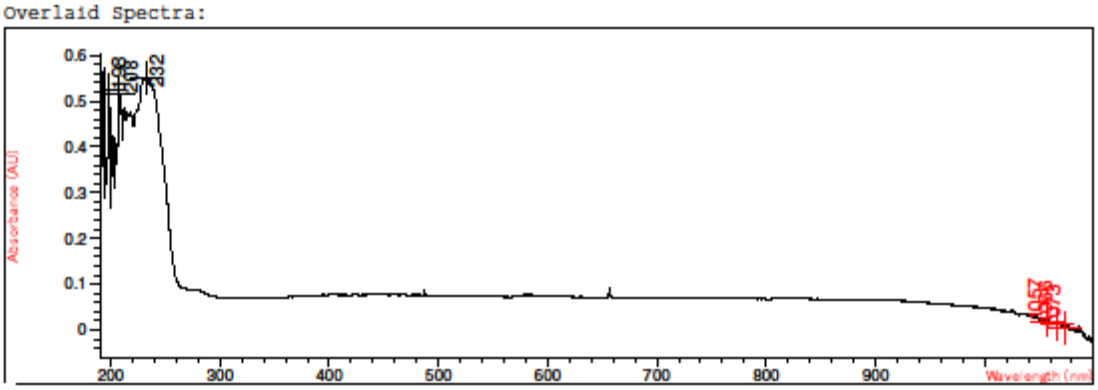

#	Name	Peaks(nm)	Abs(AU)	Valleys(nm)	Abs(AU)
1		232.0	0.55200	1073.0	4.5352E-3
1		198.0	0.52272	1066.0	1.1662E-2
1		208.0	0.51677	1057.0	1.9570E-2

Figure A 49. UV-VIS spectrum of the mixture of (±)17-HDHA and *S*-PETAD (5% excess) in dichloromethane after 3 h at 35°C

Method file : <method not saved>
Information : Default Method
Data File : C:\USERS\TVH\DESKTOP\BOJANA\080318 17 RAC 0 02 MG-ML OG PETAD 300%
OVERSKUDD ETTER 3 TIMER 30 OC T.SD Created : 3/8/18 15:39:59

Overlaid Spectra:

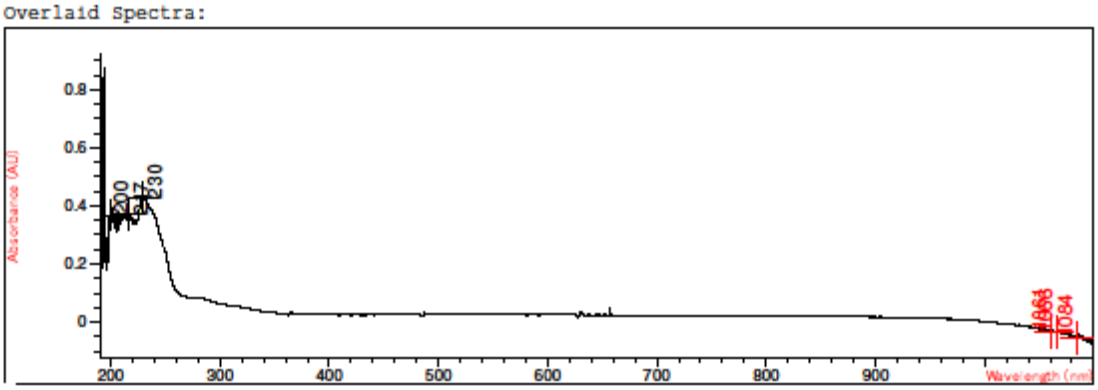

#	Name	Peaks(nm)	Abs(AU)	Valleys(nm)	Abs(AU)
1		230.0	0.42664	1084.0	-5.4168E-2
1		217.0	0.37085	1066.0	-3.6345E-2
1		200.0	0.36820	1061.0	-3.2331E-2

Figure A 50. UV-VIS spectrum of the mixture of (±)17-HDHA and *S*-PETAD (300% excess) in dichloromethane after 3 h at 35ºC

Method file : <method not saved>
Information : Default Method
Data File : C:\USERS\TVH\DESKTOP\BOJANA\090318 17 RAC 0 02 MG-ML OG PETAD OVER
NATT 30 NOC.SD Created : 3/9/18 10:29:44

Overlaid Spectra:

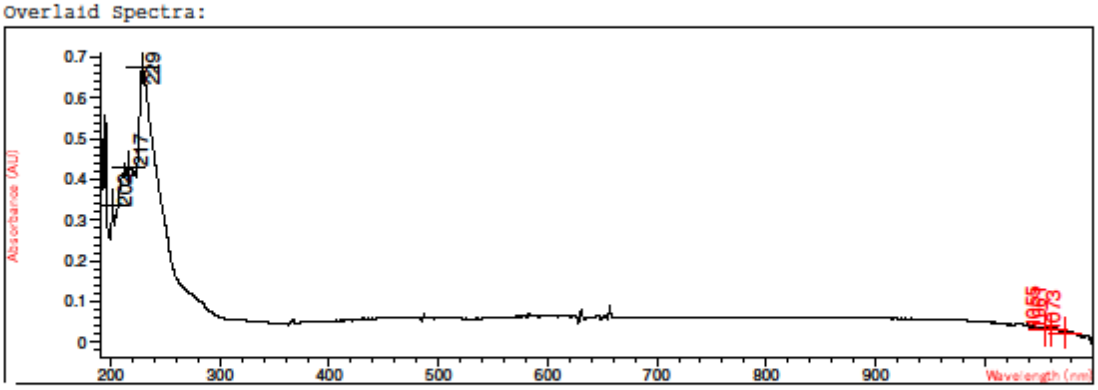

#	Name	Peaks(nm)	Abs(AU)	Valleys(nm)	Abs(AU)
1		229.0	0.67574	1073.0	2.3628E-2
1		217.0	0.43047	1061.0	3.0943E-2
1		202.0	0.33485	1055.0	3.1754E-2

Figure A 51. UV-VIS spectrum of the mixture of (±)17-HDHA and *S*-PETAD (300% excess) in dichloromethane after 24 h at 35ºC

```
Method file :          <method not saved>
Information :          Default Method
Data File   :          C:\USERS\TVH\DESKTOP\BOJANA\180318 17S-HDHA 0 02 MG-ML OG PETAD 0
                       MIN.SD     Created : 3/18/18 11:53:05
```

Overlaid Spectra:

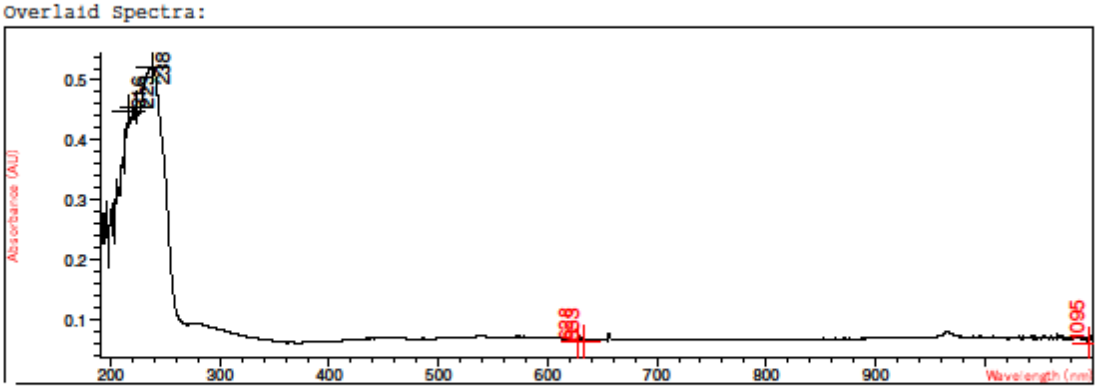

#	Name	Peaks(nm)	Abs(AU)	Valleys(nm)	Abs(AU)
1		238.0	0.52145	1095.0	6.1887E-2
1		223.0	0.45450	628.0	6.5194E-2
1		216.0	0.44877	633.0	6.5530E-2

Figure A 52. UV-VIS spectrum of the mixture of 17*S*-HDHA and *S*-PETAD (5% excess) in dichloromethane initially

```
Method file :          <method not saved>
Information :          Default Method
Data File   :          C:\USERS\TVH\DESKTOP\BOJANA\180318 17S-HDHA I OG PETAD 2H.SD
                       Created : 3/18/18 13:51:03
```

Overlaid Spectra:

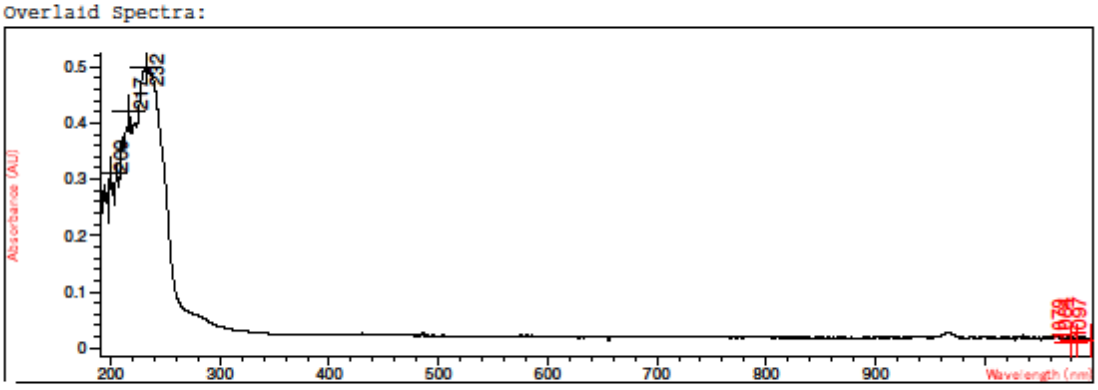

#	Name	Peaks(nm)	Abs(AU)	Valleys(nm)	Abs(AU)
1		232.0	0.49889	1079.0	9.9096E-3
1		217.0	0.42142	1084.0	1.2972E-2
1		200.0	0.30960	1097.0	1.3156E-2

Figure A 53. UV-VIS spectrum of the mixture of 17*S*-HDHA and *S*-PETAD (5% excess) in dichloromethane after 2h at 35ºC

Method file : <method not saved>
Information : Default Method
Data File : C:\USERS\TVH\DESKTOP\BOJANA\190318 17S-HDHA I OG PETAD 24H.SD
Created : 3/19/18 10:08:38

Overlaid Spectra:

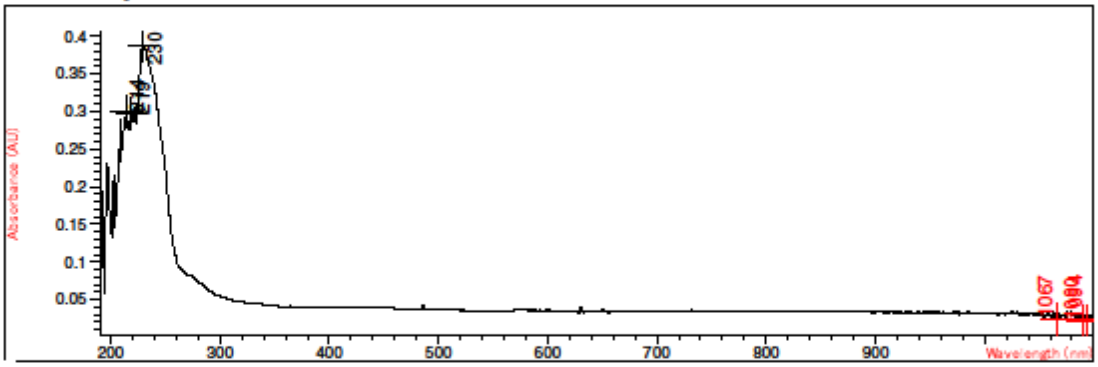

#	Name	Peaks(nm)	Abs(AU)	Valleys(nm)	Abs(AU)
1		230.0	0.38740	1090.0	2.1670E-2
1		214.0	0.29982	1094.0	2.2575E-2
1		219.0	0.29682	1067.0	2.4348E-2

Figure A 54. . UV-VIS spectrum of the mixture of 17*S*-HDHA and *S*-PETAD (5% excess) in dichloromethane after 24h at 35ºC

Method file : <method not saved>
Information : Default Method
Data File : C:\USERS\TVH\DESKTOP\BOJANA\180318 17S-HDHA 300 OVERSKUDD OG PETAD 0 MIN.SD Created : 3/18/18 12:00:51

Overlaid Spectra:

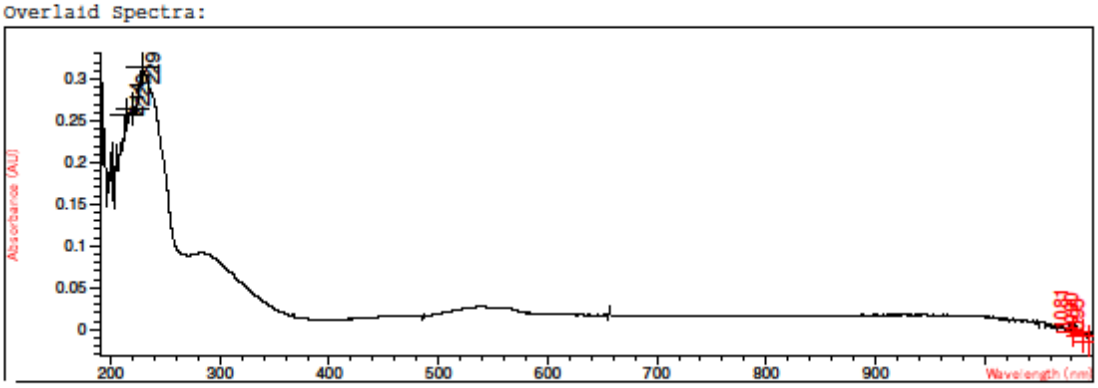

#	Name	Peaks(nm)	Abs(AU)	Valleys(nm)	Abs(AU)
1		229.0	0.31401	1095.0	-1.4363E-2
1		220.0	0.26511	1090.0	-7.3366E-3
1		214.0	0.25681	1081.0	-1.7567E-3

Figure A 55. UV-VIS spectrum of the mixture of 17*S*-HDHA and *S*-PETAD (300% excess) in dichloromethane initially

Method file : <method not saved>
Information : Default Method
Data File : C:\USERS\TVH\DESKTOP\BOJANA\180318 17S-HDHA 300 OVERSKUDD OG PETAD 2H.SD Created : 3/18/18 13:55:08

Overlaid Spectra:

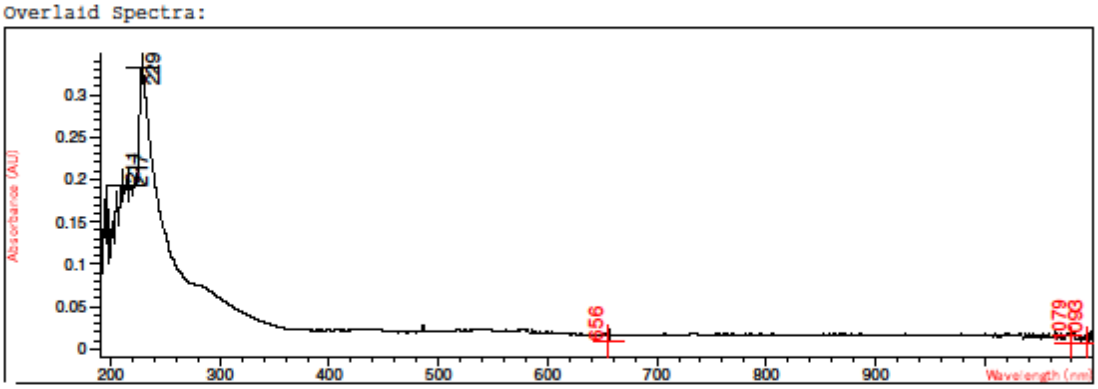

#	Name	Peaks(nm)	Abs(AU)	Valleys(nm)	Abs(AU)
1		229.0	0.33192	1079.0	7.0672E-3
1		211.0	0.19355	1093.0	7.6056E-3
1		217.0	0.19239	656.0	8.9607E-3

Figure A 56. UV-VIS spectrum of the mixture of 17*S*-HDHA and *S*-PETAD (300% excess) in dichloromethane after 2h at 35°C

Method file : <method not saved>
Information : Default Method
Data File : C:\USERS\TVH\DESKTOP\BOJANA\190318 17S-HDHA 300 OG PETAD 24H.SD
Created : 3/19/18 10:12:35

Overlaid Spectra:

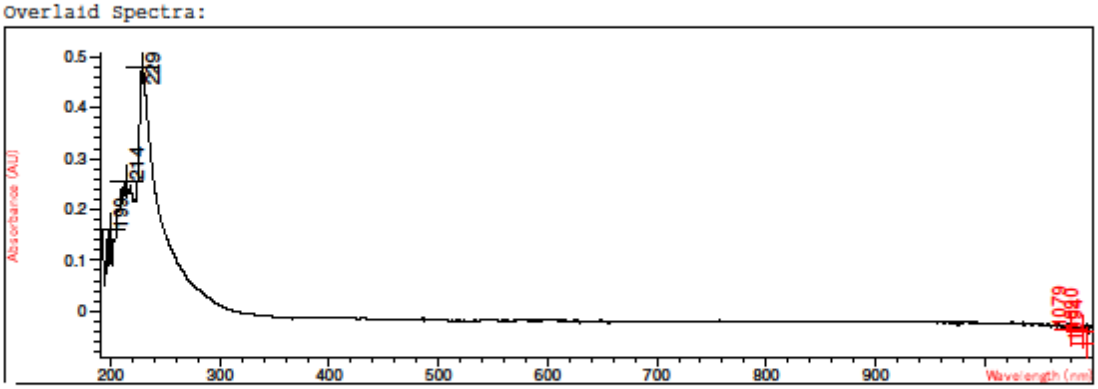

#	Name	Peaks(nm)	Abs(AU)	Valleys(nm)	Abs(AU)
1		229.0	0.47884	1094.0	-6.2924E-2
1		214.0	0.25562	1090.0	-4.0998E-2
1		199.0	0.16044	1079.0	-3.5738E-2

Figure A 57. UV-VIS spectrum of the mixture of 17*S*-HDHA and *S*-PETAD (300% excess) in dichloromethane after 24h at 35°C

Method file : <method not saved>
Information : Default Method
Data File : C:\USERS\TVH\DESKTOP\BOJANA\180318 MAR1 OG PETAD 0 MIN.SD
Created : 3/18/18 12:03:53

Overlaid Spectra:

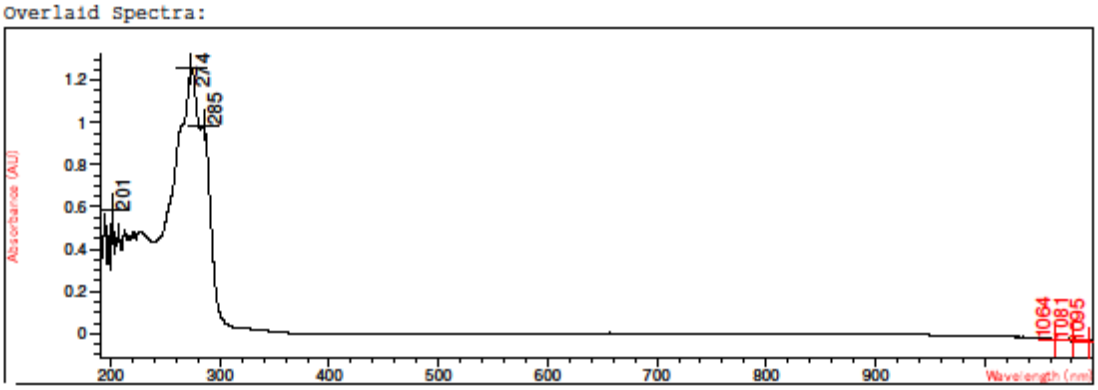

#	Name	Peaks(nm)	Abs(AU)	Valleys(nm)	Abs(AU)
1		274.0	1.25790	1095.0	-4.4278E-2
1		285.0	0.98815	1081.0	-3.4437E-2
1		201.0	0.58494	1064.0	-2.9923E-2

Figure A 58. UV-VIS spectrum of the mixture of MaR1 and *S*-PETAD (5% excess) in dichloromethane initially

Method file : <method not saved>
Information : Default Method
Data File : C:\USERS\TVH\DESKTOP\BOJANA\180318 MAR1 OG PETAD 2H.SD Created : 3/18/18 13:57:57

Overlaid Spectra:

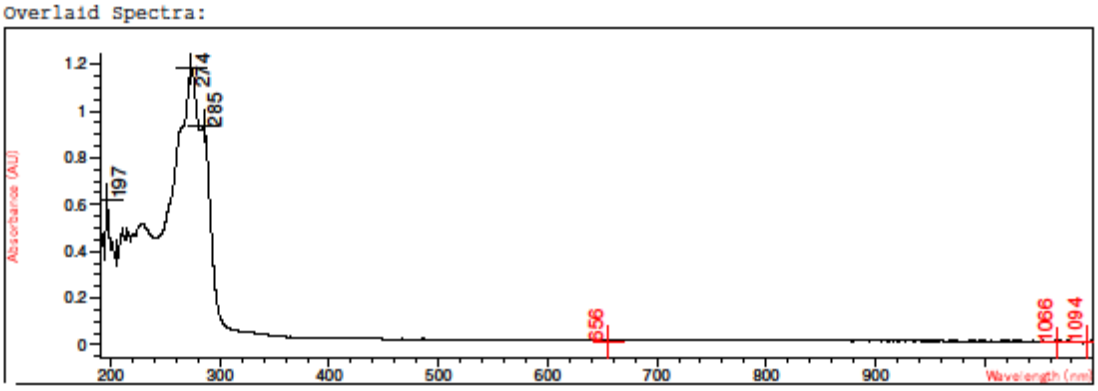

#	Name	Peaks(nm)	Abs(AU)	Valleys(nm)	Abs(AU)
1		274.0	1.18340	1066.0	8.3528E-3
1		285.0	0.93622	656.0	8.6961E-3
1		197.0	0.62016	1094.0	9.1281E-3

Figure A 59. UV-VIS spectrum of the mixture of MaR1 and *S*-PETAD (5% excess) in dichloromethane after 2h at 35°C

Method file : <method not saved>
Information : Default Method
Data File : C:\USERS\TVH\DESKTOP\BOJANA\190318 MAR1 OG PETAD 24H.SD Created : 3/19/18 10:15:26

Overlaid Spectra:

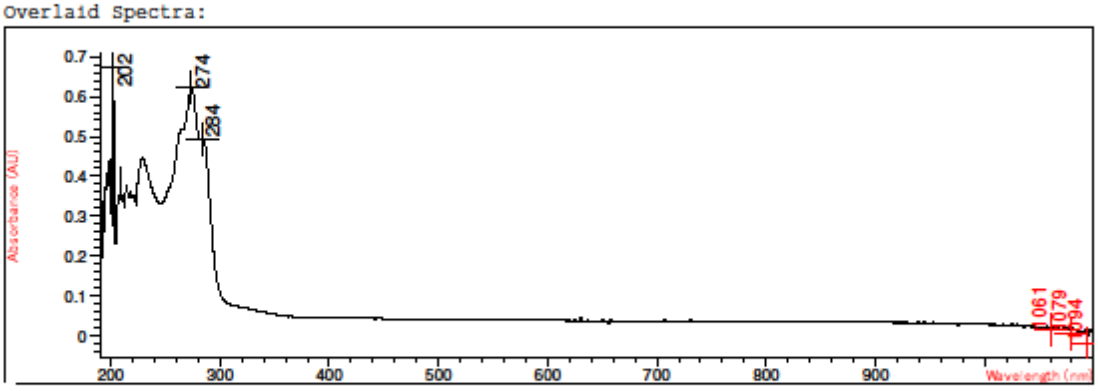

#	Name	Peaks(nm)	Abs(AU)	Valleys(nm)	Abs(AU)
1		202.0	0.67256	1094.0	-1.7838E-2
1		274.0	0.62264	1079.0	7.3328E-3
1		284.0	0.49445	1061.0	1.6109E-2

Figure A 60. UV-VIS spectrum of the mixture of MaR1 and *S*-PETAD (5% excess) in dichloromethane after 24h at 35ºC

Method file : <method not saved>
Information : Default Method
Data File : C:\USERS\TVH\DESKTOP\BOJANA\180318 MAR1 300 OVERSKUDD OG PETAD 0 MIN.SD Created : 3/18/18 12:06:11

Overlaid Spectra:

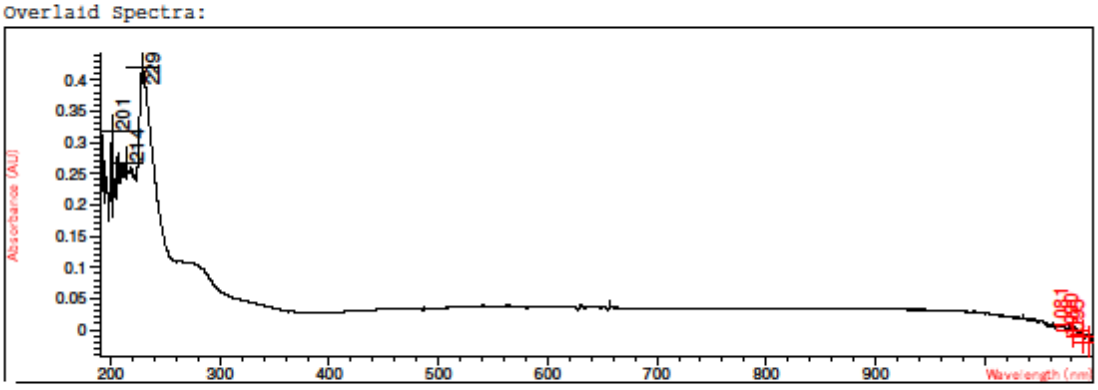

#	Name	Peaks(nm)	Abs(AU)	Valleys(nm)	Abs(AU)
1		229.0	0.41980	1095.0	-2.0009E-2
1		201.0	0.31883	1090.0	-1.1924E-2
1		214.0	0.26741	1081.0	-2.8415E-3

Figure A 61. UV-VIS spectrum of the mixture of MaR1 and *S*-PETAD (300% excess) in dichloromethane initially

```
Method file :         <method not saved>
Information :         Default Method
Data File   :         C:\USERS\TVH\DESKTOP\BOJANA\180318 MAR1 300 OVERSKUDD OG PETAD 2H.SD
                          Created : 3/18/18 14:00:28
```

Overlaid Spectra:

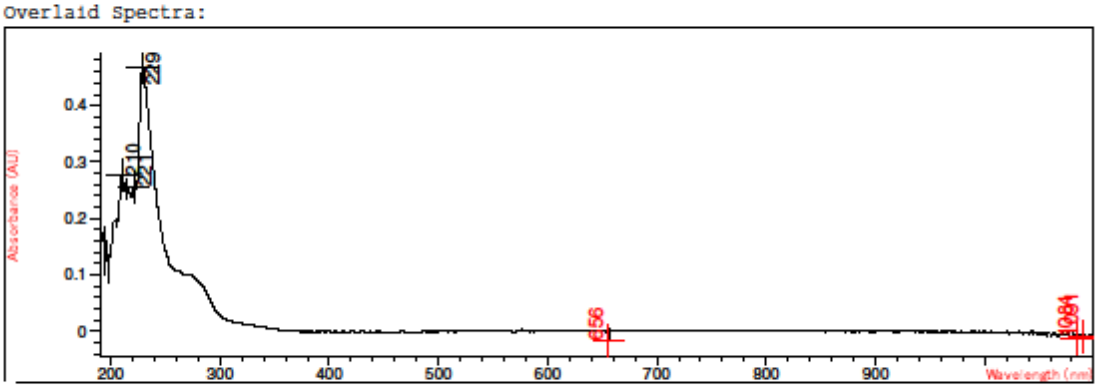

#	Name	Peaks(nm)	Abs(AU)	Valleys(nm)	Abs(AU)
1		229.0	0.46747	656.0	-1.7622E-2
1		210.0	0.27549	1084.0	-1.1853E-2
1		221.0	0.25653	1091.0	-1.0825E-2

Figure A 62. UV-VIS spectrum of the mixture of MaR1 and *S*-PETAD (300% excess) in dichloromethane after 2h at 35ºC

```
Method file :         <method not saved>
Information :         Default Method
Data File   :         C:\USERS\TVH\DESKTOP\BOJANA\190318 MAR1 300 OG PETAD 24H.SD
                      Created : 3/19/18 10:18:11
```

Overlaid Spectra:

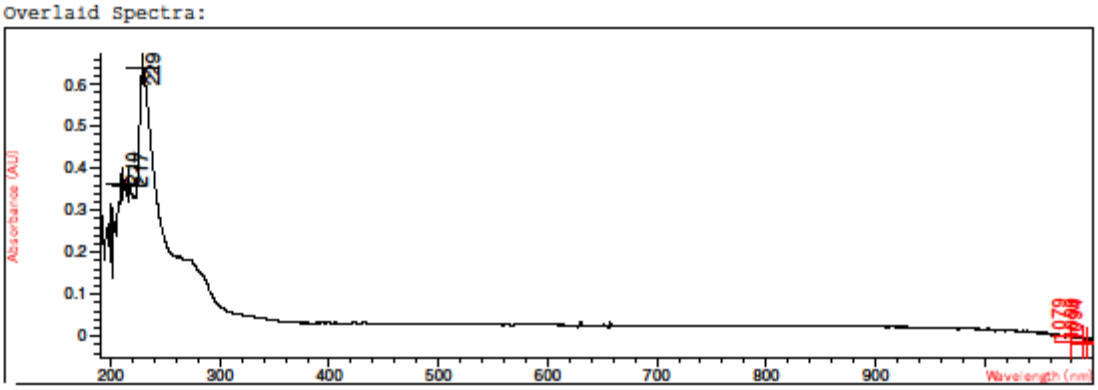

#	Name	Peaks(nm)	Abs(AU)	Valleys(nm)	Abs(AU)
1		229.0	0.63865	1094.0	-1.6886E-2
1		210.0	0.36094	1079.0	-1.3606E-2
1		217.0	0.35776	1090.0	-1.3493E-2

Figure A 63. UV-VIS spectrum of the mixture of MaR1 and *S*-PETAD (300% excess) in dichloromethane after 24h at 35ºC

6.2 MS spectra

MS Spectrum Report

Analysis Info

Sample Name
Method ESI_neg_50_1500.m

Acquisition Date 10/23/2017 1:26:11 PM
Analysis Name D:\Data\maxis2017\13396.d

Acquisition Parameter

Source Type	ESI	Ion Polarity	Negative	Set Nebulizer	0.4 Bar
Focus	Not active	Set Capillary	3500 V	Set Dry Heater	200 °C
Scan Begin	50 m/z	Set End Plate Offset	-500 V	Set Dry Gas	4.0 l/min
Scan End	1500 m/z	Set Charging Voltage	0 V	Set Divert Valve	Source
		Set Corona	0 nA	Set APCI Heater	0 °C

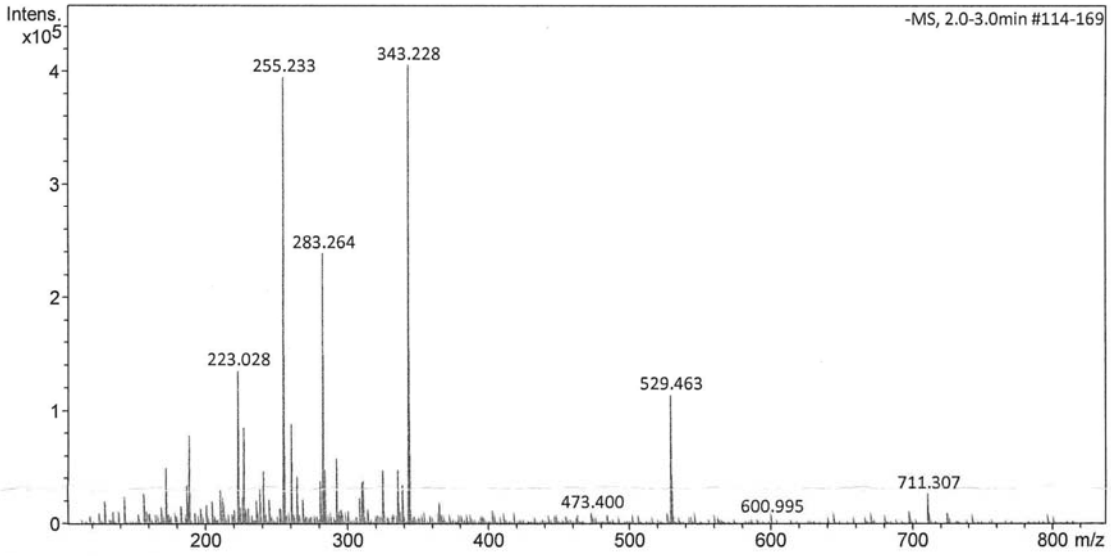

#	m/z	I %
1	173.007	12.4
2	189.092	19.4
3	223.028	33.3
4	227.202	21.1
5	241.217	11.6
6	255.233	97.3
7	256.236	17.1
8	260.873	21.9
9	265.148	10.4
10	281.249	9.4
11	283.264	58.8
12	284.268	11.8
13	293.177	14.2
14	325.184	11.8
15	325.217	9.7
16	336.327	11.9
17	343.228	100.0
18	344.231	24.8
19	529.463	28.1
20	530.466	10.8

Figure A 64. MS spectrum of 17*S*-HDHA, ESI in the negative ion mode

MS Spectrum Report

Analysis Info

Sample Name		Acquisition Date	10/23/2017 9:15:39 AM
Method	ESI_pos_50_1500.m	Analysis Name	D:\Data\maxis2017\13384.d

Acquisition Parameter

Source Type	ESI	Ion Polarity	Positive	Set Nebulizer	0.4 Bar
Focus	Not active	Set Capillary	3500 V	Set Dry Heater	200 °C
Scan Begin	50 m/z	Set End Plate Offset	-100 V	Set Dry Gas	4.0 l/min
Scan End	1500 m/z	Set Charging Voltage	2000 V	Set Divert Valve	Waste
		Set Corona	0 nA	Set APCI Heater	0 °C

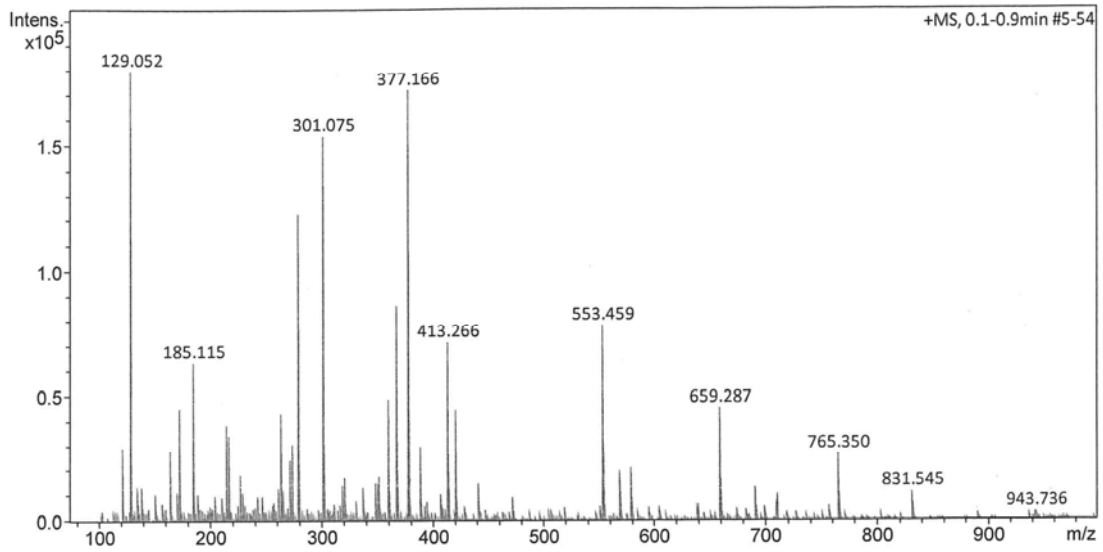

#	m/z	I %
1	129.052	100.0
2	173.078	25.0
3	185.115	35.2
4	215.125	21.5
5	217.105	19.1
6	263.056	24.0
7	273.167	17.1
8	279.093	68.1
9	301.075	85.5
10	302.079	17.4
11	360.324	27.2
12	367.224	47.9
13	377.166	95.7
14	378.170	25.1
15	389.206	16.7
16	413.266	39.7
17	421.233	24.8
18	553.459	43.4
19	554.463	17.3
20	659.287	25.1

Figure A 65. MS spectrum of 17*S*-HDHA, ESI in the positive ion mode

MS Spectrum Report

Analysis Info

Sample Name	PTAD-EtOH	Acquisition Date	10/23/2017 1:11:58 PM
Method	ESI_neg_50_1500.m	Analysis Name	D:\Data\maxis2017\13395.d

Acquisition Parameter

Source Type	ESI	Ion Polarity	Negative	Set Nebulizer	0.4 Bar
Focus	Not active	Set Capillary	3500 V	Set Dry Heater	200 °C
Scan Begin	50 m/z	Set End Plate Offset	-500 V	Set Dry Gas	4.0 l/min
Scan End	1500 m/z	Set Charging Voltage	0 V	Set Divert Valve	Source
		Set Corona	0 nA	Set APCI Heater	0 °C

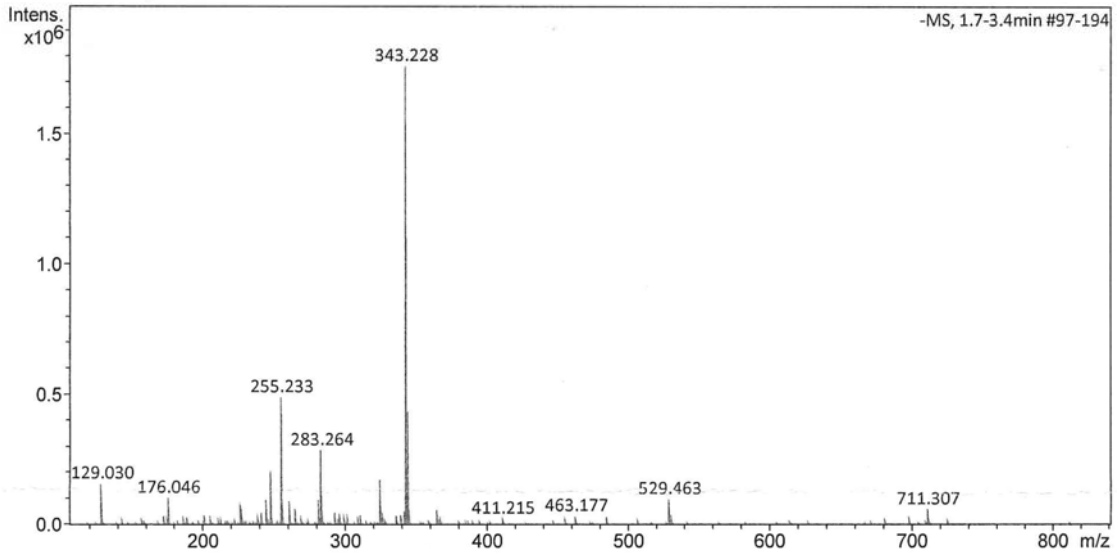

#	m/z	I %
1	129.030	8.9
2	176.046	5.8
3	227.202	4.1
4	245.155	5.5
5	248.068	11.6
6	255.233	27.8
7	256.236	4.9
8	260.873	5.2
9	265.148	3.5
10	281.228	5.3
11	283.264	16.3
12	284.268	3.3
13	325.184	3.0
14	325.217	10.0
15	343.228	100.0
16	344.231	24.9
17	345.234	3.5
18	365.210	3.3
19	529.463	5.6
20	711.307	3.3

Figure A 66. MS spectrum of 17*S*-HDHA with PTAD in ethanol, ESI in the negative ion mode

MS Spectrum Report

Analysis Info

Sample Name	PTAD-EtOH	Acquisition Date	10/23/2017 9:32:50 AM
Method	ESI_pos_50_1500.m	Analysis Name	D:\Data\maxis2017\13385.d

Acquisition Parameter

Source Type	ESI	Ion Polarity	Positive	Set Nebulizer	0.4 Bar
Focus	Not active	Set Capillary	3500 V	Set Dry Heater	200 °C
Scan Begin	50 m/z	Set End Plate Offset	-100 V	Set Dry Gas	4.0 l/min
Scan End	1500 m/z	Set Charging Voltage	2000 V	Set Divert Valve	Waste
		Set Corona	0 nA	Set APCI Heater	0 °C

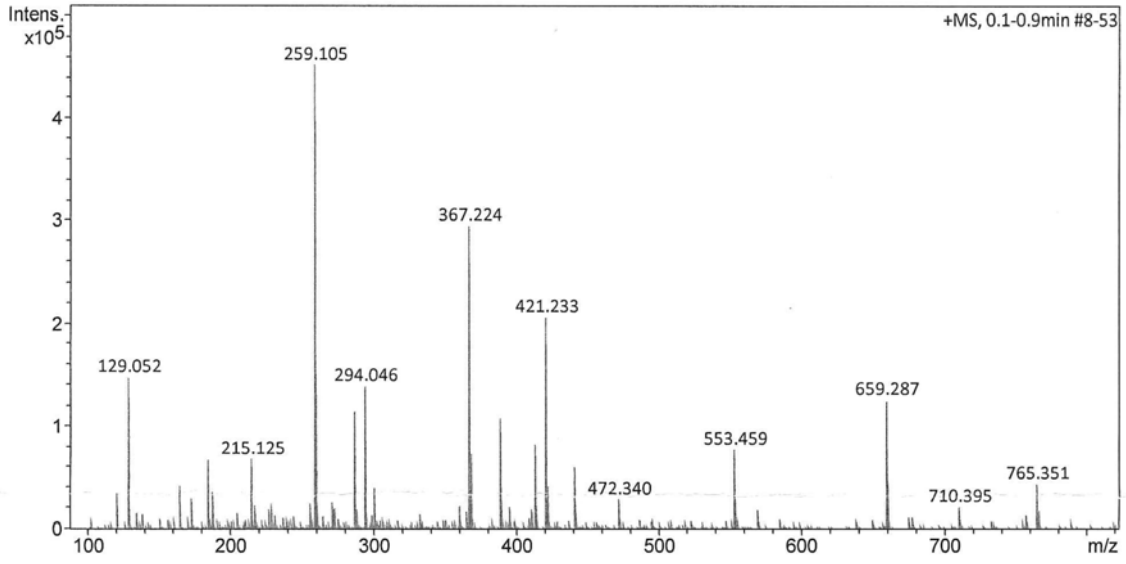

#	m/z	I %
1	129.052	32.5
2	164.921	9.4
3	185.115	14.9
4	215.125	15.2
5	259.105	100.0
6	260.089	33.1
7	260.109	13.2
8	287.137	25.6
9	294.046	30.6
10	367.224	65.1
11	368.228	16.3
12	389.206	24.1
13	413.266	18.3
14	421.233	45.7
15	422.236	9.1
16	441.298	13.2
17	553.459	17.3
18	659.287	27.8
19	660.291	10.0
20	765.351	9.6

Figure A 67. MS spectrum of 17*S*-HDHA with PTAD in ethanol, ESI in the positive ion mode

MS Spectrum Report

Analysis Info

Sample Name	PTAD-CH2Cl2	Acquisition Date	10/23/2017 12:58:10 PM
Method	ESI_neg_50_1500.m	Analysis Name	D:\Data\maxis2017\13394.d

Acquisition Parameter

Source Type	ESI	Ion Polarity	Negative	Set Nebulizer	0.4 Bar
Focus	Not active	Set Capillary	3500 V	Set Dry Heater	200 °C
Scan Begin	50 m/z	Set End Plate Offset	-500 V	Set Dry Gas	4.0 l/min
Scan End	1500 m/z	Set Charging Voltage	0 V	Set Divert Valve	Source
		Set Corona	0 nA	Set APCI Heater	0 °C

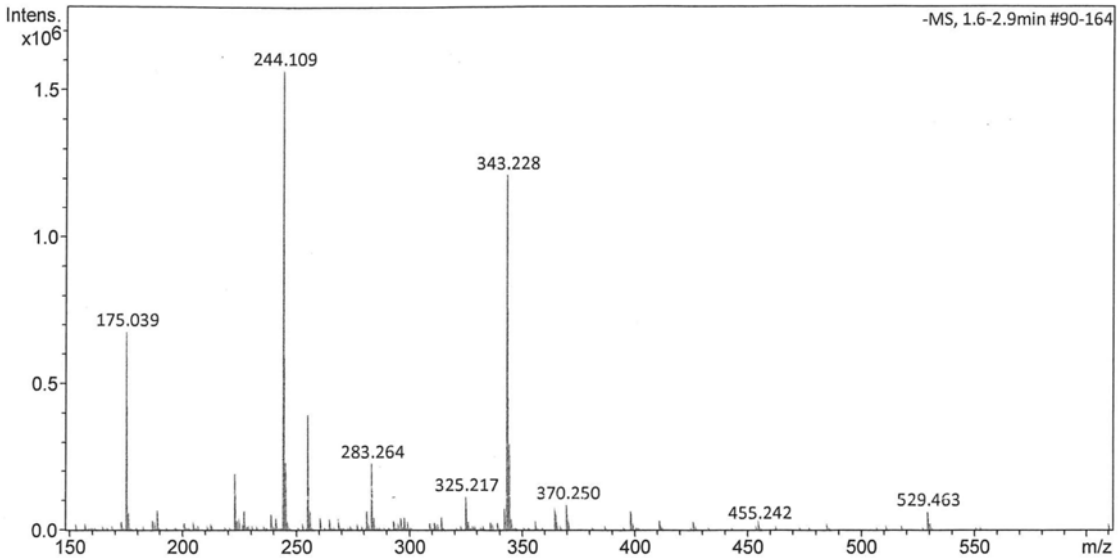

#	m/z	I %
1	175.039	43.3
2	176.042	4.0
3	189.092	4.4
4	223.028	12.4
5	227.202	4.2
6	244.109	100.0
7	245.112	14.8
8	245.155	4.0
9	255.233	25.3
10	256.236	4.5
11	281.228	4.0
12	283.264	14.8
13	325.217	7.5
14	342.219	5.0
15	343.228	77.3
16	344.231	19.0
17	365.210	4.2
18	370.250	5.7
19	398.281	4.1
20	529.463	4.1

Figure A 68. MS spectrum of 17*S*-HDHA with PTAD in dichloromethane, ESI in the negative ion mode. Dichloromethane evaporated prior to analysis, and residuals reconstituted in ethanol.

MS Spectrum Report

Analysis Info

Sample Name	PTAD-CH2Cl2	Acquisition Date	10/23/2017 9:50:28 AM
Method	ESI_pos_50_1500.m	Analysis Name	D:\Data\maxis2017\13386.d

Acquisition Parameter

Source Type	ESI	Ion Polarity	Positive	Set Nebulizer	0.4 Bar
Focus	Not active	Set Capillary	3500 V	Set Dry Heater	200 °C
Scan Begin	50 m/z	Set End Plate Offset	-500 V	Set Dry Gas	4.0 l/min
Scan End	1500 m/z	Set Charging Voltage	2000 V	Set Divert Valve	Waste
		Set Corona	0 nA	Set APCI Heater	0 °C

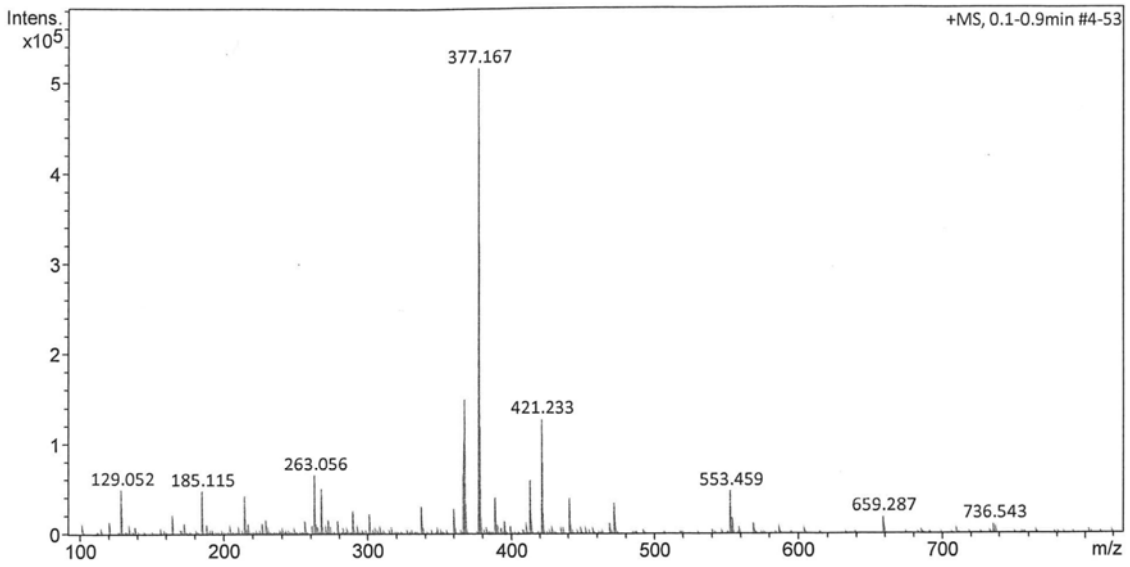

#	m/z	I %
1	129.052	9.5
2	185.115	9.2
3	215.125	8.3
4	263.056	12.8
5	268.106	9.9
6	290.088	5.1
7	301.141	4.2
8	337.075	5.7
9	360.324	5.3
10	367.224	29.1
11	368.228	7.3
12	377.167	100.0
13	378.170	26.1
14	389.206	7.9
15	413.266	11.7
16	421.233	24.8
17	422.236	4.9
18	441.298	7.8
19	472.340	6.5
20	553.459	9.3

Figure A 69. MS spectrum of 17*S*-HDHA with PTAD in dichloromethane, ESI in the positive ion mode. Dichloromethane evaporated prior to analysis, and residuals reconstituted in ethanol.

MS Spectrum Report

Analysis Info

Sample Name	S-PEM-romT	Acquisition Date	10/23/2017 11:59:43 AM
Method	ESI_neg_50_1500.m	Analysis Name	D:\Data\maxis2017\13392.d

Acquisition Parameter

Source Type	ESI	Ion Polarity	Negative	Set Nebulizer	0.4 Bar
Focus	Not active	Set Capillary	3500 V	Set Dry Heater	200 °C
Scan Begin	50 m/z	Set End Plate Offset	-500 V	Set Dry Gas	4.0 l/min
Scan End	1500 m/z	Set Charging Voltage	0 V	Set Divert Valve	Source
		Set Corona	0 nA	Set APCI Heater	0 °C

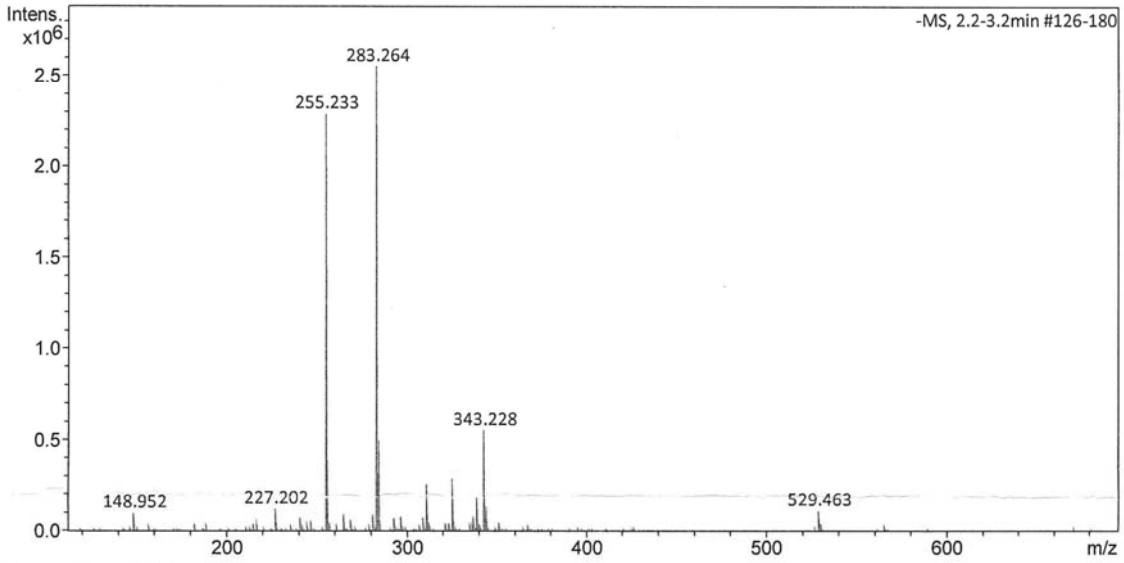

#	m/z	I %
1	148.952	4.0
2	227.202	4.8
3	241.217	2.9
4	255.233	89.7
5	256.236	15.6
6	265.148	3.6
7	269.249	2.4
8	281.249	3.7
9	283.264	100.0
10	284.268	19.6
11	293.177	3.0
12	297.153	3.0
13	309.241	2.8
14	311.169	10.0
15	325.184	11.4
16	337.273	3.1
17	339.200	7.4
18	343.228	21.8
19	344.231	5.4
20	529.463	4.4

Figure A 70. MS spectrum of 17*S*-HDHA with *S*-PEM in ethanol at room temperature, ESI in the negative ion mode

MS Spectrum Report

Analysis Info

Sample Name	S-PEM-romT	Acquisition Date	10/23/2017 10:33:52 AM
Method	ESI_pos_50_1500.m	Analysis Name	D:\Data\maxis2017\13388.d

Acquisition Parameter

Source Type	ESI	Ion Polarity	Positive	Set Nebulizer	0.4 Bar
Focus	Not active	Set Capillary	3500 V	Set Dry Heater	200 °C
Scan Begin	50 m/z	Set End Plate Offset	-500 V	Set Dry Gas	4.0 l/min
Scan End	1500 m/z	Set Charging Voltage	2000 V	Set Divert Valve	Waste
		Set Corona	0 nA	Set APCI Heater	0 °C

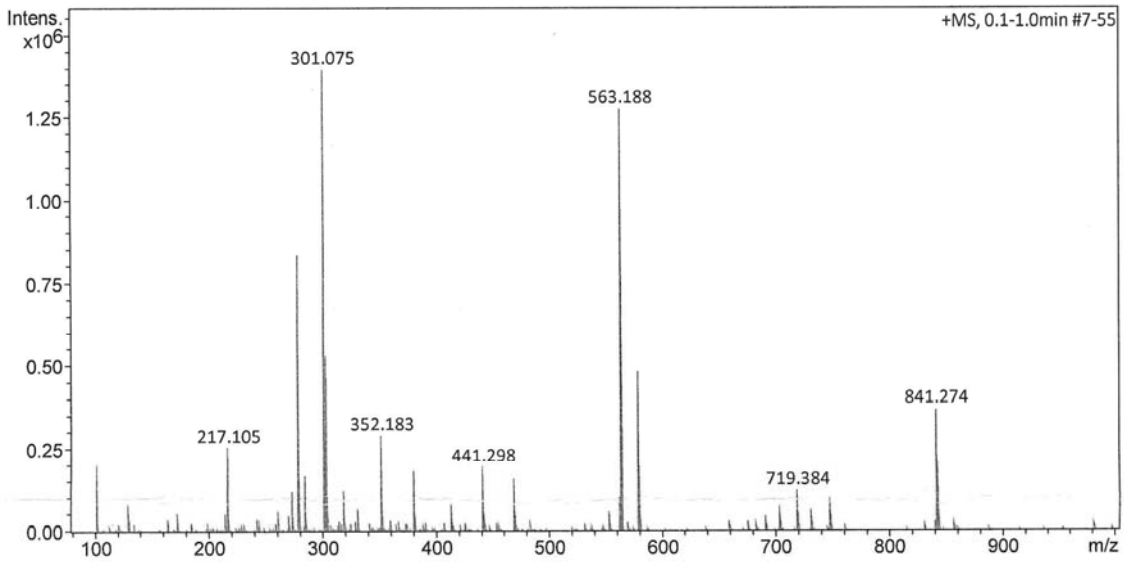

#	m/z	I %
1	102.128	14.5
2	217.105	18.3
3	279.093	59.7
4	280.097	12.2
5	285.102	12.0
6	301.075	100.0
7	302.079	19.8
8	303.112	38.0
9	319.086	8.9
10	352.183	20.9
11	380.214	13.1
12	441.298	14.1
13	469.329	11.3
14	563.188	91.3
15	564.191	36.3
16	579.161	34.5
17	580.165	14.0
18	719.384	8.8
19	841.274	26.4
20	842.277	15.2

Figure A 71. MS spectrum of 17*S*-HDHA with *S*-PEM in ethanol at room temperature, ESI in the positive ion mode

MS Spectrum Report

Analysis Info

Sample Name	S-PEM-40C	Acquisition Date	10/23/2017 11:38:47 AM
Method	ESI_neg_50_1500.m	Analysis Name	D:\Data\maxis2017\13390.d

Acquisition Parameter

Source Type	ESI	Ion Polarity	Negative	Set Nebulizer	0.4 Bar
Focus	Not active	Set Capillary	3500 V	Set Dry Heater	200 °C
Scan Begin	50 m/z	Set End Plate Offset	-500 V	Set Dry Gas	4.0 l/min
Scan End	1500 m/z	Set Charging Voltage	0 V	Set Divert Valve	Source
		Set Corona	0 nA	Set APCI Heater	0 °C

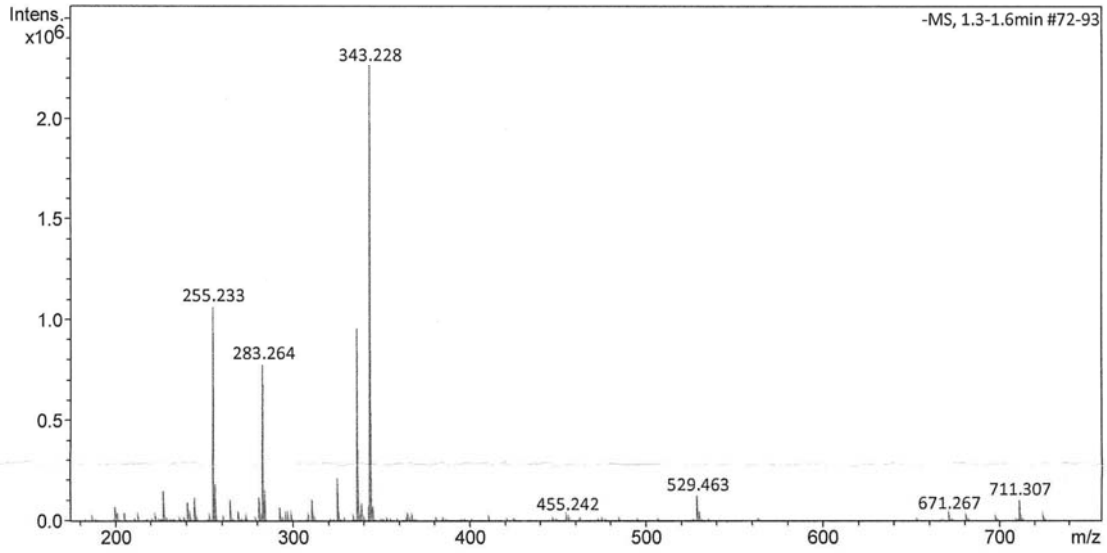

#	m/z	I %
1	227.202	6.6
2	241.217	4.2
3	245.155	5.1
4	255.233	47.2
5	256.236	8.2
6	265.148	4.6
7	281.228	5.0
8	281.249	3.7
9	283.264	34.5
10	284.268	6.9
11	311.169	4.7
12	325.184	5.9
13	325.217	9.3
14	336.327	42.5
15	337.331	10.2
16	339.200	3.9
17	343.228	100.0
18	344.231	24.6
19	529.463	5.5
20	711.307	4.5

Figure A 72. MS spectrum of 17*S*-HDHA with *S*-PEM in ethanol at 40ºC, ESI in the negative ion mode

MS Spectrum Report

Analysis Info

Sample Name	S-PEM-40C	Acquisition Date	10/23/2017 10:51:55 AM
Method	ESI_pos_50_1500.m	Analysis Name	D:\Data\maxis2017\13389.d

Acquisition Parameter

Source Type	ESI	Ion Polarity	Positive	Set Nebulizer	0.4 Bar
Focus	Not active	Set Capillary	3500 V	Set Dry Heater	200 °C
Scan Begin	50 m/z	Set End Plate Offset	-500 V	Set Dry Gas	4.0 l/min
Scan End	1500 m/z	Set Charging Voltage	2000 V	Set Divert Valve	Waste
		Set Corona	0 nA	Set APCI Heater	0 °C

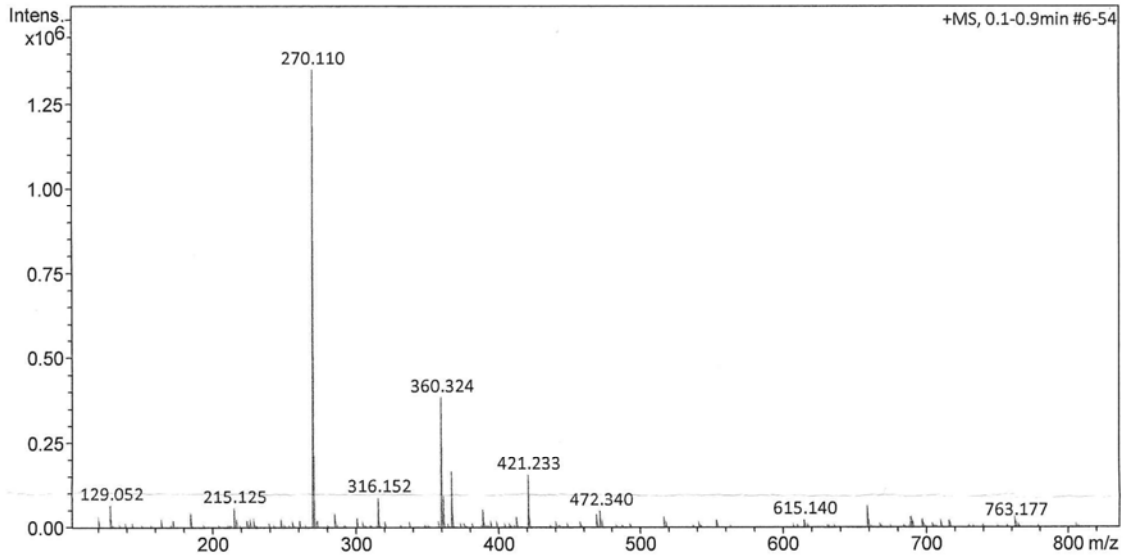

#	m/z	I %
1	129.052	4.9
2	185.115	3.2
3	215.125	4.3
4	270.110	100.0
5	271.113	15.9
6	286.084	3.1
7	316.152	6.7
8	360.324	28.4
9	361.327	7.0
10	367.224	12.4
11	368.228	3.1
12	389.206	4.0
13	413.266	2.3
14	421.233	11.6
15	422.236	2.3
16	469.329	3.0
17	472.340	3.7
18	517.231	2.5
19	659.287	4.8
20	689.159	2.3

Figure A 73. MS spectrum of 17*S*-HDHA with *S*-PEM in ethanol at 40ºC, ESI in the positive ion mode

MS Spectrum Report

Analysis Info

Sample Name	S-PEM-60C	Acquisition Date	10/23/2017 12:46:43 PM
Method	ESI_neg_50_1500.m	Analysis Name	D:\Data\maxis2017\13393.d

Acquisition Parameter

Source Type	ESI	Ion Polarity	Negative	Set Nebulizer	0.4 Bar
Focus	Not active	Set Capillary	3500 V	Set Dry Heater	200 °C
Scan Begin	50 m/z	Set End Plate Offset	-500 V	Set Dry Gas	4.0 l/min
Scan End	1500 m/z	Set Charging Voltage	0 V	Set Divert Valve	Source
		Set Corona	0 nA	Set APCI Heater	0 °C

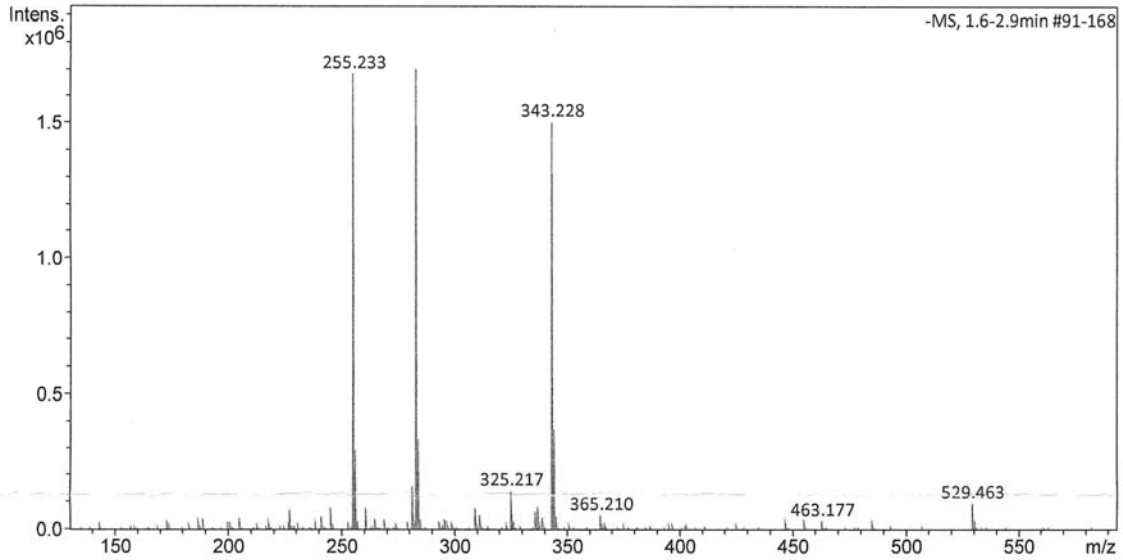

#	m/z	I %
1	227.202	4.4
2	245.155	4.6
3	255.233	99.0
4	256.236	17.5
5	260.873	4.7
6	281.228	4.8
7	281.249	9.4
8	283.264	100.0
9	284.268	20.0
10	309.241	4.7
11	311.169	3.2
12	325.184	3.9
13	325.217	8.5
14	336.327	3.9
15	337.272	4.9
16	343.228	88.3
17	344.231	21.8
18	345.234	3.0
19	365.210	3.1
20	529.463	5.7

Figure A 74. MS spectrum of 17*S*-HDHA with *S*-PEM in ethanol at 60ºC, ESI in the negative ion mode

MS Spectrum Report

Analysis Info

Sample Name	S-PEM-60C	Acquisition Date	10/23/2017 10:12:41 AM
Method	ESI_pos_50_1500.m	Analysis Name	D:\Data\maxis2017\13387.d

Acquisition Parameter

Source Type	ESI	Ion Polarity	Positive	Set Nebulizer	0.4 Bar
Focus	Not active	Set Capillary	3500 V	Set Dry Heater	200 °C
Scan Begin	50 m/z	Set End Plate Offset	-500 V	Set Dry Gas	4.0 l/min
Scan End	1500 m/z	Set Charging Voltage	2000 V	Set Divert Valve	Waste
		Set Corona	0 nA	Set APCI Heater	0 °C

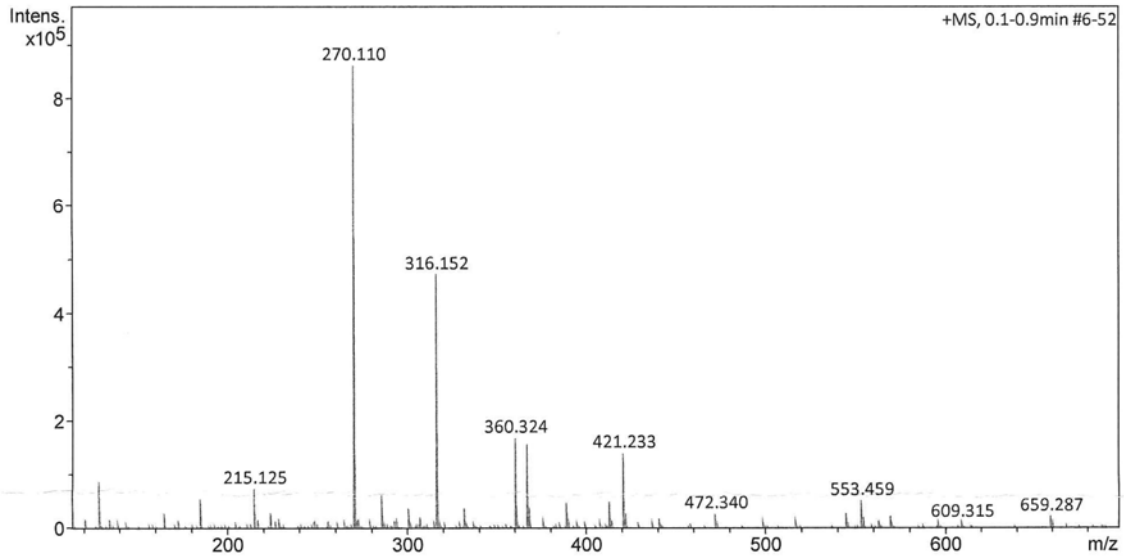

#	m/z	I %
1	129.052	10.4
2	185.115	6.4
3	215.125	8.7
4	270.110	100.0
5	271.113	16.1
6	286.084	7.3
7	301.141	4.4
8	316.152	54.8
9	317.155	9.9
10	332.126	4.5
11	360.324	19.6
12	361.327	4.8
13	367.224	18.3
14	368.228	4.7
15	389.206	5.7
16	413.266	5.9
17	421.233	16.4
18	422.236	3.3
19	545.204	3.4
20	553.459	6.0

Figure A 75. MS spectrum of 17*S*-HDHA with *S*-PEM in ethanol at 60ºC, ESI in the positive ion mode

MS Spectrum Report

Analysis Info

Sample Name	17S-HDHA-PTAD	Acquisition Date	10/30/2017 9:11:55 AM
Method	ESI_pos_50_1500.m	Analysis Name	D:\Data\maxis2017\13434.d

Acquisition Parameter

Source Type	ESI	Ion Polarity	Positive	Set Nebulizer	0.4 Bar
Focus	Not active	Set Capillary	3500 V	Set Dry Heater	200 °C
Scan Begin	50 m/z	Set End Plate Offset	-500 V	Set Dry Gas	4.0 l/min
Scan End	1500 m/z	Set Charging Voltage	2000 V	Set Divert Valve	Waste
		Set Corona	0 nA	Set APCI Heater	0 °C

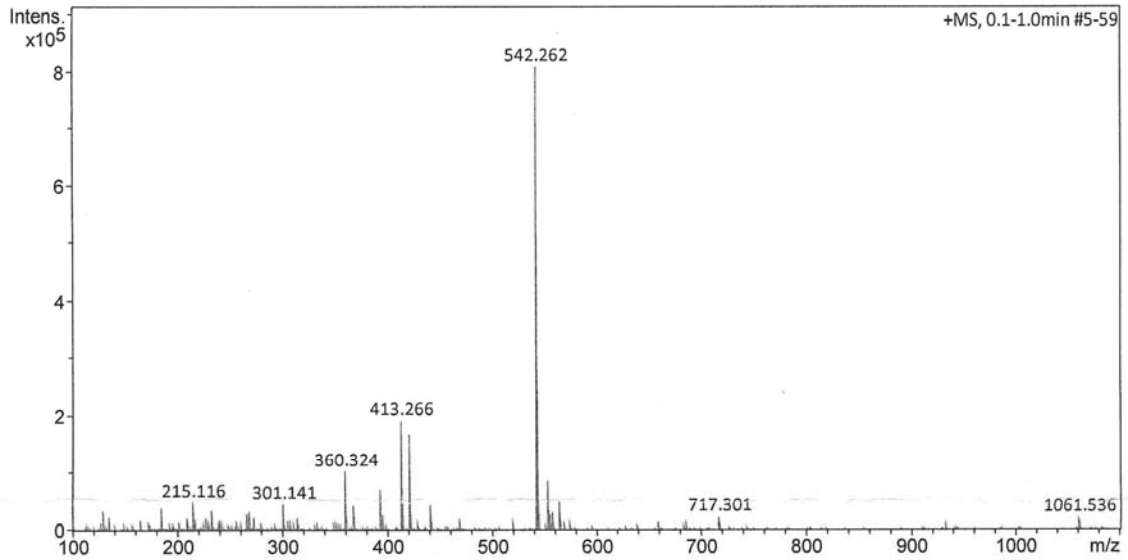

#	m/z	I %
1	129.052	4.2
2	185.115	4.8
3	215.116	6.1
4	215.125	4.5
5	233.150	4.3
6	268.106	4.2
7	301.141	5.7
8	360.324	12.7
9	367.224	5.4
10	393.298	8.7
11	413.266	23.7
12	414.270	6.1
13	421.233	20.8
14	422.236	4.1
15	441.298	5.4
16	542.262	100.0
17	543.266	34.3
18	544.269	6.7
19	553.459	10.5
20	564.245	6.1

Figure A 76. MS spectrum of 17*S*-HDHA with freshly made PTAD in dichloromethane after 2h at 35ºC. ESI in the positive ion mode. Dichloromethane evaporated prior to analysis, and residuals reconstituted in ethanol.

MS Spectrum Report

Analysis Info

Sample Name	MARI-PTAD	Acquisition Date	10/30/2017 10:17:16 AM
Method	ESI_neg_50_1500.m	Analysis Name	D:\Data\maxis2017\13436.d

Acquisition Parameter

Source Type	ESI	Ion Polarity	Negative	Set Nebulizer	0.4 Bar
Focus	Not active	Set Capillary	3500 V	Set Dry Heater	200 °C
Scan Begin	50 m/z	Set End Plate Offset	-500 V	Set Dry Gas	4.0 l/min
Scan End	1500 m/z	Set Charging Voltage	0 V	Set Divert Valve	Source
		Set Corona	0 nA	Set APCI Heater	0 °C

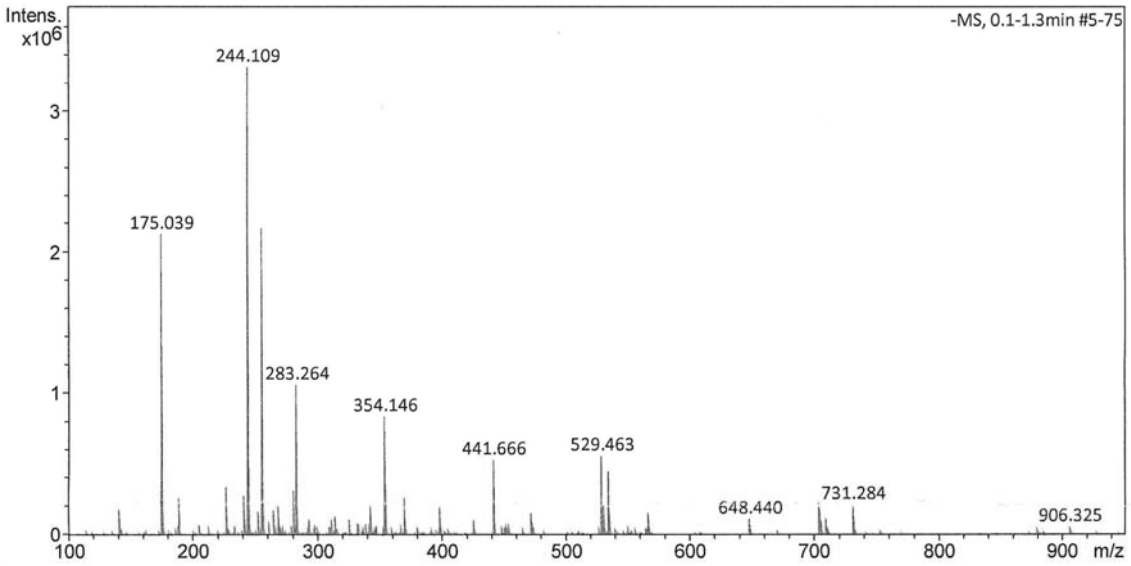

#	m/z	I %
1	175.039	64.1
2	176.046	11.2
3	189.092	7.9
4	227.202	10.1
5	241.217	8.4
6	244.109	100.0
7	245.112	14.6
8	255.233	65.4
9	256.236	11.5
10	281.249	9.4
11	283.115	12.2
12	283.264	31.9
13	354.146	25.3
14	354.648	10.7
15	370.250	7.9
16	441.666	16.1
17	442.167	8.5
18	529.463	16.9
19	534.261	13.6
20	731.284	6.5

Figure A 77. MS spectrum of MaR1 with freshly made PTAD in methanol after 2h at room temperature. ESI in the negative ion mode.

MS Spectrum Report

Analysis Info

Sample Name	MARI-PTAD	Acquisition Date	10/30/2017 9:34:15 AM
Method	ESI_pos_50_1500.m	Analysis Name	D:\Data\maxis2017\13435.d

Acquisition Parameter

Source Type	ESI	Ion Polarity	Positive	Set Nebulizer	0.4 Bar
Focus	Not active	Set Capillary	3500 V	Set Dry Heater	200 °C
Scan Begin	50 m/z	Set End Plate Offset	-500 V	Set Dry Gas	4.0 l/min
Scan End	1500 m/z	Set Charging Voltage	2000 V	Set Divert Valve	Waste
		Set Corona	0 nA	Set APCI Heater	0 °C

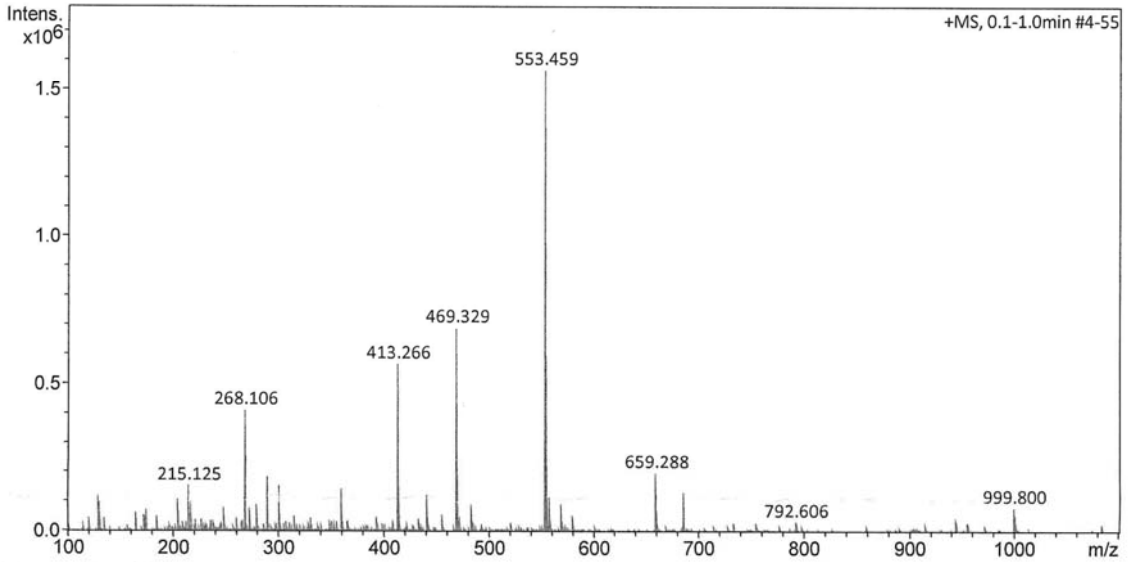

#	m/z	I %
1	129.052	7.9
2	130.159	6.4
3	205.068	6.9
4	215.125	9.8
5	268.106	26.2
6	290.088	11.8
7	301.075	7.3
8	301.141	9.8
9	360.324	9.2
10	413.266	36.2
11	414.270	9.5
12	441.298	7.9
13	469.329	44.0
14	470.332	13.8
15	553.459	100.0
16	554.463	38.1
17	555.466	7.7
18	558.258	7.3
19	659.288	12.7
20	685.436	8.3

Figure A 78. MS spectrum of MaR1 with freshly made PTAD in methanol after 2h at room temperature. ESI in the positive ion mode.

MS Spectrum Report

Analysis Info

Sample Name	17S-HDHA-S-PEM 35C	Acquisition Date	11/2/2017 11:27:16 AM
Method	ESI_neg_50_1500.m	Analysis Name	D:\Data\maxis2017\13459.d

Acquisition Parameter

Source Type	ESI	Ion Polarity	Negative	Set Nebulizer	0.4 Bar
Focus	Not active	Set Capillary	3500 V	Set Dry Heater	200 °C
Scan Begin	50 m/z	Set End Plate Offset	-500 V	Set Dry Gas	4.0 l/min
Scan End	1500 m/z	Set Charging Voltage	0 V	Set Divert Valve	Source
		Set Corona	0 nA	Set APCI Heater	0 °C

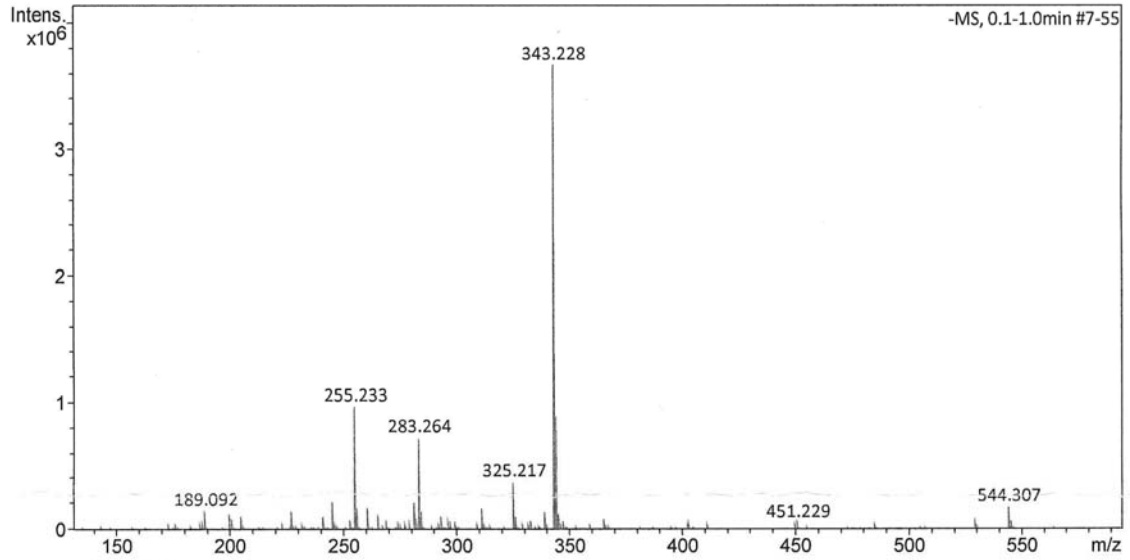

#	m/z	I %
1	189.092	3.9
2	200.072	3.4
3	227.202	3.7
4	245.155	5.9
5	255.233	26.4
6	256.236	4.6
7	260.873	4.5
8	265.148	3.1
9	281.228	5.6
10	281.249	5.0
11	283.264	19.9
12	284.268	3.9
13	311.169	4.4
14	325.184	5.3
15	325.217	10.2
16	339.200	3.7
17	343.228	100.0
18	344.231	24.5
19	345.234	3.4
20	544.307	4.6

Figure A 79. MS spectrum of 17*S*-HDHA with freshly made *S*-PEM in dichloromethane after 2h at 35ºC. ESI in the negative ion mode. Dichloromethane evaporated prior to analysis, and residuals reconstituted in methanol.

MS Spectrum Report

Analysis Info

Sample Name	17S-HDHA-S-PEM 35C	Acquisition Date	11/2/2017 12:52:50 PM
Method	ESI_pos_50_1500.m	Analysis Name	D:\Data\maxis2017\13453a.d

Acquisition Parameter

Source Type	ESI	Ion Polarity	Positive	Set Nebulizer	0.4 Bar
Focus	Not active	Set Capillary	3500 V	Set Dry Heater	200 °C
Scan Begin	50 m/z	Set End Plate Offset	-500 V	Set Dry Gas	4.0 l/min
Scan End	1500 m/z	Set Charging Voltage	2000 V	Set Divert Valve	Waste
		Set Corona	0 nA	Set APCI Heater	0 °C

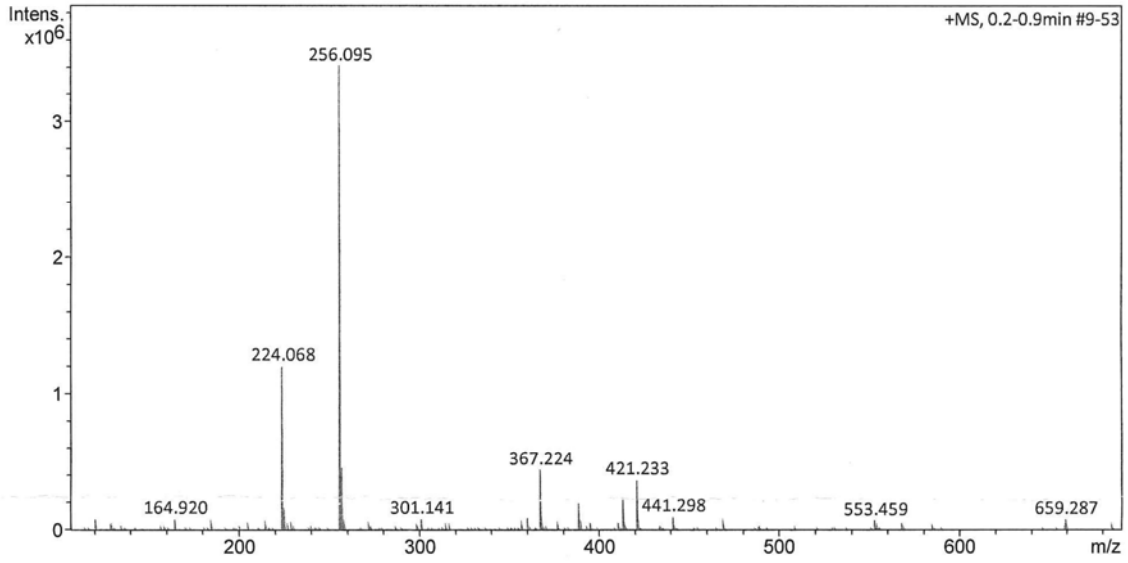

#	m/z	I %
1	120.987	2.3
2	164.920	2.4
3	224.068	35.3
4	225.072	4.9
5	256.095	100.0
6	257.098	13.6
7	301.141	2.5
8	360.324	2.6
9	367.224	13.0
10	368.228	3.2
11	389.206	5.8
12	395.313	1.7
13	411.188	1.7
14	413.266	7.1
15	414.270	1.9
16	421.233	10.9
17	422.236	2.3
18	441.298	2.9
19	553.459	2.0
20	659.287	2.3

Figure A 80. MS spectrum of 17*S*-HDHA with freshly made *S*-PEM in dichloromethane after 2h at 35ºC. ESI in the positive ion mode. Dichloromethane evaporated prior to analysis, and residuals reconstituted in methanol.

MS Spectrum Report

Analysis Info

Sample Name	17-oxo-DHA-PTAD romT	Acquisition Date	11/2/2017 11:41:48 AM
Method	ESI_neg_50_1500.m	Analysis Name	D:\Data\maxis2017\13460.d

Acquisition Parameter

Source Type	ESI	Ion Polarity	Negative	Set Nebulizer	0.4 Bar
Focus	Not active	Set Capillary	3500 V	Set Dry Heater	200 °C
Scan Begin	50 m/z	Set End Plate Offset	-500 V	Set Dry Gas	4.0 l/min
Scan End	1500 m/z	Set Charging Voltage	0 V	Set Divert Valve	Source
		Set Corona	0 nA	Set APCI Heater	0 °C

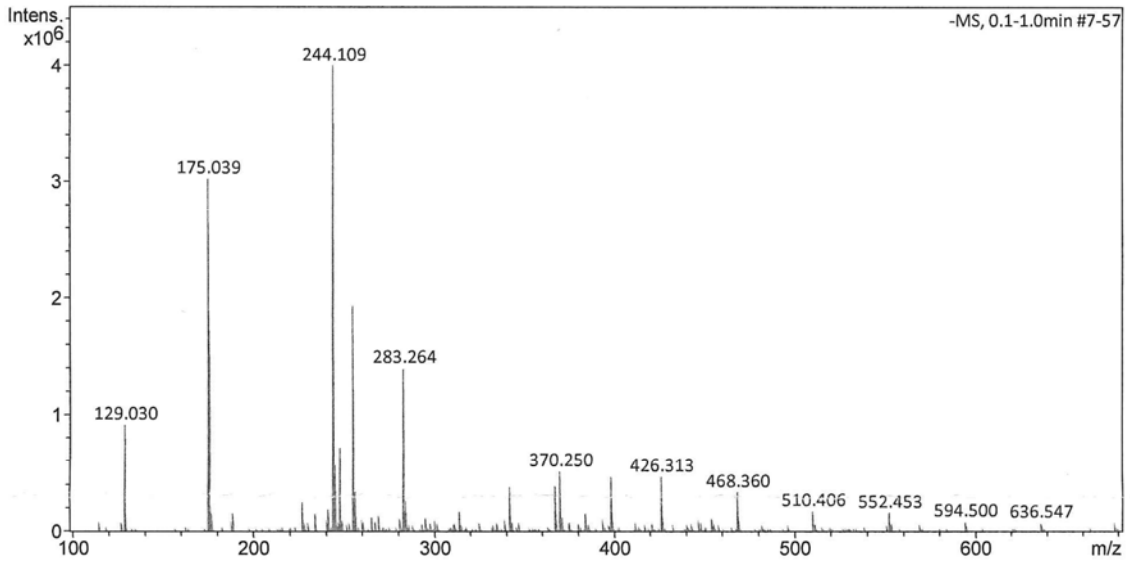

#	m/z	I %
1	129.030	22.9
2	175.039	75.7
3	176.046	43.2
4	227.202	6.3
5	241.217	5.0
6	244.109	100.0
7	245.112	14.2
8	248.068	18.0
9	248.080	5.2
10	255.233	48.4
11	256.236	8.5
12	283.264	35.0
13	284.268	6.7
14	342.219	9.6
15	367.264	9.9
16	370.250	13.0
17	398.281	11.8
18	426.313	11.9
19	468.360	8.5
20	510.406	4.4

Figure A 81. MS spectrum of 17-oxo-DHA with freshly made PTAD in dichloromethane after 2h at room temperature. ESI in the negative ion mode. Dichloromethane evaporated prior to analysis, and residuals reconstituted in methanol.

MS Spectrum Report

Analysis Info

Sample Name	17-oxo-DHA-PTAD romT	Acquisition Date	11/2/2017 12:42:53 PM
Method	ESI_pos_50_1500.m	Analysis Name	D:\Data\maxis2017\13452a.d

Acquisition Parameter

Source Type	ESI	Ion Polarity	Positive	Set Nebulizer	0.4 Bar
Focus	Not active	Set Capillary	3500 V	Set Dry Heater	200 °C
Scan Begin	50 m/z	Set End Plate Offset	-500 V	Set Dry Gas	4.0 l/min
Scan End	1500 m/z	Set Charging Voltage	2000 V	Set Divert Valve	Waste
		Set Corona	0 nA	Set APCI Heater	0 °C

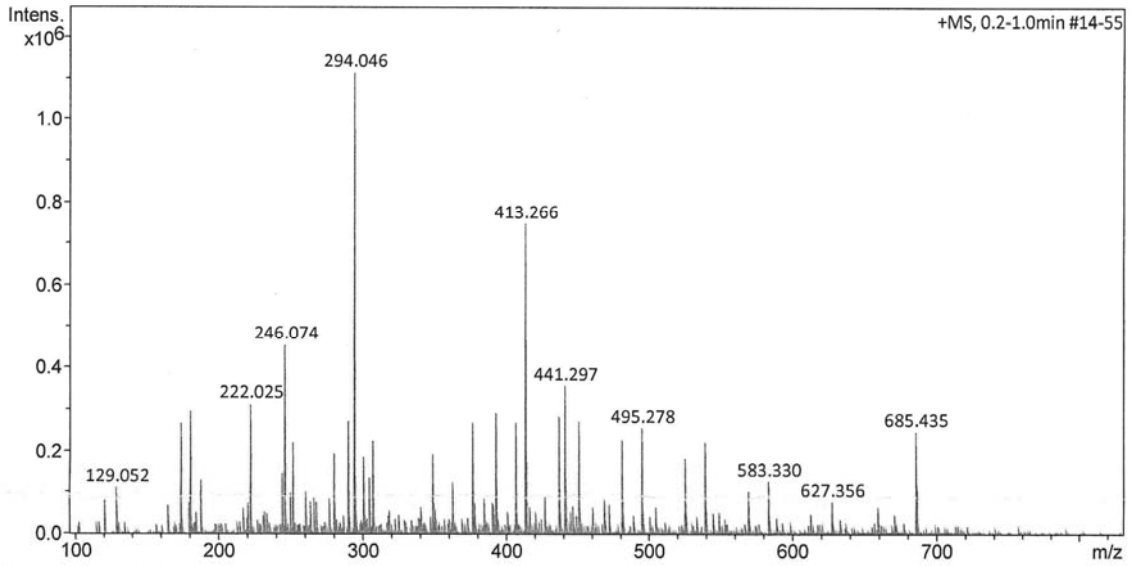

#	m/z	I %
1	174.053	23.9
2	181.062	26.8
3	222.025	28.1
4	246.074	40.8
5	252.084	20.1
6	290.088	24.5
7	294.046	100.0
8	307.105	20.3
9	377.167	24.3
10	393.210	26.2
11	407.225	24.3
12	413.266	67.1
13	414.270	17.9
14	437.236	25.6
15	441.297	32.0
16	451.251	24.6
17	481.262	20.5
18	495.278	23.0
19	539.304	20.1
20	685.435	22.3

Figure A 82. MS spectrum of 17-oxo-DHA with freshly made PTAD in dichloromethane after 2h at room temperature. ESI in the positive ion mode. Dichloromethane evaporated prior to analysis, and residuals reconstituted in methanol.

MS Spectrum Report

Analysis Info

Sample Name	17-oxo-DHA-PTAD 35C	Acquisition Date	11/2/2017 11:15:37 AM
Method	ESI_neg_50_1500.m	Analysis Name	D:\Data\maxis2017\13458.d

Acquisition Parameter

Source Type	ESI	Ion Polarity	Negative	Set Nebulizer	0.4 Bar
Focus	Not active	Set Capillary	3500 V	Set Dry Heater	200 °C
Scan Begin	50 m/z	Set End Plate Offset	-500 V	Set Dry Gas	4.0 l/min
Scan End	1500 m/z	Set Charging Voltage	0 V	Set Divert Valve	Source
		Set Corona	0 nA	Set APCI Heater	0 °C

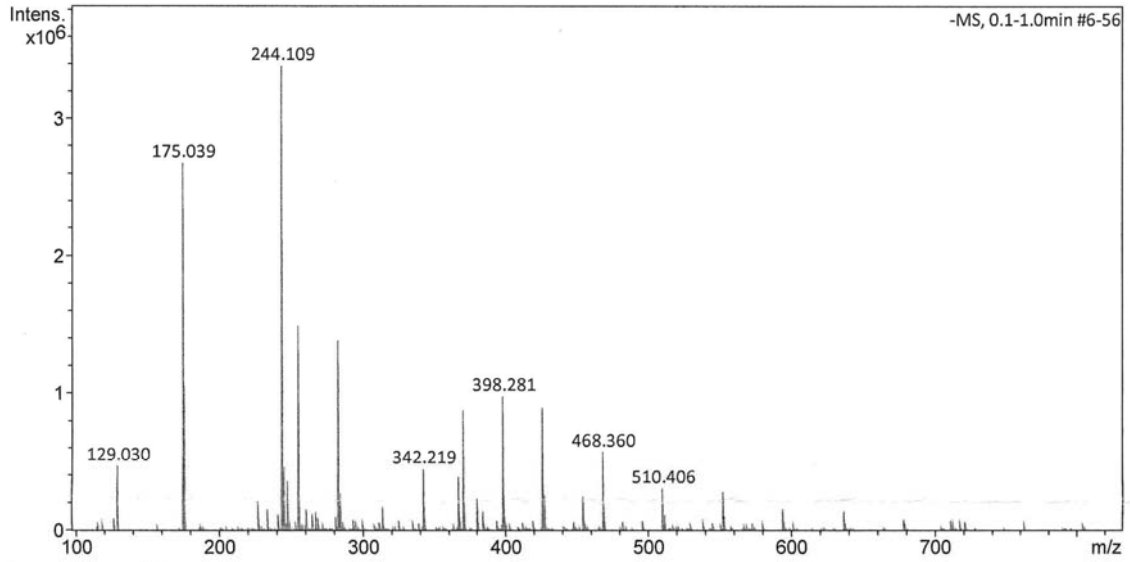

#	m/z	I %
1	129.030	14.0
2	175.039	78.9
3	176.046	31.2
4	244.109	100.0
5	245.112	13.9
6	248.068	10.9
7	255.233	44.1
8	256.236	7.7
9	283.264	41.0
10	284.268	8.0
11	342.219	13.4
12	367.264	11.7
13	370.250	26.1
14	398.281	29.0
15	399.285	7.7
16	426.313	26.6
17	427.316	7.6
18	468.360	16.9
19	510.406	9.1
20	552.453	8.4

Figure A 83. MS spectrum of 17-oxo-DHA with freshly made PTAD in dichloromethane after 2h at 35ºC. ESI in the negative ion mode. Dichloromethane evaporated prior to analysis, and residuals reconstituted in methanol.

MS Spectrum Report

Analysis Info

Sample Name	17-oxo-DHA-PTAD 35C	Acquisition Date	11/2/2017 1:04:44 PM
Method	ESI_pos_50_1500.m	Analysis Name	D:\Data\maxis2017\13454a.d

Acquisition Parameter

Source Type	ESI	Ion Polarity	Positive	Set Nebulizer	0.4 Bar
Focus	Not active	Set Capillary	3500 V	Set Dry Heater	200 °C
Scan Begin	50 m/z	Set End Plate Offset	-500 V	Set Dry Gas	4.0 l/min
Scan End	1500 m/z	Set Charging Voltage	2000 V	Set Divert Valve	Waste
		Set Corona	0 nA	Set APCI Heater	0 °C

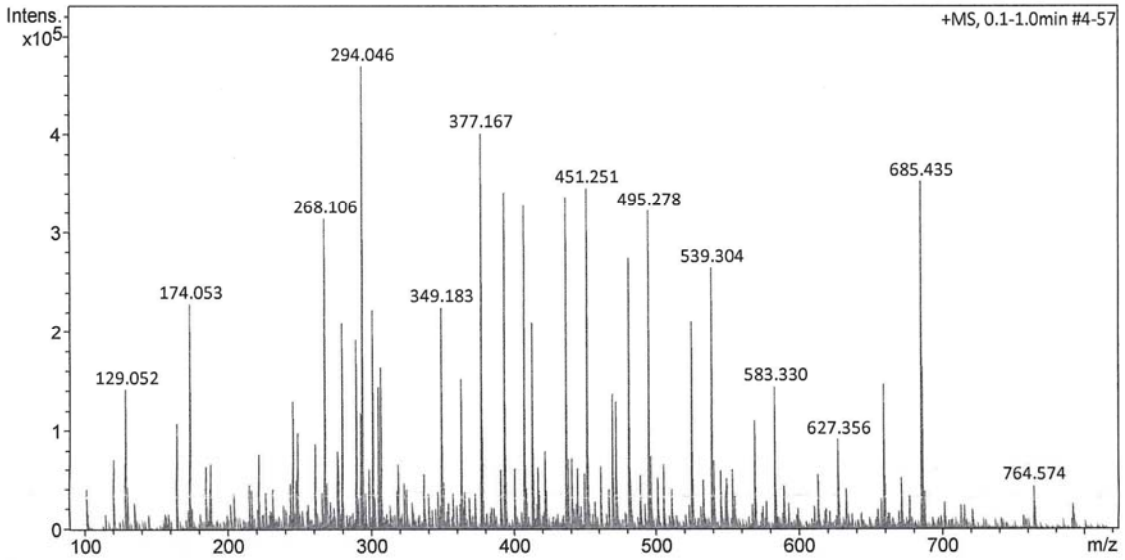

#	m/z	I %
1	174.053	48.7
2	268.106	66.9
3	280.031	44.8
4	290.088	41.0
5	294.046	100.0
6	301.075	43.3
7	301.141	47.4
8	349.183	48.0
9	377.167	85.3
10	393.210	72.7
11	407.225	69.9
12	413.266	44.8
13	437.236	71.6
14	451.251	73.5
15	481.262	58.4
16	495.278	68.6
17	525.288	44.9
18	539.304	56.3
19	685.435	75.0
20	686.439	35.1

Figure A 84. MS spectrum of 17-oxo-DHA with freshly made PTAD in dichloromethane after 2h at 35oC. ESI in the positive ion mode. Dichloromethane evaporated prior to analysis, and residuals reconstituted in methanol.

MS Spectrum Report

Analysis Info

Sample Name	17-oxo-DHA-S-PEM romT	Acquisition Date	11/2/2017 11:54:38 AM
Method	ESI_neg_50_1500.m	Analysis Name	D:\Data\maxis2017\13461.d

Acquisition Parameter

Source Type	ESI	Ion Polarity	Negative	Set Nebulizer	0.4 Bar
Focus	Not active	Set Capillary	3500 V	Set Dry Heater	200 °C
Scan Begin	50 m/z	Set End Plate Offset	-500 V	Set Dry Gas	4.0 l/min
Scan End	1500 m/z	Set Charging Voltage	0 V	Set Divert Valve	Source
		Set Corona	0 nA	Set APCI Heater	0 °C

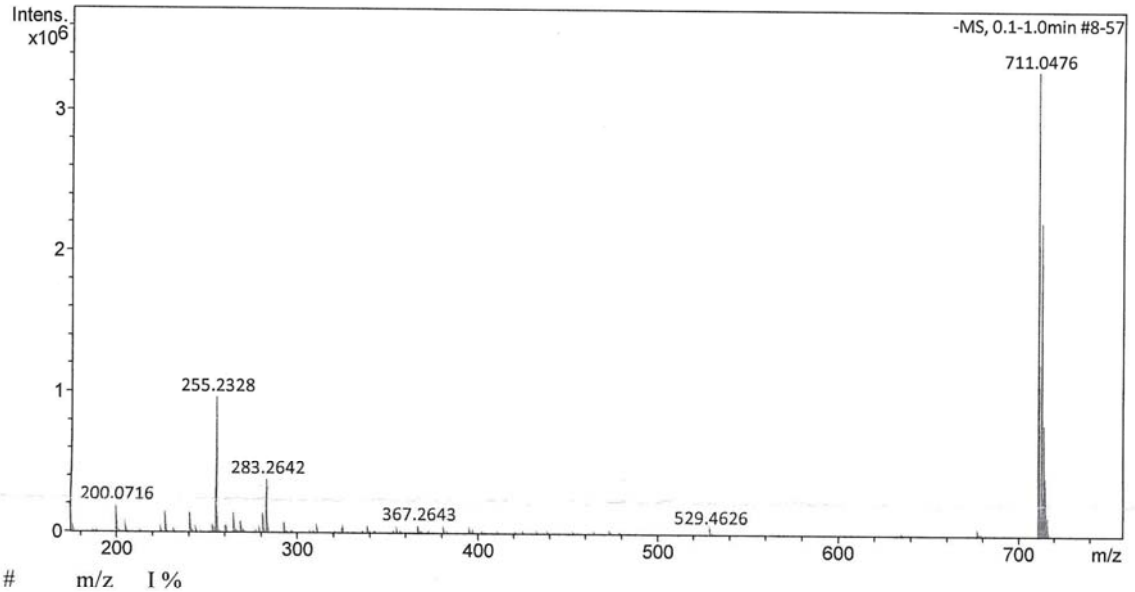

#	m/z	I %
1	200.0716	5.9
2	227.2016	4.6
3	241.2172	4.3
4	253.2172	1.8
5	255.2328	29.2
6	256.2363	5.2
7	260.8733	1.7
8	265.1478	4.3
9	269.2485	2.7
10	281.2486	4.5
11	283.2642	11.7
12	284.2676	2.3
13	293.1790	2.3
14	711.0476	100.0
15	711.1906	1.8
16	712.0506	37.0
17	713.0451	67.4
18	714.0479	24.0
19	715.0437	12.5
20	716.0455	4.1

Figure A 85. MS spectrum of 17-oxo-DHA with freshly made *S*-PEM in dichloromethane after 2h at room temperature. ESI in the negative ion mode. Dichloromethane evaporated prior to analysis, and residuals reconstituted in methanol.

MS Spectrum Report

Analysis Info

Sample Name	17-oxo-DHA-S-PEM romT	Acquisition Date	11/2/2017 12:34:37 PM
Method	ESI_pos_50_1500.m	Analysis Name	D:\Data\maxis2017\13450a.d

Acquisition Parameter

Source Type	ESI	Ion Polarity	Positive	Set Nebulizer	0.4 Bar
Focus	Not active	Set Capillary	3500 V	Set Dry Heater	200 °C
Scan Begin	50 m/z	Set End Plate Offset	-500 V	Set Dry Gas	4.0 l/min
Scan End	1500 m/z	Set Charging Voltage	2000 V	Set Divert Valve	Waste
		Set Corona	0 nA	Set APCI Heater	0 °C

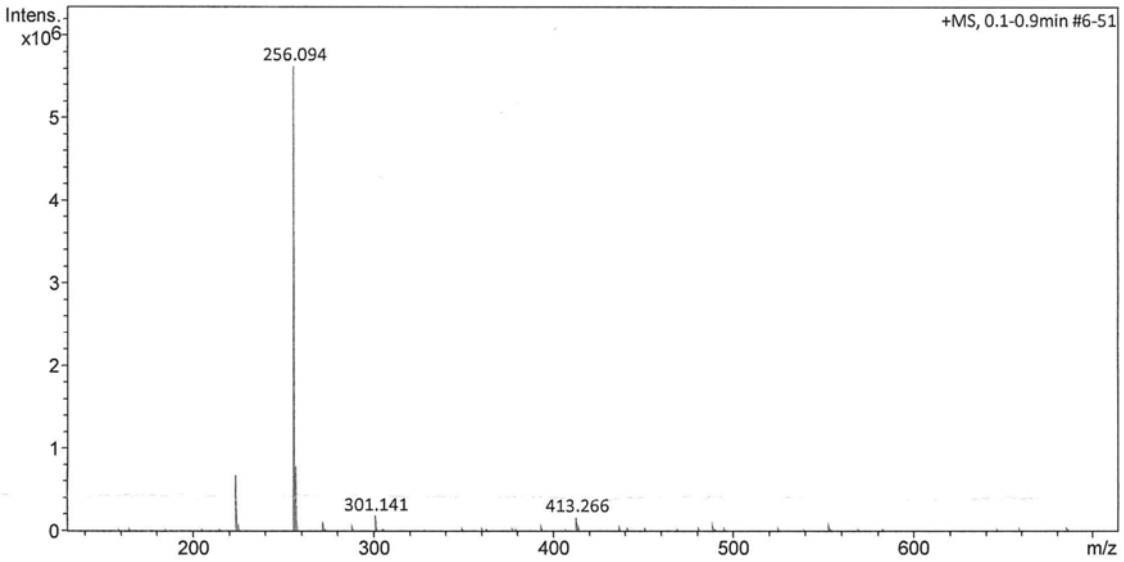

#	m/z	I %
1	164.921	0.7
2	224.068	12.0
3	225.072	1.6
4	256.094	100.0
5	256.190	1.8
6	256.254	0.8
7	257.098	13.9
8	258.100	1.4
9	272.068	2.0
10	288.121	1.0
11	301.141	3.3
12	377.167	0.7
13	393.210	0.8
14	413.266	3.1
15	414.270	0.8
16	437.236	0.8
17	481.262	0.7
18	489.200	1.1
19	553.459	1.1
20	685.436	0.7

Figure A 86. MS spectrum of 17-oxo-DHA with freshly made *S*-PEM in dichloromethane after 2h at room temperature. ESI in the positive ion mode. Dichloromethane evaporated prior to analysis, and residuals reconstituted in methanol.

MS Spectrum Report

Analysis Info

Sample Name	17-oxo-DHA-SPEM 35C	Acquisition Date	11/2/2017 10:55:50 AM
Method	ESI_neg_50_1500.m	Analysis Name	D:\Data\maxis2017\13456.d

Acquisition Parameter

Source Type	ESI	Ion Polarity	Negative	Set Nebulizer	0.4 Bar
Focus	Not active	Set Capillary	3500 V	Set Dry Heater	200 °C
Scan Begin	50 m/z	Set End Plate Offset	-500 V	Set Dry Gas	4.0 l/min
Scan End	1500 m/z	Set Charging Voltage	0 V	Set Divert Valve	Source
		Set Corona	0 nA	Set APCI Heater	0 °C

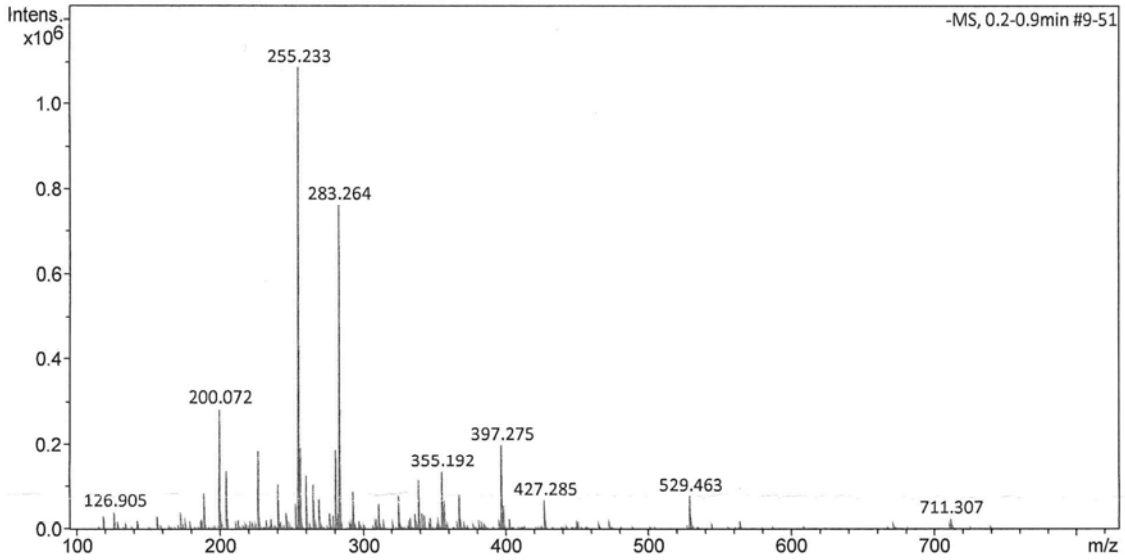

#	m/z	I %
1	189.092	7.8
2	200.072	26.2
3	205.160	12.5
4	227.202	17.1
5	241.217	9.7
6	255.233	100.0
7	256.236	17.9
8	260.873	11.6
9	265.148	9.7
10	269.249	6.4
11	281.249	17.4
12	283.264	70.1
13	284.268	13.9
14	293.178	8.0
15	325.184	7.1
16	339.198	10.5
17	355.192	12.4
18	367.264	7.4
19	397.275	18.3
20	529.463	7.0

Figure A 87. MS spectrum of 17-oxo-DHA with freshly made *S*-PEM in dichloromethane after 2h at 35ºC. ESI in the negative ion mode. Dichloromethane evaporated prior to analysis, and residuals reconstituted in methanol.

MS Spectrum Report

Analysis Info

Sample Name	17-oxo-DHA-SPEM 35C	Acquisition Date	11/2/2017 1:16:10 PM
Method	ESI_pos_50_1500.m	Analysis Name	D:\Data\maxis2017\13455a.d

Acquisition Parameter

Source Type	ESI	Ion Polarity	Positive	Set Nebulizer	0.4 Bar
Focus	Not active	Set Capillary	3500 V	Set Dry Heater	200 °C
Scan Begin	50 m/z	Set End Plate Offset	-500 V	Set Dry Gas	4.0 l/min
Scan End	1500 m/z	Set Charging Voltage	2000 V	Set Divert Valve	Waste
		Set Corona	0 nA	Set APCI Heater	0 °C

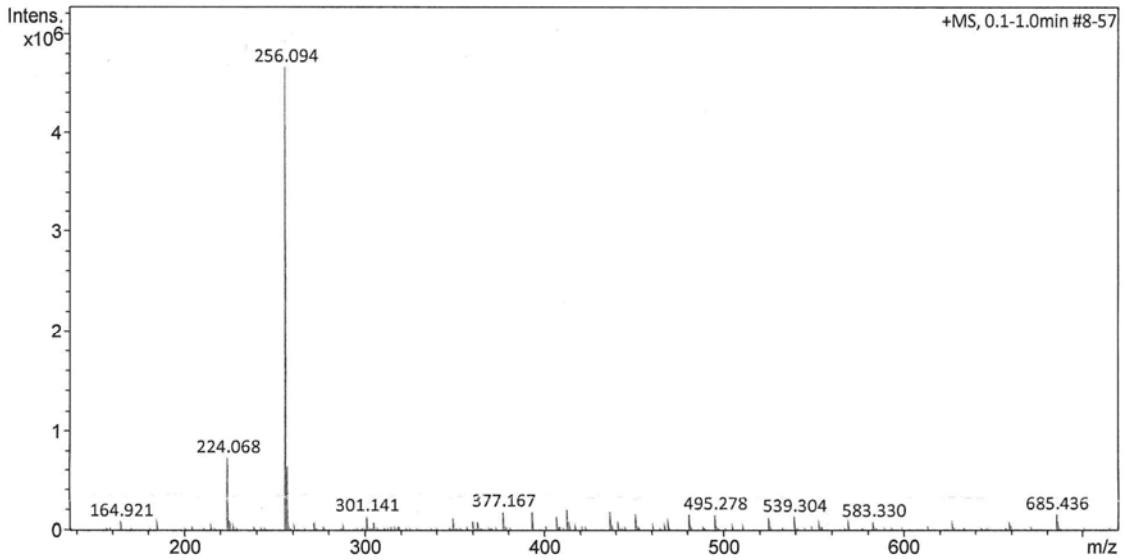

#	m/z	I %
1	164.921	1.8
2	224.068	15.7
3	225.072	2.2
4	256.094	100.0
5	257.098	13.8
6	301.141	2.9
7	349.183	2.6
8	360.324	1.7
9	377.167	3.9
10	393.210	3.9
11	407.225	3.0
12	413.266	4.4
13	437.236	3.9
14	451.251	3.4
15	481.262	3.2
16	495.278	3.3
17	525.288	2.5
18	539.304	2.8
19	659.287	2.0
20	685.436	3.2

Figure A 88. MS spectrum of 17-oxo-DHA with freshly made *S*-PEM in dichloromethane after 2h at 35ºC. ESI in the positive ion mode. Dichloromethane evaporated prior to analysis, and residuals reconstituted in methanol.

MS Spectrum Report

Analysis Info

Sample Name	17-RAC PETAD ROMT	Acquisition Date	3/12/2018 2:12:07 PM
Method	ESI_pos_50_1500.m	Analysis Name	D:\Data\maxis2018\13913.d

Acquisition Parameter

Source Type	ESI	Ion Polarity	Positive	Set Nebulizer	0.4 Bar
Focus	Not active	Set Capillary	3500 V	Set Dry Heater	200 °C
Scan Begin	50 m/z	Set End Plate Offset	-500 V	Set Dry Gas	4.0 l/min
Scan End	1500 m/z	Set Charging Voltage	2000 V	Set Divert Valve	Waste
		Set Corona	0 nA	Set APCI Heater	0 °C

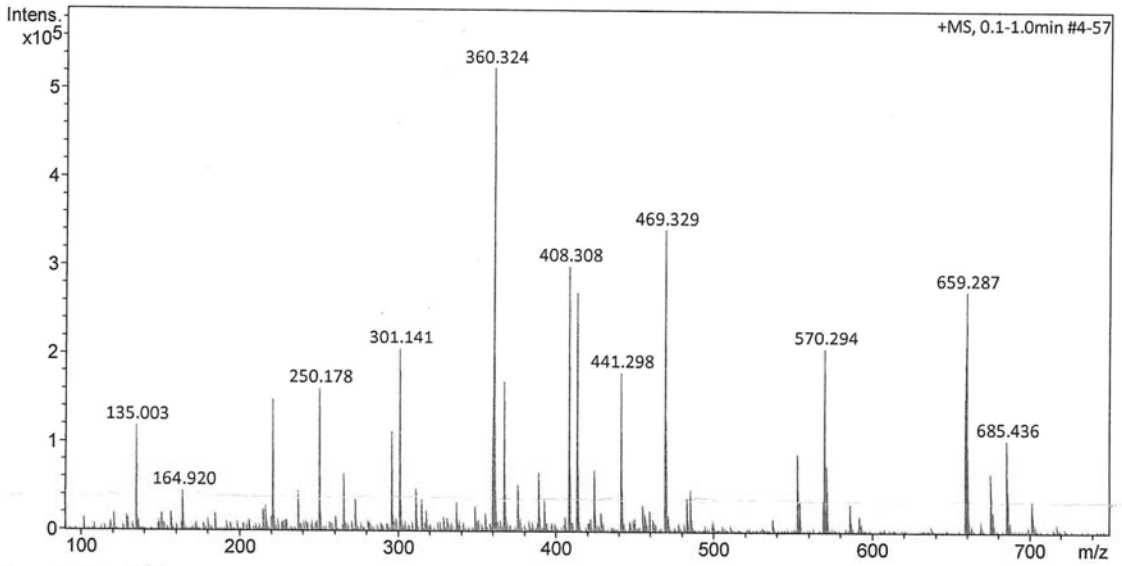

#	m/z	I %
1	135.003	22.7
2	221.175	28.5
3	250.178	30.7
4	296.137	21.6
5	301.141	39.3
6	360.324	100.0
7	361.327	23.7
8	367.224	32.4
9	408.308	57.4
10	413.266	51.7
11	414.270	14.2
12	441.298	34.4
13	469.329	65.2
14	470.332	20.5
15	553.459	17.1
16	570.294	39.7
17	571.297	14.2
18	659.287	52.1
19	660.291	18.6
20	685.436	20.1

Figure A 89. MS spectrum of (±)17-HDHA with freshly made *S*-PETAD in dichloromethane after 24h at 35ºC. ESI in the positive ion mode. Dichloromethane evaporated prior to analysis, and residuals reconstituted in methanol.

MS Spectrum Report

Analysis Info

Sample Name	17-RAC PETAD 30C 300	Acquisition Date	3/12/2018 2:44:56 PM
Method	ESI_pos_50_1500.m	Analysis Name	D:\Data\maxis2018\13915.d

Acquisition Parameter

Source Type	ESI	Ion Polarity	Positive	Set Nebulizer	0.4 Bar
Focus	Not active	Set Capillary	3500 V	Set Dry Heater	200 °C
Scan Begin	50 m/z	Set End Plate Offset	-500 V	Set Dry Gas	4.0 l/min
Scan End	1500 m/z	Set Charging Voltage	2000 V	Set Divert Valve	Waste
		Set Corona	0 nA	Set APCI Heater	0 °C

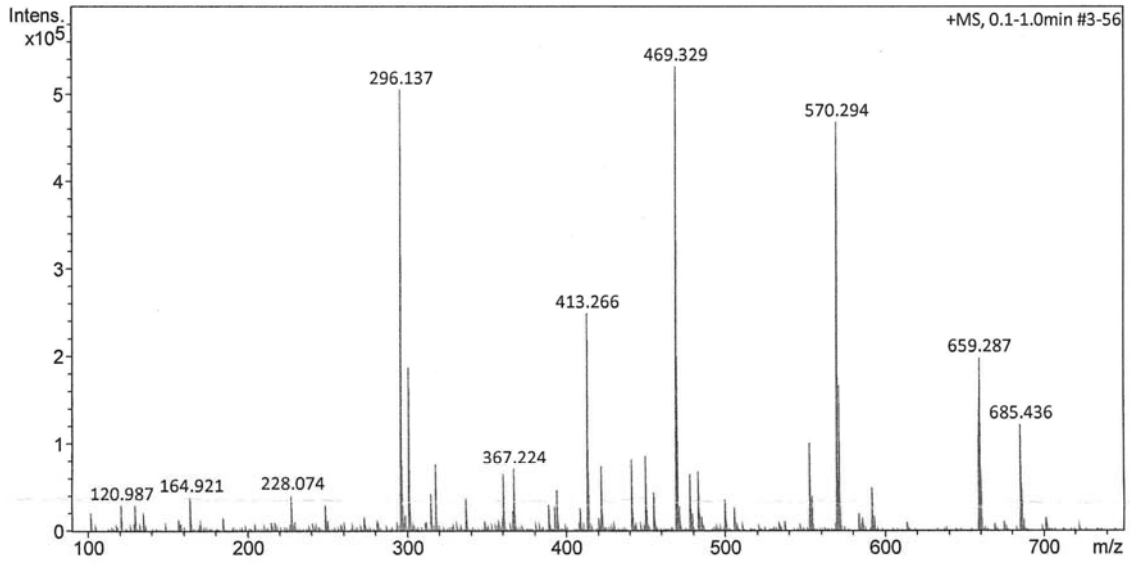

#	m/z	I %
1	296.137	95.0
2	297.140	15.5
3	301.141	35.3
4	318.119	14.5
5	367.224	13.5
6	413.266	46.8
7	414.270	12.9
8	422.278	14.1
9	441.298	15.6
10	450.309	16.2
11	469.329	100.0
12	470.332	31.1
13	478.340	12.3
14	483.344	12.8
15	553.459	19.1
16	570.294	88.0
17	571.297	31.4
18	659.287	37.2
19	660.291	13.3
20	685.436	23.1

Figure A 90. MS spectrum of (±)17-HDHA with freshly made *S*-PETAD (300% excess) in dichloromethane after 24h at 35ºC. ESI in the positive ion mode. Dichloromethane evaporated prior to analysis, and residuals reconstituted in methanol.

MS Spectrum Report

Analysis Info

Sample Name	17S-I PETAD 30C	Acquisition Date	3/20/2018 11:06:03 AM
Method	ESI_pos_50_1500.m	Analysis Name	D:\Data\maxis2018\13940.d

Acquisition Parameter

Source Type	ESI	Ion Polarity	Positive	Set Nebulizer	0.4 Bar
Focus	Not active	Set Capillary	3500 V	Set Dry Heater	200 °C
Scan Begin	50 m/z	Set End Plate Offset	-500 V	Set Dry Gas	4.0 l/min
Scan End	1500 m/z	Set Charging Voltage	2000 V	Set Divert Valve	Waste
		Set Corona	0 nA	Set APCI Heater	0 °C

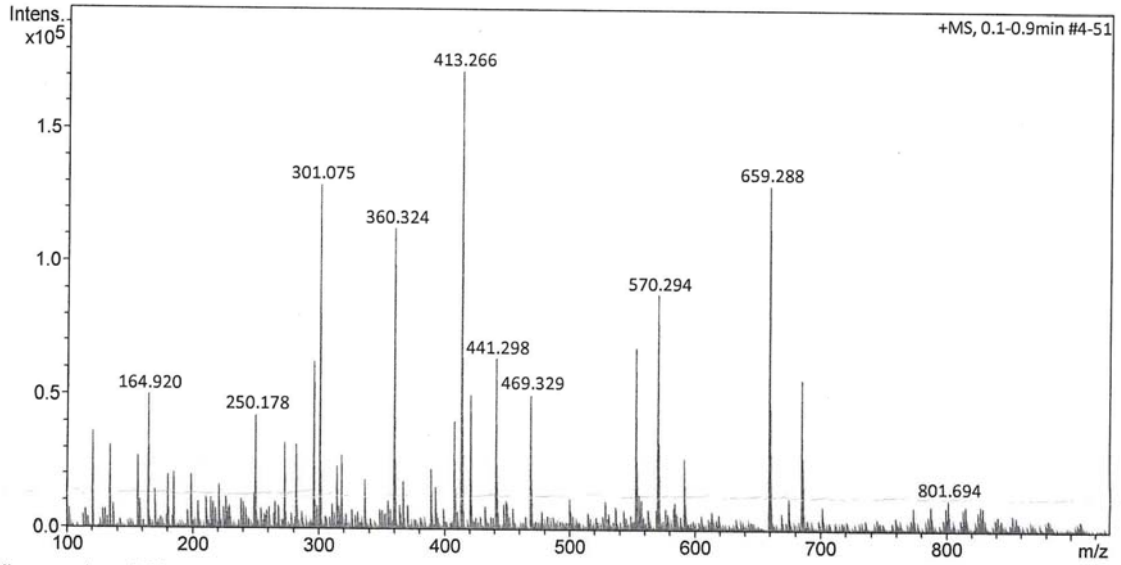

#	m/z	I %
1	120.987	21.3
2	164.920	29.1
3	250.178	25.0
4	273.167	18.8
5	296.137	36.5
6	301.075	75.1
7	301.141	73.1
8	360.324	65.4
9	408.308	23.8
10	413.266	100.0
11	414.270	25.9
12	421.233	29.5
13	441.298	37.2
14	469.329	29.4
15	553.459	39.7
16	570.294	51.4
17	571.297	18.8
18	659.288	75.3
19	660.291	26.9
20	685.436	33.0

Figure A 91. MS spectrum of 17*S*-HDHA with freshly made *S*-PETAD in dichloromethane after 24h at 35ºC. ESI in the positive ion mode. Dichloromethane evaporated prior to analysis, and residuals reconstituted in methanol.

MS Spectrum Report

Analysis Info

Sample Name	17S-300 PETAD 30C	Acquisition Date	3/20/2018 11:45:43 AM
Method	ESI_pos_50_1500.m	Analysis Name	D:\Data\maxis2018\13943.d

Acquisition Parameter

Source Type	ESI	Ion Polarity	Positive	Set Nebulizer	0.4 Bar
Focus	Not active	Set Capillary	3500 V	Set Dry Heater	200 °C
Scan Begin	50 m/z	Set End Plate Offset	-500 V	Set Dry Gas	4.0 l/min
Scan End	1500 m/z	Set Charging Voltage	2000 V	Set Divert Valve	Waste
		Set Corona	0 nA	Set APCI Heater	0 °C

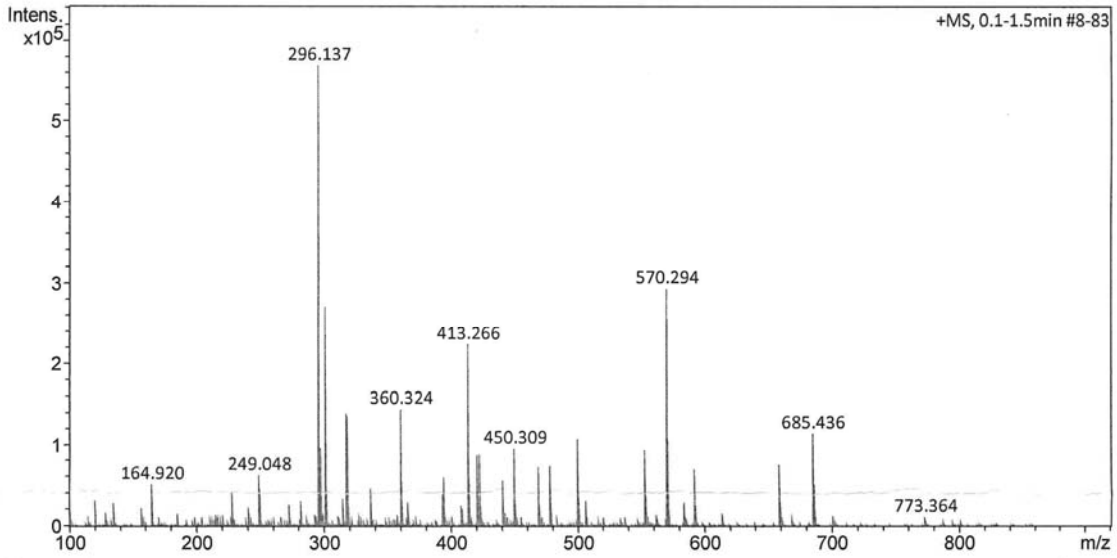

#	m/z	I %
1	249.048	10.9
2	296.137	100.0
3	297.140	17.0
4	301.141	47.7
5	318.119	24.3
6	360.324	25.4
7	413.266	39.3
8	414.270	10.6
9	421.233	15.2
10	422.278	15.6
11	450.309	16.9
12	469.329	12.8
13	478.340	13.1
14	500.288	19.0
15	553.459	16.8
16	570.294	51.7
17	571.297	18.7
18	592.276	12.2
19	659.288	13.3
20	685.436	20.2

Figure A 92. MS spectrum of 17*S*-HDHA with freshly made *S*-PETAD (300% excess) in dichloromethane after 24h at 35ºC. ESI in the positive ion mode. Dichloromethane evaporated prior to analysis, and residuals reconstituted in methanol.

MS Spectrum Report

Analysis Info

Sample Name	MaR1 PETAD 30C	Acquisition Date	3/20/2018 12:49:07 PM
Method	ESI_pos_50_1500.m	Analysis Name	D:\Data\maxis2018\13944.d

Acquisition Parameter

Source Type	ESI	Ion Polarity	Positive	Set Nebulizer	0.4 Bar
Focus	Not active	Set Capillary	3500 V	Set Dry Heater	200 °C
Scan Begin	50 m/z	Set End Plate Offset	-500 V	Set Dry Gas	4.0 l/min
Scan End	1500 m/z	Set Charging Voltage	2000 V	Set Divert Valve	Waste
		Set Corona	0 nA	Set APCI Heater	0 °C

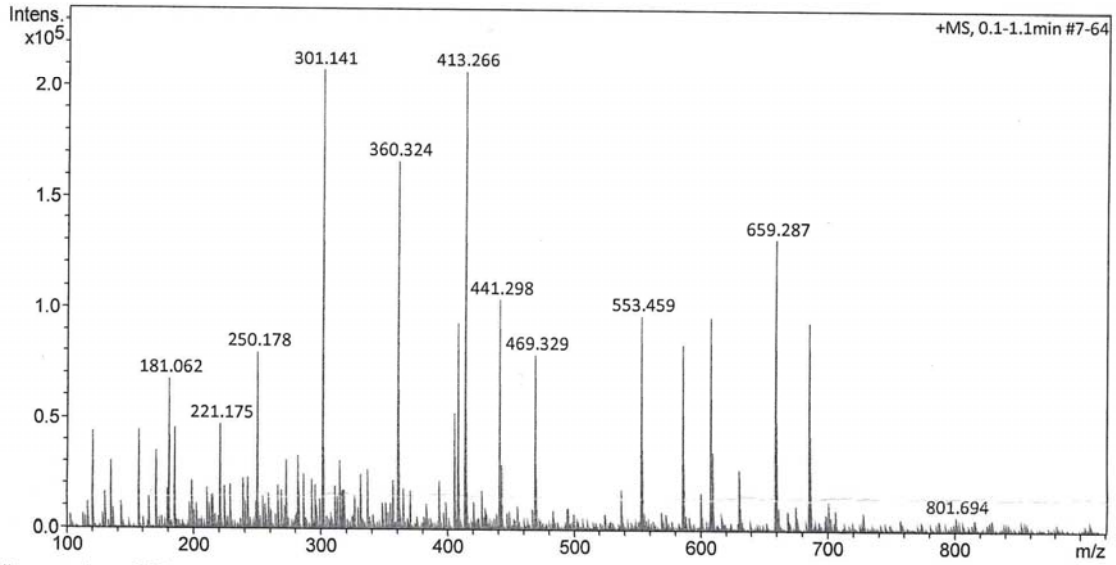

#	m/z	I %
1	120.987	21.3
2	156.984	21.6
3	181.062	32.6
4	185.014	22.2
5	221.175	22.9
6	250.178	38.3
7	301.141	100.0
8	360.324	80.1
9	405.201	25.4
10	408.308	45.0
11	413.266	99.8
12	414.270	26.3
13	441.298	50.3
14	469.329	38.1
15	553.459	46.8
16	586.289	40.4
17	608.271	46.6
18	659.287	63.2
19	660.291	23.0
20	685.436	45.6

Figure A 93. MS spectrum of MaR1 with freshly made *S*-PETAD in dichloromethane after 24h at 35ºC. ESI in the positive ion mode. Dichloromethane evaporated prior to analysis, and residuals reconstituted in methanol.

MS Spectrum Report

Analysis Info

Sample Name	MaR1 PETAD 300 30C	Acquisition Date	3/20/2018 1:07:20 PM
Method	ESI_pos_50_1500.m	Analysis Name	D:\Data\maxis2018\13945.d

Acquisition Parameter

Source Type	ESI	Ion Polarity	Positive	Set Nebulizer	0.4 Bar
Focus	Not active	Set Capillary	3500 V	Set Dry Heater	200 °C
Scan Begin	50 m/z	Set End Plate Offset	-500 V	Set Dry Gas	4.0 l/min
Scan End	1500 m/z	Set Charging Voltage	2000 V	Set Divert Valve	Waste
		Set Corona	0 nA	Set APCI Heater	0 °C

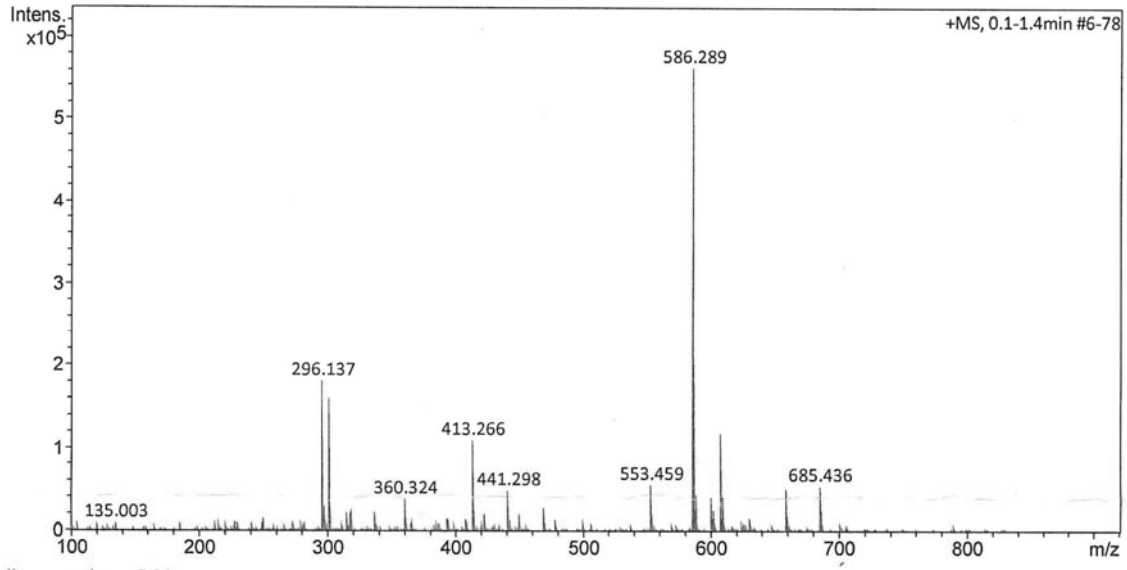

#	m/z	I %
1	296.137	32.2
2	297.140	5.4
3	301.141	28.7
4	302.144	5.2
5	360.324	6.8
6	413.266	19.7
7	414.270	5.2
8	441.298	8.7
9	469.329	5.0
10	553.459	9.9
11	586.289	100.0
12	587.292	36.1
13	588.296	7.8
14	600.305	7.1
15	602.261	4.4
16	608.271	21.0
17	609.274	7.4
18	659.287	9.1
19	685.436	9.6
20	686.439	4.5

Figure A 94. MS spectrum of MaR1 with freshly made *S*-PETAD (300% excess) in dichloromethane after 24h at 35ºC. ESI in the positive ion mode. Dichloromethane evaporated prior to analysis, and residuals reconstituted in methanol.